THE UNIVERSITY
of EDINBURGH

The role of methyl-CpG-binding domain protein-2 (MBD2) in colonic inflammation

Gareth-Rhys Jones

A thesis submitted for the degree of Doctor of Philosophy

University of Edinburgh

2016

Acknowledgements

Firstly I would like to thank my post-doctoral supervisor, colleague and friend Dr. Peter Cook. Pete has fielded endless questions, queries and always made himself available for sage advice, usually with an (on occasion) witty pun. Many thanks for his time and limitless patience in reading this manuscript, for his thoughtful comments and for truly making this last 3 years so enjoyable. To my flatmate and colleague Dr. Alex Phythian-Adams, I've never been more grateful for your culinary expertise than after a difficult day in the lab combined with your always thoughtful, always helpful, always cheerful demeanor. Your dedication to producing science of the highest quality, often whilst surrounded by seemingly insurmountable obstacles has been an inspiration.

Sheila is simply a credit to Linlithgow, and I would not be surprised if a statue is erected in the not to distant future. Only a fraction of the enclosed work would have been possible without your help and time. Many thanks in particular for creating and maintaining the chimeric mice. To the other members of the MacDonald Lab, many thanks to Lauren for taking wet-behind-the-ears, inept medic and helping create a lean-mean-FACSing machine. Many thanks also to Freya and Cecilia for MacDonald lab flaming zombie cocktail nights out, and for teaching me Swedish by diffusion.

Outwith the MacDonald Lab, many thanks to Allison Bancroft for her help, advice in performing the *T. muris* infection experiments, particularly the ELISA restimulation outputs. Many thanks also to John Worthington, who has also fielded many colon related questions, and graciously provided a significant amount of time and reagents into making the enclosed experiments possible. Depsite only meeting Dr. Calum Bain in person during the final month of my PhD he has been a constant presence throughout. Both in providing protocols, helping unravel the mysterious world of colon immune-biology and publishing beautiful and inspirational work.

To Tom Fenton and Mark Travis, many thanks for access to your database of IBD patients and flow cytometry data thereof. This was a really unexpected and wonderful addition to the project that I think really enriches its translational value. To Wellcome, many thanks for your financial support in funding the ECAT programme, in particular for allowing me to continue my studies in Manchester with the MacDonald Lab.

Finally to Andrew, thankyou for being the most wonderful person to work for, for taking me down to Manchester when most in their right mind would have left me behind, and for always making yourself available for science and life advice. But most importantly for telling me when I'm doing it all wrong, and putting me back on track. Lastly to Ciara, thank you for everything that really matters, and making me lots of tea.

Author's Declaration

I declare that all experimental data contained in thus thesis is the result of my own work, with the exception of bone marrow chimera generation which was carried out in collaboration with Sheila Brown, *Trichuris muris* ELISAs which was performed by Dr. Allison Bancroft at the University of Manchester. In addition IlluminaRef6Mouse microarrays were analysed in collaboration with Dr. Al Ivens, and 16S sequencing analysis with the assistance of Dr. Nick Kennedy, both at the University of Edinburgh. No part of this thesis has been previously submitted for any other degree at the University of Edinburgh or any other institution.

Signature…….

Printed Name……..

Contents

Acknowledgements 2
Authors Declaration 3
List of Figures 8
List of Tables 9
List of Diagrams 10
List of Abbreviations 11
Summary 14
Lay Summary 17
Chapter 1 General Introduction 18
1.1 Introduction 19
1.2 The inflammatory bowel diseases 19
1.3 The Gastrointestinal immune system 20
1.3.1 Neutrophils 21
1.3.2 Eosinophils 21
1.3.3 Monocytes 22
1.3.4 Macrophages 23
1.3.5 Dendritic cells 24
1.3.6 T Cells 27
1.3.7 Innate lymphoid cells 28
1.3.8 Intestinal epithelial cells 28
1.4 IBD is characterised by a dysregulated immune response 29
1.5 The Microbiome 31
1.6 Animal models of IBD 35
1.6.1 DSS colitis 35
1.6.2 TNBS/Oxazolone colitis 36
1.6.3 Adoptive transfer of CD45RB T cells 37
1.6.4 *Il10-/-* transgenic mice 38
1.6.5 Other transgenic models 38
1.6.6 *Trichuris Muris* 39
1.6.7 *Citrobacter rodentium* 40
1.7 Epigenetics 41
1.7.1 DNA methylation 41
1.7.2 Histone modification 42
1.7.3 Nucleosome remodelling 43
1.7.4 Methy- CpG-binding proteins 43
1.7.5 Epigenetics in innate and adaptive immunity 46
1.7.6 Epigenetics and the microbiome 47
1.7.7 Epigenetics and the "missing heritability" of IBD 48
1.8 Thesis Aims 50
Chapter 2 Materials and Methods 51
2.1 Mice 52
2.2 Isolation of mesenteric lymph node cells 52
2.3 Isolation of colon LP cells 52

2.4 Isolation of colon epithelial cells 52
2.5 Processing of whole blood 53
2.6 Histology 53
2.7 Flow cytometry and Antibodies 53
2.7.1 Surface staining 53
2.7.2 Intracellular staining 53
2.7.3 Flow cytometry assisted cell sorting (FACS) 54
2.8 Induction of DSS colitis 54
2.9 Induction of *T. muris* colitis 54
2.10 Enzyme linked immunosorbent assays (ELISAs) 55
2.11 Human samples 55
2.12 Generation of BM chimeras 56
2.13 RNA extraction 56
2.13.1 Tissue 56
2.13.2 Cells 56
2.14 cDNA sythesis from RNA and qPCR 57
2.15 Stool DNA extraction and 16S amplification 57
2.16 Illumina Ref6 Mouse Array 58
2.17 Statistical analysis 58
Chapter 3 The role of *Mbd2* in the steady state and inflamed colon 64
3.1 Introduction 65
3.2 Expression of *Mbd2/MBD2* in the GI tract 68
3.3 Analysis of *MBD2* as a candidate susceptibility locus in IBD 68
3.4 Identification of immune populations in the steady state colon LP 69
3.5 Assessment of naive *Mbd2-/-* mice 74
3.6 Assessment of *Mbd2* expression in myeloid cells 75
3.7 Assessment of *Mbd2-/-* mice after acute colitis 76
3.7.1 *Mbd2-/* display severe inflammation upon DSS treatment 76
3.7.2 mRNA expression of cytokine response 77
3.8 Effects of inflammation on the colon LP myeloid compartment 77
3.8.1 Effect of DSS on WT colon LP myeloid cells 77
3.8.2 Comparison of *Mbd2-/-* and WT colon LP cells in DSS 77
3.8.3 Assessment of the role of *Mbd2* in myeloid cytokine prduction 78
3.9 Assessment of *Mbd2-/-* response fo *Trichuris muris* infection 79
3.9.1 General observations and experimental outline 80
3.9.2 Serum antigen specific responses in WT and *Mbd2-/-* mice 80
3.9.3 Comparison of *Mbd2-/-* and WT colon LP cells in *T. muris* infection 81
3.9.3.1 Myeloid cells 81
3.9.3.2 T cells 81
3.9.4 Local and systemic cytokine responses 82
3.9.4.1 Antigen specific draining lymph node response 83
3.9.4.2 CD4 T cell response 83
3.9.4.3 CD8 T cell response 84
3.10 Colon LP cells in active IBD 84

3.10.1 Patient demographics and experimental outline 84
3.10.2 Colon LP analysis in healthy controls and IBD patients 85
3.11 Discussion 86
Chapter 4 The role of *Mbd2* deficient haematopoietic cells in colonic inflammation 109
4.1 Introduction 110
4.2 The role of haematopoietic *Mbd2* in colonic inflammation 112
4.3 The role of monocytes in the susceptibility of *Mbd2-/-* to colitis 114
4.3.1 Blood and colon LP monocyte cytokine responses 114
4.3.2 Gene expression profiles of colon LP monocytes in colitis 115
4.3.2.1 Genes upregulated in *Mbd2-/-* monocytes 116
4.3.2.2 Genes downregulated in *Mbd2-/-* monocytes 117
4.3.3 Naïve Colon LP monocyte proliferation in *Mbd2-/-* 117
4.3.4 WT and *Mbd2-/-* monocytes in mixed BM chimeras 118
4.4 The role of *Mbd2* in colon LP CD11c+ cells 119
4.4.1 Defining CD11c expressing cells in the colon LP 120
4.4.2 Selective depletion of *Mbd2* in CD11c+ cells 120
4.4.3 The role of CD11c+ cell depletion of *Mbd2* in the steady state 121
4.4.4 The role of CD11c+ cell depletion of *Mbd2* in colitis 121
4.4.4.1 Comparison of CD11cΔ*Mbd2* and control colon LP cells in colitis 122
4.4.4.2 Comparison of CD11cΔ*Mbd2* and control CD11c+ cell cytokine production 123
4.4.4.3 Gene expression of colon LP CD11c+ cells in colitis 124
4.4.4.3.1 Macrophages 124
4.4.4.3.2 CD11b- DC 125
4.4.4.3.3. Summary 126
4.4.5 TLR expression of *Mbd2-/-* CD11c+ cells *in vivo* 127
4.4.6 Co-stimulatory molecule expression of *Mbd2-/-* CD11c+ cells *in vivo* 128
4.5 Discussion 129
4.5.1 Haematopoietic sources of *Mbd2* and susceptibility to colitis 129
4.5.2 The role of *Mbd2* in monocytes 130
4.5.2.1 Key differences in *Mbd2* deficient monocyte gene expression in colitis 131
4.5.2.2 Mixed BM chimeras 134
4.5.3 The role of *Mbd2* in CD11c expressing cells 136
4.5.3.1 Key differences in *Mbd2* deficient macrophage gene expression during colitis 136
4.5.3.2 Increased CD11c+ cell pro- and anti- inflammatory pathways in colitis 138
4.5.3.3 Key differences in *Mbd2* deficient CD11b- DC gene expression during colitis 140
4.5.3.4 Activation of CD11c+ cells in *Mbd2* deficiency 141
4.5.4 Future work 141
4.6 Summary 145
Chapter 5 The role of *Mbd2* on the colonic epithelium and intestinal microbiota 170
5.1 Introduction 171
5.2 Identifying and extracting colon epithelial cells 174
5.3 Characterisation of naïve *Mbd2-/-* CECs 176
5.4 Characterisation of *Mbd2-/-* CECs in colitis 177
5.5 Gene expression analysis of *Mbd2-/-* CECs 178

5.5.1 Naïve CECs 178
5.5.1.1 Genes upregulated in *Mbd2-/-* CECs 179
5.5.1.2 Genes downregulated in *Mbd2-/-* CECs 180
5.5.2 CECs in DSS colitis 180
5.5.2.1 Genes upregualted in *Mbd2-/-* CECs 181
5.5.2.2 Genes downregulated in *Mbd2-/-* CECs 182
5.6 The composition of the intestinal microbiota in *Mbd2* deficiency 183
5.6.1 iTOL Dendrograms 184
5.6.2 Non-metric multidimensional scaling analysis 184
5.6.3 Dysbiosis in *Mbd2-/-* mice 184
5.7 Discussion 186
Chapter 6 Concluding remarks 229
6.1 Introduction 230
6.2 Concluding remarks 234
Bibliography 237

List of Figures

3.1 *Mbd2/MBD2* expression in the gastrointestinal tract and association with IBD 92
3.2 Flow cytometry gating strategy for colon LP myeloid populations 93
3.3 Colon LP non-myeloid cell comparision in naïve *Mbd2-/-* and WT mice 94
3.4 Naïve colon LP phenotyping in WT and *Mbd2-/-* mice 95
3.5 *Mbd2* expression in selected FACS purified colon LP myeloid subsets 96
3.6 Susceptibility of *Mbd2-/-* mice to DSS colitis 97
3.7 Colon mRNA expression of selected cytokines during DSS colitis 98
3.8 Flow cytometry analysis of the colon LP in DSS colitis 99
3.9 Serum antigen-specific antibody responses in *T. muris* colitis 100
3.10 Flow cytometry analysis of *T. muris* infected *Mbd2-/-* and WT mice 101
3.11 MLN antigen specific cytokine responses in *T. muris* colitis 102
3.12 Human colon LP CD14+ cells in IBD and healthy controls 103
4.1 Susceptibility of CD45.1WT versus CD45.1*Mbd2-/-* chimeras to DSS colitis 147
4.2 Colon LP flow cytometry analysis of DSS treated CD45.1WT and CD45.1*Mbd2-/-* chimeras 148
4.3 Flow cytometry identification of cytokine producing colon LP and blood monocytes 149
4.4 Gene expression analysis of DSS treated WT versus *Mbd2-/-* colon LP monocytes 150
4.5 Reconstitution of CD45.2WT/*Mbd2-/-* mixed BM chimeras 151
4.6 Flow cytometry analysis of DSS treated WT/*Mbd2-/-* mixed BM chimeras 152
4.7 CD11c expressing populations in the colon LP and effect of *Mbd2* deficiency 153
4.8 Susceptibility of CD11cΔMbd2 mice to DSS colitis 154
4.9 Flow cytometry analysis of CD11cΔ*Mbd2* colon LP cells in DSS colitis 155
4.10 Gene expression analysis of *Mbd2-/-* and WT DSS treated colon LP CD11c+ cells 156
4.11 TLR production and gene expression in *Mbd2* and WT DSS treated colon LP cells 157
5.1 Flow cytometry analysis of CECs 195
5.2 Optimising CEC isolation 196
5.3 Pre and post sort FACS purification of CECs 197
5.4 mRNA expression of epithelial cell markers and *Mbd2* in CECs 198
5.5 Surface marker expression of *Mbd2-/-* CECs in DSS and *T. muris* colitis 199
5.6 Gene expression analysis of naïve WT and *Mbd2-/-* CECs 200
5.7 Gene expression analysis of DSS treated WT and *Mbd2-/-* CECs 201
5.8 Analysis of the microbiota in naïve WT and *Mbd2-/-* mice 202

List of Tables

1.1 MBD functions 45

2.1 List of experimental animals 59

2.2 List of monoclonal antibodies used for flow cytometry 60

2.3 Clinical disease score criteria used during DSS-induced colitis 62

2.4 Histological disease score criteria used during DSS-induced colitis studies 62

2.5 Primers used in qRT-PCR 63

3.1 Summary of steady state myeloid marker expression in colon myeloid LP cells 104

3.2 Summary of colon LP myeloid population cell numbers in the steady state and after DSS colitis 105

3.3 CD4 T cell responses in *T. muris* colitis 106

3.4 Overview of IBD phenotype classification and clinical severity scores 107

3.5 Patient demographics and IBD disease characteristics 108

4.1 Summary of colon LP myeloid population cell numbers in Naïve and DSS treated, WT and *Mbd2-/-* BM chimeras 158

4.2 Blood and colon LP cytokine production in WT and *Mbd2-/-* monocytes 159

4.3 Gene expression analysis in DSS treated *Mbd2-/-* and WT colon LP monocytes 160

4.4 Gene ontology analysis of DSS treated *Mbd2-/-* and WT colon LP monocytes 161

4.5 Proportions of colon LP myeloid cells in *Mbd2-/-*:WT mixed BM chimeras 162

4.6 Blood and colon LP cytokine production in *Mbd2-/-*:WT mixed BM chimeras 163

4.7 Summary of colon LP myeloid population cell numbers in naïve and DSS treated, CD11cΔ*Mbd2* and control mice 164

4.8 Gene expression analysis in DSS treated *Mbd2-/-* and WT colon LP macrophages 165

4.9 Gene ontology analysis of DSS treated *Mbd2-/-* and WT colon LP macrophages 166

4.10 Gene expression analysis in DSS treated *Mbd2-/-* and WT colon LP CD11b- DC 167

4.11 Gene ontology analysis of DSS treated *Mbd2-/-* and WT colon LP CD11b- DC 168

4.12 Co-stimulatory molecule expression on *Mbd2-/-* MP cells 169

5.1 Comparison of proposed CEC extraction methods 175

5.2 Gene expression analysis of naïve *Mbd2-/-* and WT CECs 203

5.3 Gene ontology analysis of naïve *Mbd2-/-* and WT CECs 208

5.4 Gene pathway analysis of naïve *Mbd2-/-* and WT CECs 209

5.5 Gene expression analysis of *Mbd2-/-* and WT CECs in colitis 210

5.6 Gene ontology analysis of *Mbd2-/-* and WT CECs in colitis 217

5.7 Gene pathway analysis of *Mbd2-/-* and WT CECs in colitis 218

5.8 Co-housing and age of mice used in 16S analysis 219

5.9 OTU classification of bacteria in *Mbd2-/-* and WT microbiome 220

5.10 Gene expression analysis of naïve versus colitic WT CECs 221

5.11 Gene ontology analysis of naïve versus colitic WT CECs 227

5.12 Gene pathway analysis of naïve versus colitic WT CECs 228

5.13 Summary of dysregulated MHC loci in *Mbd2-/-* CECs 187

List of Diagrams

1.1 DC subsets in the mouse and human intestinal lamina propria 26
1.2 Interaction between colon LP immune cells and the epithelium 34
4.1 Proposed kinetics of pro and anti-inflammtory pathways in DSS colitis 136
4.2 Proposed mechanisms for *Mbd2* mediated changes in haematopoietic cells in DSS colitis 144
6.1 Proposed mechanisms for *Mbd2* mediated changes in colon homeostasis 232

List of Abbreviations

A/E	Attaching and effacing
AJ	Adherens junction
APC	Antigen presenting cell
APRIL	A proliferation-inducing ligand
BCG	Bacillus Calmette-Guerin
BMDC	Bone marrow derived dendritic cell
CAC	Colitis-associated cancer
CCR	C-C chemokine receptor
CD	Crohn's disease
cDC	Conventional dendritic cell
CEC	Colon epithelial cell
CIITA	MHC class II transactivator
CMF	Calcium-magnesium free
CX3CR1	CX3C chemokine receptor
DC	Dendritic cell
DCIR2	Mouse dendritic cell inhibitory receptor 2
DNA	Deoxyribonucleic acid
DNMT	DNA methyl transferase
DSS	Dextran sulphate sodium
EDTA	Ethylenediaminetetraacetic acid
EHEC	Enerohaemorrhagic Escherichia coli
ELISA	Enzyme linked immunosorbant assay
EpCAM	Epithelial cell adhesion molecule
FCS	Foetal calf serum
GALT	Gut-associated lymphoid tissue
GI	Gastrointestinal
GM-CSF	Granulocyte macrophage colony-stimulating factor
GWAS	Genome-wide association studies
HAT	Histone acetyltransferase
HBI	Harvey Bradshaw index
HBSS	Hanks-buffered salt solution
HDAC	Histone deacetylase
HDM	House dust mite
HMT	Histone methyltransferase
HSC	Haematopoietic stem cell
HSP	Heat shock protein
iALP	Intestinal alkaline phosphatase
IBD	Inflammatory bowel disease
IEC	Intestinal epithelial cell
IEL	Intra-epithelial lymphocyte
IFN	Interferon
IIBDGC	International IBD genetic consortium
IL	Interleukin

ILC	Innate lymphoid cell
ILF	Isolated lymphoid follicle
iNOS	Inducible Nitric oxide synthase
JAM	Junctional adhesion molecules
KGF	Keratinocyte growth factor
LP	Lamina propria
MACS	Magentic activated cell sorting
MBD	Methyl-CpG-binding protein
MDP	Macrophage DC progenitor
MFI	Mean fluorescence intensity
MHC	Major histocompatibility complex
MLN	Mesenteric lymph node
MMP	Matrix metalloproteinase
MP	Mononuclear phagocyte
mRNA	Messenger RNA
MyD88	Myeloid differentiation primary response gene 88
NEMO	NF-kB essential modulator
NF-κB	Nuclear factor-kappa B
NICE	National institute for health and care excellence
NKT	Natural killer T cell
NMDS	Non-linear multi-dimensional scaling
NOD	Nucleotide-binding oligomerisation domain
NURD	Nucleosome remodelling deacetelyase
OTU	Operational taxonomic unit
PAMP	Pathogen-associated molecular pattern
PBS	Phosphate buffered saline
PFA	Paraformaldehyde
PGE_2	Prostaglandin E2
PMN	Polymorphonuclear leucocyte
PP	Peyers Patch
PPARγ	Peroxisome proliferator-activated receptor gamma
PRR	Pattern recognition receptor
RNA	Ribonucleic acid
RORγt	RAR-related orphan receptor gamma
ROS	Reactive oxygen species
RT	Reverse transcription
SCFA	Small chain fatty acid
SCID	Severe combined immunodeficiency
SEA	*Shistosoma mansoni* soluble egg antigen
SFB	Segmented filamentous bacteria
sIgA	Secretory IgA
siRNA	Small inhibitory RNA
SIRPα	Signal-regulatory protein alpha
SNP	Single nucleotide polymorphism

SPF	Specific pathogen free
SR	Scavenger receptor
TAM	Tumour-associated macrophage
TAP	Transporter associated with antigen processing
TGF-β	Transforming growth factor
Th	T helper cells
TJ	Tight junction
TLR	Toll-like receptor
TNBS	2,4,6-Trinitrobenzenesulfonic acid
TNF	Tumour necrosis factor
TNFRSF	TNF receptor superfamily
Treg	Regulatory T cell
TRUC	*Tbet*$^{-/-}$ *Rag2*$^{-/-}$ mice
TSLP	Thymic stromal lymphopoietin
UC	Ulcerative colitis

Summary

The human GI tract has evolved to simultaneously absorb nutrients and be the frontline in host defence. These seemingly mutually exclusive goals are achieved by a single cell thick epithelial barrier, and a complex resident immune system which lives in symbiosis with the intestinal microflora and is also able to rapidly respond to invading pathogens. An immunological balance is therefore required to permit tolerance to the normal intestinal microflora, but also prevent the dissemination of pathogenic micro-organisms to the rest of the host. Inappropriate immune responses in genetically susceptible individuals are the hallmark of human inflammatory bowel disease (IBD) and are thus targeting effector immune cells and their cytokines remains the mainstay of treatment. However despite vigorous efforts to delineate the genetic contribution to IBD disease susceptibility using large multinational cohorts, the majority of disease heritability remains unknown. Epigenetics describes heritable changes in chromatin that are not conferred by DNA sequence. These incorporate changes to histones, chromatin structure and DNA methylation, which confer changes to gene transcription and thus gene expression and cellular function. Methyl-binding proteins (MBD) have the ability to bind to methylated DNA and recruit large chromatin remodeling complexes that underpin a variety of epigenetic modifications. Methyl-CpG-binding domain protein 2 (MBD2) is one such MBD that is required for appropriate innate (dendritic cell) and adaptive (T cell) immune function, though its role has not been investigated in the GI tract.

We hypothesized that alterations in chromatin are central to the reprogramming of normal gene expression that occurs in disease states. By defining the phenotype of immune cells in the absence of MBDs we hope to understand the mechanisms of chromatin-dysregulation that lead to immune-mediated diseases such as IBD. We therefore aimed to assess the role of MBD2 in colon immune cells in the steady state and in murine models of GI tract inflammation, thereafter identifying the culprit cell types and genes responsible for any observed changes. We envisaged that investigating heritable, epigenetic changes in gene expression that are inherently more amenable to environmental manipulation than our DNA code, may provide novel insight to a poorly understood mechanism of disease predisposition. In addition identifying the cellular and gene targets of *Mbd2* mediated changes to immune homeostasis that may provide exciting and novel approaches to therapeutic modulation of pathological inflammatory responses.

In chapter 3 we assessed the expression of *Mbd2/MBD2* in the murine/human GI tract. Consistent with existing mouse data, levels of *Mbd2* mRNA increased between anatomical divisions of small (duodenum, ileum, terminal ileum) and large intestine (caecum, colon, rectum). In addition *MBD2* mRNA was greater in the rectum versus ileum, with active IBD associated with lower rectal *MBD2* mRNA compared to quiescent IBD controls. Thus we

sought to understand the role of *Mbd2* in the colon, where mRNA levels were the highest in the GI tract and where appropriate immune function is central to prevent damaging inflammation. To address these aims required the development of existing methods of cell surface marker expression analysis using flow cytometry techniques to simultaneously identify multiple innate and adaptive immune populations. Using naïve *Mbd2* deficient mice (*Mbd2*$^{-/-}$) we observed CD11b^{+} CD103^{+} DCs were significantly reduced in number in *Mbd2* deficiency.

To understand the role of *Mbd2* in colonic inflammation we employed a mouse model of chemical (DSS) and infectious (*T. gondii*) colitis comparing *Mbd2*$^{-/-}$ and littermate controls (WT). *Mbd2*$^{-/-}$ were extremely sensitive to DSS and *T. gondii* mediated colonic inflammation, characterized by increased symptom score, weight loss and histological score of tissue inflammation (DSS) and increased antibody specific cytokine responses (*T. gondii*) in *Mbd2* deficient animals. Flow cytometry analysis of colon LP cells in both infectious and chemical colitis revealed significant accumulation of monocytes and neutrophils in *Mbd2*$^{-/-}$. Indeed monocytes and neutrophils were the principal myeloid sources of IL-1b and TNF in DSS colitis and the number of IL-1b/TNF+ monocytes/neutrophils was significantly greater in *Mbd2*$^{-/-}$. Lastly we employed our colon LP isolation techniques to analyse immune populations in active and quiescent IBD and healthy controls, using endoscopically acquired biopsy samples. Analysis revealed that as in murine colitis, active human IBD is characterized by the accumulation of CD14^{High} monocyte-like cells, with an associated increased ratio of macrophage:monocyte-like cells.

In Chapter 4 we sought to understand the cellular sources of *Mbd2* that may explain the pre-disposition of *Mbd2*$^{-/-}$ to colitis. Firstly we restricted *Mbd2* deficiency to haematopoietic cells using grafting *Mbd2*$^{-/-}$ bone marrow (BM) into lethally irradiated WT mice. These animals treated with DSS displayed increased weight loss, symptom score, neutrophil accumulation and histopathology score compared to mice irradiated and grafted with WT BM. Given the accumulation of monocytes in *Mbd2*$^{-/-}$ DSS treated mice, and existing literature supporting a pathogenic role in this model, we then investigated the role of *Mbd2* in monocyte function. Colon monocytes sorted from *Mbd2*$^{-/-}$ and WT DSS treated mice displayed similar expression for many pro-inflammatory genes (*Il6, Il1a, Il1b, Tnf*), but demonstrated significantly dysregulated expression for some others (*Regb, Lyz1, Ido1, C4a*). To investigate this in a more refined model, we lethally irradiated WT mice and repopulated them with a WT:*Mbd2*$^{-/-}$ BM mix. This enabled the analysis of WT and *Mbd2*$^{-/-}$ haematopoietic cells in the same animal. Colon WT and *Mbd2*$^{-/-}$ monocyte recruitment and cytokine production in DSS treated mixed BM chimeras was equivalent between genotypes suggesting that *Mbd2* deficiency in monocytes alone did not explain the increased susceptibility of *Mbd2*$^{-/-}$ to DSS colitis. We then restricted *Mbd2* deficiency to CD11c

expressing cells, given the known role for *Mbd2* in their function, and for $CD11c^+$ cells in DSS, using a CD11cCre*Mbd2*$^{Fl/Fl}$ system. DSS treated mice with *Mbd2* deficient $CD11c^+$ cells demonstrated increased weight loss, symptoms score, histolopathology score, monocyte and neutrophil colon accumulation compared to controls. To further explore the role of *Mbd2* in colon $CD11c^+$ cells, macrophage and DCs from DSS treated WT and *Mbd2*$^{-/-}$ mice were purified and their gene expression analysed. *Mbd2*$^{-/-}$ versus WT macrophages demonstrated significantly altered expression of both pro- (*Il1a, C6, Ido1, Trem2*) and anti-inflammatory (*Tgfbi, Retnla*) pathways that we hypothesized was a method for attempted host control of excessive colon damage in *Mbd2*$^{-/-}$ mice. DC gene expression analysis was hampered by small sample size, but demonstrated a large number of small expression changes, including IL-12/IL-23 (*Jak2*) and autophagy (*Lrrk2*) pathways. Lastly levels of co-stimualtory molecules (CD40/CD80) were increased in *Mbd2*$^{-/-}$ but not CD11cΔMbd2 colon LP DCs/macrophages suggesting that non-$CD11c^+$ cellular sources of *Mbd2* were required to produce increased activation phenotype in these cells.

Finally in Chapter 5 we explored the role for *Mbd2* in non-haematopoietic cells, namely the colonic epithelium. Here we first developed a novel method for identifying and purifying these cells using flow cytometry. *Mbd2* deficient colonic epithelium demonstrated increased expression of activation markers MHC II and LY6A/E in the steady state and in DSS / *T. muris* mediated colonic inflammation. Indeed FACS purified colon epithelial cells from naive and DSS treated, *Mbd2*$^{-/-}$ and WT mice revealed conserved dysregulated gene expression independent of inflammation: Both naïve and inflamed *Mbd2* deficient epithelium displayed significantly increased expression of genes responsible for antigen processing/presentation (MHC I, MHC II, immunoproteasome) and decreased expression of genes involved in cell-cell adhesion (*Cldn1, Cldn4*). Lastly we investigated whether the observed differences in *Mbd2*$^{-/-}$ cell types conferred alterations in the makeup of the intestinal microflora. Interestingly independent of co-housing of *Mbd2*$^{-/-}$ and WT animals, *Mbd2* deficiency consistently predicted the microbial composition, with increased levels of Clostridales and decreased levels of *Parabacteroides* bacteria.

Collectively we have identified $CD11c^+$ cells, monocytes and colon epithelial cells as key cell types for *Mbd2* mediated changes in gene expression that affect mucosal immune responses. These data thus identify *Mbd2* gene targets within these cell types as exciting new areas for investigation and therapeutic modulation to limit damaging GI tract inflammation.

Lay Abstract

The gastrointestinal tract is comprised of specialised tissues that permit the absorption of nutrients whilst also providing an important barrier to infection. The gastrointestinal immune system must therefore provide an ability to survey the bowel contents for potential infection, but not respond inappropriately to the 'good bacteria' that live in our gut, with the resultant damage that may cause. Inappropriate immune responses are therefore at the heart of many common illnesses today, in particular the inflammatory bowel diseases. These diseases affect young people, are in part genetic, and commonly require medicines and surgery to control bowel inflammation which is part driven by an overactive immune response. The way we understand how genetic information is passed onto our children has changed in recent years. In particular, an additional layer of information that co-ordinates how our DNA is folded and interpreted and used by our cells, but that doesn't affect our DNA sequence is now appreciated. This layer of information is termed epigenetics and can passed down the generations. Because epigenetic information isn't as tightly regulated as our DNA code, it can be altered much more easily in response to changes in our environment, such as infection, ageing, smoking etc. MBD2 is a protein that can affect epigenetic changes to our DNA and has previously been shown to be important in how immune cells function. The purpose of this thesis was therefore to understand if MBD2 can alter the way our immune cells function in our bowel, in particular in response to inflammation.

We identified that without MBD2 the bowel was more susceptible to inflammation and that this was caused in part by altered immune cell function. In particular MBD2 was important in particular cell types called dendritic cells and macrophages that co-ordinate the detection and response to microorganisms. In an additional unexpected finding, we also observed that MBD2 acts in the epithelial lining of the bowel to prevent inappropriate surveillance of the 'good bacteria'. The combination of altered epithelial and immune cell function in the absence of MBD2 also resulted in an altered make-up of the 'good bacteria' that live in our bowel.

Overall epigenetic mediated changes to how our DNA is expressed by immune and epithelial cells not only alters their function, but may explain why some people develop immune conditions like inflammatory bowel disease and others do not. Understanding how our immune system uses epigenetics may therefore in the future offer a different approach to treatment of such conditions.

Chapter 1

General Introduction

1.1 Introduction

The human gastrointestinal (GI) tract comprises the oral cavity, oesophagus, stomach, small and large intestines (1). The small intestine is subdivided into the duodenum, jejenum and ileum and the large intestine into the caecum, colon, rectum and anus (1). Each of these discreet anatomical sub divisions also confers distinct morphological and functional traits to facilitate the main purpose of this organ system, namely the absorption of nutrients and expulsion of waste (1). The former is reliant on a large, $400m^2$ surface area of single cell thick epithelium formed of fingerlike villi projections that must not only permit the passage of vital nutrients, but also form a physical barrier to separate host from environment (1). A thin epithelial surface may facilitate the absorption of foodstuffs, but has the potential to compromise host defence. The human GI tract has therefore evolved a highly selectively permeable surface, with an abundant immune presence exemplified by the copious lymphoid tissue and immune cells it harbours (1). Indeed in addition to the diverse array of dietary antigens consumed each day, the GI tract is colonised by a dense population (10^{14}) of micro-organisms that numerically exceeds both the genetic material and cellularity of the host (2). Despite a robust epithelial barrier, luminal antigens are not entirely prevented from entering tissues. Intact food proteins can be detected in the blood and small numbers of GI tract dwelling micro-organisms can be found in the draining lymph nodes of healthy animals (3). An intimate relationship therefore exists between commensal organisms, the host immune system and selective barrier function.

1.2 The inflammatory bowel diseases

Inflammatory bowel disease (IBD), including ulcerative colitis (UC) and Crohn's disease (CD), are chronic inflammatory conditions of the gastrointestinal tract. They most frequently present in the 2^{nd} and 3^{rd} decades with rectal bleeding, abdominal pain or diarrhoea (4), (5). Anti-inflammatory and/or immunomodulator therapy, although effective, does not completely eliminate the substantial morbidity associated with these conditions, which have a major population health impact given their preponderance in young people. CD is characterised by transmural inflammation, affecting any part of the GI tract, with a prevalence of 144/100,000 population (6). The incidence is highest amongst young people in Scotland and continues to rise (1.9 per 10^5/year 1981-3, 2.9 per 10^5/year 1990-2) (7). UC is characterised by inflammation confined to the mucosa and may spread proximally from the rectum to encompass the entire colon. UC is similarly common with a reported UK incidence of between 6.5-15.1 per 10^5 / year and an age-sex adjusted point prevalence in Northern England of 243/100,000 population (6), (8).

Historical data have shown up to 75% of patients will undergo surgery at least once during their disease course, with resection not curative and further surgical intervention often required (9), (10). Despite increasing use of immunomodulatory treatments such as

thiopurines, methotrexate and monoclonal antibodies against TNF, 25% of newly diagnosed patients managed with conventional medical treatment will still require intestinal surgery within 5 years of diagnosis (11). Operative management remains effective for managing disease complications and improving quality of life, but does not eliminate the pathogenic process, so most patients develop recurrence of the disease (12),(13),(14).

1.3 The Gastrointestinal immune system

Healthy individuals possess an abundant and highly active GI tract immune system that is tightly regulated to prevent excessive immune responses to foods and commensal microbiota (15). The host response to infection by pathogens are known as immune responses. A specific response to a particular pathogen or its products is known as an adaptive immune response, as it represents an organisms adaption to its environment (16). In many organisms this results in lifelong protection against said pathogen, mediated by immunological memory (16). In contrast the innate immune response mobilises immediately to combat a wide range of pathogens but does not lead to long lasting immunity or a specific response to a particular pathogen (16). The defence systems of the innate immune response rely on a limited number of receptors that recognize micro-organisms. Pattern recognition receptors (PRRs) recognize simple molecules and regular patterns of molecular structure known as pathogen-associated molecular patterns (PAMPs) present on micro-organisms but not host cells (16). PRRs include toll-like receptors (TLRs) that recognize PAMPs characteristic of bacteria, fungi and viruses (16). Stimulation of TLRs results in the release of antimicrobial peptides (AMP), with this pathway being conserved in all animals and plants (16). Another important family of PRRs are nucleotide-binding oligomerisation domain (NOD) like receptors that are intracellular sensors for microbial products that activate nuclear factor kappa-B (NF-κB) in a similar manner to TLRs (16).

Cytokines are key effectors of the immune response. They are small proteins that are released from cells in response to an stimulus that can induce responses by binding to specific receptors on the cells that secrete them (autocrine), adjacent cells (paracrine) or distant cells (endocrine) (16). Among the first cytokines released in early immune response, is a group of chemoattractant cytokines termed chemokines. These small proteins induce chemotaxis in nearby cells, resulting in movement of cells towards the source of the chemokine (16).

The systemic and mucosal immune systems differ in an anatomical separation of the inductive and effector sites. Lymphoid aggregates, such as Peyer's patches (PP) in the small intestine, contain large numbers of T and B cells, which when activated migrate via the blood, back to the lamina propria (LP) and epithelium, a process mediated by their expression of α4β7 integrin and chemokine release by effector sites in the GI tract (17), (18).

The LP in addition contains large numbers of IgA-producing plasma cells, $CD4^+$ T cells, macrophages, dendritic cells (DCs), mast cells and eosinophils, with a significant leucocyte population, notably $CD8^+$ T cells expressing the γδ T cell receptor, residing within the epithelium (intra-epithelial lymphocytes (IEL)) (19),(20). We now consider these relative cell types and their contribution to mucosal immunity in health and disease.

1.3.1 Neutrophils

Polymorphonuclear leucocytes (PMN), also called neutrophils, are critical components of the innate immune response. They protect the host from microbial pathogens and from the damaging effects of injured cells. As such they possess an arsenal of antimicrobial functions including degranulation and phagocytosis that mitigate against invading pathogens by massive release of reactive oxygen species and other toxic molecules (21). As such neutrophil depletion exacerbates certain models of mucosal inflammation suggesting a beneficial role, perhaps by limiting translocation of bacteria and producing wound-healing mediators (22). However it is also clear that neutrophils can directly contribute to disease pathology whereby excessive recruitment, such as in IBD, and activation leads to release of toxic products, trans-epithelial migration and extensive mucosal injury (23). Neutrophils similarly have the ability to produce metalloproteases (MMP) that can cleave chemokine precursors augmenting their potency, and may acquire antigen presenting and T cell activation functions during colitis (24). Thus the regulatory or inflammatory phenotype of intestinal neutrophils is determined by a range of factors, including the type of stimulus, the production of chemoattractants and the interaction with other immune cells that modulate their function.

1.3.2 Eosinophils

Eosinophils develop from eosinophil progenitor cells that are derived from haematopoietic cells, express CD34 and interleukin (IL) 5Rα and undergo differentiation on exposure to IL-5, IL-3 and granulocyte-macrophage colony stimulating factor (GM-CSF). Eosinophils are able to detect pathogens and promote innate and adaptive immune responses via the expression of complement receptors (e.g. CD11b), Fc receptors (FcαR, FcγRII) and pattern recognition receptors (PRR) (25). Upon activation eosinopihls release a variety of mediators such as cytokines (IL-12, IFN-γ, IL-4 and TGF-β), chemokines and growth factors (26). Eosinophils in the GI tract are poorly described, traffic to non-oesophageal GI tract portions in an eotaxin-1 dependent manner and are distinct phenotypically and functionally from eosinophils in other tissues (27). Eosinophils are regulated by epithelial derived cytokines such as thymic stromal lymphopoietin (TSLP) and IL-33 that directly activate eosinophils and promote their recruitment by augmenting Th2 responses (28). An important role is suggested by their abundance and low turnover *in vivo* with activated eosinophils found in greater numbers in those with active IBD compared to quiescent IBD and healthy controls (29) (30). Eosinophils

are capable of presenting antigen to $CD4^+$ T cells and releasing secretory IgA (sIgA), suggesting a role in the initiation and polarisation of adaptive immune responses (31). Indeed, murine eosinophils are able to express major histocompatibility complex class II (MHC-II), and co-stimulatory molecules (CD40, CD80 and CD86) under certain conditions (32). In addition deficiency eotaxin-1 or eosinophils themselves protects against murine models of colitis, though not in all reports, with eotaxin-1 levels in the intestine or circulation correlating with disease severity in UC (33). Lastly, Griseri et al. have shown that eosinophils accumulate in an IL-23 driven model of colitis, with blockade of IL-5 or eosinophil depletion associated with ameliorated disease (34). They further show that GM-CSF is a potent activator of eosinophil function and that eosinophil peroxidase release promotes colitis, suggesting a direct tissue-toxic mechanism for eosinophils in this model of intestinal inflammation (34). Such is the interest in the pro-inflammatory potential of mucosal eosinophils that a phase II trial assessing the role of bertilimumab, an eotaxin-1 neutralising antibody is underway assessing eosinophil depletion in the treatment of acute UC (Clinical trials no. NCT01671956).

1.3.3 Monocytes

Monocytes are mononuclear phagocytes (MP) that originate from progenitors in the bone marrow and traffic via the bloodstream to peripheral tissues. Monocytes mediate antimicrobial defence, are implicated in inflammatory diseases such as atherosclerosis and inhibit tumour-specific immune-evading mechanisms. Monocytes are divided on the basis of chemokine receptor expression and the presence of specific surface molecules (35,36). Murine expression of LY6C and CD11b defines a monocyte subset with high levels of CC-chemokine receptor 2 (CCR2) and low levels of CX_3C-chemokine receptor 1 (CX_3CR1). These are termed inflammatory or $LY6C^{High}$ monocytes, account for 2-5% of circulating white blood cells in homeostatic conditions, and are rapidly recruited to sites of inflammation ((37)). A second subset of circulating monocytes in mice expresses high levels of CX_3CR1, low level LY6C and CCR2 and adheres to the luminal surface of endothelial cells in a process termed 'patrolling' (35,36). Human monocytes are divided into subsets on the basis of surface CD14 and CD16 expression (38). $CD14^+$ $CD16^-$ (classical) monocytes are the most numerous in human blood and, like murine $LY6C^{High}$ monocytes, express CCR2. $CD16^+$ monocytes may be further subdivided into $CD16^{++}$ $CD14^+$ (intermediate) and $CD16^+$ $CD14^{++}$ (non-classical) monocyte groups (39). $CD16^{++}$ $CD14^+$ monocytes are thought similar to murine $LY6C^{Low}$ monocytes given their similar role in *in vivo* patrolling (40). Therefore whilst monocytes in humans and mice are not identical, their differentiation and function in immune response appear to be similar (41).

It has recently been reported that blood monocytes are the precursors for intestinal macrophages (42,43). Indeed the murine colonic macrophage compartment is entirely

dependent on constant replenishment from LY6C^{High} monocytes, in contrast to embryonic precursors propagating tissue macrophages in other sites (42). In addition to their role in replenishing tissue macrophages in the steady state, monocytes are recruited to infected tissue sites to mediate direct antimicrobial activity. For example infection with the intracellular Gram-positive bacterium *Listeria monocytogenes* is exacerbated in mice with CCR2 deficiency, reducing the recruitment of tumour necrosis factor (TNF) and inducible nitric oxide synthase (iNOS) capable monocytes and their progeny (44,45). However it has also been suggested that monocytes may have a regulatory role in limiting commensal-mediated damage to the GI tract. Grainger et al. have eloquently shown that in response to commensals, inflammatory monocytes can directly inhibit neutrophil-mediated pathology in response to pathogen challenge by production of the lipoid mediator prostaglandin E_2 (PGE_2) (46).

Thus whilst monocytes maintain intestinal macrophages in the steady state via a low level constitutive presence, they accumulate in inflammation, expressing high levels of IL-1β, IL-6 and PRRs, facilitating a vigorous inflammatory immune response and in addition may also have a dual regulatory role on other local inflammatory cells (43,46,47).

1.3.4 Macrophages

Macrophages are one of the most abundant immune cells in the mammalian intestine and are the largest population of MPs in the body (48). As described above, adult mouse intestinal macrophages are exclusively derived from blood-borne inflammatory monocytes, and are long-lived, present to at least 8 weeks post monocyte-differentiation (43). Within the mononuclear phagocyte pool, murine macrophages are often distinguished from DCs by differential expression of surface markers such as F4/80, CD11b, CD18, CD64, CD68 and Fc receptors (49). In contrast identifying macrophages and their M1 and M2 subsets in humans has proved challenging (49). For example human macrophages do not express *Ym1* or *Retnla*, 2 of the most studied identifiers of alternatively activated macrophages in mice (49). Similarly neither ARG1 or iNOS are expressed by *in vitro* polarized macrophages stimulated with IL-4 or IFN-γ, perhaps suggesting that macrophage effector molecules will be diverse between species based upon the specific pathogen challenges that they face (49).

Macrophage density in the intestine is poorly understood, though thought to correlate to bacterial load, and is thus highest in the colon where commensal bacteria number in excess of 10^{12} organisms/ml (50). Intestinal macrophages have been shown to demonstrate a tolerogenic phenotype, poorly responsive to TLR stimuli, which underlies one of the principal mechanisms for host control against inappropriate reactions to commensal microflora (51). As such, unlike macrophages from other tissues, mucosal macrophages in the steady state secrete low levels of pro-inflammatory cytokines and chemokines such as IL-12, Il-23, TNF,

IL-1, IL-6 or CXCL10 in response to TLR ligands but secrete higher levels of the anti-inflammatory cytokine IL-10 (52), (53), (54), (55). However intestinal macrophages retain an avid phagocytic ability, able to uptake apoptotic cells via expression of CD36, and have potent anti-bacterial activity (56). Indeed in inflammatory conditions, macrophages are capable of upregulating the expression of TLRs, co-stimulatory molecules and pro-inflammatory receptors, resulting in the production of large quantities of TNF, IL-6, iNOS, IL-1 and MMPs (57), (50), (58). Thus macrophages are a fundamental component of innate responses in the healthy and inflamed GI tract, limiting inappropriate reaction to the resident commensal microflora, but capable of facilitating a robust response in disease states.

1.3.5 Dendritic cells

DCs are specialised antigen presenting cells (APCs) that orchestrate innate and adaptive immune responses. In the intestine, DCs are present in peyers patches (PP), isolated lymphoid follicles (ILF) and the LP, constitutively migrating in lymphatics to mesenteric lymph nodes (MLN) and presenting antigen to T lymphocytes - a process fundamental to the induction of oral tolerance (59),(3).

Murine intestinal DCs are characterised by high expression of CD11c and MHC-II and a lack of expression of CD64. The majority of intestinal $CD11c^{+}$ $MHC\text{-}II^{+}$ $CD64^{-}$ cells express the integrin-αE (CD103) whose ligand E-cadherin is expressed on the basolateral surface of epithelial cells (60). It is thought that rather than representing a distinct lineage of DCs in the intestine, CD103 is likely induced on DCs during their residence in the intestine (61).

Intestinal $CD103^{+}$ DCs can be divided into 2 distinct populations on the basis of CD11b expression that differ in transcriptional factor requirements and function (Diagram 1.1). $CD103^{+}$ $CD11b^{-}$ DCs are related to lymph node resident $CD8\alpha^{+}$ DCs and share with these cells expression of the chemokine receptor XCR1 (62), (63). In addition genetic deletion of the transcription factors Id2, Irf8 and Batf3 leads to selective loss of $CD11b^{-}$ $CD103^{+}$ cells (64). By contrast, $CD103^{+}$ $CD11b^{+}$ intestinal DCs appear similar to $CD11b^{+}$ lymph node resident DCs, sharing expression of signal regulatory protein-α (SIRPα) and DC inhibitory receptor 2 (DCIR2) and are dependent on different transcription factors in their development and maintenance, namely Irf4 and Notch2 (65), (66). Both $CD103^{+/-}$ $CD11b^{+}$ DCs have been shown to promote TGF-β T helper (Th) 1 and Th17 cell differentiation with $TLR5^{+}$ $CD11b^{+}$ DCs able to induce B Cell IgA class switching via production of a proliferation inducing ligand (APRIL) (65), (67).

There are also 2 distinct, less well-defined $CD103^{-}$ populations of DC that can similarly be described by expression of CD11b. $CD103^{-}$ $CD11b^{+}$ DCs do not express CD64 or XCR1, but are under control of the DC-specific transcription factor Zbtb46 (62), (63), (65), (68) (Diagram

1.1). Lastly a population of $CD103^-$ $CD11b^-$ DCs have been described, that like $CD103^-$ $CD11b^+$ DCs migrate to MLN in a CCR7 dependent manner, expand in response to Flt3 ligand, prime T cell responses and induce T cell CCR9 (69). In addition both $CD103^-$ $CD11b^{+/-}$ cells have recently been shown to express higher levels of IL-12 and IL-23 mRNA and induce higher IFN-γ and IL-17 production from proliferating T cells compared to $CD103^+$ LP DCs, even in the absence of TLR stimulation (65).

Regarding the ontogeny of intestinal DCs, adoptive transfer of DC progenitors into CD11c depleted mice demonstrated that pre-cDCs but not $LY6C^{High}$ monocytes were able to give rise to $CD103^+$ $CD11b^+$ and $CD103^+$ $CD11b^-$ DC in the intestinal mucosa, whereas macrophage and DC progenitor (MDP) were able to give rise to all DC and macrophage subsets (70), (71). Underlining the rapid advancement in our understanding of DC surface markers, this study was not able to address the ability of MDPs or pre-cDCs to produce $CD103^-$ DCs, as markers that would have distinguished them from macrophages (such as CD64) were not used (71). However other studies of $LY6C^{High}$ adoptive transfer have shown that they give rise exclusively to $F4/80^+$ $CD64^+$ cells suggesting $CD103^-$ DCs are not monocyte derived (72), (43). Lastly, it has been shown that removing the transcription factor Zbtb64 in Zbtb46-DTR mice decreases $CD103^+$ $CD11b^+$ DCs by 50%, in contrast to $CD103^+$ $CD11b^-$ DCs which were almost completely removed (73).

Many of the initial markers used to define DC subsets in mice and humans are not conserved, leading to difficulties in generalizing data between species. However a human intestinal $CD103^+$ DC population has been identified, and can be further subdivided into 2 subsets (65), (66). A $CD103^+$ $SIRP\alpha^-$ subset that display similarities to human CD8α-like cDCs, expressing CD141 and DNGR-1, that likely represent the human equivalent of murine $CD103^+$ $CD11b^-$ DCs and a larger population of $CD103^+$ $SIRP\alpha^+$ DCs that were $CD141^-$ and $DNGR\text{-}1^-$ that likely represent the murine equivalent of $CD103^+$ $CD11b^+$ DCs (74), (75), (76), (66). Lastly, a $CD103^-$ $CD64^-$ $SIRP\alpha^+$ DC population has been identified that likely represent the human counterpart of $CD103^-$ $CD11b^+$ DC (66), (62), (63).

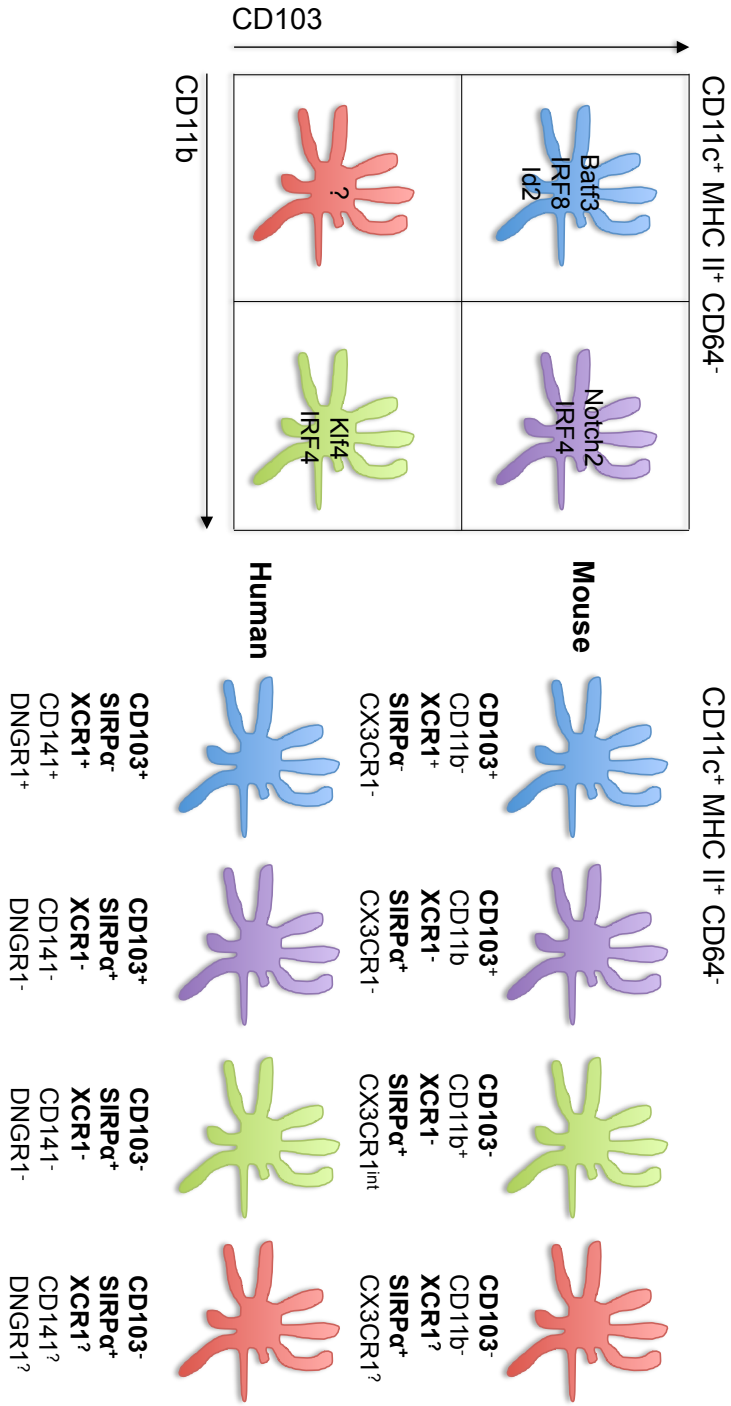

Diagram 1.1 DC subsets in the mouse and human intestinal lamina propria (adapted from Bekiaris et al. 2014)

1.3.6 T cells

The intestinal mucosa contains a large number of T cells localised within gut-associated lymphoid tissue (GALT) including PPs and ILFs, and throughout the LP and intestinal epithelium (19). Colon LP T cells express the surface markers TCRαβ and are then subdivided into 4 populations based on the expression of CD8αβ, CD8αα or CD4 ($CD8\alpha\beta^+$, $CD8\alpha\beta^+$ $CD8\alpha\alpha^+$, $CD4^+$ and $CD4^+CD8\alpha\alpha^+$). LP T cells display a previously activated or memory phenotype, entering the mucosa after priming in secondary lymphoid organs, drive excessive inflammation and cytotoxicity in response to microbiota derived antigens and may exacerbate IBD in humans (19). Intra epithelial lymphocytes (IELs) are more heterogeneous, their composition dependent on their anatomical location in the GI tract and are dominated by T lymphocytes (there are estimated to be more T cells in the intestinal epithelium than the spleen) (77), (78). Colon IELs contain the same LP T cell populations mentioned above, but in addition contain $CD4^-$ $CD8^-$ and $CD8\alpha\alpha^+$ populations that express either TCRαβ or TCRγδ ((79). IELs display both protective and inflammatory qualities dependent on the stimuli they receive and their local environment. They can condition and repair the epithelial barrier and control epithelial cell growth and turnover by secreting TGFβ1/3, keratinocyte growth factor (KGF) and junctional adhesion-like (JAM) molecule which directly interacts with the epithelium to promote restoration of barrier integrity (80), (81), (82). In contrast they can also secrete TNF and IFNγ, are found in increased numbers in patients with active IBD and coeliac disease and may promote immunopathology in mouse models of intestinal inflammation (77).

T cells can be further subdivided based upon their effector subtypes (Th1, Th2, Th17, and regulatory T cells). Th1 cells are induced by IL-12 and characteristically secrete copious amounts of IFNγ, TNF and IL-12 controlled by the master transcription factor TBET. Th2 cells by contrast secrete IL-4, IL-5 and IL-13 controlled by the master transcription factor GATA3 (83). Th17 cells are a further subset of T cells induced by IL-6 and TGFβ, secreting large amounts of IL-17A, IL-17F, IL-21 and IL-22 and controlled by the master transcription factor RORγt (84), (85), (86).

Regulatory T cells (Tregs)

Tregs characterised by the expression of CD4, CD25 and FoxP3, are defined as T cells with an ability to supress naïve T cell proliferation *in vitro* and *in vivo* (87). Mice that are depleted of Tregs spontaneously develop multiorgan autoimmunity including gastrointestinal inflammation (88). Indeed a genetic defect in *FOXP3* results in immune polyendocrinopathy enteropathy X-linked (IPEX) characterised by a lack of Tregs, producing a severe pan-enteric inflammatory enteropathy that resembles CD (89). Tregs perform a vital role in tolerance supressing abnormal immune responses to commensal micro-organisms and

dietary antigen by the expression of anti-inflammatory cytokines IL-10 and TGF-β that prevent aberrant activation and effector function of other immune cells (90).

1.3.7 Innate lymphoid cells

ILCs are an emerging and diverse group of immune cells and derive from an ID2 expressing progenitor and are defined by 3 main features: They are of lymphoid morphology, are negative for other cell-lineage markers (CD3, B220, LY6G/C, CD11c, Ter119) and lastly then lack RAG-dependent antigen receptors (91). ILCs can further be sub categorized into groups: Group 1 ILCs are T-box expressed in T-cells (TBET) dependent and are comprised of ILC1 and NK cells. Group 2 ILCs are GATA-binding protein 3 (GATA3) and retinoic acid receptor ROR dependent and are comprised of ILC2 and lastly group 3 ILCs that are RORγt dependent and are comprised of ILC3s and lymphoid tissue-inducer (LTi) cells (92). ILCs tend to mirror the cytokine profile of T-helper cells and thus are thought to be the innate counterparts of T-helper lymphocytes. Group 1 ILCs produce Th1 associated cytokines, in particular IFNγ. Group2 ILCs produce Th2 cytokines, in particular IL-5 and IL-13 (93), (94). Group 3 ILCs are defined by their ability to secrete Th17 cytokines such as IL-17 and IL-22 (95). Recent data has implicated Group3 ILCs in the development of IBD. Group 3 ILCs have been shown to be able to induce colitis in a *Helicobacter hepaticus* infection characterised by IL-17A and IFNγ production in *Rag*$^{-/-}$ mice (96). Subsequent data suggest that Group 3 ILCs can induce colitis in an IL-23R, IL-22 dependent mechanism, that *Rorγt*$^{-/-}$ mice do not develop CD40L induced colitis and lastly human ILC's were found at increased levels in the LP in an IL-23 dependent manner (97), (96), (98), (99).

1.3.8 Intestinal epithelial cells

The intestinal epithelium is the largest mucosal surface in the human body (1). This surface is a single cell thick to permit efficient ion and nutrient absorption and yet must shield the host from a diverse and sustained antigenic load (100). At its most basic intestinal epithelial cells (IECs) regulate GI tract immunity by forming a physical barrier by separating luminal contents from the underlying LP. However IECs also display innate immune function through the production of anti-microbial products, including defensins, cathelicidins and calprotectin (101). Indeed IECs are able to process and present antigen via MHC II, express PRRs including TLRs, and secrete a number of immunoregulatory mediators such as IL-10, TGF-β and IL-12p70 (102). The epithelium covering ILFs contains a specialised sub division of epithelial cells termed M cells with the ability to directly uptake luminal antigen by endocytosis, presenting antigen unmodified to T cells given the lack of M cell lysosomes (103). IECs are therefore equipped with the necessary machinery to detect, process and respond to microbial signals in the intestinal lumen to facilitate local mucosal responses (Diagram 1.2).

1.4 IBD is characterised by a dysregulated immune response

IBD is thought to be the result of a dysregulated immune system in genetically susceptible individuals. Genome wide association studies (GWAS) comparing patients with IBD to healthy controls have identified >100 polymorphic loci, including many genes involved in innate and adaptive immune response (104), (105). Susceptibility variants have been reported in genes associated with autophagy, (*ATG16L1*), the IL-23/Th17 pathway (*IL-12B*), TGFβ signaling (*SMAD3*) and T cell activation (*TAGAP*) (106), (104). *NOD2* was the first CD susceptibility gene discovered and has the largest genetic effect on disease susceptibility to date (107), (108). A recent meta-analysis of over 2,500 patients with *NOD2* mutations revealed the presence of any *NOD2* mutation increased risk for surgery by 58% and complicated disease by 48% compared to IBD patients without *NOD2* mutation (109).

How these genes confer an increased risk of developing IBD is not clear, and is an area of research interest. Autophagy refers to the cellular process of 'self-eating', a process by which lysosomal degradation to intracellular organelles, unfolded proteins of extracellular material maintains cellular homeostasis under conditions of stress, such as infection or mitochondrial damage (110). Transgenic mice generated to express a hypomorphic isoform of the ATG16L1 protein display Paneth cell abnormalities similar to those found in ileal resections of CD patients, and are more susceptible to experimental colitis (111). Similarly DCs have been shown to require intact NOD2 and ATG16L1 pathways to permit effective autophagy processes, consistent with the hypothesis that the detection and isolation of intracellular pathogens are intimately linked (112).

Infiltrating monocytes have been identified at increased levels in the intestinal mucosa of IBD patients (43). $CD14^{High}$ cells display increased production of TNF, IL-1β, IL-6 and respiratory burst activity and recruit other immune cells, such as eosinophils via release of eotaxin-1 (113). It is hypothesised that monocytes are therefore key effector cells in mediating ongoing mucosal inflammation. LP $CD14^{High}$ monocytes are derived from blood precursors, demonstrated using radio-labelled transfer of blood monocytes, and are recruited perhaps in response to increased circulating levels of chemokines such as CCL2 and CCL4 (47).

Macrophage and DC subtypes form a central part of the functional mucosal barrier of the GI tract, however the exact definition of these cells using surface markers remains controversial. One such marker is CX_3CR1, which appears to be highly expressed on macrophages but not cDCs (114), (52). CX_3CR1^+ LP macrophages are located in close proximity to the epithelium and are able to extend processes to sample luminal antigen (103). However it has also been shown that $CD103^+$ CX_3CR1^- DC also present antigen via intestinal goblet cells, thus uptake of luminal antigen may not be confined to a particular MP cell subset (115). Genetic deletion of CX_3CR1 results in decreased LP macrophage

numbers, increased bacterial translocation of commensal bacteria and increased susceptibility to experimental colitis that can be rescued by administration of CX_3CR1 sufficient macrophages or blockade of IL-17A (103), (116).

Recent studies in man have also identified intestinal monocytes and monocyte-derived macrophages as critical perpetrators in driving inflammation in IBD (113), (117), (72). The human gastrointestinal mucosa represents the largest reservoir of macrophages in the body and, as in mice, resting human GI tract macrophages are relatively inert (118), (119). Human intestinal macrophages express CD68, CD33 and low levels of CD14, CX_3CR1, CD11c and CD163 (113), (42). However under inflammatory conditions a discreet $CD14^{High}$ monocyte population accumulates which, like the analogous $LY6C^+$ $MHC\text{-}II^-$ monocyte population seen in mice, is also present at reduced numbers in the steady state (113), (120). These $CD14^{High}$ cells seem to be derived from circulating classical blood monocytes, express higher levels of CD11c, CD64, CD163 and are heterogeneous in expression of HLA-DR and CD209 (120), (121). In addition $CD14^{High}$ cells can produce large amounts of inflammatory cytokines such as IL-6, IL-23 and TNF (113), (57).

The evidence for the role of DCs in IBD pathogenesis is currently limited to observational studies in man, and transgenic studies in mice. DCs accumulate in the mucosa of IBD patients and experimental models of and interference with T cell-DC interactions via CD40/CD40L blockade can prevent T cell mediated colitis (122), (123), (124).

GWAS have identified several IBD risk susceptibility loci involving Th17 cells and their differentiation including *IL-23R, IL12B, JAK2, STAT3, CCR6* and *TNFSF15* (105), (125). Indeed IBD patients have greater *IL17A* expression in the GI tract, and display greater numbers of Th17 cells (126), (127), (128). However animal models suggest conflicting roles for the IL-17 axis in conferring susceptibility to colitis. IL-17A deficient mice, or those treated with IL-17A neutralising antibodies are more resistant to the development of experimental colitis using trinitrobenzene sulfonic acid (TNBS) (129). IL-17A has also been shown to directly inhibit Th1 cells and suppress the development of inflammation; experimental autoimmune encephalomyelitis is suppressed in $Il17^{-/-}$ mice and bone erosion is reduced in rats treated with IL-17 receptor IgG1 Fc fusion protein (130), (131). However using a model of chemical colitis, mucosal inflammation was ameliorated by IL-17F deficiency (132), (133).

In summary the patchy transmural inflammation of CD is associated with activation of Th1 and Th17 cells in response to the production of IL-12, IL-18, IL-23 and TGFβ by APCs. In turn activated Th1 and Th17 cells increase section of pro-inflammatory mediators such as IL-2, IL-17, IFNγ and TNF. This reinforces APC, macrophage and endothelial release of TNF, IL-1, IL-6, IL-8, IL-12 and IL-18. In contrast the mucosal inflammation in UC may be

associated with a Th2 immune response mediated by IL-4, IL-5 and IL-13 (134). However other reports have shown increased IFNγ and reduced IL-13 from intestinal biopsies of UC versus CD patients so distinguishing between IBD subtypes based on T cell cytokine profile alone may not be robust (126). In both CD and UC, T cells respond to presented antigen and can be regulated by anti-inflammatory mediators such as IL-10 in a similar manner. Therefore the bulk of current and emerging IBD treatments have focused on the reducing the action of pro-inflammatory cytokines, increasing anti-inflammatory cytokines, blocking T cell co-stimulation or inducing T cell apoptosis.

Tregs have a marked anti-inflammatory capability in animal models of colitis, and are found in reduced numbers in the blood of active IBD patients (135), (136), (137). However Tregs are paradoxically found in increased levels in the LP of patient with active IBD, and demonstrate equivalence in suppressing effector T cells compared to healthy patients *ex vivo*, suggesting normal function (138), (139). This may be explained by the observation that T cells that experience TCR activation in the presence of TGF-β turn on FoxP3 expression (induced Tregs) (140). Whether iTregs maintain the same anti-inflammatory functions as constitutive Foxp3 expressing T cells (natural Tregs) is debated (141).

Therefore decreased anti-inflammatory mechanisms may be equally important targets for therapeutic intervention as enhanced effector mechanisms. Lastly it has been noted that a large proportion of mucosal Tregs from IBD patients are able to produce IL-17, promoting further inflammation and neutrophil recruitment. Thus by sharing characteristics of potentially pathogenic T cells, copious Tregs in IBD may paradoxically promote rather than suppress intestinal inflammation (142), (143).

Taken together there is a strong genetic association with immunological gene polymorphisms and the likelihood of developing IBD. However our understanding of the role of the innate immune system in IBD pathogenesis is poor, with conflicting evidence for pro and anti-inflammatory effects of the adaptive immune response.

1.5 The Microbiome

The human body harbours trillions of microbes located at host-environmental interfaces such as skin, gut, genital and respiratory surfaces (2). The genetic load of our microbial co-habitants constitutes the microbiome, and outweighs the genetic contribution of the host by 10 fold (2). The last decade has permitted identification of the microbial community via sequencing and high throughput technologies and analysis of their function. Numerous studies have now profiled the healthy human microbiome, with over 90% of all phylotypes belonging to 2 divisions; *Bacteroidetes* and *Firmicutes* (144). In addition whole-genome shotgun sequencing of faecal samples from a European adult cohort revealed 98% of genes

were bacterial, with the rest constituting yeasts, viruses, archaea and protozoa (145). Indeed commensal fungi interact with the innate immune receptor DECTIN-1 and its gene *Clec7a* in mice. *Clec7a*$^{-/-}$ mice are more susceptible to DSS colitis mediated by altered responses to commensal fungi, with *CLEC7A* polymorphisms in man predisposing to a severe form of UC (146). Thus it is likely the identification of non-bacterial facets of the microbiome will become increasingly recognised and analysed over the following decade as sequencing methodologies continue to advance.

It has subsequently become apparent that our microbiota have evolved with us and are critical for normal development and homeostasis. The intestinal microflora interacts with the adjacent mucosal environment directly, affecting intestinal permeability and local immune responses, but also indirectly via microbial metabolites such as in the production of short chain fatty acids (SCFA) that mediate host responses including Treg induction (147), (148). The microbiota is a dynamic entity, its composition changing in response to age, sex, geography, diet and medication (149). Alteration in the dynamics of this balance may result in a dysbiosis, which is associated with the susceptibility to an array of GI tract and non-GI tract diseases, such as IBD, coeliac disease, obesity, multiple sclerosis, malignancy and liver disease (150).

Evidence supporting the role of luminal antigens in exacerbating IBD comes from treatments that modify the faecal stream. Notably diversion of faeces from active inflammation induces remission and mucosal healing and infusion of faeces re-activates the disease (151). In addition specific taxonomic shifts have been reported in IBD. *Enterobacteriaceae* are increased in relative abundance in both patients with IBD and animal models of intestinal inflammation (152). Adherent invasive *E. coli* (AIEC) strains in particular have been isolated from ileal CD biopsies and are enriched in patients with UC (153). This may simply represent an increased preference of these organisms to survive in an inflammatory environment, with administration of anti-inflammatory treatments, such as mesalazine, reducing their frequency (154), (155). In contrast some bacteria have known protective effects on host immunity. *Bacteroiodes* and *Clostridium* species for example have been shown to induce the expansion of Tregs, thereby reducing intestinal inflammation, with other organisms shown to attenuate inflammation by regulating NF-κB activation (156). Similarly the *Bifidobacterium, Lactobacillus* and *Faecalibacterium* genera may protect the host from inflammation by down-regulating inflammatory cytokines or augmenting IL-10 production (157,158). *F. prausnitzii* has received much attention in recent years, underrepresented in IBD patients, with lower levels of mucosa associated *F. prausnitzii* correlating with higher risk of recurrent CD after surgery (158), (159). Conversely, recovery of *F. prausnitzii* after relapse is associated with clinical remission in UC (160). In addition to the immunomodulatory effects noted above, the *Faecalibacterium* genus is also responsible for the fermentation of dietary fibre to produce

SCFAs, which are the primary energy source for colon IECs (161). Indeed IECs express a range of PRRs to sense the presence of the microflora (162). TLRs and NLRs are the best documented and play a key role in the induction of innate effectors and inflammation (162). PRR signaling in IECs therefore serves to maintain the barrier functions of the epithelium, including the production of sIgA, and setting a tolerogenic phenotype of the mucosa to inhibit overreaction to the innocuous luminal dietary and microbial antigens (163).

Host-microbial interactions are therefore pivotal in protection from pathogenic bacterial invasion. This consists of a first line defence comprised of facets of the innate immune system described above, namely mucins, the epithelium and immune cells such as DCs, monocytes and macrophages. Mice that lack an adaptive immune system, such as *Rag*$^{-/-}$ and severe combined immunodeficient (SCID) mice do not develop spontaneous colitis, though this can be potently induced by chemical (DSS), immunological (anti-CD40) and infectious (*Helicobacter hepaticus*) challenge (164), (165,166). This would suggest that the innate immune system is sufficient for IBD development. Taken together the intestinal microbial community performs a range of useful functions for the host including digesting substrate inaccessible to host enzymes (163). In addition the microbiota shape host immune responses and vice versa, with dysbiosis strongly associated with disease states (163). GI tract microflora therefore represent an attractive, potentially modifiable, candidate to account for the environmental contribution to IBD.

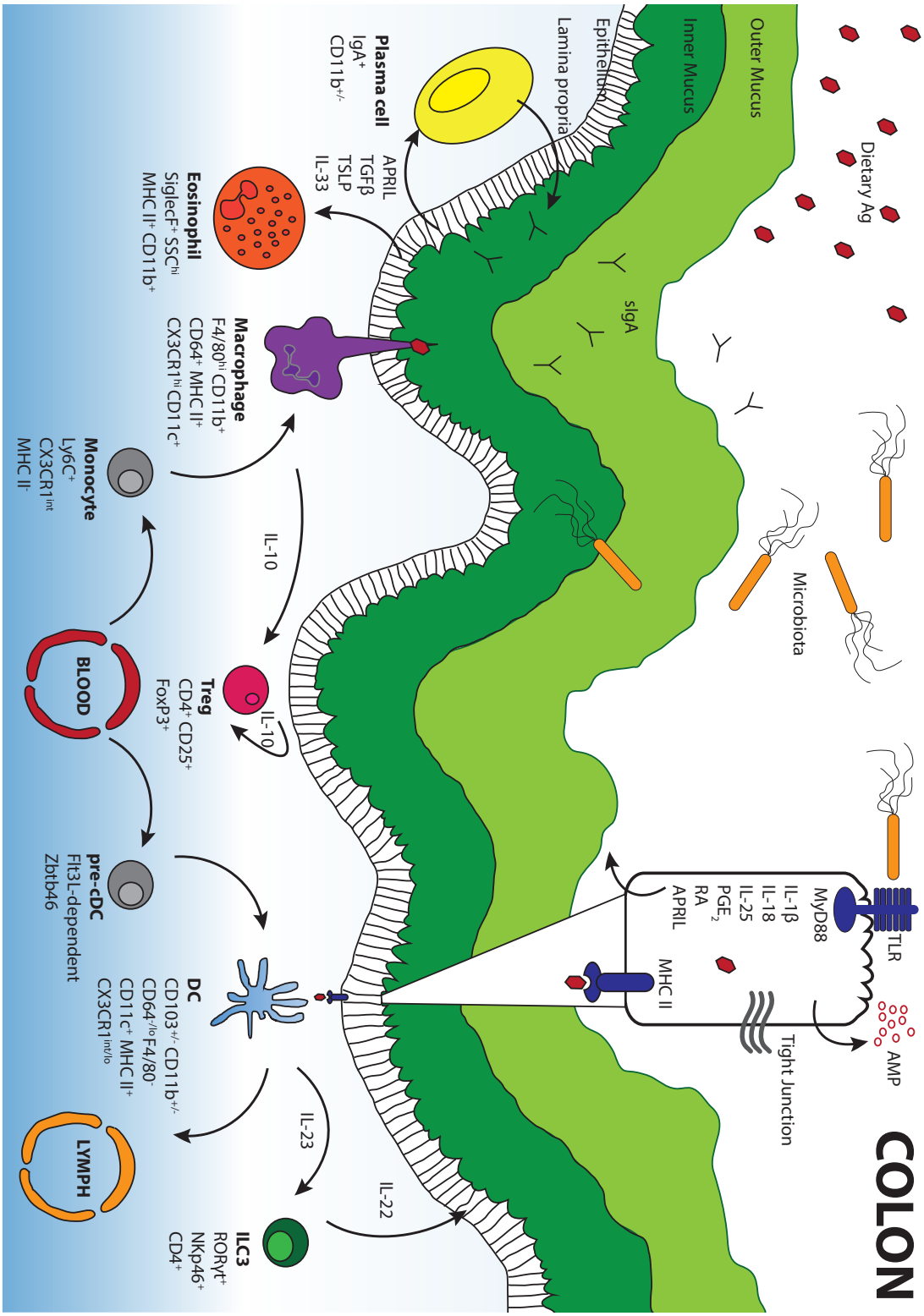

Diagram 1.2 Interaction between colon LP immune cells and the epithelium

1.6 Animal models of IBD

Much of the recent progress in understanding mucosal immunity has been achieved by the study of experimental animal models of intestinal inflammation. However no one model yet replicates all the complex facets of human IBD, nor replaces the value of studies using human material. Indeed the clinical manifestation and disease course of IBD is extremely heterogeneous; an observation reflected in the increasing transgenic mouse strains all displaying IBD-like intestinal changes (167). However animal models provide an opportunity to explore mechanisms of host response to GI tract inflammation that are not yet possible using human tissues. Animal models of intestinal inflammation can be broadly subdivided into infection, chemical induction, immune cell transfer or gene targeting (168).

A compromised epithelial barrier may be a key component in the pathogenesis of IBD by permitting increased translocation of luminal antigen and micro-organism into the mucosa, resulting in a florid inflammatory response (169). A seminal paper by Hermiston et al. demonstrated that decreased intestinal epithelial cell-cell adhesion mediated by replacing E-cadherin with a N-cadherin transgene resulted in LP inflammation but only at areas of defective epithelium, suggesting micro-organism entry can induce an inflammatory response (170). Indeed asymptomatic IBD patients display increased intestinal permeability prior to clinical relapse with variants in epithelial organic cation transporters (*OCTN*) 1 and *OCTN2* risk susceptibility loci for IBD (171).

1.6.1 DSS colitis

DSS is a sulphated polysaccharide of highly variable molecular weight ranging from 5kDa to 1400kDa. Administration of 40kDa DSS to mice in drinking water can readily traverse the mucosal membrane, found in LP macrophages and MLN within 24hrs, resulting in distal colitis, rectal bleeding, diarrhoea and weight loss (164), (166). Molecular weight of DSS, manufacturer, mouse sex or strain, and intestinal microflora, but not volume of DSS ingested, have all been shown to affect the disease severity (167). It is believed that DSS is directly toxic to IECs, thereby affecting the integrity of the mucosal barrier. As T and B cell deficient, SCID or *Rag1*$^{-/-}$ mice also develop a severe colitis to DSS, the adaptive immune system is not thought to play a dominant role in the acute phase of this model (166). Therefore the acute DSS model is a useful tool for investigating the role of the innate immune system in intestinal inflammation. Typical histological changes of acute DSS colitis include mucin depletion, epithelial degeneration and eventually epithelial necrosis (167). This is accompanied by the infiltration of the LP and submucosa by neutrophils, resulting in cryptitis and crypt abscesses. Cycles of continuous DSS treatment (7 days) interspersed with normal drinking water (14 days) results in a chronic colitis which, if combined with the carcinogen azoxymethane results in inflammation-associated colorectal cancer (CAC) (172).

1.6.2 TNBS/Oxazolone colitis

Intra-rectal administration of the haptenating agents TNBS or oxazolone renders autologous colonic or microbial proteins immunogenic to the host immune system (173), (174). This results in severe diarrhoea, weight loss and colonic thickening (175).

Intra-rectal TNBS to SJL/L or C57BL/10 mice results in transmural colonic inflammation, driven by Th1 mediated responses and characterised by the accumulation of $CD4^+$ T cells, neutrophils and macrophages in the LP (175). Given the dependence of chronic TNBS colitis on $CD4^+$ T cells, this model has proved an important vehicle for investigating T-helper mucosal responses. TNBS colitis is associated with elevated IFNγ levels, with anti-IL-12p40 treatments able to prevent its production and abrogate nascent and established disease (175), an observation that led to the development of humanised anti-IL12p40 antibody treatment for CD. However a Cochrane review of anti-IL12p40 efficacy assessed 4 randomised trials of 955 patients and revealed only a very modest treatment benefit of inducing clinical response (176). TNBS has also contributed to our knowledge of oral tolerance, with mice fed TNBS-haptenised colonic proteins less susceptible to TNBS colitis due to TGFβ producing Tregs, a process dependent on IL-10 (177), (178). TNBS colitis susceptibility varies widely among mouse strains. BALB/c mice for example develop Th2 mediated colonic hypertrophy, accentuated in the absence of IFNγ, with a Th2 component also observed in C57BL/6 mice deficient in IL-12 and IFNγ (179), (180). BALB/c mice are therefore used for modeling chronic TNBS-colitis induced fibrosis, given elevated IL-13 drives TGFβ mediated fibrosis involving early growth response protein-1 (EGR-1), IGF-1 and myofibroblast production of collagen (181). Thus TNBS has proved a useful model for investigating Th1 and Th2 immune responses as well as the factors guiding the initiation and resolution of fibrosis in the GI tract.

Oxazolone (4-ethoxymethylene-2-phenyl-2-oxazolin-5-one) is also an intra-rectally administered haptenating agent, which like TNBS elicits colonic inflammation (182). However in contrast to the transmural inflammation observed in TNBS colitis, single dose administration of oxazolone produces acute superficial inflammation more akin to the UC pathology seen in man (183), (184). Cellular and cytokine responses in oxazolone colitis also differ compared in TNBS. Data suggest that the host response to oxazolone is controlled by IL-13 production from LP $CD4^+$ natural killer (NK) T cells, as IL-13 blockade and NKT deficient mice do not develop colitis (183). The IL-13 response in oxazolone colitis is poorly defined, but may be a result of IL-33 and IL-25 release from damaged epithelial cells (185). UC-like oxazolone colitis is characterised by increased IL-9 and IL-13 production and an LP infiltrate containing IL-13 producing NKT cells (186), (187). Thus the importance

and value of oxazolone colitis lies in its resemblance to human UC not only in respect to morphology, but in addition to immunopathogenesis.

1.6.3 Adoptive transfer of CD45RB^{High+} T cells

The balance of regulatory and effector T cells in the development of intestinal inflammation was first highlighted in the transfer of distinct T cell populations into immunodeficient mice (188). The transfer of naïve $CD4^{+}CD45RB^{High}$ T cells from donor mice into immunodeficient SCID or *Rag1*$^{-/-}$ mice results in a wasting disease characterised by chronic colonic inflammation developing over 5-10 weeks (189), (188). Conversely the transfer of $CD4^{+}CD4RB^{Low}$ cells does not produce colonic inflammation, owing to the presence of $CD4^{+}CD25^{+}Foxp3^{+}$ Tregs that antagonise effector T cell function in the gut by the production of IL-10, TGFβ and IL-35 (188,189), (190), (191). Indeed Tregs deficient in the IL-10 receptor fail to protect mice from this model of colitis, and lose the ability to express FoxP3 suggesting IL-10 signaling is required for the maintenance of their function (88). In addition TGFβ deficient Tregs, or the administration of anti-TGFβ antibodies, are unable to protect recipient mice from colitis (192). Indeed if naïve T cells are rendered incapable of responding to TGFβ by overexpression of a negative TGFβ receptor, Treg TGFβ production is unable to suppress colitis (193). Despite these insights into Treg and Teffector roles, the mechanism and source of inflammatory stimuli in this transfer model of colitis have been difficult to ascribe. Early studies suggested the model to rely on Th1 mediated responses, due to the presence of IFNγ and TNF producing LP T cells and the observation that transferred T cells lacking T-bet, the master transcription factor for Th1 responses, fail to induce colitis (189), (194). Subsequent studies support a role for T cell differentiation into IL-17 producing Th17 cells under the influence of IL-23 in this transfer model, whereby transferred T cells lacking the IL-23 receptor or the Th17 master regulator RORγt and *Rag1*$^{-/-}$ recipient mice deficient in IL-23p19 do not develop colitis (195), (196). These mutually exclusive hypotheses have been combined with the observation that Th17 responses are plastic, able also to give rise to IFNγ producing Th1 cells (196), (197). Taken together, current data suggest that colitis induced by the adoptive transfer of T cells produces a Th1 IFNγ producing population that originates indirectly from a Th17 differentiation pathway dependent on IL-23, rather than exclusively from a Th1, IL-12 dependent mechanism. In addition, it underlines the importance of balance in mucosal homeostasis: balance between pro-inflammatory effector cell function and anti-inflammatory regulatory function, a balance that may be tipped by quantitative or qualitative defects in these cells in IBD. It also highlights that, as in other models of experimental colitis, bacterial antigens play a crucial role in mediating pathology, as mice treated with antibiotics or bred germ-free develop significantly ameliorated bowel inflammation.

1.6.4 *Il10*$^{-/-}$ transgenic mice

IL-10 is a well-known suppressor of multiple facets of the immune system (198). Several studies have suggested that IL-10 inhibits IL-12 and TNF production, T cell proliferation and promotes the formation of antigen-specific Tregs (199). Mice with specific deletion of IL-10 develop spontaneous colitis in specific pathogen free (SPF), but not germ free, conditions (198) suggesting an important role for the microbiota in generating IL-10 dependent immune responses. Indeed *IL10* polymorphisms are risk susceptibility loci for IBD, with a familial form of paediatric onset CD identified that is due to mutations in the IL-10 receptor, which was rescued by bone marrow transplantation (200). Intestinal inflammation in IL-10 deficient mice is characterised by a Th1 T cell LP infiltrate that is reduced by the administration of anti-IL-12p40 or anti-IFNγ (201). In addition IL-10 specific deletion in T cells or Tregs also results in spontaneous colitis, suggesting that T cell sources of IL-10 are necessary to maintain mucosal homeostasis (202), (203). Similarly IL-10R deficient macrophages or systemic anti-IL-10R antibody treatment, rendering the host unable to respond to IL-10, leads to a pro-inflammatory phenotype and spontaneous colitis (204), (205). Finally, macrophages extracted from patients with CD as a result of a loss of function mutations in the IL-10R display impaired differentiation and function (206). Taken together this model of intestinal inflammation has identified LP naïve T cells, Tregs and macrophages as important sources and response elements to the IL-10 axis that are required to prevent damaging spontaneous enterocolitis (206).

1.6.5 Other transgenic models

There are numerous other transgenic animals which display altered susceptibility to intestinal inflammation and therefore have provided vital inflammation for our understanding of mucosal homeostasis. These include mice deficient in TBET and RAG2 proteins (TRUC mice), which develop spontaneous inflammation and a colitogenic microflora, that can transmit colitis to WT mice when co-housed (such as *Proteus mirabilis* and *Helicobacter typhlonius*) (207). Mice deficient in Mucin 2 (MUC2), a large gel-forming protein secreted by the intestinal epithelium, also develop spontaneous colitis as a result of increased barrier function, resulting in increased susceptibility to DSS and colorectal cancer models, characterised by the infiltrate of TNF and IL-1β producing lymphocytes (208), (209). Intestinal epithelial specific deletion of IKK-γ (also known as NEMO) disrupts NF-κB signaling, leading to a heightened sensitivity to TNF, epithelial apoptosis and translocation of bacteria, and increased susceptibility to the nematode parasite *Trichuris muris,* highlighting a role for pro-inflammatory cytokines such as TNF in barrier protection and defence as well as disruption (210). SAMP1/YitFc (SAMP) mice represents an excellent model system to understand the disease mechanisms of CD as it one of the only animal models that produce severe inflammation in the terminal ileum, the commonest location for CD in man (211). SAMP mice were discovered by in-breeding a colony of AKR/J mice, selecting for

accelerated senescence, noticing an autoimmune phenotype (212). Genome wide scanning of cohorts of SAMP mice with ileal inflammation versus healthy controls identified 4 areas of chromosomal loci that were strongly linked to the presence of inflammatory change, including allelic differences in IL-18, PPARγ and IL-10 receptor genes (212). Therefore these mice are do not require genetic, chemical or immunological manipulation to produce intestinal symptoms.

1.6.6 *Trichuris muris*

Gastrointestinal infection with the parasite *Trichuris muris*, a mouse model of the human *T. trichiura* infection, is a much-studied model of colonic inflammation (213). Ingested infective eggs accumulate in the caecum, hatching within 2 hours, adhering and anchoring to the caecal epithelium, maturing from larval to adult life stages over the ensuing 32 days which, in the absence of appropriate immunity and expulsion, results in chronic local tissue destruction and inflammation (214). Successful resolution of infection requires a polarised Th2 immune response, with susceptibility conferred by a Th1, IFN-γ dominated response (215). The load of infected eggs delivered to the host is also critical in determining polarisation of the host immune response and thus susceptibility to chronic infection: Low dose (20 eggs) results in a Th1 polarised immune response, and therefore chronic inflammation, in immunocompetent animals. However, high dose (200eggs) results in an IL-4, IL-13 polarised Th2 response (216), (217). Supporting the role of parasite-host evolution, wild mice are thought to accumulate worms through repeated low-level infections of 5-15 eggs, with heavy infections confined to only a few individuals (218). Therefore *T. muris* infection load in nature favours parasite persistence and chronic infection by negating an expulsive Th2 response from the host. Thus the therapeutic use of helminths has been attempted in IBD to antagonise damaging host Th1 responses. Utilising the ability of helminths to modulate a Th2 host response and thus evade expulsion was hypothesised to explain the lack of IBD in less developed areas where parasites are endemic (219). However results have been conflicting with no consistent treatment benefit shown, which may be secondary to differences in methodology, dose, species and IBD phenotype (220), (219).

Clearance of *T. muris* infection requires an intact adaptive immune system. Current data support the requirement for $CD4^+$ but not $CD8^+$ or NK T cells for an effective host response, with conflicting evidence for DCs or B cells, with eosinophils and basophils in addition showing redundant functions (221), (222), (223), (224), (225). Epithelial barrier function is also key to successful parasite clearance, with susceptible mice displaying reduced mucin production, epithelial cell turnover and muscle contractility (226), (227).

1.6.7 Citrobacter rodentium

C. rodentium is a murine mucosal pathogen that induces a self-limiting colitis or death depending on strain susceptibility (228), (229). It shares several pathogenic mechanisms with enteropathogenic *Escherichia coli* (EPEC) and enterohaemorrhagic *E. coli* (EHEC), two clinically important human GI pathogens, such as the formation of attaching and effacing (A/E) lesions, characterised by the intimate attachment of bacteria to the intestinal epithelium (228), (229). *C. rodentium* is transmitted via the faecal-oral route, with most infection studies favouring delivery by oral gavage with laboratory culture bacteria (230). After colonic colonisation, adherent bacteria undergo a virulence switch that facilitates further colonisation, with the infection clearing in less susceptible strains, mediated by epithelial shedding of colonised cells into the intestinal lumen (231). Myeloid differentiation primary response protein 99 (MYD88) is a key adaptor protein in innate immune signaling downstream of TLR and IL1R families, and plays a key role in response to *C. rodentium* infection by recruiting neutrophils, macrophages and DCs to the LP, expression of iNOS and triggering the proliferation of epithelial cells (232), (233). As such TLR2 deficient mice develop severe colonic pathology, weight loss and mortality (232).

C. rodentium has also yielded insight into the role of inflammasomes in mucosal homeostasis. Inflammaosomes are scaffolds in the cytoplasm of immune cells that are responsible for the maturation of caspases and IL-1 family cytokines (234). Caspase-1 and NLRP3 mediated responses are crucial for resistance to *C. rodentium*, with caspase-1 and NLRP3 deficient mice displaying increased bacterial loads, severe immunopathology and rapid weight loss (235). *C. rodentium* triggers a florid Th17 cell response that exceeds the Th1 cell response, that is caused by epithelial cell apoptosis, as blocking apoptosis impairs Th17 responses in the LP (236). Similarly blockade of IL-17A and IL-17F results in increased mucosal inflammation, bacterial load and systemic translocation of bacteria (237). In addition to IL-17, ILC3s and other Th17 cells are important sources of IL-22, which is essential for *C. rodentium* protection (238). IL-22 is part of the IL-10 superfamily and triggers protection to *C. rodentium* by inducing the production of RegIII AMPs and promoting epithelial barrier integrity (238).

Lastly, recent investigations have suggest that transfer of the microbiota from mice resistant to *C. rodentium* to mice that are susceptible, renders protection to infection to recipient mice, with neutralisation of IL-22 removing this protective effect (239), (240). Resistance to infection is associated with increased Bacteriotedes and reduced Firmicutes at phylum level, although segmented filamentous bacteria (SFB) that promote IL-17 protective mucosal responses, are equivalent (239), (240). Taken together *C. rodentium* elicits a co-ordinated immune response dependent on Th17 and innate cell responses also underlining the importance of the host microbiota in conferring susceptibility to enteric pathogens.

1.7 Epigenetics

Epigenetics is one of the most rapidly expanding fields of biology that, like the microbiome, demonstrates an ability to interact with genetic and environmental factors. Waddington defined the term “epigenetics” as “the causal interactions between genes and their products, which bring the phenotype into being” (241). Subsequently, this term has been used to describe the molecular mechanisms that reinterpret the genetic code into a multitude of phenotypic outcomes. This has led to the modern definition of epigenetics as the heritable marking of DNA that leads to the alteration of gene expression independent of genetic information carried in the primary DNA sequence (242).

Epigenetic modifications of DNA permit an ability to influence phenotype in a heritable fashion, retained after cell division and directly or indirectly affecting the transcription of the genetic code. DNA methylation, histone posttranslational modifications and nucleosome positioning are the best described epigenetic processes, but more recently have expanded to include microRNAs (miRNAs), chromatin remodeling complexes and polycomb group proteins (243), (244). Through changes in gene transcription, DNA-protein interactions, protein translation, and gene silencing epigenetic processes determine key developmental processes including growth, differentiation, genomic imprinting and immunity (245), (246).

Epigenetic marks that are incorrectly established may confer human disease. Monozygotic twins who contain the same DNA sequence may have differing susceptibilities to autoimmune and malignant pathologies due to discordant DNA and histone modification profiles (247), (248). Whilst the relative plasticity of epigenetic marks is advantageous in adding an additional layer of cellular genetic control, it also renders them susceptible to environmental perturbations such as diet, nutrition, stress, chemical and pharmaceutical agents (249). Thus epigenetic processes may be mediators of gene-environment interactions and so may contribute to the penetrance of polygenic, environmentally influenced disorders such as IBD (250). It is now appreciated from studies in animals that environmental insult may induce specific phenotypes mediated by epigenetic processes and that are heritable (251), (252).

1.7.1 DNA methylation

DNA methylation occurs by the addition of a methyl group to the 5’ carbon of the cytosine residue of cytosine-guanine (CpG) dinucleotides. Methylation occurs at approx. 70% of CpG dinucleotides with marked region specific variation (253). Non-methylated CpG dinucleotides are often, but not exclusively clustered together at gene promoter sites and are referred to as CpG islands (253). Highly methylated areas of the mammalian genome are less transcriptionally active leading to gene silencing, a principle that is exploited by neoplastic

processes by aberrant de novo methylation of tumour suppressor genes, abrogating their function in favour of tumour development (254). DNA methylation is therefore strongly correlated with gene silencing and is widely believed to participate directly in transcriptional repression (255). Methyl-CpG-binding proteins (MBDs) serve as essential contributors for DNA demethylation independent of cell division and have potential roles in transcript splicing and chromatin compaction (256). MBDs and histone deacetylase (HDAC) recruitment may therefore represent mediators of transcriptional control through induction of heterochromatin (255). This is a developing area, and thus conflicting hypotheses exist regarding the causal nature of DNA methylation in mediating transcriptional repression (257), (258). Whether DNA methylation is a cause or consequence of repression therefore remains to be fully elucidated. DNA methyltransferases are a key family of enzymes responsible for the remethylation of hemi-methylated CpGs during cell division (DNMT1) (259). Indeed they also undertake de novo methylation in early development (DNMT3a/b), thereby conserving DNA methylation patterns, the importance of which is underlined by the embryonic lethality of DNMT1, DNMAT3a and DNMT3b deficiency (260), (261). Taken together genome methylation requires coordinated expression and function of DNMTs and MBDs to permit appropriate gene expression in normal growth and development. It is therefore perhaps unsurprising that altered DNA methylation and DNMT expression/regulation were amongst the first epigenetic changes reported in IBD and in CAC (262), (263), (264).

1.7.2 Histone modification

Eukaryotic DNA is tightly folded around specialised proteins termed histones (H) to from chromatin (265). The histone octamer forms the structural basis for which the fundamental unit of chromatin, nucleosomes, may form around (265). The nucleosome is a repeating subunit of 146base pairs of chromatin in a double helix around a core of H2A, H2B, H3 and H4 histone proteins (265). Current evidence suggest that each histone subtype maybe altered by numerous post-translational modifications including acetylation, methylation, ubiquitination, phosphorylation, sumoylation, citrullination, ADP ribosylation and proline isomerization, of which acetylation and methylation are the most widely described (266). These modifications determine the accessibility of DNA to transcriptional, replicative, recombination, condensation and mRNA splicing machinery (265). As a result, post-translational modification of histones confer a diverse range of heritable transcriptional promotion or repressive abilities. For example, trimethylation of lysine residues on H3 proteins can be associated with both open (H3K4, H3K36 and H3K79) and closed (H3K9 and H3K27) regions of chromatin (267). In contrast highly acetylated regions are generally associated with euchromatin and leads to active transcription by increasing chromatin accessibility (267). This has led to hypothesis of a ‘histone code’ whereby the overall pattern, rather than individual histone marks, of post-translational histone modification fine-tunes higher order chromatin structural organisation, expression and repression (266). Enzymes

that catalyse the addition or removal of acetyl or methyl groups to HDACs; histone acetyltransferases (HATs) and histone methyltransferases (HMTs) therefore represent important mechanisms for mediating epigenetic patterns for inheritance (268). The mechanism(s) by which histone acetylation or methylation affects transcription is poorly understood. This may be the result of acetyl neutralisation of lysine positivity, destabilising negatively charged DNA promoting dissociation from histone to an 'open' position (268).

1.7.3 Nucleosome remodeling

Whilst the structure of individual nucleosomes is highly regulated and ordered, the overall structure of nucleosomes along DNA is highly variable (269). The precise positioning of nucleosomes can therefore be regulated by transcription factors and other accessory proteins and results in functional changes in gene expression (269). Nucleosomes can therefore represent a physical barrier to gene transcription, impeding the progression of RNA polymerases, demonstrated by the eviction of nucleosomes from transcriptionally active start sites (270). Nucleosome positioning may therefore impede or facilitate gene expression and is controlled by chromatin remodeling complexes, large multi protein scaffolds that alter the composition or organisation of nucleosome core proteins. There are currently 5 recognised families of chromatin remodeling complexes, SWI/SNF, ISWI, NuRD, INO80 and SWR1 (271). Some associated family members, including the MBDs, facilitate the eviction or lateral sliding of nucleosomes and therefore gene activation. MBDs may also possess HDAC and/or methyl-CpG binding properties and thus promoting gene repression (272), (273).

1.7.4 Methyl-CpG-binding proteins

DNA methylation constitutes the addition of a methyl group to the cytosine of a CpG dinucleotide and is correlated to transcriptional repression ((274)). Approximately 70% of CpG dinucleotides in the mammalian genome are methylated (275) excluding areas of high CpG density termed 'CpG islands' that are usually unmethylated (276), but acquire methylation during differentiation (277) or be aberrantly methylated in cancer. It has been suggested that mechanisms for transcriptional repression mediated by CpG methylation involves MBDs binding to methylated cytosine and recruitment of a co-repressor complex (278). MBDs may be divided into the methyl-CpG-binding domain proteins (MBDs), Kaiso and SRA domain proteins (Table 1.1) (279). The MBD group includes MeCP2, MBD1, MBD2 and MBD4 that have methyl-CpG binding domains, and MBD3, MBD5 and MBD6 that do not bind methylated DNA (280). Using tagged MBD proteins it has recently been shown that MBD1, MBD2, MBD4 and MeCP2 binding to chromatin increases linearly with methylation density, with binding not appearing to plateau with increased local density of methylated cytosines (280). Indeed in the absence of genome methylation, MBD binding is substantially reduced (280). The same authors find a strong negative correlation with MBD binding and

promotor activity and enhancer accessibility supporting a role for MBD proteins in DNA-methlyation mediated genome regulation (280).

MBD2 is capable of recruiting a large 2MDa nucleosome-remodelling (NuRD) complex (281). This complex contains a chromatin remodelling protein (Mi-2), HDACs 1 and 2, and has been shown to establish transcriptional repression in vertebrates, invertebrates and fungi (281). MBD2 is thought to recruit the NuRD complex to methylated sites within the genome to effect chromatin remodelling, histone deacetylation and methylation (281). Given promoter methylation is a hallmark of cancer it was initially suggested that MBD2 may regulate genes critical during carcinogenesis, however more recent studies suggest that MBD2 may also regulate the activity of target genes (282). It was also initially thought from *in vitro* data that MBD2 selectively binds methylated DNA, recent data *in* vivo using genome wide mapping in mouse embryonic stem cells suggests that whilst binding largely occurs at highly methylated CpG regions, a subset of binding sites occurred at active unmethylated promoters (283), (280). Thus in one study 80% of MBD2 binding sites had DNA methylation levels between 80-100% with preferential binding to promoter and exon regions rather than introns or intergenic regions (279). The binding of MBD2 to non-methylated chromatin required protein interactions with the NuRD complex was demonstrated by engineering an MBD2 protein that lacked an MBD and assessing genome wide associations (280): Non-methylated binding sites were also DNAse I hypersensitive, low in CpG density but enriched for H3K4me1 and H3K27ac, thus showing the hallmarks of active regulatory regions (280). In contrast to methylation-dependent binding, methylation independent binding was largely cell type specific, as most binding was seen to occur at tissue-specific regulatory regions (280).

Thus based on their ability to bind methylated DNA, MBDs are prime candidates for interpreting the DNA methylome and may also be a role for binding non-methylated chromatin in a tissue specific manner. MBDs therefore represent attractive targets for investigating epigenetic regulation of chromatin expression.

Protein	Interaction partner	Effects	Loss of function phenotype in mice
MECP2	Sin3A, HDACs	Transcriptional repression	Neural, Rett-syndrome like, imparied microglial cell phagocytosis
	c-ski, N-CoR	Transcriptional repression	
	HMGB1	Unknown	
	Sin3B, HDAC2	Transcriptional repression	
	Dnmt1	Targeting of maintenance DNAmethylation	
	H3K9 methyltransferase	Transcriptional repression	
	CoREST complex	Repression of neural genes	
	Brm	Transcriptional repression	
	YB-1	Alternative splicing	
	ATRX	Epigenetic regulation required for neural development	
	HP1	Transcriptional repression	
	CREB1	Transcriptional activation	
MBD1	MPG	DNA repair	Minor neural defects, increased genomic instability
	Suv39h1-HP1	Transcriptional repression	
	MCAF1, MCAF2, SETDB1, CAF1, p150	Transcriptional repression, inheritance of epigenetic states	
	PML-RARα,HDAC3	PML-RARα mediated silencing	
MBD2	Mi02, MTA1-3, P66α/β, HDAC1/2, RbAp46/48, DOC-1. PRMT5, MEP50 (NuRD complex)	Transcriptional repression	Mild maternal phenotype, abnormal T-cell differentiation, reduced tumourigenesis, impaired DC mediated Th2 responses
	Sin3A	Transcriptional repression	
	Tax	Transcriptional activation	
	TACC3, HATs, pCAF	Transcriptional activation	
	GNCF	Oct-4 silencing	
	Dnmt1	Targeting of maintenance DNAmethylation	
	RFP	Enhancement of transcriptional repression	
MBD3	Mi02, MTA1-3, P66α/β, HDAC1/2, RbAp46/48, DOC-1 (NuRD complex)	Transcriptional repression	failure in differentation of pluripotent cells, embryonically lethal
	Dnmt1	Targeting of maintenance DNAmethylation	
	CDK2AP1, GNCF	Oct-4 silencing	
MBD4	Sin3A, HDAC1	Transcriptional repression	No apparent phenotype
	FADD	Genome surveillance/apoptosis	
	MLH1	DNA repair	
	RFP	Enhancement of transcriptional repression	
Kaiso	Tcf3	Supression of Wnt signalling	No apparent phenotype
	p120	Wnt signalling	
	N-CoR	Transcriptional repression	

Table 1.1 MBD functions (adapted from Bogdanovic et al. 2009)

1.7.5 Epigenetics in innate and adaptive immunity

Emerging evidence supports a role for epigenetic mechanisms in affecting the innate and adaptive immune response (284). Indeed the inflammatory process itself may confer epigenetic reprogramming to drive or abate aberrant responses (242). Studies of epigenetic marks in tissue macrophages are currently predominantly limited to profiling of histone acetylation and methylation, but suggest combinations of active and repressive histone marks regulate the expression of key cytokines required for appropriate M1 'classical' or M2 'alternatively activated' polarisation (285). Defined combinations of active and repressive histone marks regulate the chromatin states of inflammatory cytokines, permitting a rapid, polarised immune response into classically activated M1 and alternatively activated M2 macrophages (286). Epigenetic mechanisms might therefore explain the gene-specific signatures of tolerant GI tract macrophages.

Likewise epigenetic processes can affect monocyte programming and response to bacterial pathogens. For example H3K4 tri methylation of *NOD2* by mycobacterial components enhances innate immune responses (287). In addition bacillus Calmette-Guérin (BCG) vaccination induces methylation of cytokine promoters in human monocytes that can be reversed with methyltransferase inhibitors, suggesting plasticity of epigenetic programming (287). Thus epigenetic reprogramming may hold preventative and therapeutic roles in modulating aberrant immune response in autoimmunity and pathological inflammatory states (288).

In addition, the chemotactic ability of monocyte derived DCs and macrophages can be modulated by nucleosome remodeling. The lipid-modulating agent simvastatin, which is widely used for its cholesterol synthesis blocking properties, also has immunomodulatory function (289). Simvastatin can induce closed heterochromatin at the chemokine ligand 2 (*CCL2*) locus, accompanied by increased histone repressive marks (H3K27 and H3K9) and decreased active marks (H3ac and H3K4me3) at the *CCL2* promoter resulting in decreased gene expression in monocyte derived cells (289).

Genome-wide DNA methylation mapping of DC maturation revealed significant loss of DNA methylation across regions of binding sites for transcription factors affiliated with DC lineage fate and response to immune stimuli (290). Chronic repression of *Il12* in DCs from mice recovering from severe sepsis correlates to promoter enrichment of histone marks H3K4me3 and H3K27me2 (290). Similarly regulation of H3K9me2/3 marks by DC specific histone methyltransferases or demethylases are required for DC development and differentiation (291). Lastly, neutrophils as noted above are key cells in pathogen clearance with potent antimicrobial activity, but their migration can be paradoxically impaired in severe sepsis and

is associated with reduction in H3ac marks at the *CXCR2* promoter that mediates neutrophil migration to inflamed areas (292).

The strongest evidence for epigenetic control of immune cell development comes from $CD4^+$ T cell fate. $CD4^+$ Th1, Th2, Th17 and Treg cells display a variety of distinguishing epigenetic motifs including different profiles of DNA methylation, repressive histone marks, RNA interference, with MBDs associated with active, inactive and silenced loci in Th cell types (293), (294). The combination of these epigenetic processes ensure that lineage specific cytokines e.g. IFNγ for Th1 and IL-4 for Th2 are expressed by the appropriate cell types (293), (294), (295). Th1 cells for example demonstrate a demethylated *Ifng* promoter and repressive histone modifications at the *Il4* locus, with the reverse in Th2 cells (296). Similarly active histone modifications (H3Kac and H3K4me3) were associated with *Il17a* and *Il17f* promoters in Th17 cells with DNA methylation at the *Il17a* promoter preventing STAT3-*Il17a* promoter binding, inhibiting the regulatory effect of STAT3 on Th17 differentiation (293), (297). In addition Tregs, which constitutively express FoxP3 to maintain their immunosupressive qualities, display histone modification in a FoxP3 dependent manner of a variety of genes (298), (299). Genes activated by FoxP3 show enrichment of active marks, H3K4me3, H3K9/14ac and H4K16ac and genes repressed by FoxP3 show enrichment of the repressive mark H3K27me3 (299), (298).

Taken together, epigenetic regulation of cytokines and transcription factors within cells of the adaptive and innate immune systems can control their development, differentiation and function. This interaction between the genome and epigenome will likely have important implications for understanding the pathophysiology of heritable, immune mediated diseases such as IBD, the ultimate test of which will be the design of cell specific therapeutic epigenomic interventions to promote a favourable immunological phenotype.

1.7.6 Epigenetics and the microbiome

Recent data now suggest that intestinal bacteria can regulate epithelial cell immune responses through epigenetic mechanisms (300). Butyrate is a bacterial metabolite formed by the fermentation of dietary fibre, and is a powerful inhibitor of HDAC activity (301). Butyrate-dependent HDAC inhibition increases the expression of NOD2 and intestinal alkaline phosphatase (iALP), responsible for the metabolism of LPS, by increasing histone acetylation at these loci (301). Similarly the probiotic bacteria *Bifidobacterium breve* and *Lactobacillus rhamnosus* may confer anti-inflammatory effects by modulating host production of IL-23 and IL-17 by inhibiting histone acetylation and enhancing DNA methylation (302). The microbiota may also exert anti-inflammatory responses by direct interaction with the intestinal epithelium. TLR4, which detects the presence of LPS from Gram-negative bacteria, is suppressed by epigenetic mechanisms in IECs, presumably to prevent overactive host

response to commensals (303). In addition *Tlr4* methylation levels are directly linked to the presence of bacteria, with levels significantly lower in germ free mice, suggesting that intestinal symbiosis is promoted by bacterial-led host epigenetic modifications (304). NKT cells are recruited to the intestinal LP during inflammation under the action of the chemokine CXCL16 released from intestinal epithelial cells (184). Germ free mice display hypermethylation of the *Cxcl16* locus that normalises on the colonization of infant, but not adult murine GI tract, with commensals with corresponding reduction in *Cxcl16* expression and NKT recruitment (184). In keeping with age-related effects of the microbiome on the host epigenome, infant but not adult mice were more susceptible to DSS colitis after the administration of maternal, pre-natal methyl-donor diet that confers change in mucosal DNA methylation (184,304). These data support the intriguing assertion that dietary pre-natal modification of offspring epigenome confers long lasting reprogramming of the mucosal immune system.

These emerging studies have highlighted an important area of microbial-host crosstalk, namely that the microbiota and their products can directly influence mucosal epigenetic marks, mediating changes in expression of immune related genes and pathways. Likewise changes in host gene expression can alter the composition and function of the luminal environment, underlining the intimate inter-relationship therein.

1.7.7 Epigenetics and the "missing heritability" of IBD

To date, relatively little is understood of the role of epigenetics in IBD. Data addressing the role of epigenetic processes in IBD are thus limited to DNA methylation analyses of intestinal biopsies or peripheral blood (262), (305), (263) (264). Comparison of affected IBD patients versus healthy controls revealed several pathways previously associated with IBD, namely differentially methylated IL-23/Th17, IL-12/Th1 and host response to bacteria loci. In corroboration of GWAS loci with epigenome-wide methylation loci reveal conserved genes including *TNF, NOD2, IL19, IL27* and *CARD9*. miRNA and histone modifications on epigenetic processes and IBD susceptibility are currently poorly described and remain a research focus ((263), (125)).

MHC-II gene control represents a complex model of how immune regulatory genes are regulated by epigenetic control: The MHC is exposed to numerous modifications such as histone acetylation and deacetylation, histone methylation, and DNA methylation (306). The class II transactivator (CIITA) in particular is considered as the main factor responsible for MHC-II gene expression, and a target for epigenetic processes (307). Indeed CIITA recruits histone-modifying enzymes and ATPase–remodeling complexes to MHC-II promoters, and is itself regulated by a complex combination of DNA methylation and histone modifications (307).

The advent of GWAS has identified numerous variants conferring risk for complex disease, the primary purpose of gene discovery being to ultimately further our understanding of disease biology (105)), (308), (104). However, the possibility of using an individual's genotype to quantify risk prediction in a clinical setting based on statistical modeling (e.g. the cumulative number of risk variants) is an exciting prospect. There are >100 susceptibility loci for IBD to date with considerable overlap between CD & UC, with an area under the curve of 0.71 for CD prediction compared to 0.56 for family history alone (309). However despite successes in identifying novel areas of IBD pathogenesis such as autophagy and ER stress using these methods, <30% of the heritability of IBD is explained using the aforementioned susceptibility loci (104). The reasons for this are complex, and include an overestimation of monozygotic disease concordance, underestimation of loci effects due to multiple allelic variants (most notable the NOD2 risk variant after deep re-sequencing increased its disease heritability from 0.8-5% after the identification of 3 novel causative variants), stringent statistical genome wide statistical cut-offs, gene-gene and gene-protein interactions (105), (310), (311). Intriguingly somatic alterations associated with methylation, acetylation or remodeling changes may alter gene expression, function and therefore disease susceptibility (250). It is indeed plausible that these somatic alterations may occur separately from germline variations in response to environmental stimuli such as cigarette smoking and diet, therefore altering gene expression in the absence of inherited variants.

Taken together it has been suggested that the establishment of stable patterns of gene expression is a prerequisite of normal differentiation and is accomplished in part by a layer of lineage specific epigenetic information incorporated onto the genome. This information is plastic, changing with time and exposure to the environment, and has been shown particularly vulnerable at specific stages of human development. Intriguingly, long-term changes in gene expression patterns could therefore represent an attractive molecular hypothesis for early life experiences affecting adult phenotype. Understanding the role of DNA transcription and translation in the context of epigenomics may therefore have important and thus far poorly understood effects on human physiology, particularly in physiological and pathological immune responses.

1.8 Thesis Aims

The GI tract immune system is complex and its research rapidly evolving thanks to an ever-expanding understanding of cells within it. Indeed the GI tract immune system is not homogenous, and varies throughout its length to likely accommodate and react to the changing microbial and luminal composition therein. Importantly epigenetic processes are increasingly believed to be involved in controlling immune response at mucosal surfaces.

The main aims of this thesis are therefore:

1. Establish protocols that permit the simultaneous identification of multiple colonic LP immune populations by flow cytometry in mice and humans.
2. Establish the role of the methyl-CpG-binding protein, MBD2, in the steady state colon LP using *Mbd2* deficient mice.
3. Establish the GI tract expression of *MBD2* in healthy and IBD patients
4. Establish the role of *Mbd2* in chemical (DSS) and infectious (*T. muris*) models of colonic inflammation
5. Identify the colon cell types and genes dysregulated in the absence of *Mbd2* using targeted cell depletion and gene expression analyses
6. Establish if *Mbd2* deficient cells in the GI tract alter the steady state intestinal microbiota.

Existing data suggest that alterations in chromatin are central to the reprogramming of normal gene expression that occurs in disease states. Defining the complex and diverse epigenetic profiles that underpin phenotypic plasticity will be a crucial starting point in understanding the mechanisms of chromatin dysregulation that leads to disease. We hope to understand if methyl-CpG-binding proteins such as MBD2 can explain altered immune responses in innate cells that confer altered responses to GI tract inflammation. Despite vast investment in advancing our understanding of the genetic contribution to common heritable disease states, we can only explain a fraction of this heritability with conventional approaches. Thus investigating heritable, epigenetic changes in gene expression that are inherently more amenable to environmental manipulation than our DNA code, may provide novel insight to a poorly understood mechanism of disease predisposition. This work will therefore aim to identify the cellular and gene targets of *Mbd2* mediated changes to immune homeostasis that may provide exciting and novel approaches to therapeutic modulation of pathological inflammatory responses.

Chapter 2

Materials and Methods

2.1 Mice

All mice were maintained under SPF conditions in the School of Biological Sciences, University of Edinburgh or the Faculty of Life Sciences at the University of Manchester. Mice were used between 8-24 weeks of age on a C57BL/6 background unless specified otherwise. Table 2.1 details the mouse strains used in experiments. All procedures were carries out under license with UK Home Office Animals (Scientific Procedures) Act 1986.

2.2 Isolation of Mesenteric Lymph node cells

To obtain leucocytes from MLN, an established laboratory protocol, published by the MacDonald laboratory was used (312). Whole MLN were removed and placed in ice cold HBSS 2% FCS before mechanical disruption through a 70µm filter to liberate a single cell suspension.

2.3 Isolation of Colon LP cells

To obtain leucocytes from the colon LP, a laboratory protocol was adapted from the Mowatt Lab, University of Glasgow. The large intestines of mice were excised and soaked in ice cold PBS. Removing excess fat and faeces was an important step in improving cell yield and viability, and was performed before the intestines were opened longitudinally washed in Hank's balanced salt solution (HBSS; Gibco) 2% foetal calf serum (FCS) and cut into 0.5cm sections. The tissue was then shaken vigorously in 10ml HBSS 2% FCS and the supernatant discarded. Tissue was then incubated in 10ml of calcium and magnesium free (CMF) HBSS containing 2mM EDTA at 37^{o}C in a shaking incubator at 180rpm for 15mins to remove mucus. The supernatant was discarded, tissue washed in a further 20ml of CMF before a second incubation in CMF HBSS/2mM EDTA for 25mins to ensure removal of mucus layer and begin disruption of epithelial tight junctions. Tissue was once again washed with pre-warmed CMF HBSS before digestion in complete RPMI (RPMI 1640. 2mM L-glutamine, 100µg/ml penicillin, 100µg/ml streptomycin and 10% FCS) containing 0.5U/ml Liberase TM (Roche) and 0.1mg/ml Type IV DNAse from bovine pancreas (SimgaAldrich) for 45mins in a shaking incubator at 180rpm, 37^{O}C. Enzyme digestion of the tissue is essential to disrupt the tissue and isolation single cell suspensions. To aid successful digestion of tissue, tissue was shaken vigorously every 5-10mins until complete digestion of tissue was achieved. The resulting suspension was passed through a 40µm cell strained (BD Falcon) and then washed in complete RMPI to remove residual enzymes. Cells were pelleted for 5mins 500G at 4^{O}C before re-suspension in 1ml of complete RPMI for cell counting. Cells were kept on ice until use.

2.4 Isolation of colon epithelial cells

Optimisation of colon epithelial cell isolation is described in detail in Chapter 5.2

2.5 Processing of whole blood

Blood was isolated by cardiac puncture and combined with 200µl of 2mM EDTA 3% FCS to prevent coagulation. Serum was aspirated after pelleting of whole blood at 500G, $4^{O}C$ for 5mins before re-suspension of haematocrit in 5ml of red cell lysis buffer (SigmaAldrich) for 7mins to lyse red blood cells. Cells were then washed twice in PBS and kept on ice before use.

2.6 Histology

1cm sections of distal colon were taken for histological analysis in selected experiments. Sections were taken from the most distal 1cm to the rectum for consistency. Samples were placed directly into 10% neutral buffered formalin for 24 hours before being transferred into 20% ethanol. Samples were processed by the Queen's Medical Research Institute Shared University Research Facilities at the University of Edinburgh, for sectioning and haematoxylin and eosin staining. This allowed the identification of nuclei, cytoplasm and collagen to permit assessment of inflammation by light microscopy.

2.7 Flow Cytometry and Antibodies

2.7.1 Surface Staining

1-3x10^{6} cells were washed in PBS and stained with LIVE/DEAD Blue (Invitrogen) at a 1:2000 dilution in 10ul PBS, for 10mins at room temperature (RT) to remove any background staining artefact generated by apoptotic cells. Surface markers as described in Table 2.2 and FcR block (αCD16/CD32, 2.4G2, produced in-house) were then added to cells in 50µl of PBS 1% FCS (FACS buffer), for 20mins at $4^{O}C$ to identify different cell populations. Antibody dilutions for staining were derived by titrating a range of antibody concentrations in pilot experiments for optimum compensation parameters. Cells were then fixed in 1% paraformaldehyde (PFA) for 10mins at RT to prevent dissociation of antibody from target molecules. Marker expression was measured on BD Fortessa or LSRII (both BD Biosciences) flow cytometers and data analysed using FlowJo software (Tree Star). Flow cytometer photomultiplier tube (PMT) voltages were applies to ensure the best compensation whilst aligning with the latest cytometer setup and tracking (CS&T) settings.

2.7.2 Intracellular staining

For detection of intracellular proteins, 2x10^{6} cells were plated in a 96-well round bottom plate (Costar) and cultured with 1µl/ml GolgiStop (BD) alone, in combination with 0.5µg/ml PMA (SigmaAldrich) and 1µg/ml ionomycin (SigmaAldrich), or with the following TLR ligands: LPS 1µg/ml, Pam3Cys 1µg/ml, CpG 50mmol or Poly I:C 1µg/ml. Cells were cultured for 3hours at $37^{O}C$ with 5% CO_{2}.

Cells were then stained with LIVE/DEAD, surface markers and fixed with PFA as described above. Cells were washed three times in FACS buffer and fixed or 20mins at $4^{O}C$ in Cytofix/Cytoperm (BD Biosciences). Following this, cells were permeabilised to allow intracellular antibody staining by being washed three times in Perm/Wash (BD Biosciences) and stained with antibodies in 50µl of Perm/Wash at the concentrations described in Table 2.2 for 60mins at $4^{O}C$. FoxP3 staining was performed using the eBioscience Foxp3 staining kit, as per the manufacturers instructions. Marker expression was measured on BD Fortessa or LSRII (both BD Biosciences) flow cytometers and data analysed using FlowJo software (Tree Star). Flow cytometer photomultiplier tube (PMT) voltages were applies to ensure the best compensation whilst aligning with the latest cytometer setup and tracking (CS&T) settings.

2.7.3 Flow cytometry assisted cell sorting (FACS)

For FACS and purification of target populations, cells were isolated and stained in the same manner as detailed above and acquired using a BD influx cell sorter (BD Biosciences). To establish optimum antibody concentrations for cell sorting, antibody concentrations were titrated across a range of dilutions over several pilot experiments to derive optimal conditions for cell yield and purity.

2.8 Induction of DSS colitis

To induce acute colitis, a well established protocol was used (Chapter 1.6), whereby mice received 2% dextran sodium sulphate (DSS) salt (reagent grade; MW 36,000-50,000 kDa; MP Biomedicals) in drinking water for up to 8 days. Mice were monitored daily for change in weight, rectal bleeding and diarrhoea to generate a symptom score (See Table 2.3). Mice scoring >9 as defined in the symptom score, that developed >20% weight loss of their initial body weight or that developed rectal prolapse were sacrificed immediately as per Home Office regulations.

Assessment of histological severity was performed blinded using a well-established scoring method of DSS (Xu et al. 2008) using transverse sections of 1cm sections H&E stained colon.

2.9 Induction of *T. muris* colitis

Gastrointestinal infection with the parasite *Trichuris muris*, a mouse model of the human *T.trichiura* infection, is a much-studied model of colonic inflammation (Chapter 1.6). Ingested infective eggs accumulate in the caecum, hatching within 2 hours, adhering and anchoring to the caecal epithelium, maturing from larval to adult life stages over the ensuing 32days which in the absence of appropriate expulsion results in chronic local tissue destruction and inflammation (Hurst et al. 2013).

Stock infections of *T. muris* were maintained in susceptible mouse strains and adult worms harvested at day 42 post infection. 20-200 embryonated eggs were gavaged into mice and response to infection assessed at day 32. *T. muris* excretory antigen (ES) was prepared as described by Hayes et al. 2014: Adult worms were cultured in RPMI 1640 (Gibco) and the supernatant collected after 4 hours. ES was pelleted to remove eggs, concentrated using a Centriprep YM-10 (Ambicon) and then dialysed against PBS. Protein concentration was determined using a Lowry assay. ES was then used in restimulation assays at 50µg/ml: $2x10^6$ MLN cells in cRPMI obtained as per Chapter 2.2 were cultured for 24hours at 37^oC for 24hours, pelleted to remove cells and supernatant stored at -20^oC until use to permit assessment of antigen specific cytokine responses.

2.10 Enzyme Linked immunosorbent assays (ELISAs)

To determine levels of cytokine, ELISAs were performed on culture supernatants of murine cells using paired mAb purified in house, purchased from eBioscience or BD Pharmingen and recombinant cytokine standards purchased from PeproTech or PBL. Primary/capture antibodies were coated onto 96 well plates (NUNC) in a volume of 50µl in PBS overnight at 4^OC (IL-4, IL-5, IL-6, IL-10, IL-12p40, IL-12p70, IL-13, IL-17). Plates were blocked using 10% NCS in PBS for>1hour. Supernatants and doubling concentrations of recombinant protein standards were added to 96 well plates in a volume of 50µl in duplicate or triplicate. Secondary/detection antibodies were added in a volume of 50µl in 10% neonatal calf serum(NCS)/PBS and allowed to bind for 1hour at 37^OC (IL-4, IL-10, IL-13), 1hour at RT (IL-12p40, IL-12p70, IL-5, IL-6, IL-17). Streptavidin-peroxidase was added to all plates in a volume of 50µl and incubated at 37^OC for 30min. 100µl of the colorimetric substrate of peroxidase, TMB (Sigma) was added to each well, following development of blue colour, reaction was stopped by addition of 0.18M H_2SO_4 acid (Sigma). Between steps, plates were washed suing PBS 0.05% Tween-20 (Sigma).

2.11 Human samples

Colon biopsies were obtained from patients attending outpatient colonoscopy at Manchester Royal Infirmary. Patients were prospectively recruited for endoscopic biopsy samples and case note review for research purposes after approval from University of Manchester ethical committee. Endoscopic assessment of disease activity was made by the endoscopisy. Immune cells were liberated from samples by placement in 5mls ice cold PBS after collection, and digested over 12hours in 10mls of pre-warmed complete RPMI (RPMI 1640. 2mM L-glutamine, 100µg/ml penicillin, 100µg/ml streptomycin and 10% FCS) containing 0.5U/ml Collagenase (Roche) and 0.1mg/ml Type IV DNAse from bovine pancreas (SimgaAldrich) in a shaking incubator at 180rpm, 37^OC (313).

2.12 Generation of BM Chimeras

BM chimeras, to restrict *Mbd2* deficiency to specific cell types, were generated using 8 week old female C57BL/6 ($CD45.1^+$ or $CD45.1^+$ $CD45.2^+$) mice were irradiated with a total dose of 11 Gy 2hours apart. Mice then received $1x10^7$ BM cells from C57BL/6 ($CD45.2^+$ or $CD45.1^+$ CD45.2) or $Mbd2^{-/-}$ ($CD45.2^+$) mice and left for 8 weeks to permit BM engraftment. BM was obtained by collecting the tibias and fibulas of donor mice into ice cold PBS. Bones were then sterilized using 70% ethanol before washing in PBS to remove trace ethanol. Bone ends were removed using a scalpel and 5ml of OBS injected through the bone using a 5ml syringe (BD) and 21G needle (BD), flushing the bone marrow into a 50ml falcon tube (BD). BM cells were then combined with anti-CD90 beads and passes through a magnetic activation cell sort (MACS) column to remove $CD90^+$ cells. Recipient mice were treated from 7 days prior to irradiation to 4 weeks post irradiation with acidified water, irradiated food and enrofloxacin in drinking water to negate opportunistic infections in keeping with local guidelines. In some experiments a mixture of donor BM from $Mbd2^{-/-}$ and C57BL/6 mice was used to reconstitute chimeric mice. Starting ratios of BM were confirmed by flow cytometry by staining for CD45.1 and CD45.2 as described in section 2.7. All mice were screened at 8 weeks post irradiation to assess for successful engraftment by analysis of CD45.1 and CD45.2 expression by flow cytometry from 50 µl of tail vein blood.

2.13 RNA extraction

2.13.1 Tissue

1cm of distal colon, inferior right lobe liver or spleen were placed in 500µl of RNALater (Invitrogen) for 24hours at room temperature or 500µl of TRizol (Ambion) and kept on dry ice, before storage at $-80^{O}C$. Phase separation of DNA/protein and RNA was performed using chloroform. RNA was precipitated using 2-propanol, with 75% ethanol used to wash RNA, prior to air-drying and resuspension in RNase free DEPC water (Ambion).

2.13.2 Cells

Cells purified by flow cytometry were sorted directly into RNA later, cells pelleted at 5000*g* for 5mins, and supernatant aspirated to a residual volume of 100µl, snap frozen on dry ice and stored at $-80^{O}C$. RNA was then extracted using a protocol adapted from Pena-Llopis et al. 2013 using the *mir*Vana miRNA isolation kit: 600µl of ice cold Ambion lysis buffer was added to the cell pellet and vortexed for 2mins (314). 60µl of miRNA homogenate additive was then added, vortexed briefly for 30secs and allowed to sit on ice for 10mins. 600µl of acid-phenol:chloroform (Ambion) was then added and the mixture vortexed for a further 30secs. Samples were then centrifuged at 16,000*g* for 5 mins at room temperature to separate aqueous and organic phases. 700µl of the upper aqueous phase then transferred to a new RNAse free 1.5ml tube and mixed with 875µl (1.25 volumes) of 100% ethanol by

vortexing for 30secs. The mixture was then passed through a filter cartridge (Ambion) in 700µl aliquots by centriguation at 10,000*g* for 30secs. The filter cartridge was then washed with 700µl of miRNA solution 1 (Ambion) and then x2 500µl washes of solution 2/3 (Ambion), centrifuged at 10,000*g* at each step. 30µl of 95^{O}C RNAse free DEPC water for 1min was then used to elute the RNA. RNA was assessed qualitatively and quantitatively using BioAgilent Nano/Pico gel electrophoresis and NanoDrop respectively. Samples with a RNA integrity number (RIN) <8 were discarded.

2.14 cDNA synthesis from RNA and qPCR

50-500ng RNA was used for the synthesis of cDNA using Superscript-III and oligo-dT (Invitrogen). Relative quantification was performed by qPCR analysis using the Roche Light Cycler 480, with LightCycler SYBR Green I master mix (Roche). Five serial 1:4 dilutions of a positive control sample of cDNA were used to create standard curves. Expression was normalized to the housekeeping genes (gene expressed constitutively for the maintenance of cellular function) glyceraldehyde3-phophate dehydrogenase *Gapdh*. For primer sequences see Table 2.5

2.15 Stool DNA extraction and 16S amplification

To determine intestinal microbiota diversity, faecal contents from mouse colon was removed, snap frozen in dry ice and stored at -80^{O}C. DNA was extracted using the QIAamp Fast DNA Stool Mini kit following the manufacturers instructions with one additional step: After the addition of InhibitEX buffer to faecal contents, LysisMatrixE (MP biomedical) was added and shaken in a TissueLyser for 6mins at 30Hz to increase the yield of capsulate bacteria (Kennedy et al 2013). Briefly, the DNA of 80-120mg of WT or *Mbd2*$^{-/-}$ stool was extracted using the QIAamp Fast DNA stool mini kits with 1 notable deviation: “Bead beating” with inert spheres of ceramic, silica and glass 0.1-4mm in diameter at 30Hz has been shown to increase the detection rate of capsulate bacteria (Wu et al. 2010). Therefore this additional step was incorporated using MP biomedicals Lysing Matrix E. Faecal DNA was quantified by Nanodrop mass spectrophotometry, diluted to 5ng/µl and PCR amplified using KAPA HiFi HotStart Ready Mix and 16S amplicon primers;

Forward 5’ TCGTCGGCAGGCGTCAGATGTGTATAAGAGACAG,

Reverse 5’ GTCTCGTGGGCTCGGAGATGTGTATAAGAGACAG

as per 16S metagenomic sequencing library protocol for the Illumina MiSeq platform. Total DNA was quantified using a Nanodrop spectrophotometer. 12.5ng of microbial DNA was then used to amplify gene-specific sequences targeting the 16S V3 and V4 region using primer sequences and protocols described in the Illumina 16S Metagenomic sequencing library preparation guide for the Illumina MiSeq system.

2.16 Illumina Ref6 Mouse Array

To assess the impact of DSS treatment and mbd2 deficiency on gene expression of FACS isolated colonic populations, 50-200ng of RNA was biotin labeled with Illumina TotalPrep RNA amplification kit as per the manufacturers instructions. Samples were then hybridized to an Illumina Mouseref-6 array. Primary raw data were QC analysed using the arrayQualityMetrics Bioconductor package to identify sub-standard or outlier gene expression signatures. Arrays were scored on the basis of 3 metrics, namely mapplot, boxplot and heatmap. Raw data were then transformed using a variance stabilizing transformation method prior to normalization using the robust spline normalization method. Expression measures were then summarised in log base2 and presented as the fold change (logFC), with positive logFC representing up regulation, and a negative logFC indicating down-regulation. Statistical analysis was then performed using linear modeling and p value adjustment for multiple testing to control for false discovery (adjusted $p<0.01$ was deemed significant).

2.17 Statistical analysis

Statistical analyses were carried out using GraphPad Prism 6 and JMP v11 software. Where data for individual experiments is presented, ANOVA comparison tests were used to identify statistical differences between groups, $p<0.05$ was deemed significant. To increase the statistical power of our analysis and simultaneously comply with the 3Rs of ethical use of animals in research we consulted the advice of a local statistician and Professor of Ecological genetics, Richard Preziosi. By employing a fit model construct in the JMP 11 statistical package we were able to enter experimental day as an ordinal variable in our model, alongside nominal variables such as genotype, treatment and continuous variables such as weight loss. Thus the fit model platform in JMP allowed us to specify a model with complex effect structures to measure our variable of interest. All of the analyses used in this way in this thesis therefore used a Two-way analysis of variance fit model, with the model producing least square mean values for the *y* variable of interest.

For example, to assess whether genotype, treatment or experimental day affected weight loss, weight loss was our continuous *y* role variable with genotype, treatment and experimental day all construct model effects to assess any affect on *y.* This permitted us to pool experiments of the same format together, using experimental day as a construct model effect to ensure day-day variation did not bias the dataset. This method has been published by Prof. Preziosi and his lab in the ecological literature (315).

This had the benefit of allowing us to present data from all our experiments combined, rather than simply showing data from one experiment, which we felt was more statistically robust and more representative of our work.

Strain	Source
Mbd2$^{+/-}$ (CD45.2)	Generated in house as described by Hendrich et al. 2001. Given poor breeding and maternal instincts by *Mbd2*$^{-/-}$ mice, this strain was maintained as a heterozygous, *Mbd2*$^{+/-}$ line proceded by PCR genotyping to differentiate *Mbd2*$^{-/-}$ *Mbd2*$^{+/-}$ and *Mbd2*$^{+/+}$ animals.
Mbd2$^{Fl/Fl}$	Generated in house by Heather Owens as described by Cook et al. 2015.
Mbd2$^{Fl/Fl}$ *CD11c*Cre	Generated in house by Peter Cook as described by Cook et al. 2015.
Cd45$^{Cd45.1/Cd45.2}$	Generated by crossing C57BL/6 *Cd45*$^{Cd45.1/Cd45.2}$ and CD57BL/6 *Cd45*$^{Cd45.1/Cd45.1}$ mice
Cd45$^{Cd45.1/Cd45.1}$	Kindly donated by Graeme Couper, University of Manchester

Table 2.1 List of experimental animal lines

Antibody	Fluorochrome	Clone	Dilution	Source
CD103	BV421	M290	1/400	BD biosciences
CD103	BV421	2e7	1/400	BD biosciences
FoxP3	e450	FJK-16s	1/200	eBioscience
MHC-II	e450	M5/114.15.2	1/200	eBioscience
Rat IgG1	BV421	RTK2071	1/200	BD biosciences
Rat IgG1	e450	eBRG1	1/200	eBioscience
Rat IgG2b	e450	eB19/10H5	1/200	eBioscience
Rat IgG2a	e450	eBR2a	1/200	eBioscience
CD45	BV510	30-F11	1/400	BD biosciences
TNF	BV421	MP6-XT22	1/400	BD biosciences
CD11c	BV605	N418	1/600	BD biosciences
CD45.1	BV650	A20	1/200	BD biosciences
IL-10	BV650	JES5-16E3	1/100	BD biosciences
CD11b	BV711	M1/70	1/300	BD biosciences
Rat IgG2b	BV711	RTK4530	1/300	BD biosciences
Rat IgG2a	BV605	RTK2758	1/400	BD biosciences
Rat IgG2a	BV650	RTK2758	1/400	BD biosciences
Ki67	Alexa 647	B56	1/200	BD biosciences
CD45	Alexa700	30-F11	1/200	Biolegend
EpCAM	PE	G8.8	1/400	eBioscience
MHC-II	Alexa700	M5/114.15.2	1/200	Biolegend
SiglecF	PE-CF594	E50-2440	1/400	Biolegend
CD19	e780	eBio1D3	1/200	eBioscience
CD11b	PE	M1/70	1/200	eBioscience
CD64	PE	X54-5/7.1	1/200	BD biosciences
TNF	PE	MP6-XT22	1/200	Biolegend
TLR3	PE	TLR3.7	1/200	eBioscience
IL-5	PE	N/A	1/200	BD biosciences
Rat IgG2a	PE	N/A	1/200	BD biosciences
Rat IgG2b	PE	eB149/10H5	1/200	BD biosciences
CD45.2	PE	B169486	1/200	BD biosciences
Rat IgG2a	PE-CF594	R35-95	1/200	Biolegend
CD25	PerCP Cy5.5	PC61	1/200	eBioscience
Ly6G	PerCP Cy5.5	1A8	1/400	eBioscience
IL-10	PerCP Cy5.5	JES5-16E3	1/100	eBioscience
EpCAM	PerCP Cy5.5	G8.8	1/400	eBioscience
Ly6C	A700	HK1.4	1/400	eBioscience
Rat IgG2a	A700	RTK2758	1/400	BD biosciences

CD3	e780	17A2	1/200	BD biosciences
CD11b	e780	M1/70	1/200	BD biosciences
Ly6G	APC/Cy7	1A8	1/200	BD biosciences
NK1.1	e780	PK136	1/200	BD biosciences
TCRb	e780	H57-597	1/200	BD biosciences
Ter119	e780	TER-119	1/200	BD biosciences
Rat IgG2a	e780	eBR2a	1/200	BD biosciences
Rat IgG2b	e780	N/A	1/200	BD biosciences
MerTk	Biotinylated	N/A	1/100	Goat IgG RD systems
F4/80	APC	BM8	1/400	Biolegend
IL-6	APC	MP5-20F3	1/100	Biolegend
IL-22	APC	IL22JOP	1/100	Biolegend
TLR2	e660	6C2	1/200	BD biosciences
F4/80	PECy7	BM8	1/400	BD biosciences
Ly6C	PECy7	HK1.4	1/600	BD biosciences
IL-17	PECy7	N/A	1/200	BD biosciences
Ly6A/E	PECy7	E13-161.7	1/800	BD biosciences
Rat IgG2a	PECy7	N/A	1/200	BD Pharmigen
Rat IgG2a	APC	RTK2758	1/200	BD biosciences
MHC-II	FITC	M5/114.15.2	1/800	BD biosciences
IL-1b	FITC	NJTEN3	1/200	BD biosciences
TLR9	FITC	M9.D6	1/200	BD biosciences

Table 2.2 List of monoclonal antibodies used for flow cytometry

Parameter		Score
Weight loss (% change of Day 0 weight)	None	0
	1-5%	1
	5-10%	2
	10-20%	3
	>20%	4
Occult or Gross Blood Loss	None	0
	Blood staining around anus	2
	Gross bleeding	4
Stool Consistency	Well formed pellets	0
	Pasty/semi formed	2
	Diarrhoea that doesn't adhere to anus	4

Table 2.3 Clinical disease score criteria used during DSS-induced colitis studies
Score for each parameter summed to give the total symptom score. Score ranges from 0 (healthy) to 12 (maximum severity of colitis). Animals were euthanised if body weight loss is greater than 20%, total score is greater or equal to 9, or if rectal prolapse develops.

Criterion	Score	Add
Inflammatory cells	0-4	0.5 each ulcer
Goblet cells	0-4	0.5 each crypt abscess
Mucosa thickening	0-4	
Submucosa cell infiltration	0-4	
Destruction of architecture	0-4	

Table 2.4 Histological disease score criteria used during DSS-induced colitis studies

Gene	Primer Sequence	
	Forward	Reverse
chgA	CACAGCCACCAATACC	TCTTCCTCCTCCTCTTC
lrg5	ACCCGCCAGTCTCCTACATC	GCATCTAGGCGCAGGGATTG
Car2	CAAGCACAACGGACCAGA	ATGAGCAGAGGCTGTAGG
Klf4	GAAATTCGCCCGCTCCGAT	CTGTGTGTTTGCGGTAGTGCC
Car1	TTGATGACAGTAGCAACC	CCAGTGAACTAAGTGAAG
mbd2	CCTTAGCAGTTTTGACTTCAGG	GGCCAATGTTGTGTTCAGGT
gapdh	AATGTGTCCGTCGTGGATCT	CCCAGCTCTCCCCATACATA
il5	ACATTGACCGCCAAAAAGAG	CACCATGGAGCAGCTCAG
il4	GAGAGATCATCGGCATTTTGA	TCTGTGGTGTTCTTCGTTGC
il10	CAGAGCCACATGCTCCTAGA	TGTCCAGCTGGTCCTTTGTT
il17	TGTGAAGGTCAACCTCAAAGTC	AGGGATATCTATCAGGGTCTTCATT
ifng	GGAGGAACTGGCAAAAGGAT	TTCAAGACTTCAAAGAGTCTGAGG
tnf	TGGTGGTTTGCTACGACGT	ACCCTCACACTCAGATCAT
il1b	CCGACAGCACGAGGCTTT	CTGGTGTGTGACGTTCCCATTA

Table 2.5 Primers used in qRT-PCR

Chapter 3

The role of *Mbd2* in the steady state and inflamed colon

3.1 Introduction

One of the key facets of the vertebrate immune system is an ability to rapidly respond to invading pathogens whilst promoting tolerance to self-antigens. The GI tract differs from this mantra in that immune reactivity to the commensal microbiota must be restrained to avert damaging inflammation. The innate and adaptive compartments of the immune system must therefore co-operate to promote tolerance and simultaneously be poised to negate invasive pathogens. There is increasing evidence that GI tract myeloid cells, in particular MP cells such as DCs and macrophages have a key role in manipulating these dual regulatory and pro-inflammatory responses (51), (316). Dysregulation of this innate immune response is a key component in the development of chronic, relapsing inflammatory disorders such as UC and CD, the mucosal immunology underpinning which is poorly understood (317).

As alluded to in Chapter 1, only 30% of the heritable component to IBD can be accounted for despite multiple efforts in large multinational GWAS cohorts (104). Therefore understanding a heritable component to GI tract immune function that is not encoded in one's nucleotide sequence, for example by epigenetic processes, would represent an attractive, novel approach to developing treatments for inflammatory disorders such as IBD. As mentioned in Chapter 1.5.4, MBD2 is a methyl-CpG-binding protein that modulates dramatic changes in gene expression via recruitment of large chromatin remodelling complexes. *Mbd2* has also been shown to be pivotal in effective DC and T cell function with its expression tightly regulated in the GI tract, the evidence for which is presented below.

Firstly, it has recently been shown that *Mbd2* deficient murine bone marrow derived DCs (BMDCs) display reduced mRNA transcript of several immunologically important processes such as antigen presentation (*H2-Aam* and *Ciita*) and co-stimulation (*Cd40, Cd80* and *Cd86*) (318). *Mbd2* deficient DCs are therefore less able to induce either naïve T cell proliferation or an appropriate Th2 response against helminths or allergens (318). As a result, deficient Th2 inductive ability in *Mbd2* deficient DC resulted in significantly ameliorated pathology to house dust mite mediated bronchial inflammation in mice (318).

Secondly, it has been shown that *Mbd2* deficient naïve T cells display a disordered developmental response to *in vitro* polarization. Both the progenitors and progeny of *Mbd2* deficient T cells express ectopic levels of IL-4 in a GATA-3 independent manner (319). Naïve uncommitted T cells cultured in polarising Th1 or Th2 conditions display augmented IFN-γ (Th1), IL-4 (Th2) and uniquely dual IFN-γ/IL-4 (Th1 and Th2) positive cells in the absence of *Mbd2* (319). As such *Mbd2* mediated changes in adaptive immune cells

produces excessive cytokine production that could be postulated to alter susceptibility of *Mbd2* deficient animals to infectious challenge.

Thirdly, *Mbd2* is tightly regulated in the GI tract suggesting its expression has important physiological roles. Indeed altered *Mbd2* expression affects response to infectious colitis and colorectal cancer susceptibility. MBD2 is expressed at significantly greater levels in the distal compared to proximal GI tract and abrogating high levels of colonic MBD2 in *Mbd2*$^{-/-}$ mice results in the expression of exocrine-pancreas genes in the colon (320). Just as the GI tract has evolved along its length to perform different functions, (nutrient absorption in the small intestine, water reabsorption in the colon etc.) it is conceivable that the cellular functions of these specialised areas are in part dependent on epigenetic-co-ordinated changes in gene expression. This suggests relative abundance of *Mbd2* is essential in normal gut development and in co-ordinating region specific gene expression profiles.

Finally, *Mbd2*$^{-/-}$ mice have been shown to be resistant to the intracellular protozoan infection *Leishmania major*, but develop florid intestinal inflammation with the gut dwelling helminth *Trichuris muris*. *T. muris* produces a colitis that is swiftly resolved in immunocompetent mice, characterised by parasite clearance and a strong IgG1 antibody response (215). *Mbd2*$^{-/-}$ mice are unable to successfully negotiate parasite expulsion resulting in a chronic colitis characterised by mucosal oedema, thickening and presence of intra-luminal worms (321), . However it is not clear from previous work what aspects of mucosal immune function are perturbed in the absence of *Mbd2*, underpinning this observation.

Intestinal tumourgenesis in mice is dependent on DNA methylation (322), (323). The Min mouse lineage was observed to have multiple intestinal neoplasias, which was subsequently found to be caused by an autosomal dominant missense mutation in the tumour suppressor gene *Apc (Apc*$^{Min/+}$ or Min) (324). Min mice therefore demonstrate GI tract adenoma development in a mouse model of colorectal cancer and have been used to study the effects of methyl-CpG binding protein deficiency by crossing Min and *Mbd2*$^{-/-}$ mice. When Min mice are rendered *Mbd2* deficient, they develop 10fold fewer adenomas compared to *Mbd2* sufficient controls, doubling median life expectancy. The authors therefore suggest MBD2 interpretation of DNA methylation signals promotes gene silencing required for tumourgenesis (325). The mechanism underpinning this observation is unclear, and has not been replicated in other models of GI tract cancer.

Taken together these data demonstrate a role for *Mbd2* in key facets of the innate and adaptive immune system and requirement for GI tract homeostasis. *Mbd2* therefore represents an attractive regulatory gene of interest but this has not been examined immunologically in the GI tract. The focus in this chapter therefore is to identify where in the

GI tract *Mbd2* expression might be relevant for normal function, simultaneously developing a method to characterise the intestinal immune cells robustly in the steady state and under experimental models of inflammation:

Chapter aims:

1. Determine and characterise expression of *Mbd2/MBD2* mRNA transcript in the GI tract, confirming spatial expression and explore regional changes specifically in the colon
2. Explore *MBD2* GI tract expression changes in IBD, and *MBD2* as a candidate risk susceptibility locus for IBD
3. Define and characterise an integrated approach to identifying and phenotyping the colonic myeloid immune compartment using flow cytometry
4. Characterise the colon LP myeloid cells in active IBD
5. Characterise *Mbd2* expression in colon LP myeloid cells
6. Determine and characterise susceptibility of *Mbd2*$^{-/-}$ mice to experimental colitis with DSS
7. Determine and characterise susceptibility of *Mbd2*$^{-/-}$ mice to infectious colitis with *T. muris*

3.2 Expression of *Mbd2/MBD2* in the GI tract

Previous studies have shown a spatial relationship for MBD2 in the murine GI tract: MBD2 is found at levels 5-fold higher in the colon, ileum and jejunum compared to the duodenum by Western blot analysis when normalised for GAPDH (320). However, these data do not assess if *Mbd2* expression is uniform throughout the colon. Gene expression analysis of *Mbd2* from intestinal tissue was performed by RT-qPCR to define if this spatial relationship of expression extended to different parts of the large intestine (Figure 3.1A). Expression of *Mbd2* at the rectum was 4-fold greater than the duodenum. Similarly there was a significant 1.8-fold increase in expression when comparing the distal (rectum) to proximal (caecum) sections of the colon (Figure 3.1A). These data suggest that *Mbd2* gene expression matches previously known protein data, and that spatial changes in *Mbd2* expression extend to within the colon, with the highest levels of *Mbd2* in the GI tract found within the rectum.

To address whether *MBD2* is regulated in a similar manner in human intestine, previously published microarray data from 67 patients with UC and 31 healthy controls was examined (326). In this study, patients underwent endoscopic biopsy at specific anatomical locations for RNA extraction and whole genome microarray as previously described (326). Firstly we analysed healthy control data for mRNA levels of *MBD2* comparing the terminal ileum and rectum for normalised log2 expression. As in the murine GI tract there was a significant increase in expression within distal versus proximal GI tract (mean log2 expression terminal ileum 0.068±0.04 versus 0.16±0.02 in rectum, Figure 3.1B). Taken together these data suggest that *Mbd2/MBD2* is expressed at significantly higher levels in the distal compared to proximal GI tract in mice and man.

3.3 Analysis of *MBD2* as a candidate risk susceptibility locus in IBD

As MBD2 follows a tightly coordinated expression pattern in the gut, we hypothesized this would alter during tissue inflammation. Analysis of rectal *MBD2* expression from the above data set of patients with active UC or healthy controls was performed (Figure 3.1C) (326). This revealed that patients with active rectal UC had a significantly lower level of *MBD2* than healthy controls (mean log2 expression 0.078±0.03 versus 0.16±0.02, Figure 3.1C). We therefore hypothesized that since *Mbd2/MBD2* expression is tightly spatially regulated in the GI tract, reduced expression in pathological state could represent an important causative or contributing mechanism to inflammation. Given the existing literature suggesting a role for *Mbd2* in innate and T cells, in addition to the above observation that active IBD is associated with reduced *MBD2* expression we hypothesised that *MBD2* is required for effective mucosal homeostasis, particularly in the distal colon which demonstrates the greatest level of mRNA transcript (319), (318).

The international IBD genetics consortium (IIBDGC) is a multinational organisation that has amassed some 20,000 cases for CD and UC, along with a similar number of healthy population controls (104). Sequencing single nucleotide polymorphisms (SNPs) from this large dataset has revealed great insight into the pathogenesis of IBD by proposing 'risk-susceptibility' loci, i.e. SNPs that feature more frequently in cases versus controls to a high degree of statistical power. One notable success of this 'hypothesis-free' testing has been the identification of previously unknown autophagy pathways in the pathogenesis of CD. Hypomorphic *ATG16L1* was identified from GWAS as enriched at genome wide significance thresholds in CD patients and thereafter shown to confer aberrant bacterial handling in *ATG16L1* mutant DC (112). To assess whether mutant *MBD2* confers an increased risk of IBD the IIBDGC dataset of 16,054 CD and 12,153 UC cases with 17,575 healthy controls was examined (Figure 3.1D).

SNPs at the *MBD2* locus were not found more frequently in cases versus controls at genome wide significance, suggesting that *MBD2* SNPs do not confer an increased susceptibility of IBD.
However, this does not exclude the possibility that *MBD2* is regulating other genes up/downstream that are required for mucosal homeostasis, or that rare variants in *MBD2* genotype have been excluded from this dataset. Similarly this data does not exclude the importance of changes in MBD2 in IBD or indeed post-transcriptional/translation modifications of MBD2 on its function in disease states. However, previous murine studies have highlighted the importance of *Mbd2* in driving colitis like inflammation mediated by a skewed immune response (321). In addition no studies have assessed whether expression of *Mbd2/MBD2* by specific cell populations, rather than whole tissue expression, in the GI tract is important during health or disease.

3.4 Identification of immune populations in the steady state colon LP

Understanding the repercussions of *Mbd2* mediated changes in GI tract immune cells requires an understanding of a) the complex and heterogeneous cellular milieu at mucosal barrier surfaces and b) the confirmation and characterisation of *Mbd2* expression within these cell types. Neither of these 2 facets is completely understood, either in the steady state or inflammation and is considered below.

There have been substantial recent developments in the ability of researchers to discriminate between MPs in mucosal tissue sites using flow cytometry (43), (65). This has built upon previous work using a limited number of phenotypic markers such as CD11c, CD11b and MHC-II, which are now recognised to be insufficient to sensitively delineate the heterogeneous immune populations of the intestinal tract (36). For example CD11c, once

thought of as a DC specific marker, is now appreciated to be expressed by a variety of cell types, not least tissue resident macrophages (See Table 3.1) (36), (327). GI tract DCs and macrophages share many phenotypic and functional facets, but also have very different roles in the initiation of tolerance and induction of immune response. Therefore the ability to robustly discriminate between these populations will not only enable us to understand their role in normal mucosal physiology, but to pinpoint dysregulated responses that manifest in disease. In particular, this will allow us to characterise a role for *Mbd2* in modulating the balance and composition of immune cell types in steady state and inflammatory settings.

Mutli-colour flow cytometry using an array of additional phenotypic markers such as CD103, CX_3CR1, F4/80, MertK, CD64, SiglecF, LY6G and LY6C have been employed to characterise subdivisions of MP cells in the GI tract, predominately in the small intestine LP. These include monocytes, macrophages, eosinophils, neutrophils, and DCs based on their surface expression of CD11b and CD103. However a robust, integrated strategy to discriminate the spectrum of colon LP myeloid cells including eosinophils, neutrophils, monocytes, macrophages and $CD11b^{+/-}$ DC subsets simultaneously within the colon has not yet been shown. Recent studies have shown expression of the chemokine receptor CX_3CR1 on colon MP cells can distinguish between the maturation stages of blood derived inflammatory monocytes through to resident tissue macrophages (43). It is not currently possible to detect CX_3CR1 directly by flow cytometry due to poor antibody affinity, and thus studies have relied upon $CX_3CR1^{gfp/+}$ transgenic mice to investigate expression of this receptor (43), (114).

We therefore developed a gating strategy for colon LP myeloid cells that has previously been validated using $CX_3CR1^{gfp/+}$ mice (43), to identify different myeloid cells populations (Figure 3.2 and Table 3.1). This approach, presented in Figure 3.2 and summarised below, permitted analysis of colon LP myeloid cell types. We also adopted a similar approach for the characterisation of T, B and innate lymphoid cells and this data is presented in Figure 3.3.

Neutrophils (Figure 3.2 Population A: $CD11b^{+}$ $LY6G^{+}$)

The first set of myeloid cells identified by our newly developed gating strategy in Figure 3.2, was a $CD11b^{+}$ population positive for the lymphocyte surface antigen 6G (LY6G). LY6G identifies neutrophils, but not monocytes or lymphocytes, with anti-Ly6G monoclonal antibody offering selective depletion of neutrophils (22). Neutrophils possess an arsenal of antimicrobial functions including degranulation and phagocytosis that mitigate against invading pathogens by massive release of reactive oxygen species and other toxic molecules (21). Although these responses are clearly beneficial, excessive recruitment and

accumulation in the intestine under pathological conditions such as IBD is associated with mucosal injury and debilitating disease symptoms (21).

Eosinophils (Figure 3.2 Population B: SiglecF^{+} SCC High)

Eosinophils possess a characteristic SCC high profile and uniquely express the sialic acid-binding immunoglobulin lectin. Eosinophils in the GI tract are poorly described, and are distinct phenotypically and functionally from those in other tissues (27). An important role is suggested by their abundance and low turnover *in vivo,* with activated eosinophils found in greater numbers in those with active IBD compared to quiescent IBD and healthy controls ((30), (29). Early identification and removal from downstream gating analysis was found to be critical to avoid contamination of population E (Macrophages), due to these cells expressing CD11b and low levels of F4/80, MHC-II and CD11c.

CD11b^{-} DC (Figure 3.2 Population C: CD11b- CD11c^{+} CD103$^{+/-}$)

This was the only myeloid population seen to not express CD11b, with the majority of cells expressing the integrin-αE (CD103). Population C1 (CD103^{+}) were the most abundant DC population observed (around 1% of intact cells), while population C2 (CD103^{-}) were the least abundant (around 0.4% of intact cells). CD11b^{-} CD103^{+} DCs are CD8α^{+}, require Flt3 and GM-CSF receptors for normal development and expand upon exogenous administration of their ligands (114). In addition, genetic deletion of the transcription factors Id2, Irf8 or Batf3 leads to selective loss of SI CD11b^{-} CD103^{+} cells (64). CD11b^{-} CD103^{-} DCs are poorly described, but like CD11b^{-} CD103^{+} DCs migrate to MLNs in a *Ccr7* dependent manner, expand in response to Flt3 ligand, prime T cell responses and induce T cell CCR9 (69). CD11b^{-} CD103^{-} DCs are observed to be unique amongst colon LP DCs in expressing both CD64 and the tyrosine kinase inhibitor MerTK. Both of these markers have been used to define DCs in other tissues as monocyte derived DCs (moDCs) with CD64^{+} DCs in the lung able to induce potent chemokine response after allergen challenge (Plantinga et al. 2013).

Monocytes (Figure 3.2 Population D: CD11b^{+} Ly6C^{+} MHC-II$^{+/-}$)

It has recently been reported that blood monocytes are the precursors for intestinal macrophages in adult mice (42), (43). As such LY6C^{+} monocytes are found constitutively, though at low levels identified through our gating panel (around 1% of intact cells). On entering the colon LP, the LY6C^{+} cells enter a “monocyte-waterfall” characterised by change in surface marker expression and phenotype over 48-96 hours en route to becoming stable tissue resident macrophages (43). This process involves the acquisition of MHC-II, loss of LY6C, before upregulation of CD11c, F4/80 and finally CX_3CR1(43). Monocytes are thought to have little other role in the steady state, but accumulate in inflammation, constitutively

expressing high levels of IL-1β, IL-6 and TLR to disturb the tolerogenic status quo in preference of a vigorous, pro-inflammatory immune response (43), (47).

Macrophages (Figure 3.2 Population E: CD11b^{+} CD11c$^{+/-}$ F4/80^{+} CD64^{+})

Macrophages were the most populous myeloid cell in the steady state colon LP, accounting for just over 5.5% of all intact cells. Differentiating this population from DCs has been historically challenging, given the overlap in surface marker expression, particularly of CD11c. It is however possible to discriminate macrophages based upon their expression of CD11b, CD11c, F4/80 and CD64 (See Table 3.1). Here the inability to discriminate between population expression of CX_3CR1 may have functional relevance as it has been reported that there are minor phenotypic differences between $CX_3CR1^{int/high}$ maturation stages of macrophage. CX_3CR1^{int} macrophages demonstrate numerically lower, though non significant, expression changes of *Il10* and *Tgfb* mRNA, and numerically higher, non significant changes in *Tnf*, *Nos2* and *Ccr2* mRNA versus CX_3CR1^{High} macrophages (43). It has also been reported that CX_3CR1^{int} macrophages possess a small though significant reduction in phagocytic ability, with a lower uptake of pHrodo *E.coli* bioparticles compared to CX_3CR1^{High} macrophages, though the functional significance of this change *in vivo* has not been shown (42). Therefore with the above caveats, the CX_3CR1^{int} and CX_3CR1^{High} subsets of macrophage are considered together for subsequent analysis.

CD11b^{+} DCs (Figure 3.2 Population F: CD11b^{+} CD11c^{+} F4/80^{-} CD103$^{+/-}$)

CD11b^{+} DCs, like their CD11b^{-} counterparts, can be discriminated based on CD103 expression. CD11b^{+}CD103^{+} DCs (Population F1) were found at a frequency of 0.5% of intact cells, with CD11b^{+}CD103^{-} DCs (Population F2) found at 0.7% frequency, representing the 3rd and 2nd most abundant colon LP DC populations, respectively. This observation contrasts with the small intestine LP where CD11b^{+} DCs are the most frequent DC population, underlying the heterogeneity of immune cells even with the GI tract, and the caution required therefore in generalizing these results (114). This altered balance of DC subsets has important implications for intestinal T cell priming, as CD11b^{-} DCs are more potent at cross presentation to CD8α^{+} T cells, and far less effective at priming CD4^{+} T cells than CD11b^{+} DCs (69). Like CD11b^{-} DCs, CD11b^{+} DCs have been shown able to migrate to MLN in a *Ccr7* dependent manner, expand to Flt3 ligand and induce T cell CCR9. In addition both CD11b$^{+/-}$CD103^{-} cells have recently been shown to express higher levels of IL-12 and IL-23 mRNA and induce higher IFN-γ and IL-17 production from proliferating T cells compared to CD103^{+} LP DCs, even in the absence of TLR stimulation (65).

B Cells (Figure 3.3A Population G: CD19^{+})

The role of B-cells in intestinal inflammation and immune homeostasis is not well appreciated. At intestinal sites, B cells follow a distinct differentiation pathway and are specialised in IgA production as differentiated plasma cells (328). sIgA acts as a barrier to protect the epithelium from pathogens, and interacts within the lumen with food, self and intestinal antigens (329). As such sIgA limits access of intestinal antigens into the systemic circulation, and affects intestinal microbiota composition (329). In addition a subset of CD25 expressing B cells have been described in other tissue sites and have been termed Bregs given their immunosuppressive capabilities, mediated by IL-10 and TGF-β production (330). Indeed functional impairment of TGF-β producing B cells is associated with food-allergy pathogenesis (331). Interestingly we were unable to detect any CD25 expressing CD19 cells in the colon LP.

T cells (Figure 3.3A Population H: Naïve CD8^{+}, I: CD8^{+} CD44^{+} CD69^{+}, J: CD4^{+} FoxP3^{+}, K: Naïve CD4^{+}, L: CD4^{+} CD44^{+} CD69^{+})

CD69 is considered an activation marker of T lymphocytes and is the earliest inducible cell surface glycoprotein acquired during lymphoid activation which once expressed acts as a co-stimulatory molecules for T cell activation and proliferation (332). CD44 participates in cell adhesion, migration and lymphocyte activation with T cells expressing CD44 to permit rolling and adhesion to intestinal epithelium (333), (334). CD44 has also been extensively described as identifying memory T cells with CD44^{High} cells more sensitive than CD44^{Low} cells to TCR signaling response to antigen (335). Tregs characterised by the expression of FoxP3 may be defined as T cells able to suppress naïve T cell proliferation *in vitro* and *in vivo*. Tregs are crucially involved in the maintenance of gut homeostasis by suppressing abnormal immune responses against the commensal flora or dietary antigens, in part modulating this effect by anti-inflammatory cytokine production (IL-10 and TGF-β).

A dysregulated T cell response with disordered development of activated T cell populations can lead to an exacerbated mucosal inflammatory response. Increased T cell derived cytokines and chemokines derived from IBD mucosa have therefore led to the hypothesis of a skewed, pro-inflammatory adaptive immune response in IBD patients. Inflammatory lesions develop in foetal gut explants cultured *ex vivo* with IL-12 and anti-CD3 (336), with inhibition of gut activated T cell activation, mediated by T cell specific calcium channel blockade, leading to a reduced pro-inflammatory cytokine production (337). Indeed the national institute for clinical excellence (NICE) has recently approved the use of an α4β7 blocking monoclonal antibody (vedolizumab) which limits activated T cell recruitment to the gut mucosa, which has been shown to be superior to placebo in inducing disease remission in IBD patients (338).

ILCs (Figure 3.3B Population M: CD90.2$^+$ CD127$^+$)

ILCs are an emerging and diverse group of immune cells and derive from an ID2 expressing progenitor and have recently been implicated in the development of IBD. Group 3 ILCs have been shown to be able to induce colitis in a *Helicobacter hepaticus* infection characterised by IL-17A and IFNγ production in *Rag*$^{-/-}$ mice (96). Subsequent data suggest that Group 3 ILCs can induce colitis in an IL-23R, IL-22 dependent mechanism, that *Rorγt*$^{-/-}$ mice do not develop CD40L induced colitis and lastly human ILC's were found at increased levels in the LP in an IL-23 dependent manner (97), (96), (98), (99).

3.5 Assessment of naïve *Mbd2*$^{-/-}$ mice

In order to identify any gross pathological difference between WT and *Mbd2*$^{-/-}$ mice in the steady state, 1cm sections of distal colon were taken for histological analysis. We used H&E staining transverse sections to determine putative baseline differences in the structural architecture of *Mbd2* deficient colonic mucosa (Figure 3.4A). There was no difference observed between genotypes. In particular, there was no suggestion of spontaneous colitis in *Mbd2*$^{-/-}$ mice.

We now sought to apply the gating strategy in Figures 3.2 and 3.3 to understand, allowing for the fact there was no gross histological difference between *Mbd2*$^{-/-}$ and WT mice, whether *Mbd2* deficiency conferred changes in the cellular composition of colon LP immune populations.

Firstly, there was a small but significant reduction in the proportion of CD45$^+$ cells in *Mbd2*$^{-/-}$ mice (least square mean 40.1±1.37% versus 50.9±1.46% proportion of intact cells) (Figure 3.4B). Interestingly in each of the 6 individual contributing experiments, this difference did not reach significance; only on linear regression comparing all 6 experiments together was the difference statistically significant (Figure 3.4B). This highlights the power of such methodology to detect small differences over multiple datasets, but also suggests that careful consideration of the biological significance of such small overall changes is required.

T cells, B Cells and ILC

We then sought to assess whether there was any perturbation of the adaptive immune system or ILC compartment in the steady state conferred by the absence of *Mbd2*. There was no difference in the number or proportion of TCRβ$^+$, CD19$^+$, CD4$^+$, CD8$^+$, CD4$^+$ FoxP3$^+$, CD4$^+$ CD44$^+$ CD69$^+$ populations (Figure 3.4C), or in CD90$^+$ CD127$^+$ ILCs (Figure 3.4D).

Myeloid Cells

Within the CD45$^+$ fraction, there was no significant difference observed in colon LP neutrophil, eosinophil, or CD11b$^-$ DC (CD103$^{+/-}$) populations, either expressed as the

proportion of singlet cells or total cell number per colon, between *Mbd2*$^{-/-}$ or WT mice (Table 3.1). There was a small but significant reduction in the proportion and total cell number of macrophages in *Mbd2*$^{-/-}$ versus WT naive mice (Table 3.1). In addition there was a significant reduction in the proportion and total cell number of CD11b^{+}CD103^{+} and CD11b^{+}CD103^{-} DCs in *Mbd2*$^{-/-}$ versus WT mice (Table 3.1).

However, once the reduction in total CD45^{+} cells was factored into the regression model, only the CD11b^{+}CD103^{+} population differences were significant between genotypes, i.e. there was no difference between WT and *Mbd2*$^{-/-}$ proportion and total number of all other assessed cell types (Figure 3.4E and F).

Thus naïve *Mbd2*$^{-/-}$ and WT mice were largely comparable in both the gross mucosal architecture and myeloid composition of immune cells within the colon, with the notable exception of a small reduction in total CD45^{+} cells and CD11b^{+}CD103^{+} DCs. Given that CD11b^{+} CD103^{+} DCs did not develop normally in the absence of *Mbd2*, and that existing data support a role *in vivo* for *Mbd2* in CD11c expressing cells, we then sought to assess the level of expression in WT colon LP DC and other myeloid cells.

3.6 Assessment of *Mbd2* expression in myeloid cells

The previous expression analysis of *Mbd2* shown in Figure 3.1A was performed on RNA extracted from whole tissue. Therefore we hypothesised that the contributing cell populations within this would demonstrate differing levels of *Mbd2* expression. Given that *Mbd2* has been shown to have a key role in controlling CD11c^{+} cell responses (318), with existing literature also supporting a key role for monocytes in intestinal homeostasis (43,47), these populations were selected for further analysis by simultaneous FACS purification. To assess the relative expression of *Mbd2* within these populations, the gating strategy in Figure 3.2 was adapted to simultaneously FACS purify Ly6C^{+}MHC-II$^{+/-}$ monocytes, Ly6C^{-}MHC-II^{+}F4/80^{+} macrophages, CD11b^{-} (CD103$^{+/-}$) and CD11b^{+} (CD103$^{+/-}$) DCs from WT naïve colon LP (Figure 3.5A).

RT-PCR of isolated mRNA from these populations revealed higher levels of *Mbd2* expression in myeloid cells than whole liver tissue control, with monocytes and macrophages demonstrating the highest levels of expression (Figure 3.5B). Therefore, in addition to observing increased *Mbd2* at a tissue level in the distal GI tract, we have observed that within this, the colon LP monocyte-macrophage axis expresses more *Mbd2* than other myeloid cells types and indeed other comparable whole tissue specimens.

We have therefore built upon previous work describing steady state intestinal MP and DC subsets separately, through development of a combined multi-parameter flow cytometry phenotyping strategy that enables simultaneous identification of each distinct cell type. Our next step was to apply this new approach to the inflamed *Mbd2*$^{-/-}$ colon.

3.7 Assessment of *Mbd2*$^{-/-}$ mice after acute colitis

To assess whether *Mbd2* is important for effective function of the mucosal immune system, we utilised the flow panel detailed in Figure 3.2 to assess cellular populations from the colon LP in the steady state and after acute colitis induced by feeding 2% DSS b/w in drinking water *ad libitum* for 6 days. As described in Chapter 1.6, this much-studied model of experimental colitis is characterised by disruption of colonic barrier integrity beginning 24hrs after onset of treatment (165), (164) (Chapter 1.6.1). The exposure of luminal contents and microbiota to the underlying LP results in colonic inflammation characterised by progressive weight loss, diarrhoea and PR bleeding (167). Experimental colitis induced by DSS is considered a T-cell independent model of intestinal inflammation, borne from observations that mice lacking T and B cells develop equivalent pathology as those that are immunocompetent when treated with DSS (166). Moreover, it has previously been shown that the number of colonic $CD3^+$ T cells does not increase significantly during acute colitis, only increasing after the removal of DSS in the "resolution" phase (339). Thus T cells were not considered in subsequent analysis in this model.

3.7.1 *Mbd2*$^{-/-}$ mice display severe inflammation upon DSS treatment

Daily assessment was made of weight and symptom score as defined in Table 2.3. At necropsy, *Mbd2*$^{-/-}$ mice had shortened colons with increased macroscopic evidence of inflammation (Figure 3.6A) *Mbd2*$^{-/-}$ mice had increased weight loss at day 6 (16.32±1.17% versus 8.90±1.17% least square mean change in day 0 weight) compared to WT mice (See Figure 3.6B). There were similarly increases in *Mbd2*$^{-/-}$ versus WT mean symptom score in DSS treated mice at day 4 (3.3±0.3 versus 0.8±0.5) day 5 (6.25±0.48 versus 1.0±0.7) and day 6 (12.0±0 versus 3.5±0.3) (Figure 3.6C). This reflected an increase in all parameters of the symptom score (PR bleeding, weight loss and diarrhoea). There were no symptoms recorded in untreated mice independent of genotype, with a non-significant increase in weight of both genotypes at day 6 (Figure 3.6B and C).

Histological analysis (Table 2.4) of 1cm H&E stained sections of distal colon revealed a significantly greater tissue architecture destruction, goblet cell depletion and inflammatory infiltrate in DSS treated *Mbd2*$^{-/-}$ versus WT mice in keeping with a severe colitis (least square mean histology score 14.6±0.64 versus 4.8±0.54) (Figure 3.6D and E). This would suggest

that expression of *Mbd2* is required to limit damaging inflammation incurred by DSS mediated intestinal barrier breakdown.

3.7.2 mRNA expression of cytokine response

To characterise the inflammatory cytokine response upon DSS treatment, mRNA was isolated from whole colonic tissue and analysed by RT-PCR (Figure 3.7). DSS treated *Mbd2*$^{-/-}$ mice displayed significantly greater mRNA transcript for *Ifng*, *Il1b*, *Il17*, *Tnf* and *Il10* with no significant difference seen in *Il4* and *Il5*, compared to WT (Figure 3.7). In keeping with other naïve phenotyping data, there was no difference in cytokine expression between the genotypes in untreated mice.

3.8 Effects of inflammation on the colon LP myeloid compartment

Together, the above data showed the presence of an acute inflammatory infiltrate in *Mbd2*$^{-/-}$ DSS treated mice with significant tissue architecture disruption corresponding to a profound pro-inflammatory cytokine response. To understand the cellular biology underpinning these results, we next analysed the impact of MBD2 deficiency on colon LP myeloid populations during inflammation, using the logic outlined in Figure 3.2. Given that DSS colitis is considered a model of innate immune response, the myeloid compartment was the focus of all subsequent analysis (166).

3.8.1 Effect of DSS on WT colon LP myeloid cells

After the onset of intestinal inflammation with DSS there was a dramatic alteration in the cellular composition of the colon LP. At day 6 there was a 1.7 fold increase in the total number of CD11b^{+} cells comparing DSS treated versus control WT mice (Table 3.2). As previously reported, the myeloid populations with the largest increase in total number conferred by DSS treatment in WT mice were eosinophils (2.21 fold increase), neutrophils (8.93-fold increase) and monocytes (3.73 fold increase) (Table 3.2). There were smaller increases in the remaining myeloid cells examined, with between 1.2 and 1.8 fold increases in WT DC and macrophage total cell numbers. We then sought to compare changes in myeloid cells between WT and *Mbd2*$^{-/-}$ DSS treated mice:

3.8.2 Comparison of *Mbd2*$^{-/-}$ versus WT colon LP in DSS

There was a significant increase in the proportion of CD45^{+} cells comparing *Mbd2*$^{-/-}$ DSS versus steady state, but not in WT DSS versus steady state or *Mbd2*$^{-/-}$ versus WT in DSS (Figure 3.8A). This intriguingly suggested that despite a reduction in *Mbd2*$^{-/-}$ versus WT CD45^{+} cells in the steady state, DSS preferentially expands the CD45^{+} compartment in *Mbd2*$^{-/-}$ mice. When analysing the CD45^{+} compartment further, additional differences emerge. There was a 2.49 fold increase in *Mbd2*$^{-/-}$ CD11b^{+} cells after DSS treatment which represented a significantly greater increase in the number of CD11b^{+} cells compared to WT

mice (Table 3.2). Given the increased accumulation of *Mbd2*$^{-/-}$ CD11b^{+} cells in DSS, we next investigated which myeloid populations accounted for this change:

Monocytes and neutrophils, but not eosinophils, were found at significantly greater proportion and also in total cell number in *Mbd2*$^{-/-}$ mice (Table 3.2 and Figure 3.8B and C). As in naïve *Mbd2*$^{-/-}$ mice, there remained a significant reduction in the proportion and total number of CD11b^{+} DC (CD103$^{+/-}$) after DSS treatment compared to WT, however the *Mbd2*$^{-/-}$ macrophage compartment increased in proportion by 1.6-fold (compared to 1.1-fold in WT mice) such that there was subsequently no difference in proportion or total cell number between WT or *Mbd2*$^{-/-}$ DSS treated colon LP macrophages (See Table 3.2).

Thus the myeloid composition in DSS was defined by a substantial increase in monocytes, neutrophils and eosinophils, with *Mbd2*$^{-/-}$ treated mice displaying a significantly greater proportion and total number of neutrophils and monocytes compared to WT.

3.8.3 Assessment of the role of *Mbd2* in myeloid cytokine production

Treatment of *Mbd2*$^{-/-}$ mice with DSS resulted in infiltration of pro-inflammatory cell populations along with an increase of gene expression of inflammatory cytokine burden (Figure 3.7 and 3.8A). In order to ascertain if the observed myeloid cell influx was a major factor in driving pro-inflammatory cytokine production (Figure 3.7), DSS treated or control *Mbd2*$^{-/-}$ or WT colon LP cells were cultured *ex vivo* with a protein transport inhibitor (Golgistop© 1ug/ml), to assess IL-1β, TNF and IL-10 production by flow cytometry.

In line with the total tissue cytokine expression in naïve mice (Figure 3.7), there was no difference in the total numbers of myeloid IL-1β^{+} or TNF^{+} cells between genotypes in untreated mice (Figure 3.8D and E). However, the total number of all IL-1β^{+} myeloid cells increased significantly in both genotypes after DSS treatment (mean fold change 4.03 in WT and 6.52 in *Mbd2*$^{-/-}$) (Figure 3.8D). Indeed there was a significantly greater increase in total IL-1β^{+} cells in *Mbd2*$^{-/-}$ versus WT mice (0.51±0.040 versus 0.24±0.038 x10^{6} cells). Similar changes were seen in TNF expression, with a significantly greater increase in total TNF^{+} myeloid cells in *Mbd2*$^{-/-}$ versus WT mice (0.101±0.0083 versus 0.066±0.0080 x10^{6} cells) (Figure 3.8E). In keeping with previous data suggesting a pro-inflammatory role for monocyte recruitment in DSS, this population was the largest overall contributor to myeloid IL-1β and TNF production.

Alongside this increase in pro-inflammatory cytokine production, there was no observed difference in the number of IL-10^{+} populations between treated groups. Macrophages

expressed the greatest levels of IL-10, in agreement with previous studies suggesting they are the key IL-10^{+} regulatory cell type in the colon (least square mean total number IL-10^{+} macrophages 0.012±0.0022 versus 0.017±0.0023 x10^{6} cells in *Mbd2*$^{-/-}$ and WT respectively) (43). These data suggested that the increased pro-inflammatory phenotype in *Mbd2*$^{-/-}$ DSS treated mice was not due to an alteration of IL-10 production, a key regulatory cytokine in the GI tract.

Taken together, the colon LP in DSS colitis was defined by a florid influx of IL-1β^{+} TNF^{+} monocytes disturbing the steady state myeloid composition of IL-10^{+} resident macrophages. This imbalance describes an inflamed mucosal surface ready to respond to invading pathogens brought about by a breakdown in barrier integrity. Indeed this polarization towards a pro-inflammatory response is dramatically increased in the absence of *Mbd2*, suggesting that *Mbd2* is required to limit damaging tissue pathology induced by DSS-associated epithelial challenge.

3.9 Assessment of *Mbd2*$^{-/-}$ response to *Trichuris muris* infection

Despite normal colonic T cell development (Figure 3.4C) in the absence of *Mbd2, in vitro* data suggest that *Mbd2*$^{-/-}$ naïve T cells have the capability to co-express Th1 (IFN-γ) and Th2 (IL-4) lineage specific cytokines. We therefore wanted to explore whether there was a role for *Mbd2* in other experimental models of colitis that rely on the adaptive immune system for effective host response (Chapter 1.6.6). In contrast to DSS in which an innate immune response predominates, *T. muris* produces a vigorous T adaptive immune response. Successful resolution of infection requires a polarised Th2 immune response, with susceptibility conferred by a Th1, IFN-γ dominated response (215). The load of infected eggs delivered to the host is also critical in determining polarisation of the host immune response and thus susceptibility to chronic infection: Low dose (20 eggs) results in a Th1 polarised immune response, and therefore chronic inflammation, in immunocompetent animals. However, high dose (200eggs) results in a IL-4, IL-13 polarised Th2 response (216) (Chapter 1.6.6).

A previous report showed that *Mbd2*$^{-/-}$ mice are susceptible to high dose *T. muris* infection displaying chronic inflammation, increased worm burden and IFN-γ mediated IgG2a antibody production (321). However the authors did not assess the infiltrating inflammatory cell types in the colon LP, the cellular sources of putative increased IFN-γ, or indeed if there was a dose-dependent effect on pathology. We sought to address these questions utilising our newly developed colon LP multi-parameter flow cytometry techniques:

3.9.1 General observations and experimental outline

WT and *Mbd2*$^{-/-}$ mice were gavaged with either 20 or 200 infective *T. muris* eggs at day 0 and monitored for 35 days. The main comparison was to be the effect of genotype at low and high dose infection on the development of colonic inflammation, in a pilot experiment. The below data therefore represent a single experiment with n=1 for the WT naïve control group, which prevented statistical comparison of naïve versus infected animals.

There were no adverse effects (weight loss etc.) noted during the course of the experiment in either genotype or infection dose. As expected, in the low dose infection group at day 35 there was evidence of mild colonic inflammation (caecal dilatation, increased colon weight), and scanty intraluminal worms, independent of genotype. Similarly at day 35 in the high dose infection group, WT mice as predicted had no evidence of colonic inflammation or intra-luminal worms, consistent with previous work suggesting immunocompetent mice induce a Th2 response favouring worm clearance (215). In high dose infected *Mbd2*$^{-/-}$ mice, however, there was evidence of chronic colonic inflammatory change and heavy intraluminal adult worm burden, replicating the findings of Hutchins et al (321). However the worm count and therefore burden of parasitology was not formally enumerated in this pilot experiment, as the tissues were used for cellular analysis by flow cytometry.

3.9.2 Serum antigen-specific responses in WT and *Mbd2*$^{-/-}$ mice

The serum of *Mbd2*$^{-/-}$ and WT day 35 infected mice was analysed by ELISA for the presence of *T. muris* specific IgG2a and IgG1 to confirm successful infection of the experimental mice and to give an indication of the skewing of the T cell response - IgG1 being IL-4 and IgG2a being IFNγ driven (Figure 3.9A and B). Consistent with the expected immune response to *T. muris*, there was a significant increase in the presence of parasite specific IgG2a and IgG1 in all infected versus control mice (Figure 3.9A and B) (321). In low dose infected mice, there was no significant effect of genotype observed on serum IgG2a or IgG1 at any of the dilution ranges analysed (Figure 3.9A and B). Similarly, in high dose infected mice there was no effect of genotype on the levels of parasite specific Th2 associated IgG1. This is consistent with previous published data, suggesting any altered susceptibility of *Mbd2*$^{-/-}$ mice to high dose infection is not mediated by an inability to mount a Th2 response (321). In contrast, and again consistent with previous data, there was a dramatic increase in the levels of parasite specific, IFN-γ associated IgG2a (1.15±0.16 versus 0.22±0.18 relative OD units at 1/1280 dilution) (Figure 3.8A) (321). These data confirm that all mice gavaged with *T.* muris were successfully infected, that WT mice produced an appropriate Th1-low dose and Th2-high dose antibody response, with *Mbd2*$^{-/-}$ mice developing an increased Th1 and equivalent Th2 antibody response in high dose infection (Figure 3.9).

3.9.3 Comparison of *Mbd2*$^{-/-}$ and WT colon LP cells in *T. muris* infection

The colon LP cells from infected and control mice were isolated, enumerated and surface stained for the antibody cocktail of myeloid and T-cell markers as described in Figures 3.2 and 3.3A.

3.9.3.1 Myeloid cells

The proportion of LP cells expressing CD45 was equivalent between genotypes in low dose infection. However, in keeping with a florid inflammatory process and increased total cell numbers (Figure 3.10A), there were a significantly greater number of CD45^{+} *Mbd2*$^{-/-}$ cells compared to WT in the high dose group (65.0±2.48 versus 34.3±3.9% of intact cells, Figure 3.10B). Exploring colon LP CD45^{+} cells in more detail revealed no effect of genotype on the total cell number of any of the myeloid sub-populations assessed in the low-dose group. However, in the high dose group, there were a significantly greater total number of colon LP monocytes (4.50±0.73 versus 0.19±0.17 x10^{6} cells), neutrophils (1.96±0.42 versus 0.015±0.0050 x10^{6} cells) and macrophages (3.42±0.71 versus 0.56±0.44 x10^{6} cells) in *Mbd2*$^{-/-}$ versus WT mice (Figure 3.10C). Thus, whilst there were increases in monocyte, neutrophil and eosinophil number in low dose infected versus naïve control, there was no effect of *Mbd2* deficiency in altering the myeloid composition between low dose infected mice (Figure 3.10C). In stark contrast, the myeloid compartment in high dose infection differed greatly depending on the presence or absence of *Mbd2*.

The colon LP of high dose infected WT mice closely resembled uninfected WT control, in keeping with existing data supporting parasite clearance in immunocompetent mice (213). However a significant proinflammatory monocyte and neutrophil dominated composition in *Mbd2*$^{-/-}$ high dose infection was observed (Figure 3.10C).

3.9.3.2 T cells

A robust host response to parasite infection requires an intact adaptive immune system. Indeed it has been suggested that the protective immunity against *T. muris* is almost completely dependent on CD4^{+} T lymphocytes (213).

In the low dose infection group there was no difference in the total cell numbers of any of the T cell populations analysed between genotypes. Given this was a pilot experiment it may be that numerically greater differences between the genotypes will become statistically significant in follow up work. Thus there was no difference in the number of colon LP TCRβ^{+} cells (3.16±0.76 versus 1.77±0.46 x10^{6} cells), which was predominately composed of CD4^{+} T cells (1.98±0.51 versus 1.15±0.56 x10^{6} cells, Figure 3.10D). In addition there was no significant difference in the total number of CD8^{+}, FoxP3^{+} regulatory T cells or CD44^{+}CD69^{+}

effector T cells (Figure 3.10D). Although there was no difference in the total number of Tregs between genotypes, *Mbd2* deficiency did affect the proportion of $CD4^+$ T cells expressing FoxP3; with a significant decrease seen in *Mbd2*$^{-/-}$ mice (5.33±0.47 versus 12.8±0.66 % of $CD4^+$ T cells expressing FoxP3).

In the high dose infection group, there were once again stark differences between genotypes (Figure 3.10D). There was a significant increase in the total number of *Mbd2*$^{-/-}$ $TCR\beta^+$ cells (3.87±0.50 versus 0.60±0.47 $x10^6$ cells) and again this was predominately composed of $CD4^+$ T cells (2.47±0.32 versus 0.38±0.34 $x10^6$ cells). Because of the substantial increase in the global *Mbd2*$^{-/-}$ T cell compartment, there was in addition a significant increase in the total number of *Mbd2*$^{-/-}$ $CD8^+$ T cells (0.71±0.13 versus 0.055±0.041 $x10^6$ cells). However, the total number of Tregs and Teff were equivalent between *Mbd2*$^{-/-}$ and WT mice. In addition, and in contrast to low dose infection, the proportion of $CD4^+$ T cells expressing FoxP3 was no different between genotypes (Figure 3.10D).

To ascertain whether local (i.e. colonic) changes in T cell populations conferred changes at a systemic level, draining mesenteric lymph nodes from low and high dose, WT and *Mbd2*$^{-/-}$ mice were obtained and analysed as above. There was interestingly no difference between genotypes in the proportions or total numbers of any of the T cell populations analysed (Figure 3.10E).

Thus, similar to the myeloid data, *Mbd2* deficiency exerted its greatest effect in the high dose infection group, with large increases in the $CD4^+$ T cell compartment. In addition there were also large numerical though not significant increases in colon LP T cells numbers in the low dose *Mbd2* deficient group, which one might expect to reach statistical significance in a further work.

3.9.4 Local and systemic cytokine responses in WT and *Mbd2*$^{-/-}$ mice

Clearance of *T. muris* requires an appropriate Th2 response. IL-4 has subsequently been identified as the key Th2 cytokine dictating the host response, with IL-4 deficient mice, or treatment with IL-4 depleting monoclonal antibody, negating parasite clearance (340). In addition IL-13 and TNF mediated effects have also been identified to be required for resolution of infection and mediating downstream Th2 responses (341), (342). In contrast, an inappropriate Th1 response leads to chronic infection, with transgenic mice producing high levels of IFN-γ, IL-12 or IL-18 demonstrating increased susceptibility to chronic infection (215). Thus we next assessed host cytokine responses to help delineate the relative contribution of Th1/Th2 responses to *Mbd2* deficient host susceptibility.

3.9.4.1 Antigen specific draining lymph node response

Draining MLN cells from day 35 low and high dose infected WT or *Mbd2*$^{-/-}$ mice were isolated and cultured for 72 hours with *T. muris* antigen, the supernatants of which were then assessed for Th1/2 cytokines by ELISA (Figure 3.11). In low dose infection, there was no difference in IL-4, IL-13 and IFN-γ from *Mbd2*$^{-/-}$ restimulated lymph nodes (Figure 3.11). In contrast, high dose infection was associated with significant increases in detected levels of IL-4, IL-5, IL-10, IL-13 and IFN-γ from *Mbd2*$^{-/-}$ restimulated MLN (Figure 3.11).

Given that the proportion and number of CD4^{+} T cells in draining MLN was equivalent independent of *Mbd2* deficiency or infection load (Figure 3.10E), this suggested the increased antigen specific cytokine detection was not a by-product of unbalanced T cell proportions in the cultures.

3.9.4.2 CD4^{+} T cell cytokine production

To assess whether there was an increased per cell production of cytokines in *Mbd2*$^{-/-}$ high dose infection, we assessed cytokine production by flow cytometry from colon LP or MLN T cells. Day 35 colon LP or MLN cells were isolated as described above and cultured with PMA/ionomycin for 3 hours before being surface stained with the T cell markers described above and thereafter stained intracellularly for the presence of IL-4, IL-5, IL-10, IL-13, IL-22, TNF and IFN-γ. The proportion of CD4^{+} T cells expressing these cytokines was then calculated, and is presented in Table 3.3A and B.

MLN

In the low dose infected MLN, there was no significant difference in the proportion of CD4^{+} cells expressing any of the cytokines analysed.

However, in the high dose infected MLN there was a significant increase in the *Mbd2*$^{-/-}$ CD4^{+} production of IFN-γ (4.56±0.30 versus 1.09±0.11 % CD4^{+} cells), IL-4 (6.13±0.21 versus 3.28±0.97 % CD4^{+} cells) and IL-13 (4.66±0.65 versus 2.73±0.72 % CD4^{+} cells) (Table 3.3A).

Colon LP

Regarding the low dose infected colon LP, there were no significant differences in the CD4^{+} T cell production of any of the cytokines analyzed, with the exception of IL-13. Here there was a surprising decrease in *Mbd2*$^{-/-}$ versus WT CD4^{+} T cell production of IL-13 (15.0±2.57% versus 43.40±4.18% proportion of CD4^{+} cells).

Unfortunately, in the high dose infected colon LP there was an unacceptable amount of dead cells (defined as >80% LiveDeadBlue staining of all events as assessed by flow cytometry) in 2 of the 3 WT samples that prohibited statistical analysis between high dose genotype groups (Table 3.3B).

3.9.4.3 $CD8^+$ T cell cytokine production

Colon LP $CD8^+$ T cells were too few in number to permit analysis independent of genotype or infection load. In addition there were no significant differences in any cytokine in each of the infection groups between genotypes in isolated MLN cells. This supports previous data reporting $CD8^+$ T cells as dispensable for host response to *T. muris* infection (343).

3.10 Colon LP monocytes in active IBD

In the work described above, we have observed that both infectious and chemical models of murine colitis are defined by a dramatic accumulation of LP monocytes. These effector cells capable of producing large amounts of inflammatory cytokines have been the subject of a recent study (see below) to assess their role in man, and indeed therefore whether common pathways exist between experimental colitis and IBD.

As described in Chapter 1.4, recent studies have identified intestinal monocytes and monocyte-derived macrophages as critical perpetrators in driving inflammation in IBD (113), (72). There is in addition heterogeneity seen in mice and human monocyte-macrophage expression of surface markers depending on their location within the GI tract (50). We therefore sought to identify whether $CD14^{High}$ monocyte-like and $CD14^{Low}$ resident macrophage populations could be identified in this homogenous colonic dataset both in healthy controls, quiescent and active IBD.

3.10.1 Patient Demographics and experimental outline

20 patients were consented for biopsy sampling for research purposes whilst undergoing a clinically indicated endoscopic procedure. Clinical phenotype data was collected on those patients with IBD including Vienna (CD) or Montreal (UC) classification of disease distribution and Harvey-Bradshaw (HBI) (CD) or Partial-Mayo (UC) clinical assessors of disease activity (Table 3.4 and Table 3.5). In addition a drug history was taken detailing the presence of any immunomodulator therapy. The mean age of the study population was 40.0 years, with an equivalent sex distribution.

Healthy controls

4 of the 20 patients underwent colonoscopy for the investigation of IBS symptoms in the absence of any other past medical history, had a normal procedure and were thus considered normal, healthy controls.

Quiescent IBD

10 of the 20 patients (3 UC, 7 CD) underwent colonoscopy for IBD assessment, 5 patients of which (3 UC, 2,CD) were asymptomatic, the remaining 5 patients (1 UC, 4 CD) had a mean HBI of 7.5 or partial Mayo score of 3 indicating mild disease activity. Only 1 patient was on immunomodulator therapy (azathioprine and infliximab). All 10 patients had a normal procedure; biopsies were taken of the transverse or sigmoid colon in areas of macroscopically normal mucosa and were thus considered quiescent IBD.

Active IBD

5 patients (2UC, 3CD) underwent colonoscopy for IBD assessment (note for 1 case biospes were taken from inflamed and uninflamed areas), with only 1 patient (CD) having clinical evidence of disease activity (HBI=7). 2 patients were taking azathioprine (1UC, 1 CD) with 1 patient taking methotrexate and adalimumab (CD). All 5 patients had macroscopic evidence of inflammation thought by the treating clinician to be caused by disease activity and were thus considered active IBD.

3.10.2 Colon LP analysis of healthy controls and IBD patients

Colon LP cells were isolated and surface stained for a range of markers (HLA-DR, CD11c, CD45, CD163, CD64, CD14 and CD209) before analysis by flow cytometry (See Figure 3.12A). As in mice, the number of $CD14^{High}$ monocyte-like cells in the steady state human colon was very low, accounting for approx. 0.2% of all intact cells (Figure 3.8B and (43)). This was similarly low in quiescent IBD, representing 0.4% of all intact cells. However in active IBD this population accumulated significantly in number to 2.0% of intact cells. In the active IBD group there was concordantly a significant increase in the ratio of $CD14^{High}$: $CD14^{Low}$ cells compared to quiescent IBD (0.90±0.090 versus 0.067±0.070) or healthy controls (0.90±0.090 versus 0.11±0.11) (Figure 3.12B). The ratio of monocytes:macrophages was similarly disturbed in DSS colitis with day6 DSS treated WT mice demonstrating significant bias of this ratio towards monocyte accumulation (Figure 3.12C). Thus, in mouse and human colonic inflammation there is an accumulation of monocyte-type cells.

3.11 Discussion

In chapter 3 we identified a key role for *Mbd2* in intestinal homeostasis. *Mbd2* displayed a tightly regulated spatial expression, with mRNA transcript increasing proximally to distally through anatomical divisions of murine GI tract (Figure 3.1A). *Mbd2* was therefore expressed at greatest levels in the rectum, significantly greater than proximal colon and small intestine. This relationship was preserved in human GI tract, with significantly greater *MBD2* mRNA transcript observed in human rectum versus small intestine (Figure 3.1B).

However rectal *MBD2* transcript fell significantly in patients with active IBD versus healthy controls (Figure 3.1C). We then interrogated the IIBDGC GWAS dataset to address whether *MBD2* polymorphisms conferred an increased risk of developing IBD. *MBD2* was not seen to be a risk susceptibility locus for IBD using this methodology (Figure 3.1D). It should be pointed at there are limitations in this observation, namely GWAS rely on the comparison of a large number of cases and controls to detect risk susceptibility at genome wide significance (104). Rare variants in putative susceptibility loci that are either not in the affected cohort, or present at low numbers, will clearly not be detected. In addition IBD is an extremely heterogeneous set of conditions. Two patients presenting with similar initial disease may have very different disease natural histories reflecting a poor understanding of the predictors of disease and treatment response (344). In addition, whilst GWAS will detect common variations in DNA sequence, this does not permit us insight into any role of post transcription or translation modification or splice variants in altering disease susceptibility.

As such analysing exosome sequencing of cases and controls may allow us to address the relationship of MBD2 and IBD pathogenesis more fully. In the case of *Mbd2* it is notoriously difficult to identify epigenetic regulators without simultaneously monitoring for MBD targets, DNA methylation and histone acetylation status (345). Lastly *MBD2* may not be a true IBD risk susceptibility locus, but has already been shown to control facets of the immune response in mice that may influence important areas of intestinal homeostasis in non-IBD pathways (318), (321), (319).

Therefore we suggest the next step to address the role of *MBD2* as an epigenetic risk locus in IBD will be to compare the acetylome, methylome and exosome of human intestinal samples comparing active IBD, quiescent IBD and healthy controls. As noted in Chapter 1.7, epigenetic processes are plastic, affected at key points in development and open to manipulation by environmental stimuli. Therefore it is perhaps more feasible that *MBD2* mediated changes in gene expression will be more likely detected by epigenetic analysis at mucosal surfaces, rather than germline changes in DNA sequence.

We next built upon previous work by simultaneously identifying multiple colon myeloid populations by flow cytometry (Figure 3.2) and used this gating logic to understand phenotypic differences in WT and *Mbd2*$^{-/-}$ mice in the steady state and under two models of GI tract inflammation (Figure 3.8 A,B,C and Figure 3.10 A,B,C).

There have been substantial recent developments in the ability of researchers to discriminate between mucosal MPs by flow cytometry analysis of surface marker expression. We have therefore built upon previous work to produce adapted gating logic from others using $CX_3CR1^{gfp/+}$ mice, utilising an array of MP markers to produce an integrated strategy for identifying myeloid cells. As noted in Chapter 3.4, the fact that we have not used CX_3CR1^{gfp} mice in our studies is a limitation to our gating strategy. The absence of this tool precludes the discrimination of CX_3CR1^{int} and CX_3CR1^{High} macrophage stages of differentiation, and confirmation that the previously presented CX3CR1 expression data matches our dataset. With these caveats, and the resultant time delay that crossing *Mbd2* deficient and CX_3CR1^{gfp} mice would have produced, we decided to accept these limitations.

Using these flow cytometry analysis techniques we have found that in the steady state there is a small but significant reduction in the proportion and number of $CD45^+$ colon LP cells in steady state *Mbd2*$^{-/-}$ mice (Figure 3.3B). In addition there was a selective reduction in the $CD11b^+$ $CD103^+$ DC subset (Figure 3.3C). It has been shown that *Notch2* and *Irf4* transcription factors are required for the normal development of $CD11b^+$ $CD103^+$ DCs (68) (65). However DC specific deletion of *Notch2* for example has been shown to have alterations on DC subsets in other tissues (68). Given that DC development in *Mbd2*$^{-/-}$ mice is normal in other tissues (318) we consider 2 possible hypotheses for intestinal specific depletion of *Mbd2* deficient $CD11b^+$ $CD103^+$ DCs; 1) that *Mbd2* is required for appropriate DC development that occurs after pre-cDC differentiation or 2) that *Mbd2* is required for surivival and/or conditioning of resident $CD11b^+$ $CD103^+$ DCs in the intestine.

$CD11b^+$ $CD103^+$ DCs have previously been show to be indispensable for effective clearance of the colonic pathogen *Citrobacter rodentium*, and suggested to be the obligate source of IL-23, a cytokine essential in promoting epithelial barrier defense and integrity via their stimulation of innate lymphoid cell subsets to produce IL-22 (346).

We then observed a striking susceptibility of *Mbd2*$^{-/-}$ mice to both chemical and infectious colitis. *Mbd2*$^{-/-}$ mice were exquisitely sensitive to the epithelial toxin DSS, resulting in increased weight loss, histological assessment of inflammation (Figure 3.6 B,C,D,E) and mRNA transcript of pro-inflammatory cytokines IL-1β and TNF (Figure 3.7). Flow cytometric analysis of the inflammatory infiltrate in the colon LP of *Mbd2*$^{-/-}$ mice revealed a significantly greater accumulation of monocyte and neutrophil populations compared to WT (Figure 3.8B

and C). In addition there was a significantly increased accumulation in the number of cells expressing TNF or IL-1β as assessed by Intracellular flow cytometry, with monocytes and neutrophils the largest producers of these cytokines (Figure 3.8D).

Taken together, DSS treated mice demonstrated a marked accumulation of IL-1β and TNF expressing monocytes and neutrophils, with *Mbd2* deficiency augmenting these aspects of the intestinal inflammatory response. Both in murine and human IBD it is now appreciated an inflammatory monocyte population accumulates with IL-1β and TNF producing capabilities (113). We speculate that *Mbd2* maybe acting in WT mice by directly limiting the pro-inflammatory potential within monocytes that are recruited to mucosal surfaces.

To test an intrinsic defect within monocytes, we will seek to address whether *Mbd2*$^{-/-}$ monocytes worsen colitis when in the presence of other *Mbd2* sufficient cells. Given a satisfactory monocyte specific transgenic system or antibody does not currently exist, we could employ lethally irradiated WT BM chimeras repopulated with WT and *Mbd2* deficient haemopoetic cells. This would permit assessment of both *Mbd2* deficient and WT monocytes in the same inflammatory system, therefore normalising for the overall level of inflammation that may be affecting monocyte response in *Mbd2*$^{-/-}$ mice.

To further pursue a monocyte specific role for *Mbd2* we could also assess the pro-inflammatory potential for these cells before they reach inflamed tissue sites. By performing analysis in this way, we negate the level of tissue inflammation as a variable in producing the observed phenotype. Alternatively, monocytosis in *Mbd2*$^{-/-}$ mice may simply represent an increased burden of inflammation, i.e. a readout of increased tissue destruction. In this hypothesis, other *Mbd2* deficient cell types may be the primary catalyst for dysregulated immune response. Such candidate cell types would include macrophages, based on their known role in tolerating the intestinal surface to the microbiota, DCs based on existing data supporting the role of CD11c^{+} cells in DSS colitis, the epithelium, based on existing data supporting its role in barrier function and antigen presentation and lastly neutrophils, which have well documented pro-inflammatory potential. These candidates and methods to explore their function in *Mbd2* deficient states is considered in Chapter 4.

Taken together we have built upon previous work by suggesting a global role for *Mbd2* that prevents aberrant accumulation of pathogenic cell types to the intestine thereby limiting inflammation after barrier disruption. Subsequent analysis in chapters 4 and 5 will seek to address the relative role of *Mbd2* deficient epithelial and haematopoetic cells in producing this effect.

Whilst DSS is a well-described innate model of animal colitis, we also sought to address whether *Mbd2* deficiency conferred increased predisposition to colonic inflammation mediated by adaptive immune responses. Indeed *Mbd2* deficiency resulted in dramatic colonic inflammation with *T. muris* at high dose in contrast to parasite clearance and minimal pathology in *Mbd2* sufficient mice. This was characterised by dramatic increases in $CD4^+$ T cell, monocyte and neutrophil numbers (Figure 3.10B,C,D), in addition to exaggerated parasite-specific Th1 associated antibody responses (Figure 3.9A). There was in combination increased Th1 cytokine from $CD4^+$ T cells both locally within the colon LP and distally in tissue draining lymph nodes (Table 3.3 A and B). However this was juxtaposed to an exaggerated Th2 cytokine response, and WT-equivalent Th2 antibody production that would normally herald successful parasite expulsion (Figure 3.9B and Table 3.3 A and B). Based upon the observed phenotype of increased susceptibility to infection, we expected to see an increased Th1-susceptibility conferring response and an absent Th2-resistance conferring response in *Mbd2*$^{-/-}$ mice.

The observation of an augmented bilateral Th1 and Th2 response therefore was surprising. That said there are data supporting the role of *Mbd2* in dual Th1/Th2 responses. *Mbd2*$^{-/-}$ naïve T cells and *in vitro* differentiated Th1/Th2 cells are capable of producing both increased IL-4 and IFN-γ under *in vitro* culture conditions with the mitogen PMA (319).

An alternate hypothesis however would be that the dysregulated inflammatory response we have observed in *Mbd2* deficient animals is due to worm persistence. *Mbd2* may be required by epithelial cells to prevent effacement of worms to the mucosal surface, or indeed for appropriate mucus production from colon epithelial goblet cells. Indeed the absence of *Mbd2* may confer a dysbiosis that renders the local environment more favourable for *T. muris* development in the colon. To address this hypothesis we could employ cell specific knockdown of epithelial (VillinCre), T cell (VavCre) or macrophage/DC (CD11cCre) *Mbd2* to restrict *Mbd2* deficiency to these cell types and assess the development of infection. Similarly pre-treating mice with broad-spectrum antibiotics to remove the gut microflora before *T. muris* infection could address the role of dysbiosis in infection development in WT and *Mbd2*$^{-/-}$. Lastly we could perform a timecourse experiment assessing worm burden and inflammation at Day 5,10,15,20,25 and 30. In this way we could see if excessive inflammatory responses occur at equivalent levels of parasite burden.

Taken together, we have expanded on the existing literature regarding the role of *Mbd2* in modulating response to Th2 infection. We have replicated the findings of Hutchins et al. of increased Th1 (IgG1) and Th2 (IgG2a) *T. muris* antibody responses in chronic high dose infection in *Mbd2* deficient mice, but in addition have suggested that *Mbd2* is required to limit

a $CD4^+$ rich colon LP infiltrate and concurrent Th1 and Th2 responses, both locally and systemically.

In the work described above, we have observed that both infectious and chemical models of murine colitis are defined by a dramatic accumulation of LP monocytes in WT animals. These effector cells, capable of producing large amounts of inflammatory cytokines, have been the subject of recent study (described below). To assess their role in man, and indeed therefore whether common pathways exist between experimental colitis and IBD we sought to understand whether analogous populations existed in man.

Human intestinal macrophages express CD68, CD33 and low levels of CD14, CX_3CR1, CD11c and CD163 (113), (43). However under inflammatory conditions a discreet $CD14^{High}$ monocyte population accumulates, which like the analogous $Ly6C^+$ $MHC\text{-}II^-$ monocyte population seen in mice is also present at reduced numbers in the steady state (120). These $CD14^{High}$ cells seem to be derived from circulating classical blood monocytes, express higher levels of CD11c, CD64, and CD163 and are heterogeneous in expression of HLA-DR and CD209 (121), (120). In addition $CD14^{High}$ cells produce large amounts of inflammatory cytokines such as IL-6, IL-23 and TNF (347).

There is in addition heterogeneity seen in murine and human monocyte-macrophage expression of surface markers depending on their location within the GI tract. Study inclusion criteria and reporting of tissue site sampling is therefore critical in interpreting surface expression data. Previous studies have employed either the pooling of endoscopic biopsies / surgical resection specimens from IBD patients or healthy controls independent of anatomical location (43), (113), (120), (347). There are no published data to our knowledge that report the phenotype of monocytes/macrophages exclusively sampled from colons of IBD patients and healthy controls.

These results support previous data reporting colonic inflammation in mouse and man is characterised by accumulation of pro-inflammatory TLR-expressing monocyte populations, capable of producing large amounts of IL-6, IL-23 and TNF and distinguished from resident inert macrophage populations by discreet surface marker expression (51), (113). Whilst endoscopic assessment of inflammation correlated very well with monocyte influx, with all 5 patients having a raised $CD14^{High}$: $CD14^{Low}$ ratio, only 1 patient with monocyte influx reported symptoms of disease activity. This disparity is entirely in keeping with the current paradigm of objective assessment of intestinal inflammation correlating poorly with clinical symptoms, supporting the need for regular mutli-modality assessments of disease activity to limit the damaging effects of sustained disease activity (348).

We have also replicated previous work in a homogenous patient dataset of colon specific sampling, identifying a $CD14^{High}$ monocyte-like cell accumulation in active IBD analogous to $LY6C^{+}$ $MHC\text{-}II^{+/-}$ cells in mice (Figure 3.12A). These data employed specific endoscopic biopsy sampling of inflamed (and in some cases non-inflamed areas in the same patient) tissues, in contrast to previously published data that has used a combination of whole tissue resections ± biopsy samples, often again combining multiple sections of GI tract (e.g. small and large intestine) and disease behaviours (stricturing, penetrating and pure inflammatory disease). One advantage of our dataset therefore is the more specific sampling of affected tissue (endoscopic sampling alone), from a single section of GI tract (colon) and from a single IBD disease behaviour (inflammatory).

The identification of a $CD14^{High}$ monocyte-like cell infiltrate in IBD highlights perhaps the similarity in colon inflammatory responses in mouse and man, suggesting there are common, currently poorly understood, pathways of immunological recruitment to mucosal surfaces. In particular the cellular sources of chemokines and associated breakdown in barrier function remain unanswered questions.

There are clearly caveats to the above observations. Pilot data from *T. muris* infection data will need to be investigated and replicated in larger group sizes, similarly human colonic samples are limited by a small number of cases and controls, with the inherent difficulties of IBD patient stratification well documented. Indeed $CD14^{High}$ expression of surface markers CD64 and CD163 has been shown to be increased compared to $CD14^{Low}$ cells in our and other cohorts, but not in all, underlining the distinction and perhaps ontogeny of the monocyte-macrophage axis is less clear in man.

In the next chapter we sought to refine our investigation of *Mbd2* deficiency to specific key cell types, to understand the respective roles of haemopoetic versus stromal cells and define the causative dysregulated genes in *Mbd2* deficiency.

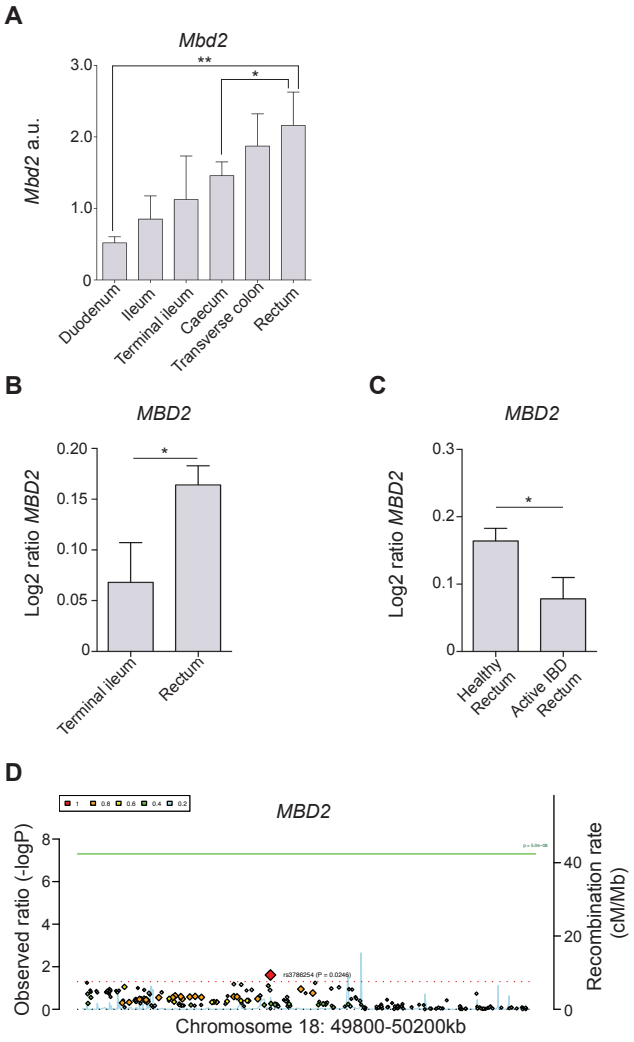

Figure 3.1 *Mbd2/MBD2* expression in the gastrointestinal tract and association with IBD

A. qPCR of 1cm sections of GI tract taken at measured intervals from the stomach pylorus*. *Mbd2* mRNA expression was determined by qRT-PCR, the mean value relative to *Gapdh* expression is presented. Mean values were obtained from 4 individual mice, data representative of 3 separate experiments. Primer sequences are in Table 2.5 **B.** Log2 ratio of *MBD2* expression from whole human genome microarray analysis of colonoscopic biopsies taken by Noble et al. 2008 from 31 healthy controls and **C.** 67 patients with active ulcerative colitis. **D**. Manhattan plot of the genome-wide association meta-analysis of 9 independent IBD case control series (16,054 Crohn's disease cases, 12,153 ulcerative colitis cases and 17,575 healthy controls) assessing *MBD2* as a putative risk susceptibility loci for IBD. The *x* axis is position on chromosome 18, the *y* axis is significance ($-\log_{10} P$ 2 tailed) of association derived by logistic regression, the green line shows genome wide significance level ($5x10^{-8}$). Statistical analysis for **(B), (C)** was performed by 2-way ANOVA, (* $p<0.05$)

* Duodenum 1cm, Ileum 18cm, Terminal Ileum 35cm, Caecum 37cm, Transverse colon 41cm, Rectum 46cm

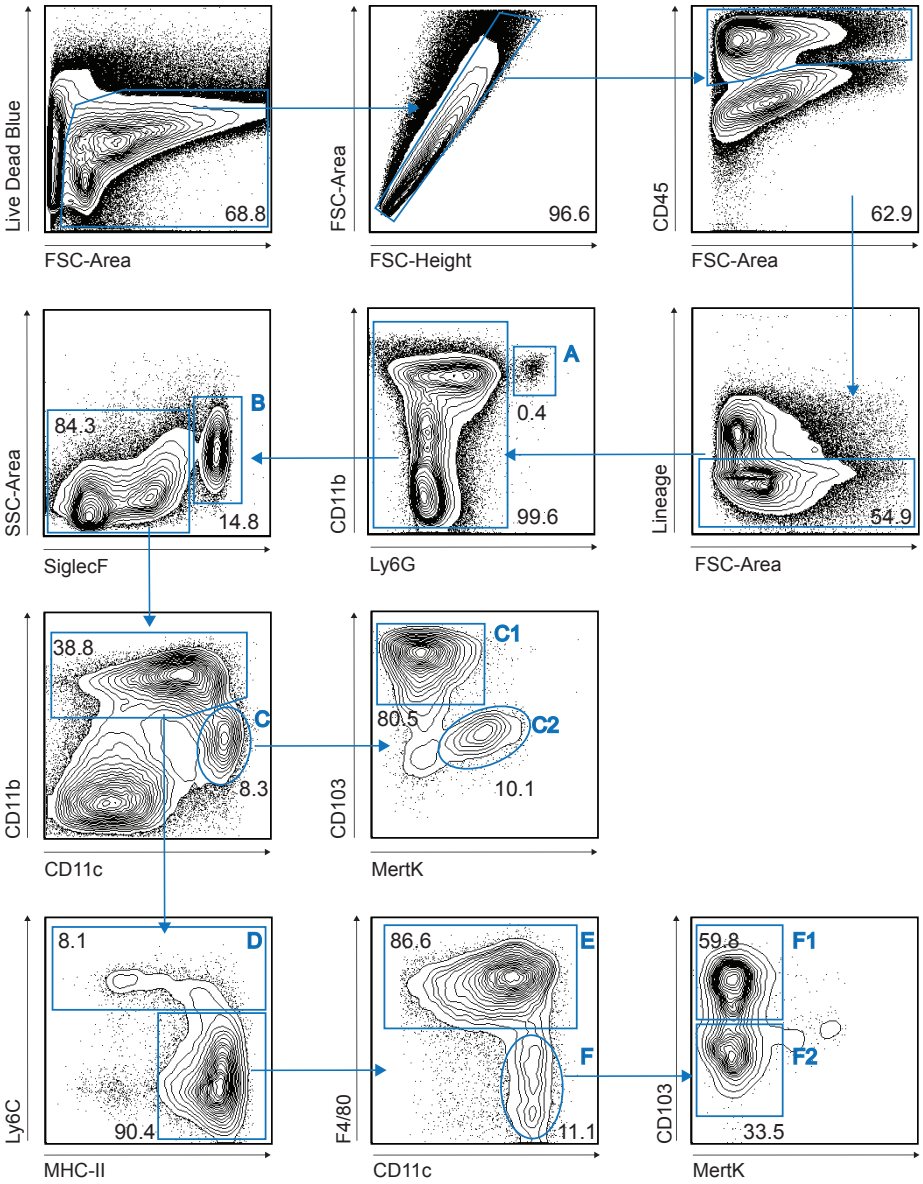

Figure 3.2 Flow cytometry gating strategy for colon lamina propria myeloid populations

Colon lamina propria cells were isolated from naive WT mice and analsyed for the expression of the following by flow cytometry; Live Dead Blue, CD45, Lineage (NK1.1,CD19,CD3,Ter119), CD11b, Ly6G,SiglecF,CD11c,CD103,Mert-K,Ly6C,MHC-II and F4/80. Representative contour plots display the following populations (as per Table 3.1) **A**. Neutrophils, **B**. Eosinophils, **C**. CD11b^{-} DC (subdivided on CD103 and MertK expression), **D**. Monocytes, **E**. Macrophages, **F**. CD11b^{+} DC (subdivided on CD103 and MertK expression).

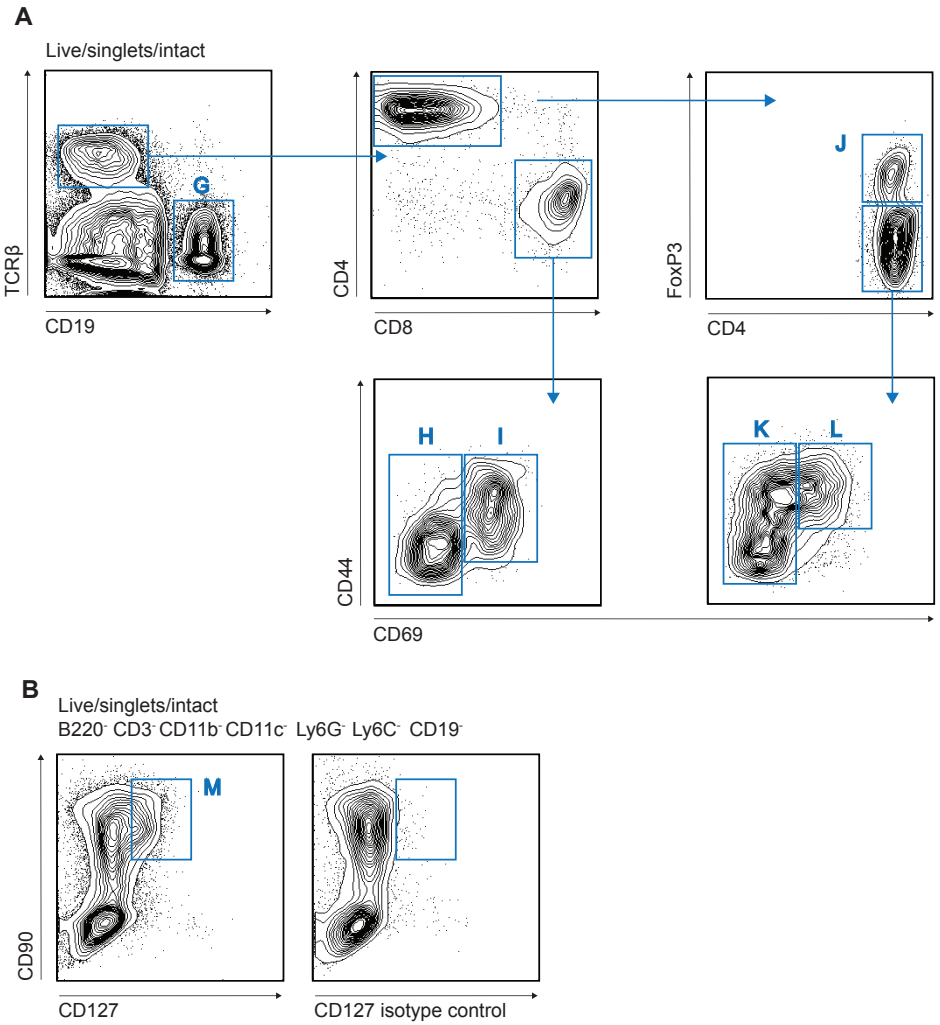

Figure 3.3 Colon LP Non-myeloid cell comparison in naive *Mbd2*$^{-/-}$ and WT mice
Colon lamina propria cells were isolated from naive WT mice and analsyed for the expression of the following by flow cytometry; Live Dead Blue, CD45, TCRβ, CD19, CD4, CD8, FoxP3, CD44, CD69, CD90, B220, CD3, CD11b, CD11c, Ly6G and Ly6C. Representative contour plots display the following populations **G**. B Cells, **H**. Naive CD8^{+} T cells **I**. CD8^{+} CD69^{+} T cells **J**. Tregs, **K**. Naive CD4^{+} T cells, **L**. CD4^{+} CD69^{+} T cells, **M** ILC

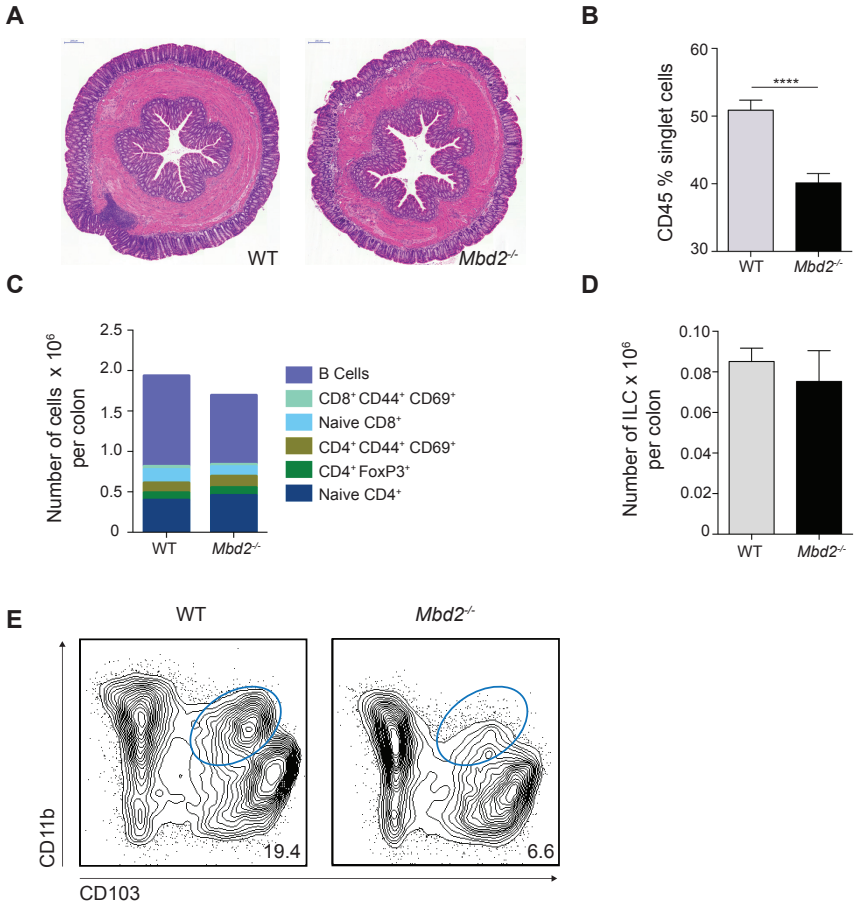

Figure 3.4 Naive Colon LP phenotyping in WT and *Mbd2*$^{-/-}$ mice

A. H&E stained transverse sections of 1cm distal colon from WT or *Mbd2*$^{-/-}$ mice at x10 magnification. Colon LP cells were isolated and surface stained as per gating strategy in Figure 3.2 and 3.3 from WT and *Mbd2*$^{-/-}$ mice. **B.** The proportion of colon LP singlet cells expressing CD45. **C.** the total number of cells from populations identified using the gating strategy in Figure 3.3A per colon **D.** The total number of ILCs per colon identified using the gating strategy in Figure 3.3B. **E**. Representative flow cytometry contour plots of colon LP cells isolated from WT or *Mbd2*$^{-/-}$ mice. Live, singlet, CD45^{+}, Lin^{-} (SiglecF, CD3, Ly6G, CD19), CD11c^{+}, F4/80^{-} gated cells showing DC subsets. **F**. Least square mean proportion of singlet cells for selected populations comparing WT and *Mbd2*$^{-/-}$ mice after adjustment for differences in total CD45 cells using linear regression modelling. n=15-20 per group analysed over 5 independent experiments (**p<0.01, ****p<0.0001).

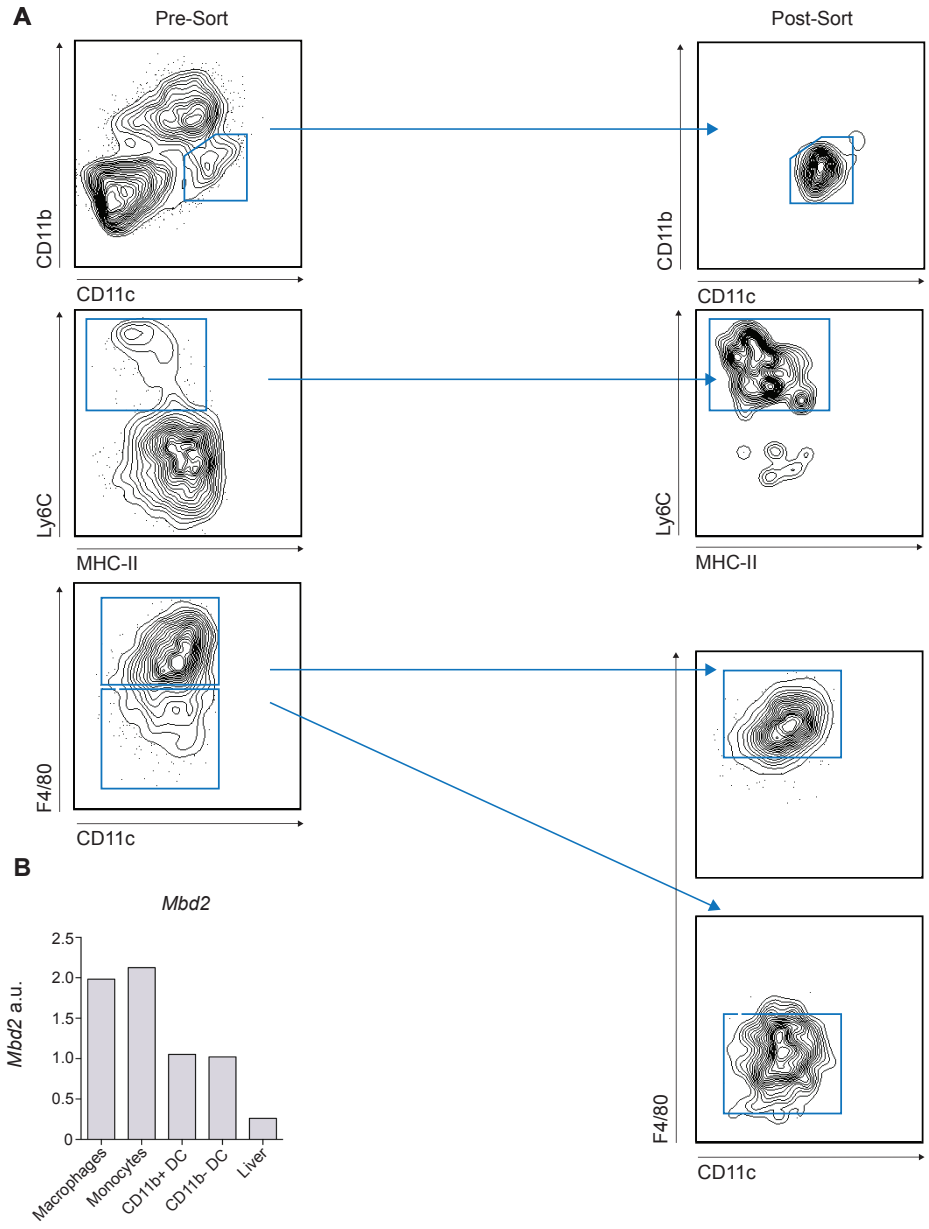

Figure 3.5 *Mbd2* expression in selected FACS purified colon LP myeloid subsets

A. Contour plots of naive WT colon LP cells stained for expression of Live Dead Blue, CD45, CD11b, CD11c, F4/80, MHC-II and Lineage (CD3, NK1.1,Ly6G) markers. Representative pre- and post- sort purity is presented for the populations described. **B**. mRNA expression of *Mbd2* assessed by RT-PCR of the myeloid subsets in **(A)**. Mean values are presented normalised for *Gapdh*, n=5 per group, representative of 3 independent experiments.

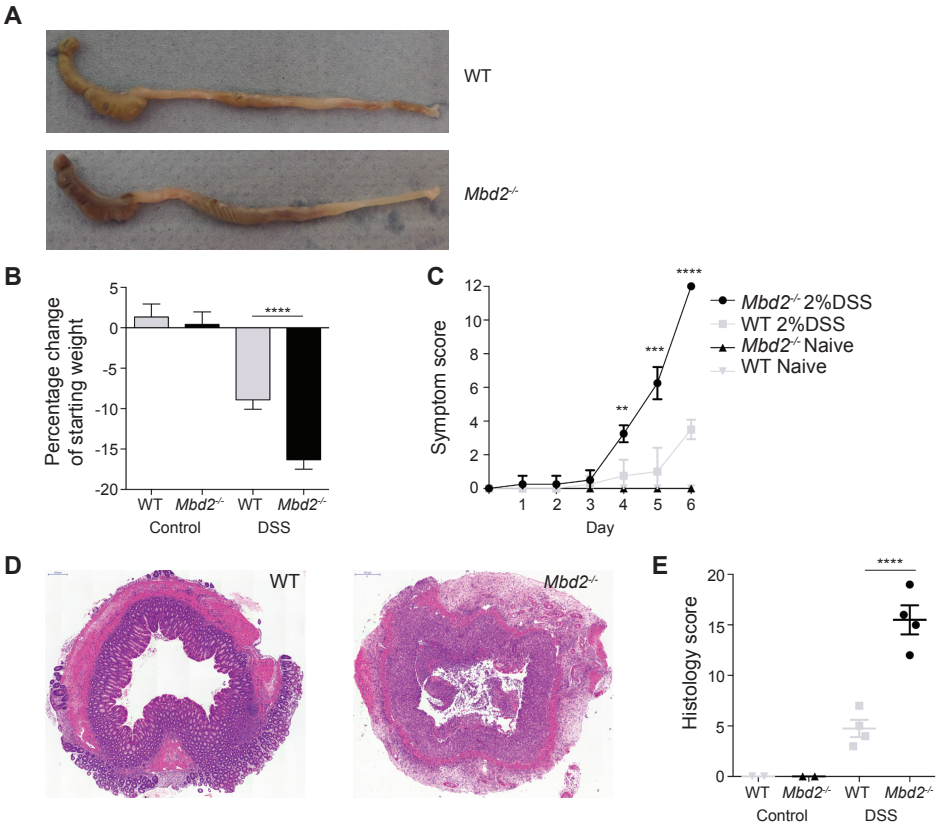

Figure 3.6 Susceptibility of *Mbd2*$^{-/-}$ mice to DSS colitis

Mbd2$^{-/-}$ or littermate WT mice recieved 2% DSS b/w in drinking water or normal drinking water for 6 consecutive days **A**. Photograph of WT and *Mbd2*$^{-/-}$ caecum and colon after division at the terminal ileum and anus post dissection. **B**. Least sqauare mean day 6 weight change of DSS treated and naive control, WT and *Mbd2*$^{-/-}$ mice as a percentage of starting body weight, n=15-25 analysed by linear regression modelling of 4 separate experiments. **C**. Mean symptom score per day over the duration of DSS treatment. Cumulative score as per Table 2.3 of weight loss (0-4), diarrhoea (0-4) and per rectal bleeding (0-4). n=4 per group, representative of 4 independent experiments **D.** H&E stained transverse sections of distal WT or *Mbd2*$^{-/-}$ DSS treated colon, x10 magnification. **E.** Least square mean±SEM blinded histology score of inflammation of (**D**), as per Table 2.4, comprising inflammatory cell infiltrate (0-4, +0.5 per ulcer), Goblet cell depletion (0-4, +0.5 per crypt abscess), Muscosal thickening (0-4), submucosal cell infiltration (0-4) and architecture destruction (0-4), n=8 per group analysed by linear regression modelling of 2 separate experiments. Representative data from 4 independent experiments (*p<0.05, **p<0.001, ***p<0.0005, ****p<0.0001).

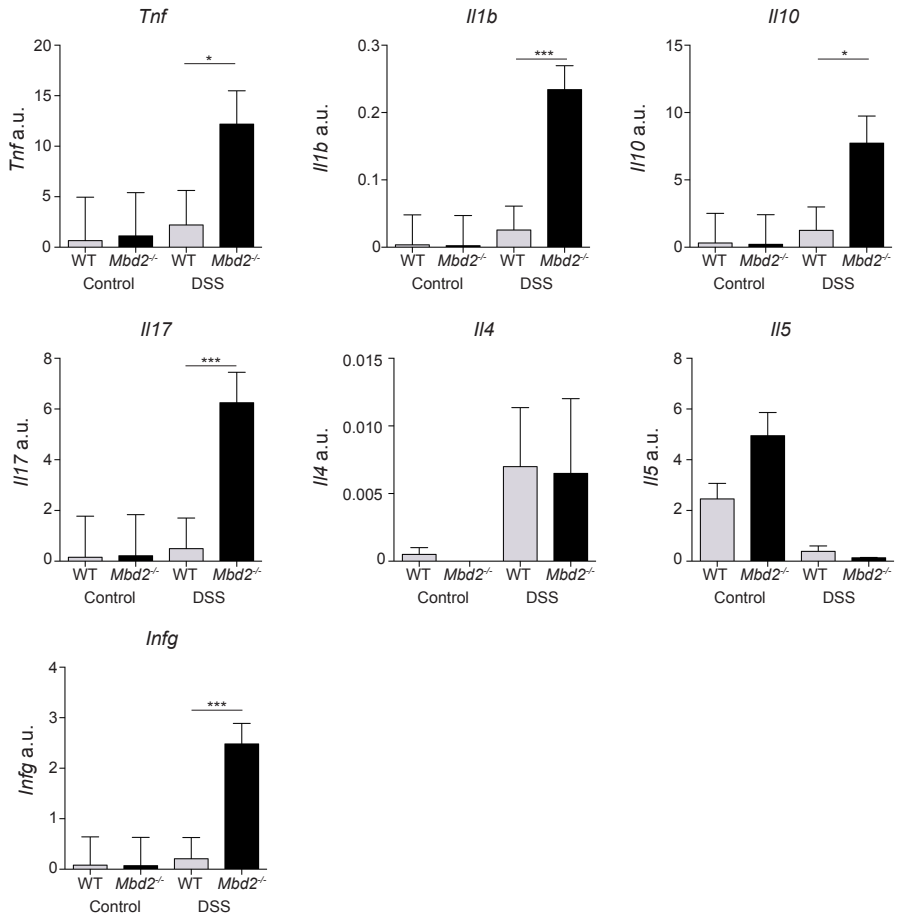

Figure 3.7 Colon mRNA expression of selected cytokines during DSS colitis

qPCR of 1cm sections of distal colon from Day6 2%DSS treated or drinking water control WT or *Mbd2*$^{-/-}$ mice. Selected cytokine mRNA expression was determined by qRT-PCR, the least square mean value relative to *Gapdh* expression is presented. Least square mean values were obtained from linear regression of 3 independent experiments, n=8-15 per group. Primer sequences are in Table 2.5. (*p<0.05, ***p<0.001).

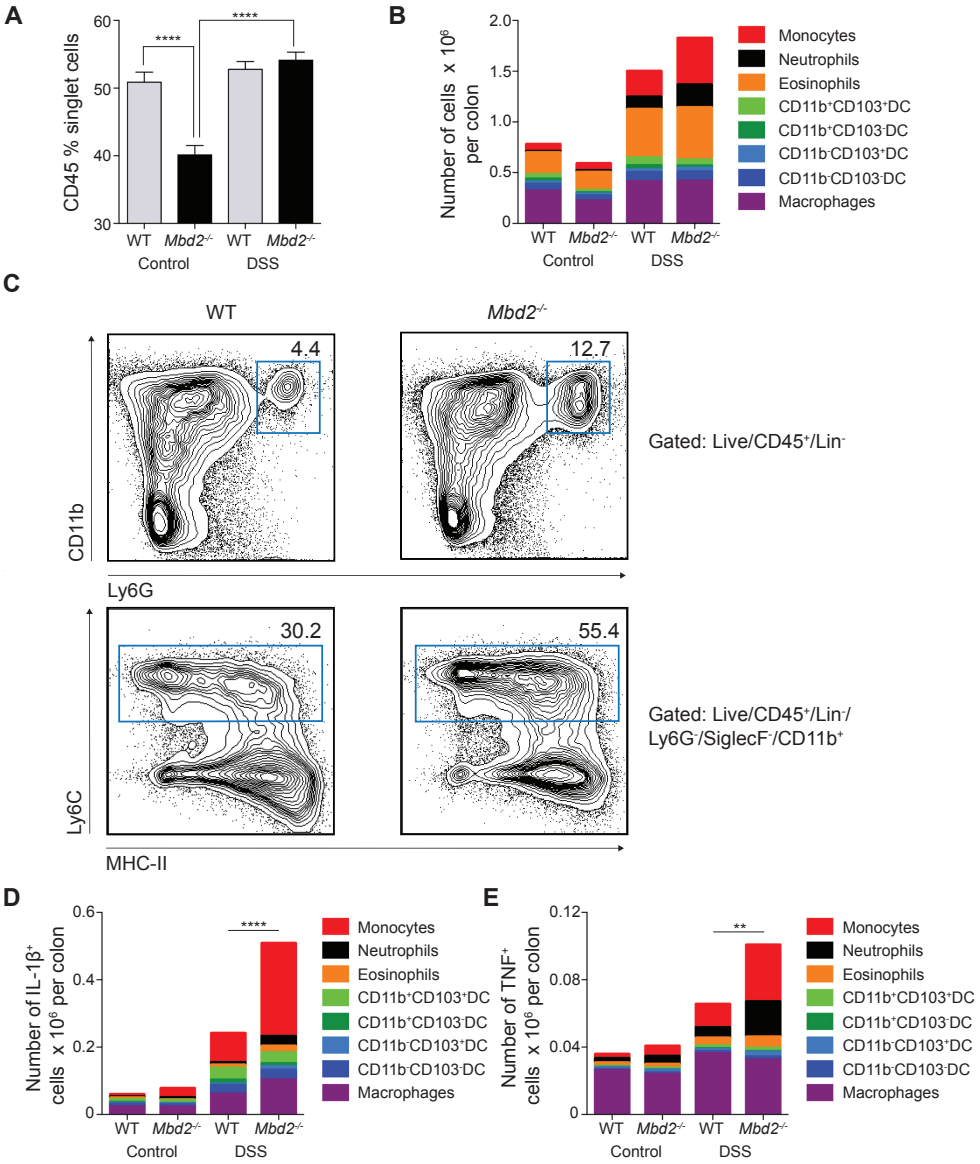

Figure 3.8 Flow Cytometry analysis of the colon lamina propria in DSS colitis

Mbd2$^{-/-}$ or littermate WT mice recieved 2% DSS b/w in drinking water or normal drinking water for 6 consecutive days, colon LP cells were isolated and assessed for the expression of SiglecF, Ly6G, CD11b, CD11c, F4/80, MertK, CD64, CD45, CD103, and Lineage markers (CD3, CD19, NK1.1, Ter119) by flow cytometry. **A**. The proportion of singlet cells expressing CD45 in naive and DSS treated WT and *Mbd2*$^{-/-}$ mice. **B**. The least square mean total number of cells x10^6 per colon is presented for the populations outlined in Figure 3.2, n=15-25 per group, analysed by linear regression of 6 independent experiments. **C**. Representative flow cytometry contour plots in Day6 DSS treated WT and *Mbd2*$^{-/-}$ mice for neutrophil and monocyte populations as defined in Figure 3.2. The least square mean number of colon LP myeloid cells x10^6 per colon after 3 hr incubation with 1µl/ml GolgiStop expressing IL-1β **(D)** or TNF **(E)** as assesed by intracellular staining and flow cytometry compared to isotype antibody control, n=12-15 mice per group analysed by linear regression of 3 independent experiments. **p<0.01, ****p<0.0001

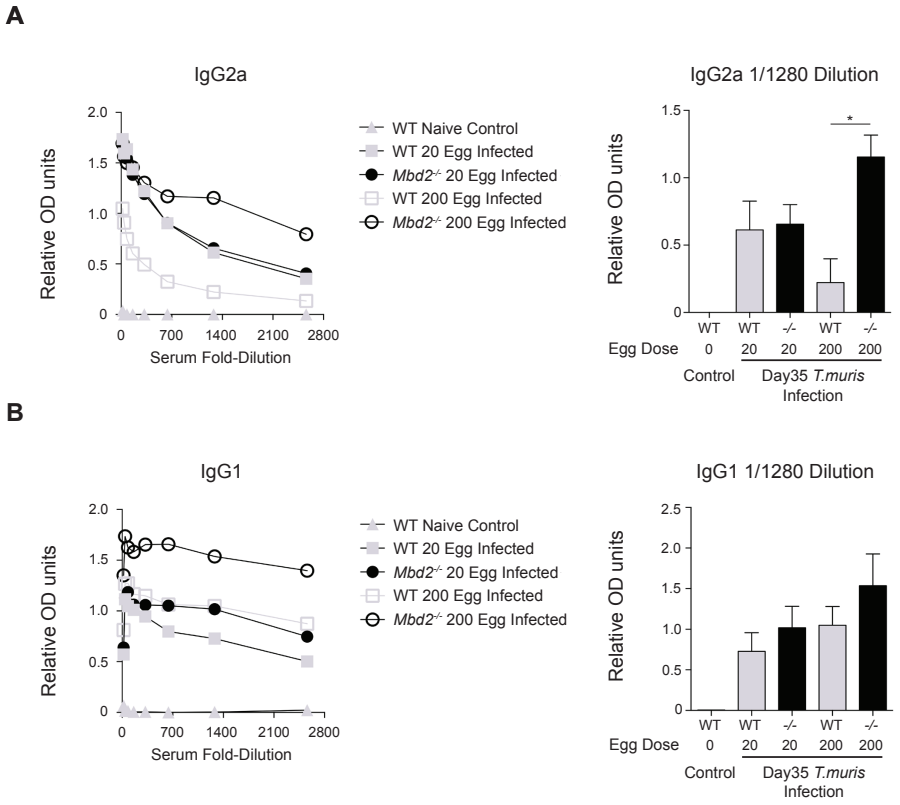

Figure 3.9 Day35 20 or 200egg *T.muris* infection *Mbd2*$^{-/-}$ verus WT antigen specific serum IgG1 and IgG2a

Serum from day 35, 20 or 200egg *T.muris* infected *Mbd2*$^{-/-}$ or WT mice was collected and parasite-specific serum antibody titers performed by ELISA with *T. muris* Ag-coated dishes and anti-isotype detection antibody for IgG2a **(A)** and IgG1 **(B)** mean flouresence data is presented from n=1-4 mice per group analysed in duplicate**.** 1/1280 dilution data is presented in bar chart format, showing data±SEM from 1 pilot experiment n=1-4 per group analysed by 2-way ANOVA. (*p<0.05).

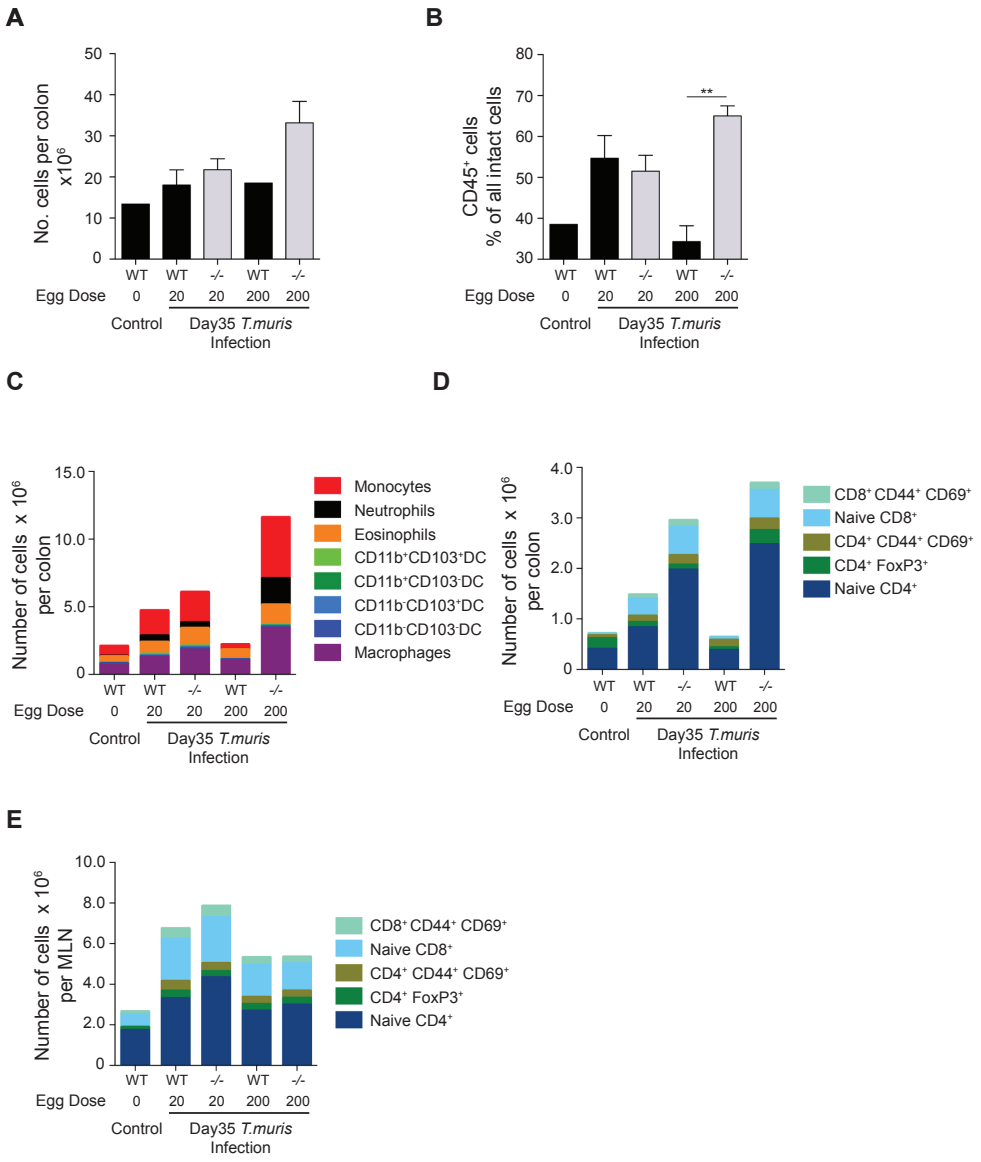

Figure 3.10 Day35 20 or 200egg *T.muris* infection *Mbd2*$^{-/-}$ verus WT FACS analysis of T cell and myeloid populations

Colon LP and MLN cells were isolated and assessed for the expression of SiglecF, Ly6G, CD11b, CD11c, F4/80, MertK, CD64, CD45, CD103, CD4, Foxp3, CD8, CD44, CD69 and Lineage markers by flow cytometry. **A**. Mean±SEM total LP cell counts enumerated per colon. **B**. The proportion of intact colon LP cells expressing the surface marker CD45. The mean total number of cells x10^6 per colon (**C** and **D**) and per MLN (**E**) is presented for the populations outlined in Figure 3.2 (**D**) and for Treg ($CD4^+$ $Foxp3^+$), Teff ($CD4^+$ $Foxp3^-$, $CD44^+$ $CD69^+$), $CD4^+$ ($CD4^+$, $Foxp3^-$ $CD44^-$ $CD69^-$) and $CD8^+$ T cells (**C** and **E**). n=1-4 mice per group from 1 pilot experiment analysed by 2 way ANOVA (**p<0.01).

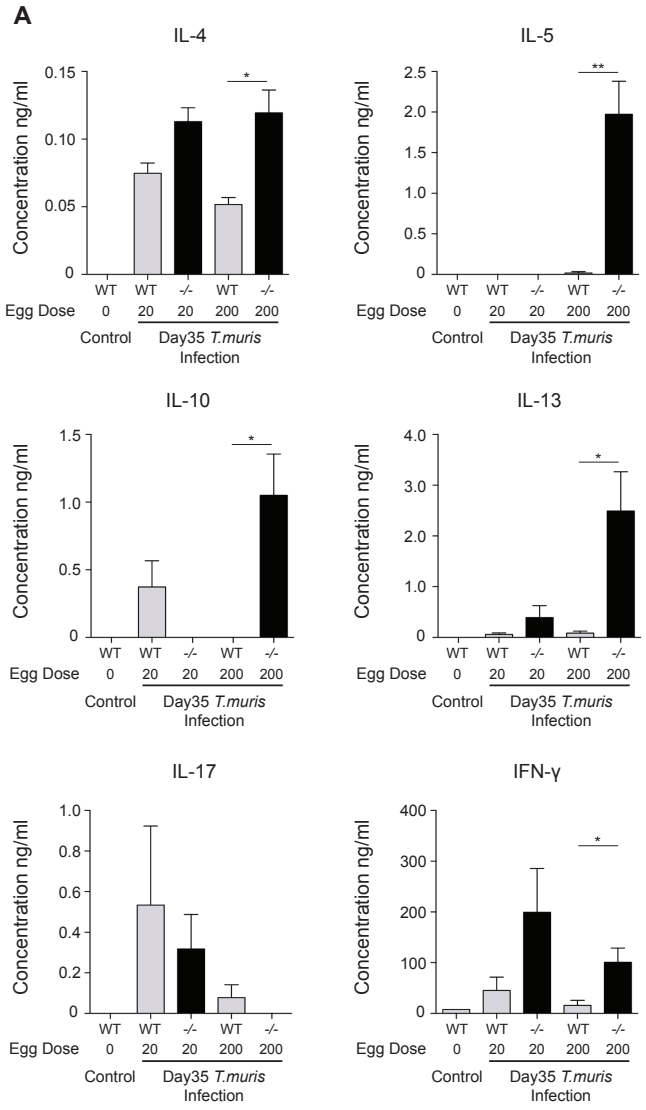

Figure 3.11 Day35 20 or 200 egg *T.muris* infection WT versus *Mbd2*$^{-/-}$ MLN antigen specific cytokine response

MLN cells were isolated and stimulated for 72 hours with 1µg/ml *T.muris* antigen and cytokine levels in supernatants assessed by ELISA, performed in triplicate. n-1-4 mice per group, from 1 pilot experiment analysed by 2-way ANOVA (*p<0.05, **p<0.01).

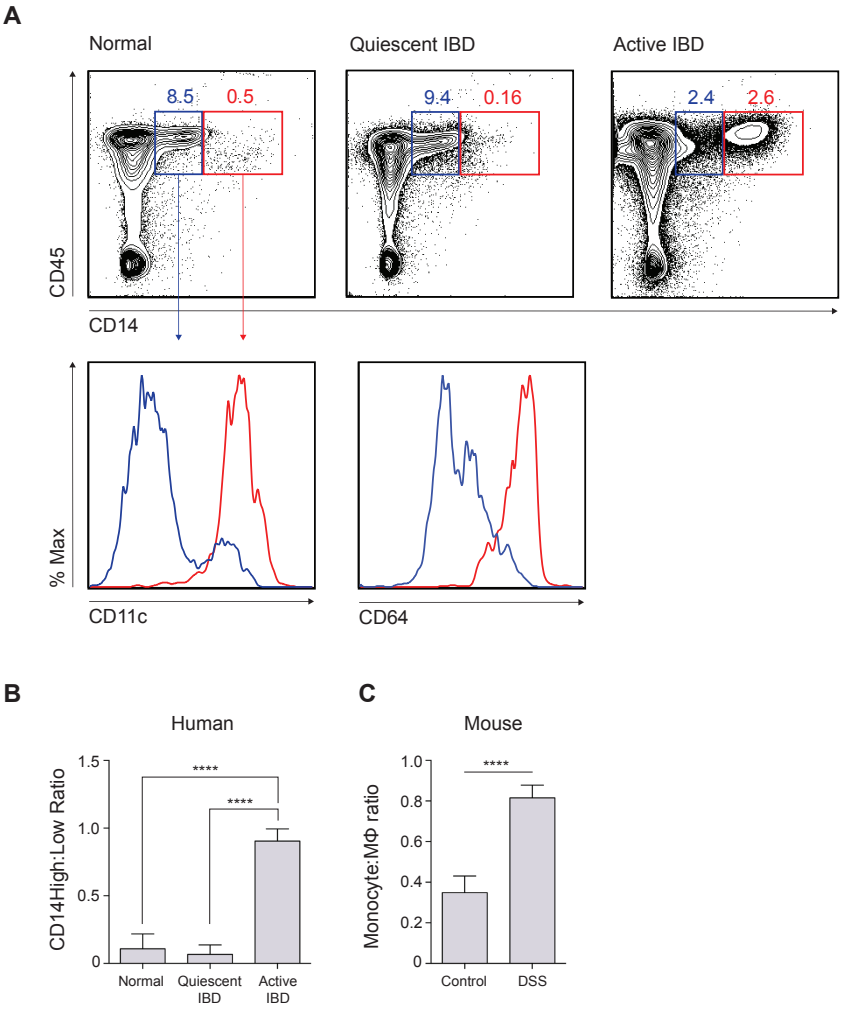

Figure 3.12 Human colon LP CD14^{+} cells in IBD and healthy controls

Colon LP cells from endoscopic biopsies were isolated from patients with endoscopically active or quiescent IBD or healthy controls, enumerated and surface stained with the following antibody cocktail; CD45, HLADR, CD103, CD172a, CD141, CD11c, CD1c, CD64, CD163, CD14 and lineage markers CD3, CD19, CD20 and CD56 and analysed by flow cytometry. **A**. Representative FACS contour plots of Live, Lin^{-} gated cells showing CD14^{high} and CD14^{low} populations. **B**. Mean±SEM for the ratio of CD14^{high} to CD14^{low} cells, n=4-10 per group analysed by 1-way ANOVA (****p<0.0001).

Population	Surface Phenotype										Proposed Population
	CD11b	Ly6G	SiglecF	CD11c	Ly6C	MHC-II	MertK	CX3CR1*	CD64	CD103	
A	+	+	-	-	-	-	-	+	-	-	Neutrophil
B	+	-	+	+	-	+	-	+	-	-	Eosinophil
C1	-	-	-	+++	-	++	-	-	-	+	CD11b- CD103+ DC
C2	-	-	-	+++	-	++	+	+	+	-	CD11b- CD103- DC
D	+	-	-	+	++	+	+	+	++	-	Monocyte
E	+	-	-	++	-	+	++	+++	+++	-	Macrophage
F1	+	-	-	+++	-	++	-	-	-	+	CD11b+ CD103+ DC
F2	+	-	-	+++	-	++	-	+	+	-	CD11b+ CD103- DC

Table 3.1 Summary of steady state myeloid marker surface expression in colon myeloid LP cells

Expression of surface markers as assessed by flow cytometry of the myeloid subsets discussed in Figure 3.2. *CX3CR1 expression was not directly measured due to the absence of a CX3CR1$^{gfp/+}$ mouse in these experiments, but was inferred from previous work utilizing a similar gating strategy.

Population	Naïve		DSS		Fold change		p value	
	WT	*Mbd2-/-*	WT	*Mbd2-/-*	WT	*Mbd2-/-*	Naïve	DSS
Neutrophils	0.013	0.015	0.121	0.226	9.234	14.85	0.933	0.0001
Monocytes	0.068	0.070	0.254	0.459	3.736	6.57	0.9722	0.0001
Eosinophils	0.216	0.180	0.477	0.515	2.204	2.87	0.4215	0.2959
CD11b+ CD103-	0.043	0.022	0.078	0.060	1.805	2.69	0.011	0.0063
CD11b- CD103-	0.021	0.018	0.026	0.035	1.245	1.97	0.46	0.02
Macrophages	0.321	0.222	0.413	0.417	1.286	1.88	0.0396	0.914
CD11b- CD103+	0.067	0.050	0.090	0.092	1.352	1.84	0.0881	0.7542
CD11b+ CD103+	0.031	0.014	0.042	0.023	1.353	1.63	0.0002	0.0001

Table 3.2 Summary of colon LP myeloid population cell numbers in the steady state and after DSS colitis.

The total number of colon LP myeloid cells x10^6 per colon was identified by analyzing the proportion of singlet cells per million cells acquired by flow cytometry and enumerating against the total number of cells isolated per colon. Fold change in least square mean total number is presented, ordered from largest to smallest change after DSS treatment. n=15-25 per group, analysed by linear regression of 6 independent experiments. Statistical significance is presented for the difference between WT and *Mbd2-/-* least square mean total number of cells in either steady state or after 6days continuous DSS treatment, shaded grey for $p<0.05$.

A) MLN CD4 T cells

Dose	Low			High			Naïve
Genotype	WT	*Mbd2*$^{-/-}$	p value	WT	*Mbd2*$^{-/-}$	p value	WT
IFN-γ	2.88	3.89	0.5042	1.09	4.67	0.0003	0.73
IL-4	1.94	4.43	0.0615	3.28	6.13	0.0461	1.41
IL-5	0.72	1.13	0.2171	0.82	1.32	0.1521	0.28
IL-10	7.87	5.81	0.1335	5.62	6.83	0.1542	5.78
IL-13	3.75	4.12	0.7594	1.93	4.66	0.0191	0.70
IL-17	25.87	30.07	0.173	28.03	34.40	0.4592	18.10
IL-22	1.23	1.80	0.3342	0.45	1.57	0.0082	0.33
TNF	16.60	11.70	0.3777	21.37	9.64	0.0685	9.16

B) Colon LP CD4 T cells

Dose	Low			High			Naïve
Genotype	WT	*Mbd2*$^{-/-}$	p value	WT	*Mbd2*$^{-/-}$	p value	WT
IFN-γ	49.93	56.80	0.6783	30.30	53.13	N/A	41.00
IL-4	6.85	4.12	0.4241	14.00	14.38	N/A	1.77
IL-5	7.93	3.51	0.372	8.22	16.00	N/A	3.12
IL-10	8.97	9.28	0.9474	4.60	7.21	N/A	7.30
IL-13	43.40	15.00	0.0044	10.90	42.03	N/A	5.71
IL-17	18.40	12.45	0.3947	7.34	8.82	N/A	8.93
IL-22	2.90	0.63	0.1251	1.52	4.95	N/A	1.52
TNF	10.89	4.53	0.1665	4.36	18.50	N/A	3.05

Table 3.3 CD4^{+} T cell responses in *T. muris* colitis

MLN (A) and Colon LP (B) cells were isolated, enumerated and cultured for 3 hours with 10ng/ml PMA and 1μg/ml ionomycin from 20 (low) or 200 (high) egg *T.Muris* infection in WT or *Mbd2*$^{-/-}$ mice. Cells were surface stained for CD45, CD4, CD3 and TCRβ before intracellular staining for the above cytokines and analysis by flow cytometry. The mean proportion of CD4 T cells producing the above cytokines compared to isotype antibody control is presented. n=1-4 per group and TCRβ before intracellular staining for the above cytokines and analysis by flow cytometry. The mean proportion of CD4 T cells producing the above cytokines compared to isotype antibody control is presented. n=1-4 per group

Disease Classification

Vienna Classification for Crohn's disease		
A1	Age at diagnosis	<40y
A2		>40y
L1	Location	Ileal
L2		colonic
L3		Ileocolonic
L4		Upper
B1	Behaviour	Non-stricutring, non-penetrating
B2		stricturing
B3		penetrating
+p		perianal disease, added to B1-3 if concomitant perianal involvement is present

Montreal Classification for Ulcerative colitis		
E1	Ulcerative proctitis	Involvement limited to the rectum
E2	Left sided	Involvement limited to the colorectum distal to the splenic flexure
E3	Extensive	Involvement extending proximal to the splenic flexure

Clinical Scoring

Partial Mayo score for Ulcerative Colitis		
Component	*Score*	*Description*
Stool frequency	0	Normal
	1	1-2stools/day more than normal
	2	3-4stools/day more than normal
	3	>4stools/day more than normal
Rectal Bleeding	0	None
	1	Visible blood with stool less than half the time
	2	Visible blood with stool half of the time or more
	3	Passing blood alone

Harvey Bradshaw Index for Crohn's disease		
Component	*Score*	*Description*
General well being	0	very well
	1	slightly below average
	2	poor
	3	very poor
	4	terrible
Abdominal pain	0	none
	1	mild
	2	moderate
	3	severe
Number of liquid stools per day		
abdominal mass	0	none
	1	dubious
	2	definite
	3	tender
Complications	1 point for each	arthralgia
		iritis / uveitis
		erythema nodosum, pypderma gangrenosum or apthous ulcers
		anal fissures, fistulae or abscesses
		other fistula
		fever during previous week

Table 3.4
Overview of the classification of IBD phenotype and clinical severity scores

				Vienna Classification (CD)						Drugs		Clincal Activity		Endoscopic score	
Disease category	IBD	Sex	Age	Age	Location	Behaviour	Montreal Classification (UC)	Biopsy Location	Inflammed?	Immunomodulators	Other	Harvey-Bradshaw index (CD)	Partial Mayo (UC)	SES (CD)	Full Mayo (UC)
Normal	-	M	57					Duodenum	N						
Normal	-	F	39					Sigmoid	N						
Normal	-	F	56					Sigmoid	N						
Normal	-	F	47					Sigmoid	N						
Quiescent	CD	M	41	A1	L2	B1		Ileum	N	AZA, IFX		5-7			
Quiescent	CD	F	35		L3	B1		Transverse	N			8-16		12	
Quiescent	CD	F	35		L3	B1		Rectum	N			8-16		12	
Quiescent	CD	M	42	A1	L1	B2		Transverse	N			5-7		4.6	
Quiescent	CD	M	42	A1	L1	B2		Sigmoid	N			5-7		4.6	
Quiescent	CD	F	27		L1			Transverse	N					2	
Quiescent	CD	F	27		L1			Sigmoid	N					2	
Quiescent	UC	F	65					Pouch	N				N/A		
Quiescent	UC	M	45					Pouch	N						
Quiescent	UC	F	27				E2	Sigmoid	N				3-5		5
Active	CD	M	49	A1	L1	B2		IC anastomosis	Y			<5		4.6	
Active	CD	M	27		L2			Colon	Y	MTX, ADA		5-7		66	
Active	CD	M	52	A2	L1	B2		Transverse	Y	AZA		<5			
Active	CD	M	30	A1	L3	B1		Transverse	Y			<5		7.2	
Active	UC	M	27				E3	Rectum	Y	AZA	5'ASA		3-5		5
Active	UC	F	27				E2	Rectum	Y				3-5		5

Table 3.5 Patient demographic and clinical phenotyping data for human samples

Patient demographic and clinical phenotyping data. IBD classification, disease behavior, drug history and clinical activity was assessed in patients with active or quiescent IBD as adjuded on endoscopy by the consenting physician or healthy controls (AZA=azathioprine, IFX=Infliximab, MTX=methotrexate, 5'ASA=aminosalicylic acid)

Chapter 4

The role of *Mbd2* deficient haematopoietic cells in colonic inflammation

4.1 Introduction

In Chapter 3 we identified a role for *Mbd2* in modulating an increased susceptibility to colonic inflammation. This was characterised by an accumulation of IL-1β^{+} and TNF^{+} myeloid cells, particularly monocytes and neutrophils. We also identified myeloid cells as displaying high levels of *Mbd2* transcript. Clearly in animals in which all cell types are *Mbd2* deficient, it is difficult to make inferences on the respective roles of *Mbd2* deficient populations to this phenotype. We therefore sought to delineate *Mbd2* deficient populations in more detail, and hypothesized that *Mbd2* deficient haematopoietic cells were likely candidates for further analysis for several reasons.

Firstly, there is an increasing body of evidence to suggest inflammatory monocytes as directly pathogenic in DSS colitis: mice deficient in CCR2, a chemokine receptor expressed by blood monocytes, are less susceptible to colonic inflammation (51). Similarly, administration of an anti-CCR2 depleting antibody thought to selectively affect LY6C^{High} blood monocytes, ameliorates colitis with lower levels of IL-6 and IL-1β in colonic tissue (47). Additionally, DSS colitis is significantly reduced in mice whose monocytes are unable to produce TNF (71). Supporting a more dominant role in intestinal inflammation for monocytes versus neutrophils, mice deficient in CCL2/CCR2 mediated monocyte recruitment are more susceptible to *Toxoplasma gondii* (*T. gondii*) infection, whereas *in vivo* neutrophil depletion has no effect on disease progression (349), (350), (351).

Other candidate haematopoietic cells for *Mbd2* mediated predisposition to colitis include macrophages and DCs. Both are critical in maintaining the immunological balance between tolerance and inflammation by pivoting the adaptive response through antigen presentation and local contribution to the cytokine milieu. DCs have the capacity to manipulate local inflammatory responses by release of cytokines and chemokines through activation of PRRs, which in turn can influence other myeloid cells (352). Indeed a dysregulated immune response to the commensal microbiota is one of the hallmarks of IBD in man, with mutations in the *NOD2* pathogen recognition molecule (expressed by both DCs and macrophages), being the strongest heritable risk factor for CD (107), (108), (353).

Previous data directly assessing the contribution of DCs in the DSS model again suggest a role in pathogenesis. For example, Berndt et al. reported an exacerbated day 7 colitis conferred by transfer of BMDCs before DSS treatment, characterised by increased histological severity score and earlier development of PR bleeding (354). In addition, using a CD11c-DTR/GFP mouse to selectively deplete CD11c expressing cells, they identified a reduced severity of day 7 colitis characterised by less rectal bleeding and histological severity in those mice depleted of CD11c cells. Abe et al. similarly report an ameliorated

phenotype of DSS colitis in CD11c depleted animals, also suggesting that colon DC sources of IFN-I induced by TLR9 ligands, have an anti-inflammatory role by reducing neutrophil and monocyte trafficking (355).

These data suggest a dual role for DCs in pro- and anti- inflammatory modes of action. It has been suggested this dual role "permits DCs to respond to a variety of biological signals" (355). However, as described in Chapter 3.4, whilst the terms 'CD11c$^+$ cells' and DCs have previously been used interchangeably, this issue appears to be much more complex (Table 3.1). It is therefore conceivable that said dual 'DC' roles in intestinal inflammation are actually conveyed by different CD11c$^+$ populations. Therefore to build upon and clarify previous work, in this chapter we sought to interrogate the identity of colonic CD11c expressing cells during DSS colitis, before determining the impact of restricting *Mbd2* deficiency to defined populations. As published data would support the role of monocytes and CD11c expressing cells as key cell types in controlling host response to colonic inflammation the role of *Mbd2* in these cells was the focus for further investigation in this chapter.

Chapter aims:

1. Examine the role of haematopoietic sources of *Mbd2* in colonic inflammation
2. Examine the role of *Mbd2* in monocytes
3. Describe the heterogeneity of CD11c$^+$ cells in the colon LP
4. Examine the role of CD11c sources of *Mbd2* in colonic inflammation
5. Compare the gene expression of colon MPs in *Mbd2* deficiency
6. Examine the role of *Mbd2* in colon MPs activation *in vivo*

4.2 The role of haematopoietic *Mbd2* in colonic inflammation

To address the role of *Mbd2*$^{-/-}$ haematopoietic cells in the induction of DSS colitis, bone marrow chimeras were generated. Host haematopoietic cells were depleted by exposure of mice to lethal doses of radiation, thereafter mice were administered WT or *Mbd2*$^{-/-}$ BM such that haematopoietic cells were selectively rendered *Mbd2* sufficient/deficient whilst non-haematopoietic cells were *Mbd2* sufficient. In addition, by using variant CD45 isoforms for host or donor chimera components it was possible to discriminate between residual host and donor haematopoietic cells by flow cytometry.

Mice expressing the CD45.1 isoform were lethally irradiated and reconstituted with CD45.2 WT (CD45.1^{WT}) or *Mbd2*$^{-/-}$ (CD45.1$^{Mbd2-/-}$), CD90 depleted bone marrow and monitored for successful engraftment (See Chapter 2.12). At 8 weeks post irradiation mice were assessed for the proportion of host (CD45.1) versus donor (CD45.2) cells in the colon LP.

The frequency of donor CD45.2^{+} colon LP monocytes, neutrophils, eosinophils and macrophages was equivalent between CD45.1^{WT} and CD45.1$^{Mbd2-/-}$ chimeras, with less than 5% of each total population expressing the host CD45.1 isoform (Table 4.1). As in global *Mbd2*$^{-/-}$ mice, there was a reduced proportion of CD45.2^{+} CD11b^{+} CD103^{+} DCs in CD45.1$^{Mbd2-/-}$ chimeras (0.085 versus 0.189% of all intact cells in CD45.1$^{Mbd2-/-}$ versus CD45.1^{WT} chimeras) (See Figure 4.1A). In addition the proportion of donor CD45.2^{+} colon LP CD11b^{-} DCs was lower in CD45.1$^{Mbd2-/-}$ chimeras, however the overall number of host and donor CD11b^{-} DCs was equivalent i.e. there were significantly greater CD45.1 host CD11b^{-} DCs in CD45.1$^{Mbd2-/-}$ versus CD45.1^{WT} chimeras, (79.1 versus 24.9% of all CD11b^{-} CD103^{+} DCs and 83.8 versus 50.1% of all CD11b^{-} CD103^{-} DCs were CD45.2^{+}) (See Figure 4.1B).

These data suggest there is an inherent defect in the development of *Mbd2*$^{-/-}$ CD11b^{+} CD103^{+} DCs, and this is not rescued by the presence of *Mbd2* sufficient stromal cells. In addition, on the presumption that radioresistance of host CD45.1^{+} cells was equivalent across the irradiated mice, the decreased CD45.2$^{Mbd2-/-}$ CD11b^{-} DC populations would suggest these cells are being selectively outcompeted by the remnant CD45.1^{+} host populations.

Thus we have observed both dysregulated development and maintenance of mature *Mbd2*$^{-/-}$ DCs in the colon LP. We next sought to assess the role of *Mbd2*$^{-/-}$ haematopoietic cells during colonic inflammation.

Consistent with best practice in our animal facility, mice were treated with the oral fluroquinolone antibiotic enrofloxacin from weeks minus 1 to 4 relative to irradiation, to minimise the risk of opportunistic infection. Concurrent antibiotic use with DSS has been

shown to produce an ameliorated phenotype consistent with the key role of host microbiota in this model (356). Similarly pre-administration with antibiotics immediately followed by DSS treatment has been shown to increase susceptibility to colonic inflammation in a MYD88 dependent manner (162). For these reasons, there was a 5-week washout period between cessation of the above prophylactic antibiotics and the commencement of DSS to permit commensal recolonisation.

CD45.1^{WT} or CD45.1$^{Mbd2-/-}$ chimeras were treated for 8 consecutive days with 2% DSS and monitored for weight loss and symptom severity as defined in Chapter 2.3. CD45.1$^{Mbd2-/-}$ chimeras lost a significantly greater percentage of starting weight at day 6 (-1.5 versus +2.1±1.4%, CD45.1$^{Mbd2-/-}$ versus CD45.1^{WT} chimeras respectively, p=0.04), though there was no significant difference seen by day 8 (Figure 4.1C). There was a significantly increased symptom score at day 8 in *Mbd2*$^{-/-}$ donor chimeras (7.3 versus 2.5±1.5, *Mbd2*$^{-/-}$ versus WT respectively) (See Figure 4.1D). Histological assessment of 1cm sections of distal colon similarly revealed an increased severity score in *Mbd2*$^{-/-}$ donor chimeras (10.3±2.2 versus 4.4±1.2) (Figure 4.1E and F). Taken together, there was a small but significant increased susceptibility of CD45.1$^{Mbd2-/-}$ versus CD45.1^{WT} chimeras to DSS colitis. Assessment of the cellular composition of the colon LP by flow cytometry similarly revealed subtle differences. Firstly, as in the naïve chimeras, there was a significant reduction in the proportion and total number of CD45.2^{+} CD11b^{+} CD103^{+} DCs in CD45.1$^{Mbd2-/-}$ chimeras (Table 4.1). Similarly, there was a significant reduction in the proportion of CD45.2^{+} CD11b^{-} DCs in CD45.1$^{Mbd2-/-}$ chimeras (Table 4.1 and Figure 4.1B).

In assessing the remaining colon LP populations, there were no significant differences seen in the total number of CD45.2^{+} eosinophils, monocytes or macrophages (Figure 4.2A and B). There was however a significant increase in the total number of CD45.2^{+} neutrophils in CD45.1$^{Mbd2-/-}$ chimeras (Figure 4.2C and Table 4.1).

Whilst this experiment did not directly compare DSS treated CD45.1$^{Mbd2-/-}$ chimeras to global *Mbd2*$^{-/-}$ (i.e. global *Mbd2* deficient animals), CD45.1$^{Mbd2-/-}$ chimeras displayed an increased predisposition to DSS mediated inflammation, though less severe than that seen in global *Mbd2*$^{-/-}$ mice (Figure 3.6). Overall these data support a role for *Mbd2* deficient haematopoietic lineage cells in controlling the increased predisposition to colonic inflammation seen in *Mbd2*$^{-/-}$ mice and we therefore sought to understand which *Mbd2* deficient populations were culprit.

4.3 The role of monocytes in the susceptibility of *Mbd2*$^{-/-}$ to colonic inflammation.

Based on the work detailed in Chapter 3, we proposed that infiltrating monocytes are the principal inflammatory population in the DSS model of colitis. Monocytes are the largest changing population by cell number comparing naïve to DSS treated mice, and are simultaneously the largest source of IL-1β and TNF (Figure 3.8D and E, Table 3.2). Despite equivalent accumulation of monocytes in CD45.1$^{Mbd2-/-}$ versus CD45.1^{WT} DSS treated chimeras (Figure 4.2B and Table 4.1), based on the existing literature presented above and the results in Chapter 3, we hypothesized a role for *Mbd2* in preventing uncontrolled pro-inflammatory response in tissue monocytes in *Mbd2*$^{-/-}$ mice.

4.3.1 Blood and colon LP monocyte cytokine response in *Mbd2*$^{-/-}$ and WT mice

To assess this, we exposed WT or *Mbd2*$^{-/-}$ blood monocytes from naïve or DSS treated mice to TLR ligands and assessed cytokine response by flow cytometry. *Mbd2*$^{-/-}$ or WT whole blood was cultured with LPS (TLR4 ligand), Pam3Cys (TLR2 ligand) or CpG (TLR9 ligand), surface stained with LY6C, CD68 and CD11b and then stained intracellularly for the cytokines IL-1β, IL-6, IL-10, IL-12p40 or TNF.

There was no significant difference between *Mbd2*$^{-/-}$ or WT naïve monocyte (LY6C^{High}, CD11b^{+}, CD68^{+}) production of IL-1β, IL-6, IL-12p40, IL-10 or TNF in response to any of the TLR ligands as defined by the percentage of monocytes staining positive for these cytokines by flow cytometry versus isotype controls (See Figure 4.3A, B and Table 4.2). In addition, though we observed blood monocytes independent of genotype displayed a significantly increased IL-1β and IL-6 response to LPS and Pam3Cys after treatment with DSS (See Table 4.2), there was no significant difference between day 6 DSS treated *Mbd2*$^{-/-}$ or WT monocyte production of the assessed cytokines to TLR stimulation (See Table 4.2). These data suggest that circulating *Mbd2*$^{-/-}$ blood monocytes display equivalent production of cytokine for a given TLR stimulus, either in the steady state or during colonic inflammation.

We next sought to assess whether *Mbd2*$^{-/-}$ monocytes on recruitment to the colon LP more readily promoted tissue inflammation. Naïve or day 6 DSS treated colon LP cells from WT or *Mbd2*$^{-/-}$ mice were isolated and cultured *ex vivo* and cytokine production determined by intracellular staining and flow cytometry. Monocytes were identified as in Figure 3.2 and assessed for IL-1β and TNF expression compared to isotype controls (See Figure 4.3B):

As with blood monocytes, there was no significant difference in IL-1β or TNF production between *Mbd2*$^{-/-}$ or WT naïve colon LP monocytes (30.0±3.84 versus 23.6±4.42% of monocytes IL1β^{+}, *Mbd2*$^{-/-}$ versus WT respectively). Similarly there was no difference in the

IL-1β^{+} production between *Mbd2*$^{-/-}$ or WT DSS treated monocytes (51.8±3.44 versus 43.8±3.28 % monocytes IL-1β^{+}, *Mbd2*$^{-/-}$ versus WT respectively) (See Figure 4.3B & Table 4.2). These data would support the assertion that like TLR ligand stimulated blood monocytes, *Mbd2*$^{-/-}$ colon LP monocytes are not inherently more able than WT to produce damaging cytokines.

Additionally, as in the TLR-stimulated blood monocytes, there were interesting differences in the effect of treatment on monocyte cytokine response. Both *Mbd2*$^{-/-}$ and WT DSS treated LP monocytes produced significantly more IL-1β and TNF than monocytes from naïve mice of the same genotype, again suggesting that priming of circulating monocytes predisposes to an enhanced pro-inflammatory tissue phenotype on migration to inflamed mucosal surfaces (See Table 4.2).

4.3.2 Gene expression profiles of colon LP monocytes from DSS treated *Mbd2*$^{-/-}$ and WT mice

Whilst these data suggest equivalent monocyte pathogenicity in the absence of *Mbd2*, they did not assess the putative role of *Mbd2* in monocyte migration, recruitment, or indeed IL-1β/TNF independent pro-inflammatory pathways. To assess whether *Mbd2* deficiency conferred such dysregulation, we undertook gene expression analyses of purified colon LP monocytes.

We hypothesized that *Mbd2*$^{-/-}$ monocytes might display aberrant gene expression profiles for migration, recruitment or pathogen detection that could explain the increased susceptibility of *Mbd2*$^{-/-}$ mice to colonic inflammation. Using the sort logic in Figure 3.5, LY6C^{High} MHC-II^{+} cells were purified by flow cytometry to sort colon LP cells from DSS treated *Mbd2*$^{-/-}$ or WT mice. The RNA component of these cells was isolated, purified and its integrity quantitatively and qualitatively assessed by spectrophotometry and gel electrophoresis before hybridization to an IlluminaMouseRef6 microarray. To ensure sufficient RNA yield, mice were pooled, n=2/3 per pool, with 5 biological replicates per genotype (See Figure 4.4A).

Primary raw data were QC analysed using the arrayQualityMetrics Bioconductor package to identify sub-standard or outlier gene expression signatures. Arrays were scored on the basis of 3 metrics, namely maplot, boxplot and heatmap. Raw data were then transformed using a variance stabilizing transformation method prior to normalization using the robust spline normalization method. Expression measures were then summarized in log base2 and presented as the fold change (logFC), with positive logFC representing up regulation, and a negative logFC indicating down-regulation. Statistical analysis was then performed using

linear modeling and p value adjustment for multiple testing to control for false discovery (adjusted p<0.01 was deemed significant).

In comparing *Mbd2*$^{-/-}$ relative to WT monocytes; 98 array features were statistically significant (57 genes upregulated, 41 downregulated), of which no genes were logFC>2 (Table 4.3). 12 GO terms were statistically enriched (Table 4.4). Of the 11 upregulated genes logFC>±1, the following were selected for further discussion based on putative relationship to monocyte function, and analysing the current literature.

4.3.2.1 Genes upregulated in *Mbd2*$^{-/-}$ monocytes

Lyz1 (LogFC+1.8) encodes the lysozyme LYZ, which is a potent bacterolytic enzyme present in phagolysosomes that displays activity against Gram negative and positive bacteria (357). Lysozyme is found upregulated in the inflamed GI tract in conditions such as IBD, coeliac disease and collagaenous colitis, is influenced by the microbiota and is postulated in enhance mucosal defense against pathogenic bacteria (358), (359), (357).

Apoc1 (LogFC+1.6) encodes the apolipoprotein C1 (APOC1), which plays a pivotal role in lipid metabolism and monocyte-macrophage differentiation. Modified lipoproteins such as APOC1 are thought to bind scavenger receptors including FCLRS and SCARB1-3, facilitating the clearance and uptake of pathogens and apoptotic cells (360).

Immunoresponsive gene 1 (*Irg1*, LogFC+1.6) is an LPS-inducible gene encoding a highly conserved enzyme that catabolises short chain fatty acids (361). IRG1 localises to mitochondria, is rapidly induced within macrophages on bacterial infection and is required by mitochondria to use fatty acid substrates in the formation of reactive oxygen species (ROS) and thus effective bacteriocidal activity (362).

Reg3b (LogFC+1.4) encodes the REG3b protein (also known as pancreatitis associated protein1 (PAP1)), which is overexpressed in patients with active IBD and experimental models of colitis (363). It has anti-inflammatory properties, reducing pro-inflammatory cytokine release in a dose-dependent manner from epithelial and monocyte cells by preventing TNF induced NF-κB activation (363).

C4a (*C4a,* LogFC+1.5) is an anaphlyatoxin that can trigger smooth muscle contraction, increased capillary permeability and chemotaxis of leucocytes in the direction of increasing concentration (364). C4b (*C4b*, LogFC+1.3) covalently binds to pathogen, thereafter forming part of the C3-convertase complex, which catalyses the proteolytic cleavage of C3 into C3a and C3b and the eventual formation of the membrane attack complex via C5, 6,7,8 (364). Serum C4 levels have been found to be increased in patients with active IBD (365).

4.3.2.2 Genes downregulated in *Mbd2*$^{-/-}$ monocytes

Mucosa-associated lymphoid tissue (MALT) lymphoma translocation protein 1 (MALT1, *Malt1,* LogFC-1.0) is an intracellular NKKb activator provides both anti-apoptotic and proliferative signals (366). MALT1 is also a paracaspase which is able to cleave roquin1, 2 and regnase-1, all of which are able to negatively regulate pro-inflammatory cytokine mRNA including *Il6, Tnf, Icos* and *Tnfrsf4* mRNA by reducing their respective half lives (367).

Fcrls LogFC-1.0

Fc receptor-like S, scavenger receptor (FCRLS, formerly known as macrophage scavenger receptor 2 (MSR2)), is a poorly described transmembrane surface protein with scavenger receptor (SR) and immunoglobulin domains. FCRLS has been shown to be upregulated on the surface of tumour-associated macrophages (TAM), but its precise functional role is unknown (368).

The absence of significant genes >2 logFC suggested a paucity of striking differences between the WT and *Mbd2*$^{-/-}$ gene expression. In particular there was no difference in mRNA expression for pro-inflammatory cytokines (IL-1β, TNF, IL-6, IL-12, IL-15, IL-18, iNOS, ROS), chemokines (CXCL9, CCR1, CCR2, CCR5), pattern recognition receptors (TLR2, 3, 4, 9), or adhesion molecules (CD62L, CD11b, ICAM1).

Taken together these data support the assertion that *Mbd2*$^{-/-}$ monocytes display small increases in pro-inflammatory gene signatures such as *Reg3b* and *Lyz1*, but - more notably - there was a lack of difference in the majority of other regulatory genes that the existing literature would suggest could explain the increased susceptibility of *Mbd2*$^{-/-}$ mice to DSS colitis.

4.3.3 Colon LP monocyte proliferation in naïve and DSS treated *Mbd2*$^{-/-}$ and WT mice

To address the upregulated cell cycle and metabolic genes seen in *Mbd2*$^{-/-}$ monocytes from KEGG pathway analyses, we sought to address whether there was increased proliferation of *Mbd2* deficient monocytes *in vivo*. Ki67 protein is a cellular marker of proliferation, present during all active phases of the cell cycle (G_1, S, G_2 and mitosis), but is absent from resting cells (G_0). Colon LP cells were isolated from WT and *Mbd2*$^{-/-}$, naïve and day 6 DSS treated mice, surface stained for the myeloid markers in Figure 3.2 and stained intracellularly for Ki67 (Figure 4.4B). The cells were assessed for the proportion of a given population that was in active cell cycle as an indicator of proliferation. There was no significant difference in WT or *Mbd2*$^{-/-}$ Ki67 staining in steady state or DSS treated monocytes (Figure 4.4B). Similarly monocyte turnover did not increase substantially with DSS treatment, in keeping with our

hypothesis that dramatic increases in this population are mediated by rapid recruitment rather than increased proliferation of resident colon monocytes (Figure 4.4B).

4.3.4 *Mbd2* deficient and sufficient monocytes in the same inflamed tissue site – generating mixed BM chimeras

To further address whether there may be a monocyte intrinsic role for *Mbd2*, we generated mixed BM chimeras to permit concurrent analysis of *Mbd2*$^{-/-}$ and WT monocytes in the presence of *Mbd2* sufficient non-haematopoietic cells. We surmised this would permit simultaneous functional readouts of monocyte recruitment and pro-inflammatory ability, whilst controlling for other confounding factors, most notably the degree of colonic inflammation between treated mice.

Mice homozygous for the haematopoietic cell surface marker CD45.1 (CD45^{host}) were lethally irradiated and reconstituted with equal proportions of WT BM that co-expressed both CD45.1 and CD45.2 isoforms (CD45^{WT}) and *Mbd2*$^{-/-}$ CD45.2^{+} (CD45$^{Mbd2-/-}$) BM. Thus CD45^{host}, CD45^{WT} and CD45$^{Mbd2-/-}$ haematopoietic cells could be discriminated by flow cytometry based upon their expression of CD45.1 and CD45.2. 8weeks post irradiation, the blood of chimeric mice was examined to assess reconstitution of adoptively transferred CD45^{WT} and CD45$^{Mbd2-/-}$ cells. To our surprise, there was an almost complete absence of CD45$^{Mbd2-/-}$ cells (Figure 4.5A). We hypothesized therefore that *Mbd2*$^{-/-}$ BM displays a developmental disadvantage compared to WT. To address this possibility, we titrated the starting proportion of CD45$^{Mbd2-/-}$ BM. Despite starting with a 9:1 (CD45$^{Mbd2-/-}$:CD45^{WT}) starting BM ratio, at 8 weeks this ratio had reversed to 2:5, consistent with an increased differentiation ability of *Mbd2* sufficient derived BM cells (Figure 4.5A).

Examination of *Mbd2* mediated changes in haematopoietic development is an intriguing prospect, but falls outwith the main aims and focus of this project. With this in mind we proceeded to treat mixed BM chimeras with a starting ratio of CD45$^{Mbd2-/-}$:CD45^{WT} of 9:1, with 2% DSS or normal drinking water for 8 consecutive days.

We observed that in keeping with our previous titration data, *Mbd2*$^{-/-}$ cells were significantly less frequent in all populations and tissues examined, despite the striking starting excess of their BM progenitors (Figure 4.5B and Table 4.5). In keeping with previous DSS experiments, there was a significant increase in the eosinophil, monocyte and neutrophil populations in the colon LP (Figure 4.6A).

Intriguingly we also observed that DSS treatment had no effect on the proportion of colon LP cells that were CD45^{WT} or CD45$^{Mbd2-/-}$ i.e. colonic inflammation did not result in preferential recruitment of *Mbd2*$^{-/-}$ cells, particularly monocytes or neutrophils given their role in tissue inflammation (Figure 4.6B).

As *Mbd2* deficiency did not significantly alter cellular recruitment to the colon, we next sought to address whether *Mbd2* deficient myeloid cells displayed a more pro-inflammatory phenotype. *Ex vivo* culture of LPS stimulated blood, or unstimulated colon LP cells was undertaken from DSS treated or naïve chimeric mice. Cells were then surface and intracellularly stained for flow cytometry markers as described in chapter 4.2. The proportion of $CD45^{WT}$ and $CD45^{Mbd2-/-}$ myeloid populations expressing the cytokines IL1-β, TNF and IL-10 (colon LP) or IL-1β, TNF, IL-6 and IL-12p40 (blood monocytes) is summarized in Table 4.6 and Figure 4.6C. There was no significant affect of genotype for any of the cytokines measured in any of the myeloid populations described. We therefore concluded that *Mbd2* deficient blood monocytes and colon LP myeloid cells have the same pro-inflammatory ability as WT cells in the steady state or during DSS colitis.

Taken together *Mbd2* deficient monocytes have been observed to have equivalent pro-inflammatory cytokine expression in the blood after TLR challenge and colon LP, in DSS and the steady state. This remained true after internally controlling for inflammatory signals and local milieu by combining *Mbd2* sufficient and deficient monocytes in the same model. We hypothesise that increased susceptibility to DSS mediated inflammation in $Mbd2^{-/-}$ mice may therefore be secondary to the kinetics of monocyte recruitment, rather than intrinsic inflammatory capacity, and is considered further in the discussion.

4.4 The role of *Mbd2* in colon LP $CD11c^+$ cells

Given that genes coordinating response to bacteria and inflammation were increased in *Mbd2* deficient monocytes (*Lyz1, Ido1, Bdkrb1*, Table 4.4) and that APCs such as macrophages and DCs are critical in coordinating such responses, not only in the steady state but also in DSS, we felt these represented attractive candidates for further investigation (355), (354). Indeed data presented in Figure 4.1D, E, F and 4.2C suggest an increased susceptibility of mice to DSS where *Mbd2* is restricted to haematopoietic cells. Given $CD11c^+$ cells are derived from bone marrow progenitors, and their development is altered in the absence of *Mbd2* (Figure 3.4E and 4.1A), we hypothesized these cells may be important in explaining the $Mbd2^{-/-}$ susceptibility to experimental colitis.

As described above (Chapter 4.1), $CD11c^+$ cells may have dual pro- and anti- inflammatory roles in DSS colitis, and it is not clear which $CD11c^+$ cells are responsible. In addition *Mbd2* has been recently shown to control expression of molecules that enable $CD11c^+$ cell promotion of Th2 immunity, with *Mbd2* deficient $CD11c^+$ cells displaying significantly impaired Th2 cytokine induction in response to *S. mansoni* egg Ag (SEA) or house dust mite

(HDM) and down regulated transcript of antigen presentation and co-stimulation genes (318).

Thus, given that CD11c expressing cells have the ability to exacerbate or ameliorate DSS colitis and that *Mbd2* controls key immunological pathways in these cells in other models, we hypothesized that *Mbd2*$^{-/-}$ predisposition to DSS colitis may in part due to dysregulated coordination of inflammatory responses by *Mbd2* deficient CD11c expressing cells (355), (354).

4.4.1 Defining CD11c expressing cells in the colon LP

To address the range of colonic CD11c^{+} populations, colon LP cells were isolated from naïve mice and surface stained with the antibody cocktail described in Figure 3.2. All singlet, CD11c^{+} cells were then identified and gated as per the logic in Figure 3.2, which successfully categorized >95% of cells. Figure 4.7 shows the proportional breakdown of all CD11c^{+} cells (Figure 4.7A) and the MFI of the identified contributing cell types (Figure 4.7B). These data revealed that macrophages were the most frequent CD11c expressing cell in the colon LP (48.0%) followed by DCs (24.9%). However, per cell, macrophages displayed an overall low expression of CD11c as measured by mean fluorescent intensity (MFI) (6620±299), in contrast to DCs, which displayed the highest overall expression of CD11c (35660±2423 and 51591±1898 MFI respectively for CD11b^{+}CD103^{+} and CD11b^{-}CD103^{+} DCs) (Figure 4.7B). Taken together, macrophages and DCs accounted for 94% of CD11c expressing cells in the colon LP. It also underlines the caution one must take in interpreting previous data attributing the action of CD11c^{+} cells in the GI tract to DCs alone.

4.4.2 Selective depletion of *Mbd2* in CD11c^{+} cells

Given the previous literature supporting a role for *Mbd2* in CD11c^{+} cells, and a role for CD11c^{+} cells in DSS colitis, we sought to restrict *Mbd2* deficiency to these cells to understand their contribution to our DSS *Mbd2*$^{-/-}$ phenotype. We took advantage of a *CD11c-Cre*$^{+}$ *Mbd2*$^{Fl/Fl}$ mouse (CD11cΔ*Mbd2*), whereby mice with *lox*P sites flanking the first exon of *Mbd2* were generated and bred with mice that express Cre recombinase in CD11c expressing cells, as previously described (318). To confirm reduction in *Mbd2* transcript in CD11c^{+} cells, colon LP cells were sorted as per Figure 3.5 from CD11cΔ*Mbd2* and *CD11c-Cre*$^{-}$ littermate controls and *Mbd2* expression assessed by RT-PCR (Figure 4.7C). There was an 85% reduction in CD11cΔ*Mbd2* macrophage *Mbd2* expression, with a 91% and 93% reduction in CD11cΔ*Mbd2* CD11b^{-} and CD11b^{+} DCs respectively. In comparison monocytes, which account for 1.5% of CD11c expressing cells had only a 19% reduction in *Mbd2* transcript. There was therefore a selective depletion of between 85-93% of *Mbd2* in those

cells that account for 73% of CD11c expressing populations in the colon in CD11cΔ*Mbd2* mice (Figure 4.7A and C).

4.4.3 The role of CD11c$^+$ cell depletion of *Mbd2* in the steady state

CD11cΔ*Mbd2* mice have been shown to have normal splenic DC development (318). To ensure that myeloid development was equivalent between CD11cΔ*Mbd2* and *CD11c-Cre*$^-$ littermate controls in non-lymphoid tissue sites we assessed colon LP myeloid cells by flow cytometry using the antibody cocktail and gating strategy described in Figure 3.2 (Table 4.7). There were no significant differences in any of the populations examined. Indeed in contrast to global *Mbd2*$^{-/-}$ mice, which had a reduced proportion of CD45$^+$ and CD11b$^+$CD103$^+$ cells (Figure 3.4B and E), these populations were equivalent between CD11cΔ*Mbd2* and *CD11c-Cre*$^-$ mice (Figure 4.7D). This data would be in keeping with the BM chimera data presented above (Figure 4.1A and B) suggesting a role for *Mbd2* in DC progenitors. However, given CD11c expression occurs later in development, restricting *Mbd2* deficiency to CD11c$^+$ cells and thus more differentiated cell types, overcomes this dysregulated development.

To ensure CD11c specific depletion of *Mbd2* did not affect the normal intestinal structure or confer a spontaneous colitis, we examined transverse sections of colon by histology. This revealed no significant differences between CD11cΔ*Mbd2* and *CD11c-Cre*$^-$ naïve littermate controls in gross morphology and structure of the colonic epithelium and LP (Figure 4.7E).

4.4.4 The role of CD11c$^+$ cell depletion of *Mbd2* in colonic inflammation

We then sought to test whether CD11c restricted *Mbd2* deficiency influenced the development of colonic inflammation by feeding CD11cΔ*Mbd2* and *CD11c-Cre*$^-$ littermate controls 2% DSS or normal drinking water for 8 consecutive days. Daily assessment was made of weight and symptom score as defined in Table 2.3. There was a significant increase in CD11cΔ*Mbd2* versus *CD11c-Cre*$^-$ mean symptom score in DSS treated mice at day 4 (2.2±0.3 versus 0.0±0), day 5 (3.6±0.6 versus 0.2±0.2), day 6 (4.2±0.6 versus 0±0), day 7 (4.6±0.6 versus 1.8±0.5) and day 8 (5.4±1.0 versus 2.4±0.6) (Figure 4.8A). This reflected an increase in all parameters of the symptom score (PR bleeding, weight loss and diarrhoea) and a significantly increased weight loss at day 8 (8.7±1.17% versus 1.8±1.8% least square mean change in day 0 weight) in CD11cΔ*Mbd2* versus *CD11c-Cre*$^-$ mice (Figure 4.8B). There were no symptoms recorded in untreated mice independent of genotype.

Histological analysis (Table 2.4 for scoring methodology) of 1cm H&E stained sections of distal colon revealed a significantly greater tissue architecture destruction, goblet cell depletion and inflammatory infiltrate in DSS treated CD11cΔ*Mbd2* versus *CD11c-Cre*$^-$ mice, indicative of elevated colonic inflammation (least square mean histology score 13.5±0.9

versus 9.8±0.9)(Figure 4.8C and D). In keeping with this, whole colonic tissue from DSS treated CD11cΔ*Mbd2* mice displayed significantly greater mRNA transcript for the inflammatory cytokine *Ifng* (least square mean expression 0.92±0.21 versus 0.12±0.20), but not *Il1b* or *Tnf*, as analysed by RT-PCR (Figure 4.8E).

Taken together these data suggest $CD11c^+$ cell expression of *Mbd2* is required to limit colonic inflammation characterised by increased weight loss, symptom and histology score. However, in contrast to global $Mbd2^{-/-}$ mice, *Il1b and Tnf* colon transcript was equivalent in WT and CD11cΔ*Mbd2* mice.

4.4.4.1 Comparison of CD11cΔ*Mbd2* and *CD11c-Cre*$^-$ colon LP cells in colonic inflammation

Once again, DSS induced a significant increase in the number of eosinophils, neutrophils and monocytes, compared to untreated mice (Table 4.7). There was an 11.0 fold change in the total number of neutrophils in CD11cΔ*Mbd2* mice (7.0 in *CD11c-Cre*$^-$), 9.4 fold change in monocytes in CD11cΔ*Mbd2* mice (6.2 in *CD11c-Cre*$^-$) and 1.4 fold change in eosinophils in CD11cΔ*Mbd2* mice (1.8 in *CD11c-Cre*$^-$) (Table 4.7) in DSS animals relative to untreated. There was, however, no significant difference between genotypes in total numbers of these cells present.

Four independent experiments of CD11cΔ*Mbd2* versus *CD11c-Cre*$^-$ DSS treated and drinking water control animals were conducted, with notable variation that may have affected statistical significance. Two of the four experiments displayed significant experimental variation in the proportion of $CD45^+$ cells, but with no effect of genotype, suggesting that inter-experimental variation rather than true biological variation was manifest (Figure 4.9A), as this was not present in other DSS experiments presented in Chapter 3, 4 and 5. The combination of this variation biased the dataset in linear modeling, which limited the interpretation of the enumerated total colon population data. To counter this, statistical analysis was performed on the data normalized for the variation in CD45 proportions (i.e. by expressing proportional data as a % of all $CD45^+$ rather than intact cells). Once this was performed, we observed a significant increase in the proportion of CD11cΔ*Mbd2* colon LP monocytes compared to *CD11c-Cre*$^-$ treated controls (8.63±0.72 versus 6.42±0.80 % of $CD45^+$ cells) but not neutrophils (6.21±0.66 versus 4.50±0.74 p=0.06) or any other myeloid population (Figure 4.9B and C).

By way of contrast to other assessments of *Mbd2* deficiency in DSS colitis, CD11cΔ*Mbd2* had 1.57 fold more colon LP neutrophils and 1.51 fold more colon LP monocytes relative to WT after DSS, compared to 1.61 fold and 1.75 fold increases in $Mbd2^{-/-}$ mice and 1.56 fold

and 1.20 fold increases in 100% BM chimeras. Thus *Mbd2* deficiency in the haematopoietic compartment, $CD11c^+$ cells or all cells resulted in a 1.5-1.6 fold greater colon LP neutrophil accumulation post DSS, which was significant in all experiments except CD11cΔ*Mbd2* (p=0.06). However monocyte accumulation was more variable (range of fold increase 1.2-1.8) and was significant in all experiments except haematopoietic restricted *Mbd2* deficiency. These different experiments and animals are clearly not directly comparable, but serve as an overview of the effect of *Mbd2* deficiency when restricted to different cell types. This suggested that increased neutrophil accumulation is consistent independent of the cell types that lack *Mbd2,* in those we have examined, and that the greatest increases in monocyte recruitment occur when non-haematopoietic cells are deficient in *Mbd2* i.e. in $Mbd2^{-/-}$ animals

4.4.4.2 The role of *Mbd2* in $CD11c^+$ cell cytokine production.

We had therefore observed that DSS treatment of either CD11cΔ*Mbd2* and *CD11c-Cre*$^-$ littermate controls resulted in eosinophil, monocyte and neutrophil accumulation in the colon LP and increased gene expression of *Il1b, Tnf* and *Ifng* (Figure 4.8E and Figure 4.9B). However there was no significant effect of *Mbd2* deficiency in $CD11c^+$ cells on the colonic gene expression of *Il1b* or *Tnf* after DSS treatment (Figure 4.8E). We next sought to understand whether, despite equivalent tissue levels of cytokine mRNA, there were changes in individual population cytokine expression conferred by $CD11c^+$ cell *Mbd2* deficiency.

Colon LP cells from CD11cΔ*Mbd2* and *CD11c-Cre*$^-$ littermate controls treated either with 2% DSS or normal drinking water for 8 consecutive days were surface, then intracellularly, stained for the myeloid markers and cytokines detailed in Figure 4.9D, then analysed by flow cytometry. Following normalisation of the datasets as mentioned above for inter-experiment variation in $CD45^+$ proportions, we observed that there were significant increases in IL-$1\beta^+$ (1.95±0.34 versus 0.69±0.34 % of $CD45^+$ cells) and TNF^+ (1.00±0.10 versus 0.48±0.11 % of $CD45^+$ cells) neutrophils and IL-$1\beta^+$ monocytes (4.47±0.63 versus 2.62±0.59 % of $CD45^+$ cells) in DSS treated CD11cΔ*Mbd2* mice, when expressed as % $CD45^+$ cells (Figure 4.9D).

Therefore, we have observed that CD11cΔ*Mbd2* mice were more susceptible to DSS colitis, characterised by increased weight loss, symptom and histological score, with significant accumulation of IL-$1\beta^+$ neutrophils and monocytes, as compared to *CD11c-Cre*$^-$ littermate controls.

4.4.4.3 Gene expression profiles of colon LP CD11c$^+$ cells from DSS treated *Mbd2*$^{-/-}$ and WT mice

Given that *Mbd2* deficiency in CD11c$^+$ cells appeared to have an important role in the response to colonic inflammation, we next sought to identify the genes controlled by *Mbd2* in CD11c$^+$ cells that might be responsible for the increased inflammation observed in global *Mbd2*$^{-/-}$ or CD11cΔ*Mbd2* mice. We therefore isolated colon LP cells from global *Mbd2*$^{-/-}$ or WT DSS treated mice, and purified macrophages and CD11b$^-$ DCs, as per the sort logic in Figure 3.5. RNA was isolated from these cells, purified, and its integrity quantitatively and qualitatively assessed by spectrophotometry and gel electrophoresis before hybridization to an IlluminaMouseRef6 microarray. To ensure sufficient RNA yield, mice were pooled (n=2/3 for macrophages and n=5 for CD11b$^-$ DCs), with 2-5 biological replicates per genotype.

4.4.4.3.1 Colon LP Macrophages

There were 40 genes logFC >±1 (38 up regulated and 2 down regulated) in day 6 DSS treated *Mbd2*$^{-/-}$ versus WT colon LP macrophages with an adjusted p value <0.05 that were considered for further analysis (Table 4.8). Candidate dysregulated genes based on GOterm pathway analysis (Table 4.9) and literature review were selected and presented below (Figure 4.10A):

Genes upregulated in *Mbd2*$^{-/-}$ macrophages

Lyz1 (LogFc +2.1), *Irg1* (LogFc +1.7), *Reg3b* (LogFc +1.3) and *Reg3g* (LogFc +1.2) see entry in Chapter 4.3.2

IL-1α (*Il1a* LogFc +1.8) and IL-1β, are the major IL-1 agonists and have been long recognised as integral components of innate immune processes (369). IL-1 expression corresponds to disease activity in the colons of IBD patients (370), (371).

Transforming growth factor (TGF)-β1 has a decisive role in limiting inflammatory pathways, with IBD patients displaying defective downstream TGF-β signaling (372), (373). TGF-β1 causes expression of TGF-β-induced (TGFBI, *Tgfbi* LogFc +1.5) which is produced by macrophages in response to apoptotic cell ingestion, leading to reduced fibroblast MMP levels and subsequent accumulation of collagen, thought to be pivotal in the resolution process post-inflammation (374).

Indoleamine 2,3 dioxygenase (IDO1, *Ido1* LogFc +1.1) catabolises tryptophan along the kynurenine pathway (375). Kynurenine metabolites act to promote T cell tolerance and exert antimicrobial effects that are attributed to IDO1 activity. IDO1 expression is stimulated by

TNF, IFN-γ and IL-1β and is one of the most highly upregulated genes in human IBD and animal models of colitis (376), (377).

Genes downregulated in *Mbd2*$^{-/-}$ macrophages

Fcrls (LogFc -1.6) see entry in Chapter 4.3.2

Resistin-like molecule (RELM) α (*Retnla* LogFc -1.1) belongs to a family of secreted mammalian proteins with immunomodulatory properties and is upregulated in several infectious and inflammatory settings (378), (379). RELM-α administration promotes immune cell activation, pro-inflammatory chemokine and cytokine expression in DSS treated mice, with reduced IL-23p19 expression from RELM-α deficient macrophages thought to exacerbate colitis (380).

Triggering receptor expressed on myeloid cells (TREM-2, *Trem2* LogFc -0.99) is a surface receptor found on macrophages, DCs and microglia that binds motifs on bacteria and yeasts (381). TREM-2 is expressed at higher levels on CD11c^{+} LP cells isolated from patients with active IBD and mice with experimental colitis versus controls suggesting myeloid sources of TREM-2 are important in regulating inflammation (382).

4.4.4.3.2 Colon LP CD11b^{-} DCs

There were 26 genes with logFC >1 (10 upregulated and 16 down regulated) in day 6 DSS treated *Mbd2*$^{-/-}$ versus WT colon LP CD11b^{-} DCs with an adjusted p value <0.05 that were considered for further analysis (Table 4.10). Candidate dysregulated genes based on pathway analysis (Table 4.11) and literature review were selected and presented below. In addition, both significant and pertinent non-significant genes (genes that have previously been published to be important in DC responses in inflammation) are presented in heat maps of average expression in Figure 4.10B

In total 370 (180 up, 182 down) genes were significantly affected irrespective of fold change, it was clear that the absolute difference for the majority of significantly dysregulated genes in CD11b^{-} DCs was small. Indeed the mean LogFC for upregulated and downregulated genes was 0.41 (median 0.38), suggesting that there are a large number of small effect size dysregulated genes in *Mbd2*$^{-/-}$ CD11b^{-} DCs. Thus significant genes with LogFc>0.5 were considered for analysis of candidiate genes.

Given the analysis was limited by the presence of n=2 biological replicates for WT and n=3 for *Mbd2*$^{-/-}$ due the rarity of these cells in the LP (aprox. 0.1% of total cells), it is possible that a larger sample size may have produced more differentially expressed genes. To investigate

the possibility of low sample number excluding genes with large fold changes that did not reach significance; the statistical threshold was relaxed to an adjusted p value of 0.1. However this did not further the number of candidate dysregulated genes with known immunological function.

Genes upregulated in *Mbd2*$^{-/-}$ CD11b^{-} DCs

Reg3b (LogFc 0.94) See entry in Chapter 4.3.2

Complement protein C1q (*C1qb* LogFc 0.75) is able to bind apoptotic cells, opsonizing and increasing their removal by phagocytes. Deficiency in *C1Q* is the strongest genetic predictor of systemic lupus erythematosis (SLE) in humans, thought to be due to persistence of apoptotic cells contributing to autoimmunity (383). In addition DCs are important cellular sources of C1q, its release acting in autocrine fashion to increase DC induction of Th1 cells (384), (385).

Genes downregulated in *Mbd2*$^{-/-}$ CD11b^{-} DCs

CD103 (*Itgae* LogFc-1.5) expression defines DC populations that exhibit roles in co-ordinating effector and Treg responses (386). The function of CD103 is poorly understood, thought to facilitate cellular adhesion via its ligand E-cadherin, expressed on the basolateral surface of epithelial cells, and affecting cell shape and motility to promote cellular attachment (387).

Janus kinase-2 (JAK2, *Jak2* LogFc -0.97) is an important component of the IL-12 and IL-23 signaling pathway (388). Subsequent phosphorylation steps of STAT 1,3,4,5 eventually lead to STAT4 mediated changes in gene expression, particularly Th17 differentiation (389). Polymorphisms in *JAK2* and other components of the IL-23 signaling pathway (*IL23R, IL12* and *STAT3*) have been identified as risk susceptibility loci for both CD and UC (308).

Leucine-rich repeat kinase 2 (LRRK2, *Lrrk2* LogFc -0.7) is large protein with 2 distinct enzymatic domains, although the precise physiological function is unknown (390). LRRK2 is known to associate with autophagy proteins p62 and LC3, is expressed preferentially by LP leucocytes, is found to be upregulated in inflamed CD colonic biopsy specimens, with LRRK2-deficient mice been shown to have poorer outcomes in response to DSS (391), (392), (393).

4.4.4.3.3 Summary of dysregulated gene expression in *Mbd2* deficient CD11c^{+} cells

Taken together, colon LP *Mbd2* deficient macrophages in DSS colitis displayed differentially expressed genes that would be hypothesised to dampen damaging inflammation, with increased expression of anti-inflammatory mediators (*Il1a, Tgfbi, Reg3b, Reg3g*) and

decreased pro-inflammatory response mechanisms (*Retnla, Trem2, Ido1*). However, in keeping with the dual role of GI tract macrophages, bacteriocidal pathways are also upregulated in *Mbd2* deficiency (*Lyz1, Irg1*) consistent with previous literature supporting combined tolerogenic and pro-inflammatory capabilities (51), (43). An unexpected finding was the reduction of the scavenger receptor FCLRS. This poorly described scavenger receptor has no previous documented function in macrophage function. However given deficiency in other scavenger receptors, notably MSR1 confers up to a 50% reduction in macrophage phagocytic ability, one would hypothesise other scavenger receptor dysregulation could confer altered bacterial handling abilities, resulting in pathogen persistence.

As can be seen in principal component analysis (Figure 4.10C), whilst displaying a number of significantly dysregulated genes, the effect size of each individual gene in the $CD11b^-$ analysis was small with few candidate genes with known or hypothesised function logFC >±1 between genotypes. As such, the overall gene expression differences conferred by *Mbd2* deficiency in $CD11b^-$ DCs was low. Given that DC-dogma would suggest these cells have a dominant role in antigen presentation to the adaptive immune system, and that DSS colitis is considered a T cell independent model, it is perhaps unsurprising that these cells do not appear to be the dominant *Mbd2* deficient cell type conferring increased susceptibility to acute colonic inflammation.

Given the above gene expression changes in *Mbd2* deficient macrophages, particularly in bacterial handling, and previous data underlining the importance of different TLRs in macrophage function (51), we sought to consolidate TLR expression data taken from the above dataset with detected levels of TLRs *ex vivo* using flow cytometry.

4.4.5 Assessment of MP cell TLR expression *in vivo*

Intestinal macrophages occupy a unique niche in the GI tract by demonstrating an anergy to TLR ligands incumbent to their tolerogenic phenotype and role in negating damaging host response to the commensal microbiota (51). We thus considered whether PRR and, in particular, TLRs were dysregulated in $Mbd2^{-/-}$ MP cells that might contribute to the increased myeloid inflammatory response in experimental colitis. Colon LP cells from $Mbd2^{-/-}$ or WT DSS treated (Figure 4.11A) or control mice were isolated and analysed by flow cytometry for TLR 2,3,4 and 9. In keeping with published data, colon monocytes were overwhelmingly positive for TLR2, 4 and 9, with macrophages demonstrating lower levels for these receptors, in both naïve and DSS treated settings (51) (Figure 4.11A). There were however no significant differences between $Mbd2^{-/-}$ and WT MP either in the steady state or in DSS colitis for TLRs as assessed by gene expression for TLR transcript or by flow cytometry for detected protein. Indeed the significant changes in TLR 2 and TLR4 protein seen between

monocytes and macrophage populations independent of genotype were not reflected in significant change in *Tlr2/Tlr4* gene transcript.

4.4.6 Assessment of MP cell co-stimulatory molecule expression *in vivo*

CD40 is a 48kDa transmembrane glycoprotein that is a member of the TNF receptor superfamily (TNFRSF) (394). CD40 signaling in APCs induces upregulation of MHC II and co-stimulatory molecules CD80/CD86, and is used to distinguish between inactivated and activated DCs the end result leading to production of cytokines such as IL-12p40 and IL-6. Indeed *Cd40*$^{-/-}$ mice or WT mice treated with a CD40-CD40L inhibitor, treated with DSS develop attenuated colitis compared to controls, characterized by a reduction in colon leucocyte recruitment. We therefore looked to assess whether *Mbd2* deficiency in colon LP APCs conferred an increased surface expression of the cell markers (Table 4.12). Interestingly, in keeping with the increased level of inflammation seen in *Mbd2*$^{-/-}$ DSS treated mice, all *Mbd2* deficient colon LP MP cells examined displayed significantly greater CD40 expression as assessed by MFI (Table 4.12). In addition, all *Mbd2* deficient colon LP MP cells, except CD11b^{-} CD103^{+} DCs, displayed significantly greater CD40 expression in the steady state. However there was once again a discrepancy between gene expression and observed protein, in that *Cd40* differences were not significant in colon LP macrophages and CD11b^{-} DCs between *Mbd2*$^{-/-}$ and WT DSS treated mice.

To understand whether increased CD40 on CD11c^{+} cells was dependent on *Mbd2* deficiency in these cells alone, we performed the above analysis of CD40 expression on CD11cΔ*Mbd2* colon LP cells and controls (Table 4.12). Interestingly in the absence of other *Mbd2* deficient cell types, the increased CD40 expression was abrogated. This suggested that non-CD11c^{+} cell sources of *Mbd2* are required to increase surface activation of DCs and macrophages.

4.5 Discussion

In chapter 4 we have identified the importance of haematopoetic *Mbd2* in controlling susceptibility to colonic inflammation. We have built upon the work in Chapter 3 that demonstrated a marked susceptibility of *Mbd2*$^{-/-}$ mice to chemical and infectious colitis. In order to refine our understanding of the cellular sources of *Mbd2* that were important in producing this observation, we sought to restrict *Mbd2* to specific populations.

4.5.1 Haematopoietic sources of *Mbd2* and susceptibility to intestinal inflammation

Firstly, using single BM chimeras, we restricted *Mbd2* deficiency to haematopoetic cells and observed an increased susceptibility of these mice to DSS colitis. This was characterised by increased weight loss, symptom score histological severity score and neutrophil accumulation in the colon LP. There was a less severe phenotype in these DSS treated chimeric mice compared to *Mbd2*$^{-/-}$ animals (Weight loss 6.1±3.0 versus 16.32±1.2 % change in starting weight, histology score 10.3±2.2 versus 14.6 ±3.6, CD45.1$^{Mbd2-/-}$ chimeric versus *Mbd2*$^{-/-}$ day 6 DSS treated mice respectively). Clearly to control for inter-experimental variation both these animals should be synchronously exposed to DSS and monitored for treatment effect. Unfortunately, there were no DSS treated global *Mbd2*$^{-/-}$ mice or global *Mbd2*$^{-/-}$ irradiated host/*Mbd2*$^{-/-}$ BM reconstituted, control components to this experiment. This was considered in the experimental design as it would have served as a comparison for the severity of the phenotype observed in the chimeric mice, and in addition would have controlled for the effect of irradiation and antibiotic treatment on inflammation severity. However, as noted in Table 2.1 *Mbd2*$^{-/-}$ mice are maintained as a heterozygous line due to poor breeding, with a less than Mendelian yield of *Mbd2*$^{-/-}$ offspring. This meant the requisite number of *Mbd2*$^{-/-}$ mice for *Mbd2*$^{-/-}$ recipient chimeric controls was prohibitively large to undertake this experiment.

Consistent with best practice in our animal facility, mice were treated with the oral fluroquinolone antibiotic enrofloxacin from weeks minus 1 to 4 relative to irradiation, to minimise the risk of opportunistic infection in the bone marrow reconstitution period. Concurrent antibiotic use with DSS has been shown to increase severity of inflammation, consistent with the key role of host commensal microbiota in limiting disease severity in this model (356). Similarly pre-administration with antibiotics immediately followed by DSS treatment has been shown to increase susceptibility to colonic inflammation in a MYD88 dependent manner (162). For these reasons, there was a 5-week washout period between cessation of the above prophylactic antibiotics and the commencement of DSS to permit commensal recolonisation.

One must be mindful that in the process of generating these chimeric animals, they have undergone a) lethal irradiation and b) broad-spectrum antimicrobial treatment, which one could argue may have irrevocably altered their subsequent response to inflammatory challenge. For example 10-12Gy murine irradiation results in extensive p53 mediated crypt shortening, followed by a burst of proliferation in remaining cells and increased MHC-I and –II expression (395), (396). Whether this perturbation affects future response to, or handling of, the commensal microbiota is not well described. Whilst this experiment was not designed to compare DSS treated CD45.1$^{Mbd2-/-}$ chimeras versus *Mbd2*$^{-/-}$ animals, and accepting the other above limitations, whilst we have observed an increased pre-disposition of CD45.1$^{Mbd2-/-}$ chimeras to DSS mediated inflammation, this did not recapitulate the severe phenotype seen in *Mbd2*$^{-/-}$ mice. Overall these data support a partial role for *Mbd2* deficient haematopoietic lineage cells in controlling the increased predisposition to colonic inflammation seen in global *Mbd2*$^{-/-}$ mice, but highlight that non-haematopoietic sources of *Mbd2* may also confer increased susceptibility.

We therefore sought to understand in Chapter 4 the haematopoietic sources of *Mbd2* that could be important. There is strong literature support for a dominant role of monocytes in the pathogenesis in the DSS model (47), (43). We therefore hypothesised that *Mbd2* was acting in WT mice to limit damaging monocyte driven inflammation, and thus explain the increased susceptibility of CD45.1$^{Mbd2-/-}$ BM chimeras to DSS colitis described in Figure 4.1 and 4.2.

4.5.2 The role of *Mbd2* in monocytes

Mbd2 deficient blood or colon LP monocytes from *Mbd2*$^{-/-}$ DSS treated or naïve mice demonstrated equivalent levels of pro-inflammatory cytokines when cultured *ex vivo* in isolation (colon) or with TLR ligands (blood). Interestingly, DSS treatment conferred increased IL-1β and IL-6 production from TLR stimulated blood monocytes independent of genotype. Whilst it is known that monocyte recruitment is in part CCL2/CCR2 dependent, and may depend on type-1 IFN and TLR dependent egress of monocytes from bone marrow, activation signals to circulating monocytes are poorly understood (397), (47). These data suggest that blood monocytes may receive currently undefined pro-inflammatory priming signals from distant inflamed tissue sites; perhaps to permit rapid response either locally e.g. to disseminated septiceamia, or once successfully migrated to sites of inflammation. Indeed it has recently been shown that monocytes may be pre-emptively educated during development based on their micro-environment to promote tissue specific function; during acute gastrointestinal infection with *T. gondii* NK cell derived IFN-γ promoted a regulatory program in monocyte progenitors that occurred before bone marrow egress or systemic inflammation (398).

In addition we undertook gene expression profiling of purified DSS treated colon LP monocytes to further understand *Mbd2* mediated changes in other monocyte-inflammatory pathways such as recruitment, pattern recognition and bacterial handling (Figure 4.4A and 4.10C).

4.5.2.1 Key differences in *Mbd2* deficient monocyte gene expression during DSS

Lyz1 (*Lyz1* LogFC +1.8) encodes a lysozyme enzyme, which is a bacterolytic enzyme present in phagolysosomes that displays activity against gram negative and positive bacteria (357). Indeed lysozyme was discovered by Alexander Fleming in 1921 during a search for medical antibiotics, functioning by damaging bacterial cell walls via hydrolysis of peptidoglycan residues (399). Lysozyme is found upregulated in the inflamed GI tract in conditions such as IBD, coeliac disease and collagaenous colitis, suggesting that the bacterial flora plays an important role in its expression (358), (359). Indeed lysozyme production is increased in patients with active colonic IBD, increases postulated to provide enhanced mucosal protection against proliferating pathogenic bacteria (357). Increased LYZ presence in *Mbd2*$^{-/-}$ monocytes could therefore be postulated to be a compensatory mechanism to the increased inflammation mediated microbial burden seen in *Mbd2*$^{-/-}$ DSS treated mice. To test this hypothesis future work could encompass measuring serum lysozyme before and during the induction of colitis to ascertain the kinetics of its expression (serum lysozyme has been shown to be a biomarker for monocyte/macrophage activity in rheumatoid arthritis) (400), or indeed we could purify monocytes using FACS during colitis from our mixed BM chimera mice and compare *Lyz1* expression i.e. we would have *Mbd2* deficient and sufficient monocytes from the same inflammatory system. Lastly, to ensure that *Mbd2* does not affect post-transcriptional modification of *Lyz1* to render it less efficient at cleaving bacterial proteins (with compensatory increased levels of expression in *Mbd2* deficient cells) we could assess LYZ1 structure and function in *Mbd2* deficient and sufficient monocytes.

Apoc1 (*Apoc1* LogFC +1.6) encodes the apolipoprotein C1 (APOC1), which plays a pivotal role in lipid metabolism and monocyte-macrophage differentiation, and was significantly upregulated in *Mbd2*$^{-/-}$ monocytes. Apolipoprotein functions in metabolic processes have consistently been found to be one of the most upregulated pathways in the macrophage differentiation process, and this is mirrored in our dataset (401). Modified lipoproteins such as APOC1 are thought to bind scavenger receptors including FCLRS and SCARB1-3, facilitating their function consistent with the role of macrophages in avid clearance and uptake of pathogens and apoptotic cells (360). The presence of upregulated metabolic and cell cycle pathways in *Mbd2*$^{-/-}$ monocytes could be hypothesised to suggest an increased ability to traverse the macrophage differentiation 'waterfall' via increases in turnover and proliferation. It could also be hypothesised that *Mbd2*$^{-/-}$ monocytes are recruited earlier to

inflamed tissue sites and that, at a given time point, *Mbd2*$^{-/-}$ monocytes may be at a later differentiation stage than WT counterparts.

Identified as an LPS-inducible gene in macrophages, immunoresponsive gene 1 (*Irg1)* (*Irg1* LogFC +1.6) encodes a highly conserved enzyme which catabolises short chain fatty acids (361). IRG1 localises to mitochondria, is rapidly induced within macrophages on bacterial infection and is required by mitochondria to use fatty acid substrates in the formation of reactive oxygen species (ROS) and thus effective bacteriocidal activity (362). *Irg1* therefore represents a key component of the immunometabolic axis connecting infection, macrophage function and the increased lipid metabolic pathways seen in monocyte-macrophage differentiation (402). The presence of upregulated *Irg1* in *Mbd2*$^{-/-}$ monocytes would be consistent with the hypothesis of increased DSS mediated colonic inflammation, barrier breakdown and thus bacterial infiltration seen in *Mbd2*$^{-/-}$ mice.

The Reg protein family is a group of small secretory proteins classified within the lectin super family (403). REG3B (also known as pancreatitis associated protein1 (PAP1)) (*Reg3b* LogFC +1.4), is overexpressed in intestinal tissues during inflammation and is found at elevated levels in patients with active IBD and in experimental models of colitis (363). It is believed to have anti-inflammatory properties, reducing pro-inflammatory cytokine release in a dose-dependent manner from epithelial and monocyte cells in part by preventing TNF induced NF-κB activation (363). Similarly, serum REG3B levels in IBD patients correlate with clinical and endoscopic assessment of disease severity (404). Thus one could hypothesise that elevated monocyte *Reg3b* levels in *Mbd2*$^{-/-}$ monocytes may reflect a compensatory anti-inflammatory control mechanism to counter the vigorous colonic inflammation seen in *Mbd2*$^{-/-}$ mice. To test this hypothesis, we could assess the level of *Reg3b* expression in steady state WT and *Mbd2*$^{-/-}$ monocytes, to confirm that *Mbd2* deficient monocytes are not pre-programmed to have anti-inflammatory tendencies. Similarly a time-course of *Reg3b* monocyte expression, or serum REG3B during DSS colitis might help confirm the dynamics of inflammation v compensatory mechanisms in the absence of *Mbd2*.

Complement component C4 is a large glycoprotein that serves as a opsonin and anchor for the proteases of the classical and lectin complement pathways (364). C4a (*C4a* LogFC +1.5) is an anaphlyatoxin that can trigger smooth muscle contraction, increased capillary permeability and chemotaxis of leucocytes in the direction of increasing concentration (364). C4b (*C4b* LogFC +1.3) covalently binds to pathogens, thereafter forming part of the C3-convertase complex, which catalyses the proteolytic cleavage of C3 into C3a and C3b and the eventual formation of the membrane attack complex via C5, 6,7,8 (364). Serum C4 levels are increased in patients with active IBD (365). Increased *Mbd2*$^{-/-}$ monocyte C4 expression would be in keeping with increased complement mediated binding to infiltrating

pathogens or commensals to control and contain bacterial invasion in a DSS-induced barrier-deficient environment. To test the hypothesis that *Mbd2* deficient monocytes have the same ability to use complement to control invading pathogens, and that increased monocyte *C4a* and *C4b* in these cells is secondary to an increased bacterial exposure, we propose to culture naïve *Mbd2* deficient and sufficient monocytes with a known concentration of luminal commensals from WT or *Mbd2*$^{-/-}$ mice and assess *C4a/b* expression. This would also have the benefit of comparing whether the composition of *Mbd2*$^{-/-}$ intestinal commensals have an increased pro-inflammatory effect on the innate immune system compared to WT microbiota.

Mucosa-associated lymphoid tissue (MALT) (*Malt* LogFC-1.0) lymphoma translocation protein 1 (MALT1) is an intracellular NF-κB activator that is involved in human MALT lymphoma tumorigenesis via constitutive NF-κB activation (366). This constitutive activation induced by translocation provides both anti-apoptotic and proliferative signals. MALT1 is also a paracaspase which is able to cleave roquin1,2 and regnase-1, all of which are able to negatively regulate pro-inflammatory cytokine mRNA including *Il6, Tnf, Icos* and *Tnfrsf4* by reducing their respective half lives (367). In addition *Malt1*$^{-/-}$ mice are resistant to experimentally induced autoimmune encephalitis (405). Thus the reduced *Malt1* expression seen in *Mbd2*$^{-/-}$ monocytes would be hypothesised to reduce NF-κB activation and expression of pro-inflammatory mediators, consistent with an anti-inflammatory control mechanism to counter the vigorous inflammatory environment seen in *Mbd2*$^{-/-}$ DSS mediated colonic inflammation. We therefore hypothesise that *Mbd2*$^{-/-}$ mice have an earlier onset of inflammation during DSS colitis than WT mice. This would be supported by the data in Figure 3.6B and C which show an increased weight loss and symptom score from day4. To pursue this in more depth however, we propose to measure monocyte *Malt1* expression earlier in the disease model, and would hypothesise that expression in *Mbd2* deficient cells is greater at earlier time points compared to WT to permit a robust response to invading pathogens, before being switched off in an attempt to limit pathological, damaging inflammation.

Fc receptor-like S, scavenger receptor (FCRLS, formerly known as macrophage scavenger receptor 2 (MSR2)) (*Fclrs* LogFC-1.0), is a poorly described transmembrane surface protein with scavenger receptor (SR) and immunoglobulin domains. FCRLS has been shown to be upregulated on the surface of tumour associated macrophages (TAM), but its precise functional role is unknown (368). The SR family however has been shown to have diverse roles, including in the innate immune response, cellular adhesion and phagocytosis of apoptotic cells, in addition to lipid uptake. MSR1 is the best-described scavenger receptor, with critical roles in phagocytosis and bacterial clearance (406). MSR1 and FCLRS share the same Cys-rich scavenger receptor domain (smart00202). MSR1 deficient mice are more susceptible to intraperitoneal infection with *S. aureus*, poorly clearing bacteria from the site

of infection and eventually succumbing to disseminated sepsis (407). Similarly MSR1 deficient macrophages are unable to effectively phagocytose gram positive bacteria despite normal phagocytosis machinery (407). Monocytes are generally thought to play a limited role in phagocytosis, though clearly downregulation of SR in *Mbd2*$^{-/-}$ macrophage intermediaries could be hypothesised to decrease bacterial clearance, propagating inflammatory response. To test this hypothesis, we propose to assess the ability of *Mbd2* deficient monocytes to phagocytose pathogen in comparison to WT. For example, we could assess the monocyte uptake of phRodo *E. Coli* bioparticles by flow cytometry, which fluoresce after uptake into phagolysosomes.

However, as suggested by the absence of significant genes that were logFC>2 there were not striking differences between the datasets. In particular there was no significant difference in the expression of pro-inflammatory cytokines (IL-1β, TNF, IL-6, IL-12, IL-15, IL-18, iNOS, ROS), chemokines (CXCL9, CCR1, CCR2, CCR5), pattern recognition receptors (TLR2, 3, 4, 9), or adhesion molecules (CD62L, CD11b, ICAM1).

4.5.2.2 The role of *Mbd2* in monocytes using mixed BM chimeras

Given the increased severity of inflammation seen in the *Mbd2*$^{-/-}$ mice and upregulated bacteriocidal pathways seen in *Mbd2* deficient monocytes, we sought to control for inter-mouse variation in inflammation by combining *Mbd2* deficient/sufficient monocytes within the same organism, using mixed BM chimeras. Once again this demonstrated equivalent pro-inflammatory cytokine producing abilities irrespective of *Mbd2* sufficiency or deficiency. Clearly we cannot exclude the possibility that *Mbd2* sufficient cells, particularly residual radio-resistant host cells or WT transferred cells, in these mixed BM chimeras were modulating *Mbd2* deficient cell types, particularly monocytes, to an ameliorated phenotype. To explore this possibility we would seek in future work to perform non-chimeric experiments to test the role of *Mbd2* in monocytes. This would overcome the issue, albeit low, of radioresistant cells and could include the use of monoclonal antibodies to deplete monocytes *in vivo* during intestinal inflammation to address the relative contribution of *Mbd2* versus WT monocytes in driving inflammation. Similarly we could purify monocytes from WT or *Mbd2*$^{-/-}$ mice and administer them to WT mice during DSS mediated inflammation to address if *Mbd2* deficient monocytes are delivered into a system that lacks any other *Mbd2* deficient cell types, they can mediate increased susceptibility to colitis. Lastly if administration of WT or *Mbd2*$^{-/-}$ monocytes is performed at different time points one could discern whether a critical mass of inflammation is required early in the DSS time course that results in the inherent control mechanisms, or 'brakes' on the inflammatory cascade being irrevocably removed, and thus explain why anti-inflammatory genes are upregulated in *Mbd2* deficient macrophages (Figure 4.10A).

One of the most striking findings derived from the production of mixed BM chimeras, was the out competition of *Mbd2*$^{-/-}$ BM by WT in producing differentiated progeny 8weeks post re-constitution. Epigenetic changes are crucial in haematopoiesis as they regulate the successive gene expression programmes that give rise to all immune cell populations (408). Investigation into the participation of epigenetic events in haematopoiesis has revealed that both DNA and histone modifications are important in this process (408). For instance, the ablation of *Hdac1* and *Hdac2* in mouse bone marrow progenitor cells impedes the development of erythrocytes and megakaryocytes (409). In addition mice with reduced DNMT1 activity have a myeloerythroid bias, unable to develop lymphoid progeny (410). Given that *Mbd2*$^{-/-}$ mice display comparable development of terminally differentiated haematopoietic cells compared to WT in steady state tissues, it is conceivable that *Mbd2* deficiency renders the differentiation of HSC into myeloid progenitors less efficient, such that they are outcompeted in the presence of *Mbd2* sufficient stem cells. To test this hypothesis we could raise short interfering RNAs (siRNAs) to MBD2 mRNA, and expose HSC from WT mice *in vitro* to MBD2 siRNA or control, assessing for effect on HSC development in particular the ability to generate differentiated progeny. We could interrogate this further by adding siRNA at defined time points to ascertain at what point in the differentiation pathway MBD2 is exerting its effects.

Gene expression analysis of *Mbd2*$^{-/-}$ monocytes isolated from the site of inflammation revealed a subtly more pro-inflammatory signature, with increased expression of bacteriocidal genes (*C4a, Irg1, Lyz1*) and compensatory promotion of anti-inflammatory pathways (*Reg3b*, *Malt1*). This initially appeared counter-intuitive, that anti-inflammatory pathways were upregulated in the presence of a marked pro-inflammatory environment. We concluded therefore that the kinetics of inflammatory gene expression were important in this model, whereby had we sampled monocytes earlier in inflammation e.g. day 3, the dominant pathway may have been a pro-inflammatory, pro-antigen response mediated mechanism, and that compensatory anti-inflammatory genes are only expressed later in disease course (Diagram 4.1).

We also observed that a monocyte maturation marker (*ApoC1*) associated with macrophage differentiation was increased in *Mbd2* deficient monocytes, though this was not associated with changes in monocyte proliferation. Indeed monocyte egress to the inflamed colon was equivalent when both *Mbd2*$^{-/-}$ and WT populations were present in the same model. We therefore suggest that colon LP monocyte recruitment is a marker of the increased inflammatory burden in DSS colitis, and hypothesise that other *Mbd2* deficient cell types in *Mbd2*$^{-/-}$ DSS treated mice are precipitating an earlier monocyte recruitment to the inflamed colon.

Diagram 4.1

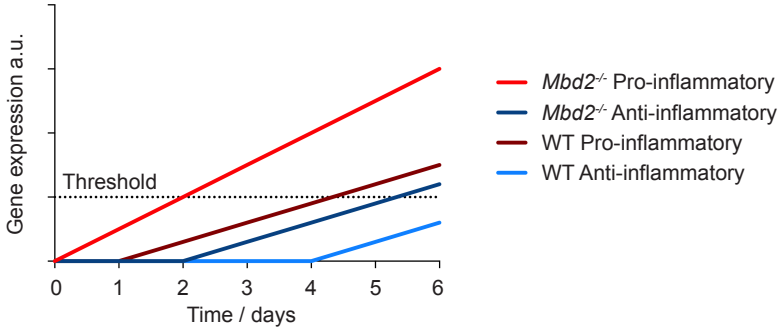

Proposed kinetics of pro- and anti- inflammatory pathways in DSS coltiis
To explain the increased pro- and anti- inflammatory pathways in Day6 DSS treated *Mbd2*$^{-/-}$ versus WT mice we propose the above hypothetical response to intestinal inflammation. We suggest that pro-inflammatory response is earlier and greater in *Mbd2*$^{-/-}$ mice, expemplifed by greater weight loss at earlier time points in the disease model (Figure 3.4). This triggers anti-inflammatory control mechanisms at an earlier stage in *Mbd2*$^{-/-}$ mice after reaching tissue limits for physiological infammation. Thus at our observed time point, day 6, both pro- and anti- inflammatory mechanisms can be seen to be increased in *Mbd2*$^{-/-}$ mice

4.5.3 The role of *Mbd2* in CD11c expressing cells

Given the known role of CD11c expressing cells in DSS colitis, and *Mbd2* in DC function, we sought to understand the role of *Mbd2* expression in CD11c^{+} cells during colonic inflammation (355), (354), (318). First, we confirmed the relative abundance and composition of CD11c expressing cells, noting that >75% of this population was composed of macrophages and DC subsets (Figure 4.7A). Second, we confirmed that in a Cre-flox system of CD11c specific *Mbd2* deletion, transcript levels from purified colon LP myeloid subsets demonstrated appropriate knock down in CD11c expressing cells to over 85% compared to *CD11c-Cre*$^{-}$ controls. Interestingly we did not see a reduced number of CD11b^{+} CD103^{+} DCs in CD11c^{+} cell deletion of *Mbd2*. Referring to our early hypothesis in Chapter 3.11 of 2 possible hypotheses for intestinal specific depletion of *Mbd2* deficient CD11b^{+} CD103^{+} DCs; 1) that *Mbd2* is required for appropriate DC development that occurs after pre-cDC differentiation or 2) that *Mbd2* is required for surivival and/or conditioning of resident CD11b^{+} CD103^{+} DCs in the intestine, we can now refine this hypothesis. Namely appropriate development of CD11b^{+} CD103^{+} DCs in CD11cΔ*Mbd2* but not chimeric or *Mbd2*$^{-/-}$ animals would suggest it is less likely that *Mbd2* is intrinsically required as a survival factor in CD11b^{+} CD103^{+} DCs. It is perhaps more likely that *Mbd2* deficiency in other haematopoietic cells is required for impaired CD11b^{+} CD103^{+} DC development in chimeric or *Mbd2*$^{-/-}$ mice, or indeed that *Mbd2* is required for appropriate development after pre-cDC differentiation but before CD11c expression in a currently unknown DC precursor specific to CD11b^{+} CD103^{+} DCs.

We then observed that CD11c restricted deficiency in *Mbd2* resulted in an increased susceptibility to DSS mediated colonic inflammation, characterised by increased weight loss, symptom and histology scores, neutrophil and monocyte accumulation with an increased proportion of TNF^+ neutrophils and IL-1β/TNF^+ monocytes. Gene expression analyses of the 2 largest CD11c expressing colon LP populations (macrophages and $CD11b^-$ DCs) revealed macrophage *Mbd2* deficiency conferred increased expression of bacteriocidal, pro-inflammatory and anti-inflammatory genes consistent with an ability of these cells to have dual roles in tolerance and pathogen response (Figure 4.10A and Table 4.8).

4.5.3.1 Key differences in *Mbd2* deficient macrophage gene expression during DSS

The IL-1 family consists of eleven proteins, which are further organised into 3 subfamilies. IL-1α and IL-1β are the major IL-1 agonists and have been long recognised as integral components of innate immune processes (369). As such they are implicated in the pathogenesis of several inflammatory diseases, with high levels of IL-1 expression corresponding to disease activity in the colons of IBD patients (370), (371). There are 3 approved IL-1 axis blocking treatments in clinical trials. Anakinra, an IL-1R anatagonist blocking IL-1α/β activity, Rilonacept, a soluble IL-1-decoy receptor and Canakinumab, a neutralising monoclonal anti-IL-1β antibody (411). IL-1α (*Il1a* LogFC+1.8) is a preformed intracellular precursor that can translocate to the nucleus upon inflammatory stimuli to control gene expression, proliferation and differentiation (369). Bersudsky et al. have recently reported the importance of IL-1α in exacerbating colonic inflammation as mice with global ($Il1a^{-/-}$) or epithelial specific ($Villin\text{-}Cre^+ Il1a^{fl/fl}$) removal of IL-1α displayed a less severe epithelial driven response to DSS (412). However the same study reported IL-1α co-staining with MPO^+ cells in acute colitis and notably WT BM transplanted into $Il1a^{-/-}$ irradiated mice had the same severity of colitis as WT BM transplanted into WT mice, suggesting a conflicting role for IL-1α sources, that includes haematopoietic cells.

Indoleamine 2,3 dioxygenase (IDO1) (*Ido1* LogFC+1.1) is the first and rate-limiting step in tryptophan catabolism along the kynurenine pathway (375). Kynurenine metabolites act to promote T cell tolerance and exert antimicrobial effects that are attributed to IDO1 activity. In the steady state GI tract expression of IDO1 is low and occurs predominately within LP cells (413). IDO1 expression is stimulated by TNF, IFN-γ and IL-1β and is one of the most highly upregulated genes in human IBD and animal models of colitis (376), (377). GI tract APCs, notably $CD103^+$ DCs, have been shown to demonstrate potent, IDO1 dependent suppressive effects on T cell proliferation mediated by Treg induction and by limiting Th1/Th17 differentiation (414). Indeed $Ido1^{-/-}$ exhibit greater colitis in a model of graft versus host disease, with TLR7/8 agonist mediated increases in APC sources of IDO1, limiting colon injury in the same model (415). Thus one would hypothesise increased *Ido1* expression from *Mbd2* deficient macrophages is another mechanism for limiting intestinal

inflammation in *Mbd2*$^{-/-}$ colitic mice. To test this hypothesis, we propose culturing day6 *Mbd2* deficient and sufficient macrophages with naïve T cells, to confirm that increased *Mbd2* deficient macrophage sources of *Ido1* can inhibit T cell proliferation, particularly the development of Th1/Th17 cells. In addition we propose an assessment of colon LP macrophages sources of *Ido1* in *Mbd2* deficient and sufficient animals earlier in the DSS inflammation model, to confirm that *Ido1* is switched on earlier in *Mbd2*$^{-/-}$ to mirror earlier onset of inflammation, rather than constitutive activation.

Resistin-like molecule (RELM) α (*Retnla* LogFC-1.1) belongs to a family of secreted mammalian proteins with putative immunomodulatory properties (416). RELM-α is upregulated in several infectious and inflammatory settings including helminth infection, allergic airway inflammation and colitis (378), (379). RELM-α administration promotes immune cell activation, pro-inflammatory chemokine and cytokine expression in DSS treated mice (379). In addition, *Retnla*$^{-/-}$ mice demonstrate less severe DSS and *C. rodentium* induced colonic pathology that has been suggested to be a result of reduced IL-23p19 expression from RELM-α deficient macrophages (380). Taken together, reduced expression of *Retnla* by *Mbd2*$^{-/-}$ macrophages in the context of severe intestinal inflammation would be hypothesised as a limiting mechanism to further damaging inflammation. To test this hypothesis, as discussed above we could once again assess for expression of *Retnla* during the induction of intestinal inflammation, to confirm increased levels in *Mbd2*$^{-/-}$ earlier in the proposed pure pro-inflammatory stage of disease. Similarly to confirm that decreased pro-inflammatory response in *Mbd2* deficient macrophages is indeed a secondary response rather than a constitutive one, we propose to purify naïve colon LP macrophages from *Mbd2*$^{-/-}$ and WT mice, culturing them *ex vivo* with bacterial products to confirm or refute an equivalent ability to uptake, process and respond to antigenic challenge.

Triggering receptor expressed on myeloid cells (TREM-2) (*Trem2* LogFC-0.99) is a surface receptor found on macrophages, DCs and microglia that binds motifs on bacteria and yeasts (417), (381). TREM-2 is expressed at higher levels on CD11c^{+} LP cells isolated from patients with active IBD and mice with experimental colitis versus controls suggesting myeloid sources of TREM-2 are important in regulating inflammation (382). Indeed *Trem2*$^{-/-}$ are protected from DSS colitis with *Trem2* deficient CD11c^{+} cells demonstrating reduced pro-inflammatory cytokine production, bacterial killing and T cell activation abilities (382). In addition administration of a TREM-1 agonist ameliorates DSS colitis and decreases TNF, IL-6 and IL-1β production from CD11c^{+} cultured cells (418). However it has also been shown that TREM-2 blockade with mAb impairs apoptosis in microglial cells via a reduced interaction with TREM-2 ligands on apoptotic neurons leading to reduced neuronal healing (419). Similarly *Trem2*$^{-/-}$ display reduced wound healing, epithelial proliferation and increased M1 macrophage infiltrate (420). It is similarly not understood why increased expression of

TREM2 is found in IBD patients if it is indeed a pro-inflammatory mediator. To explore the role of TREM2 in DSS colitis further therefore, we would propose to use TREM-2 mAb to block TREM-2 downstream effects in WT mice in acute and chronic models of DSS colitis, to confirm firstly the results of Correale et al. in ameliorating acute colitis, and thereafter in the chronic phase of DSS ingestion its putative role in intestinal wound healing (382).

4.5.3.2 Increased pro- and anti- inflammatory pathways in DSS colitis, possible explanations and relation to the literature

The combination again of both pro- and anti-inflammatory gene dysregulation led us to speculate that in the context of severe disease pathology in *Mbd2*$^{-/-}$ DSS treated mice that a complex feedback mechanism may exist (Diagram 4.1). Reduced *Mbd2*$^{-/-}$ *Retnla* and *Trem2* macrophage expression for example would be expected to result in ameliorated macrophage response by limiting pro-inflammatory cytokine secretion, however increased *Il1a* should favour an increasing inflammation response by promoting further cytokine release. We speculate this dichotomous response likely represents a compensatory mechanism to limit overwhelming inflammation that is secondary to altered kinetics of immune response in *Mbd2*$^{-/-}$ mice. We suggest that due to an earlier onset of inflammation, precipitated perhaps by increased barrier dysfunction to DSS, that the role of pro-inflammatory mediators such as *Retnla* occurs at an earlier timepoint, and this reverses once the inflammatory response exceeds a given level and itself becomes pathological. Indeed initial inflammatory response is a necessary physiological response to protect the host, a response that must be mitigated by resolution of inflammation using anti-inflammatory and pro-resolution pathways (421). Inability to resolve inflammation is thought to be one of the key drivers for critical illness, the leading cause for admission to intensive care units, irrespective of the initial cause for inflammation (422), (423), (421). Decision fates after acute inflammation depend on appropriate class switch of pro-inflammatory eicosanoid mediators such as leukotriene B_4 to pro-resolution lipid mediators such as lipoxins, resolvins and protectins that promote a return to homeostasis versus chronic inflammatory response (424). We therefore consider 3 different explanations: that increased pro- and anti- inflammatory gene expression in *Mbd2* deficient populations represents an ongoing exposure to the initial inflammatory insult mediated by 1) an inability to appropriately clear the influx of antigenic commensals or 2) because the initial inflammatory insult is much greater and more rapidly converted from local to systemic inflammation due to a primary defect in appropriate host response, namely defects in barrier function or lastly 3) that this imbalance represents a failure of pro-resolution mediators to overcome the level of inflammation in *Mbd2*$^{-/-}$ mice that favour a chronic inflammatory state.

Interestingly, a novel gene (*Fclrs*) with scavenger receptor domains not previously known to be important in macrophage function was significantly down regulated, in *Mbd2* deficient

macrophages suggesting *Mbd2* may promote bacterial uptake and/or processing by colon LP macrophages that may also explain the increased susceptibility of CD11cΔ*Mbd2* mice to DSS colitis. To test this hypothesis we would need to perform assays of phagocytosis and/or bacterial persistence and this may form the basis of future work. As mentioned above, we would propose to investigate this via assays of phagocytosis, pinocytosis and macro-pinocytosis using *E. coli* bioparticles, FITC and DQ-OVA labelled beads in *ex vivo* culture of naïve and DSS treated *Mbd2* versus WT colon LP macrophages.

Taken together, colon LP *Mbd2* deficient macrophages in DSS colitis displayed differentially expressed genes that would be hypothesised to dampen damaging inflammation, with increased expression of anti-inflammatory mediators (*Il1a, Tgfbi, Reg3b, Reg3g*) and decreased pro-inflammatory response mechanisms (*Retnla, Trem2, Ido1*). However, in keeping with the dual role of GI tract macrophages, bacteriocidal pathways were also upregulated in *Mbd2* deficiency (*Lyz1, Irg1*) consistent with previous literature supporting combined tolerogenic and pro-inflammatory capabilities (51). An unexpected finding was the reduction of the scavenger receptor *Fclrs*. This poorly described scavenger receptor has no previous documented function in macrophage function. However given deficiency in other scavenger receptors, notably MSR1 confers up to a 50% reduction in macrophage phagocytic ability, one would hypothesise other scavenger receptor dysregulation could confer altered bacterial handling abilities, resulting in pathogen persistence.

4.5.3.3 Key differences in *Mbd2* deficient CD11b^{-} DC gene expression during DSS

Janus kinase-2 (JAK2) (*Jak2* LogFC-0.97) is an important component of the IL-12 and IL-23 signaling pathway (388). It is thought to bind to membrane bound IL-23R and IL-12Rβ2 components in response to the p35 and p19 subunits of IL-12 and IL-23 respectively (388). Subsequent phosphorylation steps of STAT 1,3,4,5 eventually lead to STAT4 mediated changes in gene expression, particularly Th17 differentiation (389). Polymorphisms in *JAK2* and other components of the IL-23 signaling pathway (*Il23r, Il12* and *Stat3*) have been identified as risk susceptibility loci for both CD and UC (308). Whilst it is not understood how these loci confer their increased risk in man, it has been shown that IL-23 production from murine LP CD11b+ DCs induces production of the antimicrobial peptide REG3G in an IL-22 dependent manner, suggesting that aberrant IL-23 signaling may impair barrier function (346). However IL-23 has also been suggested to have a pro-inflammatory role in innate and T cell models of colitis. Administration of anti-IL-23p19 treatment reduced pathology in a *H. hepaticus* model of intestinal inflammation and, similarly, mice incapable of producing p19 were less susceptible to a well-established T-cell dependent model of colitis, with ROR-γt^{+} ILC3 suggested as the IL-23 responsive pro-inflammatory cell mediating this effect (96), (195). Aberrant IL-23 signaling in *Mbd2*$^{-/-}$ CD11b^{-} DCs could therefore be hypothesised to

confer pro- or anti-inflammatory changes based on Th17 differentiation, ILC function or epithelial production of antimicrobial peptides.

Leucine-rich repeat kinase 2 (LRRK2) (*Lrkk2* LogFC-0.70) is large protein (2527 amino acids), with 2 distinct enzymatic domains, although its precise physiological function is unknown (390). It has been identified as a risk susceptibility locus for CD, leprosy and is the most common genetic cause for familial and sporadic Parkinsons disease (425). Alterations in autophagy have been proposed as potential pathogenic mechanisms in all 3 disorders (425). LRRK2 is known to associate with autophagy proteins p62 and LC3, is expressed preferentially by LP leucocytes, and is found to be upregulated in inflamed CD colonic biopsy specimens, with LRRK2-deficient mice been shown to have poorer outcomes in response to DSS (391), (392). Other autophagy genes have been identified as IBD-susceptibility loci (ATG16L1, IRGM and NOD2) with macroautophagy of intracellular microbes hypothesised to be one of the defining features of CD (308). Thus dysregulated *Lrrk2* mediated autophagy in *Mbd2*$^{-/-}$ CD11b^{-} DCs would be hypothesised to perpetuate intracellular pathogens, potentially prompting cell death and further inflammatory response. To test this hypothesis, we could induce and compare autophagy in naïve *ex vivo* *Mbd2*$^{-/-}$ or WT colon LP CD11b^{-} DCs by exerting a state of starvation. By culturing in nutrient rich medium versus control, and using immunohistochemistry assessing induction of LC3 or p62, or scanning electron microscopy to detect autophagosomes. Lastly we could cross our existing *Mbd2*$^{-/-}$ mouse with a GFP labelled LC3 transgenic mouse, which would permit the direct visualisation of LC3 in a range of colon LP cell types *ex vivo* without the need to perform FACS to purify cells in advance.

4.5.3.4 Activation of CD11c^{+} cells in *Mbd2* deficiency

The data presented in Table 4.12 suggested that *Mbd2* deficient DCs and macrophages displayed higher levels of surface CD40 in DSS colitis and also in the steady state. In addition levels of CD80 on all DSS treated colon LP MP cells (except CD11b^{-} CD103^{+} DCs), and in naïve macrophages / CD11b^{+} CD103^{+} DCs were higher in *Mbd2* deficiency. We hypothesise that increased levels of APC CD40 in the steady state and inflamed colon would promote pro-inflammatory cytokines release (such as IL-12p40 and IL-6) and further leucocyte recruitment (426). Given that CD40/CD80 levels were equivalent to controls in CD11c^{+} cell specific *Mbd2* deficiency, this would suggest that non-CD11c^{+} cell sources of *Mbd2* are required to increase MP activation phenotype (Table 4.12). IECs have a well documented role in antigen presentation to LP APCs, therefore we hypothesise IEC sources of *Mbd2* may alter the ability of IECs to process and present luminal / dietary antigens to colon LP cells, thereby altering their activation and function.

To test this hypothesis, and further address whether increased CD40 in *Mbd2* deficient cells is a primary (i.e. intrinsic to CD11c^{+} cells) or secondary (e.g. a byproduct of a more inflamed

microenvironment) phenomenon, we could use the CD40-CD40L inhibitor trapidil in naïve and DSS treated *Mbd2*$^{-/-}$ and WT mice. We would propose to assess the response to inflammation (e.g. weight loss, pathology score, inflammatory cell recruitment) and function of *Mbd2* deficient CD11c^{+} cells (e.g. cytokine release, antigen processing and migration capabilities) in a system where CD40 signaling is impaired. Finally we would restrict *Mbd2* deficiency to IECs by generating a VillinCreΔMbd2 mouse, assessing the activation of colon LP MPs in the steady state and experimental colitis, thereby addressing a non-CD11c source of *Mbd2* that might be expected to alter DC/macrophage function.

4.5.4 Caveats to array data and proposed future genomic work

Whilst microarray data has the advantage of hypothesis-free testing to limit investigator bias in understanding the role of key gene expression changes, there are clearly limitations to the interpretation of this data. For example, validation of the observed changes in gene expression should be performed by correlation to expression assessed by qPCR and then continue with assays to measure changes in protein. Similarly it is possible that in the analysis of the above array data, we have overlooked important gene expression changes due to a) limitation of sensitivity of the array process compared to other techniques, for example qPCR and b) an assumption that meaningful changes in cell biology are underwritten by large changes in fold expression. This is exemplified by the data presented in Figure 4.11, whereby significant differences in protein levels (CD40 and CD80) assessed by flow cytometry between *Mbd2*$^{-/-}$ and controls was not observed in gene expression. This underlines the importance of future work to correlate the observed changes in gene/protein by analysis of both in tandem, in addition to assessments of post-translational protein modification.

Similarly we would look to address the possibility that mRNA alterations do not account for the entire phenotype we have observed. For example we have not measured changes in miRNAs, non-coding RNAs or pre-stored proteins, all of which may exert an important effect on the biology of intestinal inflammation that we have not addressed in these experiments thus far. There is an arbitrary limit of fold change that is set by individual investigators being deemed as biologically significant, however there is no accepted value for what this level might be, underlining the difficulties scientists face in ascribing biological and statistical significance. It is similarly conceivable that a multitude of small, yet statistically significant changes in a repertoire of key immune-regulatory genes confer together a profound biological effect that investigators may overlook by focusing simply on large quantitative rather than functional changes in expression.

As can be seen in principal component analysis (Figure 4.10C), whilst displaying a number of significantly dysregulated genes, the effect size of each individual gene was small with no

candidate genes with known or hypothesised function logFC >±1 between genotypes. As such, the overall gene expression differences conferred by *Mbd2* deficiency in CD11b^{-} DCs was low. Given that DC-dogma would suggest these cells have a dominant role in antigen presentation to the adaptive immune system, and that DSS colitis is considered a T cell independent model, it is perhaps unsurprising that these cells do not appear to be the dominant *Mbd2* deficient cell type conferring increased susceptibility to acute colonic inflammation.

As noted above, given the rarity of these cell types, it is possible that increasing the number of biological replicates would have increased sensitivity of detecting dysregulated genes. Similarly, due to the technical limitations of small numbers of the other DC subsets post isolation, we have only purified and assessed mRNA expression in CD11b^{-} DCs. Thus, in combination with the macrophage data, we have performed expression analysis on approximately 65% of CD11c expressing cells, and cannot exclude that the remaining DC subsets are the most dysregulated in the absence of *Mbd2*. Adopting a different methodology that is less reliant on cell yield to permit analysis, e.g. single-cell RNAseq or laser capture dissection, would be an attractive method to address this. Given the variety of antigenic stimuli to APC in the GI tract, it is likely that a single isolated cell may not be representative of the entire population, despite recent advances in phenotyping by flow cytometry. Indeed a recent review of single cell sequencing technology suggest that "hundreds or thousands" of single cells must be analysed so that all representative cell types may be observed (427).

RNA-seq offers many additional benefits compared to arrays. For example they permit the unbiased detection of novel transcripts. RNA-seq technology does not require species or transcript specific probes. It can therefore detect novel transcripts, gene fusions, SNP variants and other previously unknown changes that arrays cannot detect, based on their reliance on existing probes. There is also a broader dynamic range with RNA-seq technology. Array hybridization technology means that gene expression measurement is limited by background at the low end and signal saturation at the high end of expression. Lastly sequencing coverage depth is increased to detect rare transcripts or weakly expressed genes.

It should also be noted that the gene expression analyses were performed from purified populations from global *Mbd2*$^{-/-}$, not CD11cΔ*Mbd2* mice. Thus whilst we may hypothesise the same culprit genes may be dysregulated in both strains, it is possible that *Mbd2* deficiency in other cell types in the global *Mbd2*$^{-/-}$ mice modulates the mRNA expression profiles observed. Quantitative RT-PCR validation of key dysregulated genes identified from the global *Mbd2*$^{-/-}$ microarrays in purified macrophages and DCs from the CD11cΔ*Mbd2*

mice would be helpful to address this. Taking this a step further, we propose that an unselected microarray of all colon LP cells taken at day 0 and day 6 would be helpful in discerning the overall balance of gene expression in *Mbd2*$^{-/-}$ and WT mice. This would also have the added benefit of allowing analysis between our existing purified populations and the whole tissue, to delineate overlapping and distinct areas of mRNA expression to better understand the role of *Mbd2* in other cell types and guide future investigation.

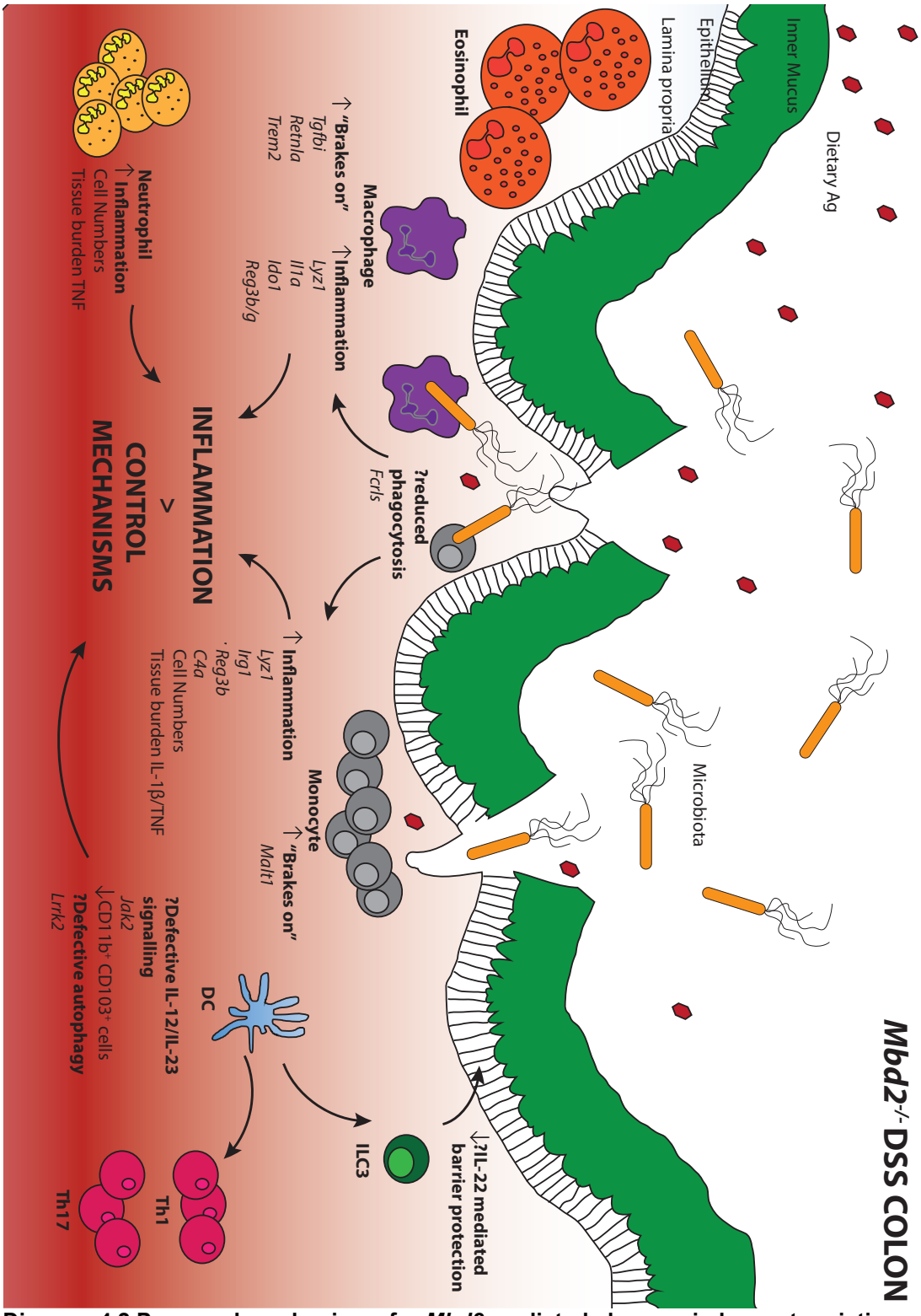

Diagram 4.2 Proposed mechanisms for *Mbd2* mediated changes in haematopoietic cells in DSS colitis

4.6 Summary

In the work detailed in this thesis, we have made several interesting observations regarding haematopoetic development and *Mbd2* deficiency. In Chapter 3 we observed a decrease in the abundance of $CD11b^{+}CD103^{+}$ DCs. In Chapter 4 we similarly observed a decrease in this population when *Mbd2* deficiency was limited to haematopoetic cells but, in addition, $CD11b^{-}$ DCs were found at reduced number when WT radioresistant host cells were present. We suggest that whilst $CD11b^{-}$ DCs develop normally in $Mbd2^{-/-}$ mice they are vigorously outcompeted when WT counterparts are present, which we speculate is unlikely due to intrinsic survival defects given normal levels of differentiated cell types in $Mbd2^{-/-}$ mice, but due to defective development from less differentiated progenitors. In support of this, CD11cΔ*Mbd2*mice showed equivalent proportions and numbers of fully differentiated DCs to WT mice, suggesting *Mbd2* mediated affects on DC development occur in less differentiated precursors. CD11c expression occurs in differentiated DCs, but also in $MHC\text{-}II^{-}$ pre-DC precursors, but not common lymphoid or myeloid precursor cells. Pre-DCs are a population of DC committed precursors present in mouse blood that can fully reconstitute the $CD8^{-}$, $CD8^{+}$ and plasmacytoid $B220^{+}$ DC subpopulations after transfer into irradiated recipients (428). This would argue that *Mbd2* mediated changes in DC differentiation occur at early stages of development before CD11c expression occurs, perhaps at the common precursor stage.

The most striking changes in DC development, however, were evident in the generation of mixed BM chimeras. We observed that equal starting proportions of WT and $Mbd2^{-/-}$ donor BM resulted in an absence of $Mbd2^{-/-}$ cells 8 weeks after reconstitution. It was necessary to titrate the starting proportion of $Mbd2^{-/-}$ BM to a nine fold excess to overcome this. Despite this starting excess, at 8 weeks post reconstitution this ratio had reversed such that WT differentiated cells were more now abundant than $Mbd2^{-/-}$ by more than two fold. Given starting viability of BM cells was equivalent between genotypes, we hypothesise that *Mbd2* deficiency renders HSC less able to enter lineage specific differentiation pathways, particularly given the importance of other epigenetic mechanisms notably in controlling differentiation dependent transcription factor function.

Whilst we have used the literature to guide the identification and interrogation of candidate haematopoietic cell types important in colonic inflammation it was not possible to analyse all cell types. It is therefore possible that there is a role for *Mbd2* in regulating additional cell types, for example neutrophil, eosinophil or ILC function that we have not accounted for. Future work will therefore include the analysis of dysregulated genes identified above in monocytes/macrophages and DCs by qPCR, in other purified cell types including eosinophils and neutrophils. Similarly the use of *in vivo* depleting antibodies (such as anti-Ly6G for

neutrophil depletion) could be employed to assess the role of other *Mbd2* expressing populations.

Taken together we have observed an increased susceptibility to colonic inflammation conferred by deficiency of *Mbd2* in haematopoietic cells. The existing literature would support a role for monocytes as a pro-inflammatory cell type in colitis and were thus targeted for a role for *Mbd2*. Whilst colon monocytes isolated for colitic *Mbd2*$^{-/-}$ mice displayed increased expression of some genes involved in inflammatory response (*Irg1, Ido1, C2, C4a/b*) the majority of gene expression was similar between genotypes. Indeed we then have shown that *Mbd2* deficient monocytes do not possess a more pro-inflammatory phenotype compared to *Mbd2* sufficient monocytes when present in the same inflamed colon using mixed BM chimeras. We therefore suggest that per cell pro-inflammatory capacities of monocytes are equivalent independent of *Mbd2* deficiency, and that increased tissue numbers of these cell types represent a readout rather than primary cause of increased DSS mediated colonic inflammation in *Mbd2*$^{-/-}$ mice.

Overall we therefore propose a model where *Mbd2* mediated changes in gene expression in CD11c expressing cells predisposes to pathological inflammation that exceeds local control mechanisms in DSS colitis (Diagram 4.2). Candidate gene targets identified by gene expression analysis of CD11c^{+} cells isolated from *Mbd2*$^{-/-}$ mice suggest predominately increased pro- but also some anti- inflammatory processes the balance of which ultimately favours increasing monocyte and neutrophil recruitment. Given that haematopoietic restriction of *Mbd2* expression did not appear to recapitulate the phenotype of *Mbd2*$^{-/-}$ response to DSS, and the intriguing observation that non-CD11c^{+} cellular sources of *Mbd2* are required to increase MP activation phenotype, we proposed to investigate further non-haematopoietic souces of *Mbd2* in colonic inflammation.

Given the suggestion from our chimera data that non-haematopoetic sources of *Mbd2* may confer a significant burden of disease susceptibility of *Mbd2*$^{-/-}$ mice to colonic inflammation, particularly given the pathogenesis of DSS thought primarily due to breakdown of barrier integrity, we hypothesised that epithelial sources of *Mbd2* may also have an important role in colonic homeostasis.

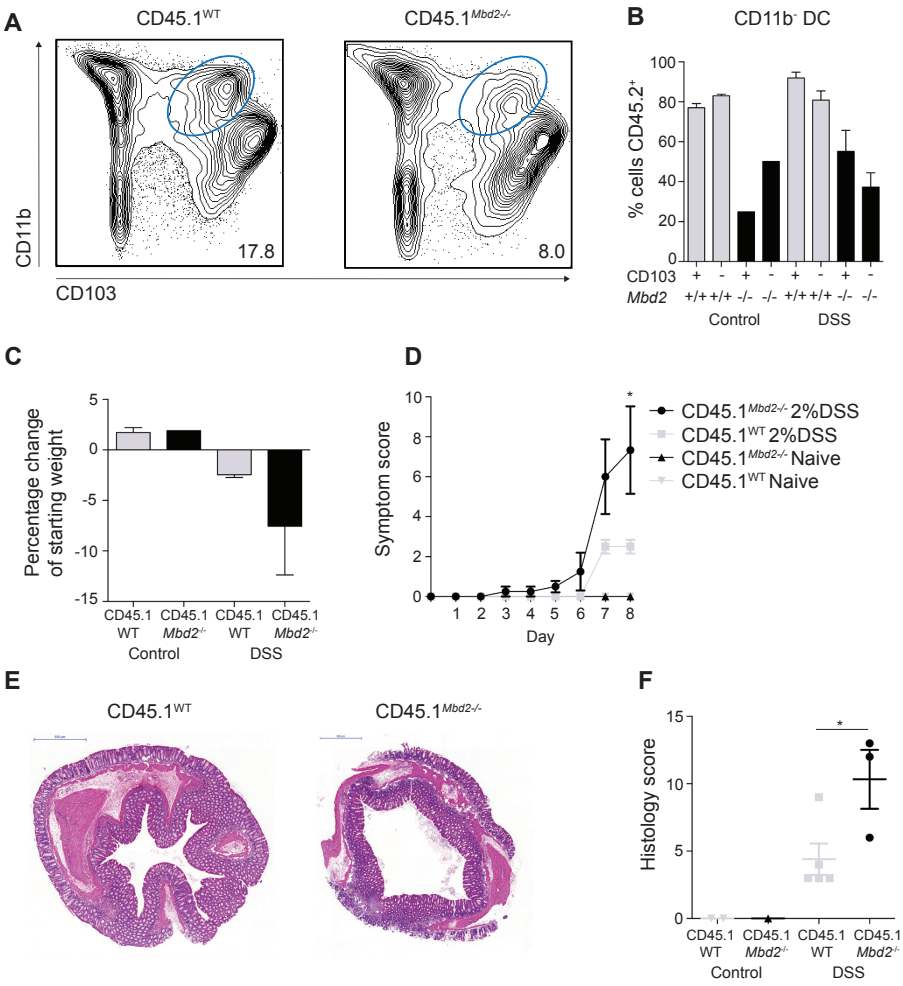

Figure 4.1 Susceptibility of CD45.1^{WT} versus CD45.1$^{Mbd2-/-}$ chimeras to DSS colitis

BM chimeras were generated by lethally irradiating CD45.1 congenic mice before reconstituion with either CD45.2^{+} *Mbd2*$^{-/-}$ (CD45.1$^{Mbd2-/-}$) or CD45.2^{+} WT (CD45.1^{WT}) CD90 depleted BM. Chimeras recieved 2% DSS b/w in drinking water or normal drinking water for 8 consecutive days. Colon LP cells were isolated and surface stained for the following antibodies; CD11b, CD45.1, CD45.2, CD11c, CD103, Ly6G, Ly6C, MHC-II, SiglecF, CD64 and analysed by flow cytometry as described in Figure 3.2. CD45.2^{+}, CD11c^{+}, Ly6G^{-}, SigelcF^{-} gated cells are presented **(A)** comparing DSS treated CD45.1^{WT} and CD45.1$^{Mbd2-/-}$ chimeras and **B** CD11b^{-}, CD11c^{+}, F480^{-}, Ly6G^{-} and SiglecF^{-} DC showing the CD45.2^{+} (i.e. donor) proportion of each CD103 subset**.** Proportion of **C**. Least square mean day 8 weight change of DSS treated and naive control, CD45.1^{WT} and CD45.1$^{Mbd2-/-}$mice as a percentage of starting body weight, n=1-8 analysed by linear regression modelling of 2 separate experiments. **D**. Mean symptom score per day over the duration of DSS treatment. Cumulative score as per Table 2.3 of weight loss (0-4), diarrhoea (0-4) and per rectal bleeding (0-4). n=4 per group, representative of 2 independent experiments **E.** H&E stained transverse sections of distal CD45.1^{WT} and CD45.1$^{Mbd2-/-}$DSS treated colon, x10 magnification. **F.** Least square mean±SEM blinded histology score of inflammation of (**E**), as per Table 2.4, comprising inflammatory cell infiltrate (0-4, +0.5 per ulcer), Goblet cell depletion (0-4, +0.5 per crypt abscess), Muscosal thickening (0-4), submucosal cell infiltration (0-4) and architecture destruction (0-4), n=8 per group analysed by linear regression modelling of 2 separate experiments. (*p<0.05).

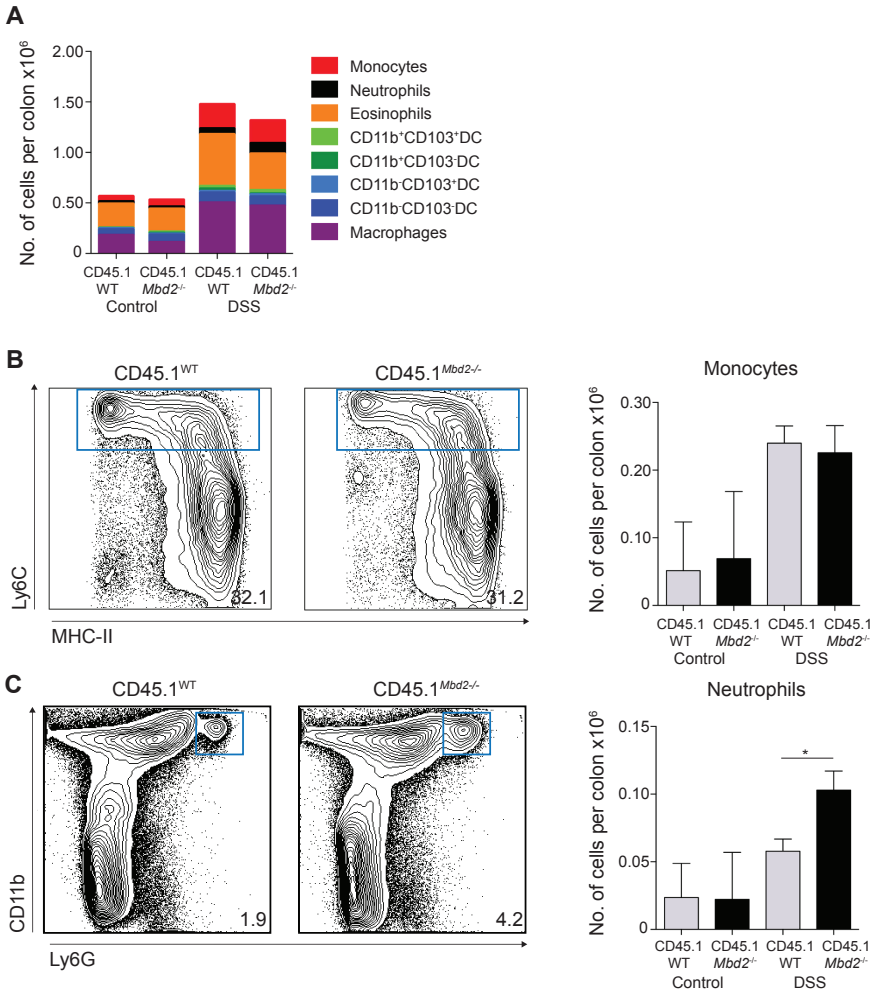

Figure 4.2 Colon LP Flow Cytometry analysis of DSS treated CD45.1^{WT} versus CD45.1$^{Mbd2-/-}$ chimeras

BM chimeras were generated by lethally irradiating CD45.1 congenic mice before reconstituion with either CD45.2^{+} *Mbd2*$^{-/-}$ (CD45.1$^{Mbd2-/-}$) or CD45.2^{+} WT (CD45.1^{WT}) CD90 depleted BM. Chimeras recieved 2% DSS b/w in drinking water or normal drinking water for 8 consecutive days. Colon LP cells were isolated and surface stained for the following antibodies; CD11b, CD45, CD11c, CD103, Ly6G, Ly6C, MHC-II, SiglecF, CD64 and analysed by flow cytometry as described in Figure 3.2. The least square mean total number of cells x10^{6} per colon is presented for the populations **(A)** n=1-8 per group, analysed by linear regression of 2 independent experiments. **B**. Representative flow cytometry contour plots in Day8 DSS treated CD45.1^{WT}and CD45.1$^{Mbd2-/-}$ mice for neutrophil and monocyte populations as defined in Figure 3.2. n=1-8 mice per group analysed by linear regression of 2 independent experiments. (*p<0.05)

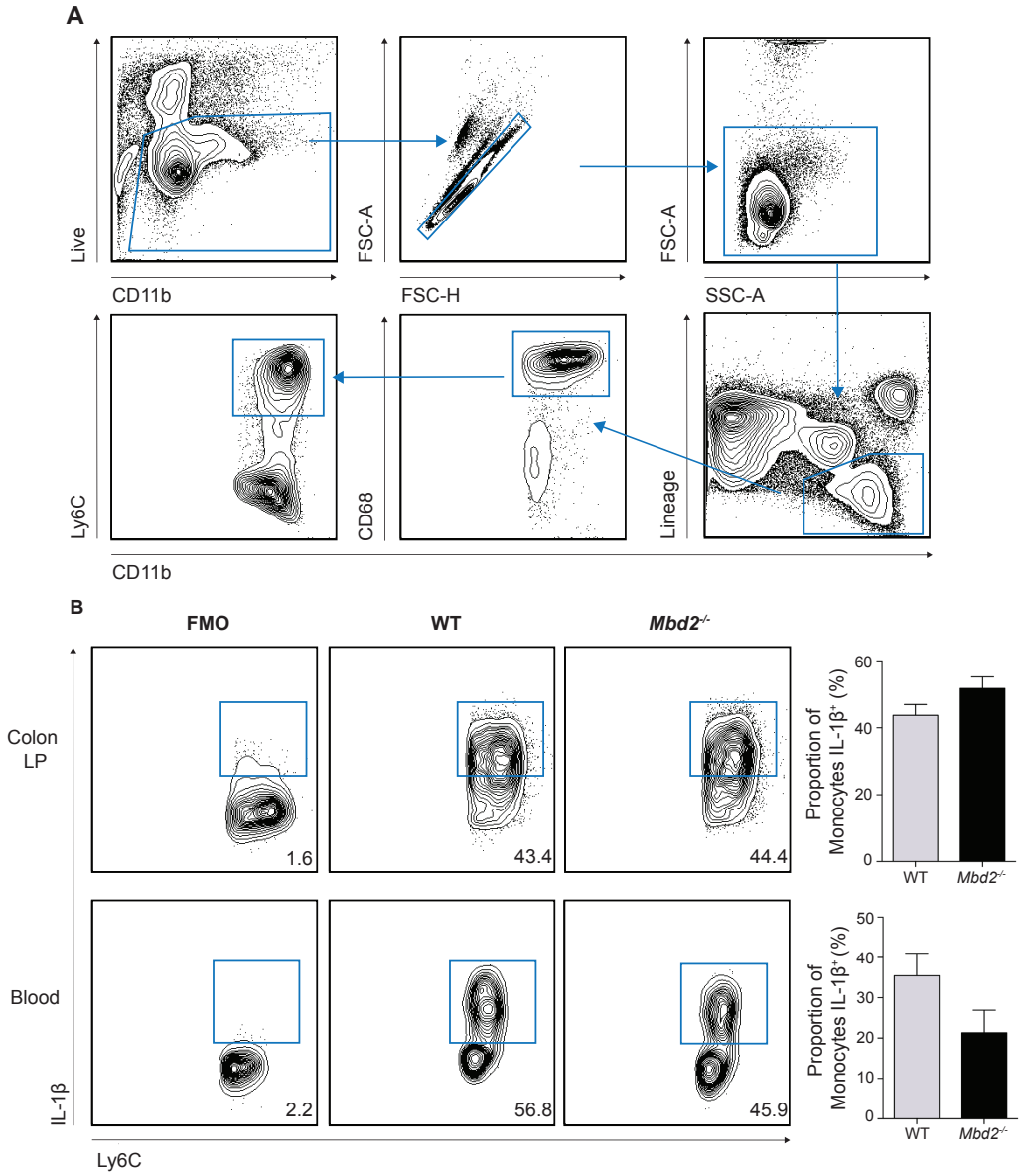

Figure 4.3 Flow cytometry idenitification of cytokine producing colon LP and blood monocytes

A. The cellular component of murine blood was isolated from naive WT mice and analsyed for the expression of the following by flow cytometry; Live Dead Blue, Ly6C, Lineage (NK1.1,CD19,CD3,Ter119,B220), CD11b and CD68.Representative contour plots display the following sequential geting logic to identify blood monocytes; Live, Singlet cells, SSC/FSC-A low 'intact' cells, Lin^{-} $CD11b^{+}$, CD68+ $CD11b^{+}$, $Ly6C^{Hi}$ $CD11b^{+}$ **B**. Representative contour plots (left) of colon LP cells and blood isolated from Day6 DSS treated WT or littermate *Mbd2*$^{-/-}$ mice and analysed for by flow cytometry for the above markers (blood) or CD11b, CD45, CD11c, CD103, Ly6G, Ly6C, MHC-II, SiglecF, CD64 (colon LP) in addition to intracellular IL-1β staining. Cells were stimulated *ex vivo* for 3 hours with 1ug/ml LPS and GolgiStop 1ul/ml(blood) or GolgiStop 1ul/ml alone (colon LP), (right) least mean square proportion of $IL\text{-}1\beta^{+}$ monocytes analysed by linear regression n=12-16 per group, 3 independent experiments.

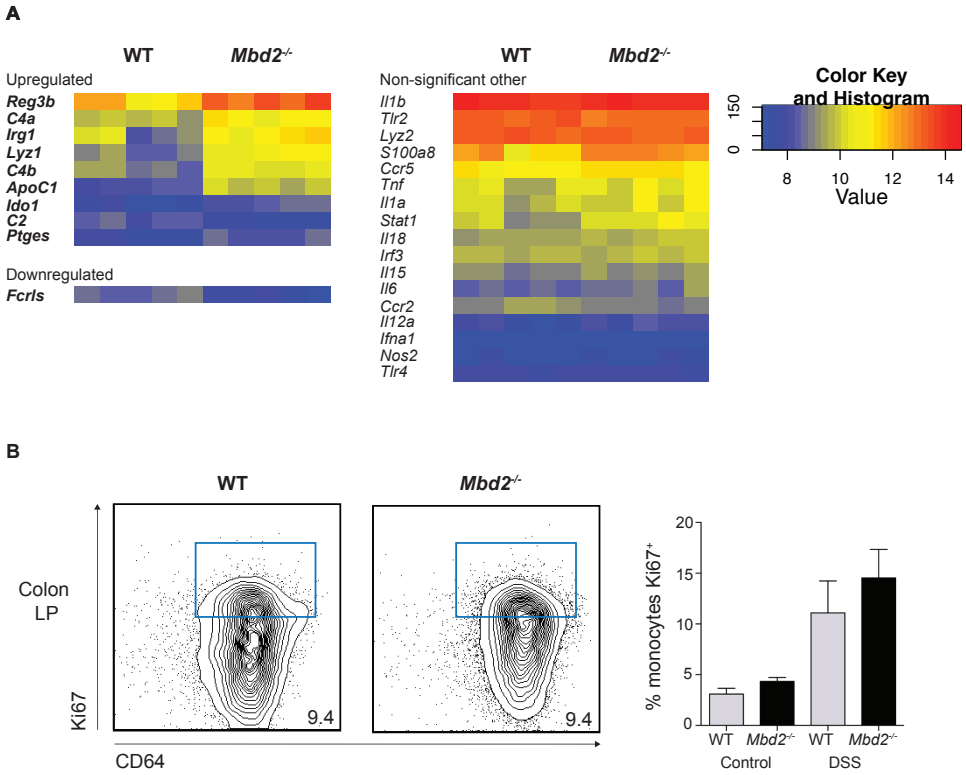

Figure 4.4 Gene expression analysis of DSS treated WT versus *Mbd2*$^{-/-}$ colon LP monocytes

Colon LP cells from Day 6 2% DSS treated *Mbd2*$^{-/-}$ or littermate WT mice were isolated. **A**. Heat map of normalised gene expression from FACS purified WT or *Mbd2*$^{-/-}$, Ly6C^{+} MHC-II$^{+/-}$ monocytes. Each group is comprised of 5 biological replicates, n=2-3 mice pooled per biological replicate. Significant (adj p<0.01) genes presented (left, gene names in bold) with other selected non-significant genes (right). **B.** Representative flow cytometry contour plots and corresponding bar chart detailing proportion of colon LP *Mbd2*$^{-/-}$ or WT monocytes idenitifed as CD11b^{+} CD11c^{-}, Ly6G^{-}, SiglecF^{-}, Ly6C^{+} MHC$^{+/-}$ expressing Ki67 compared to isotype control. representative data from 2 independent experiments.

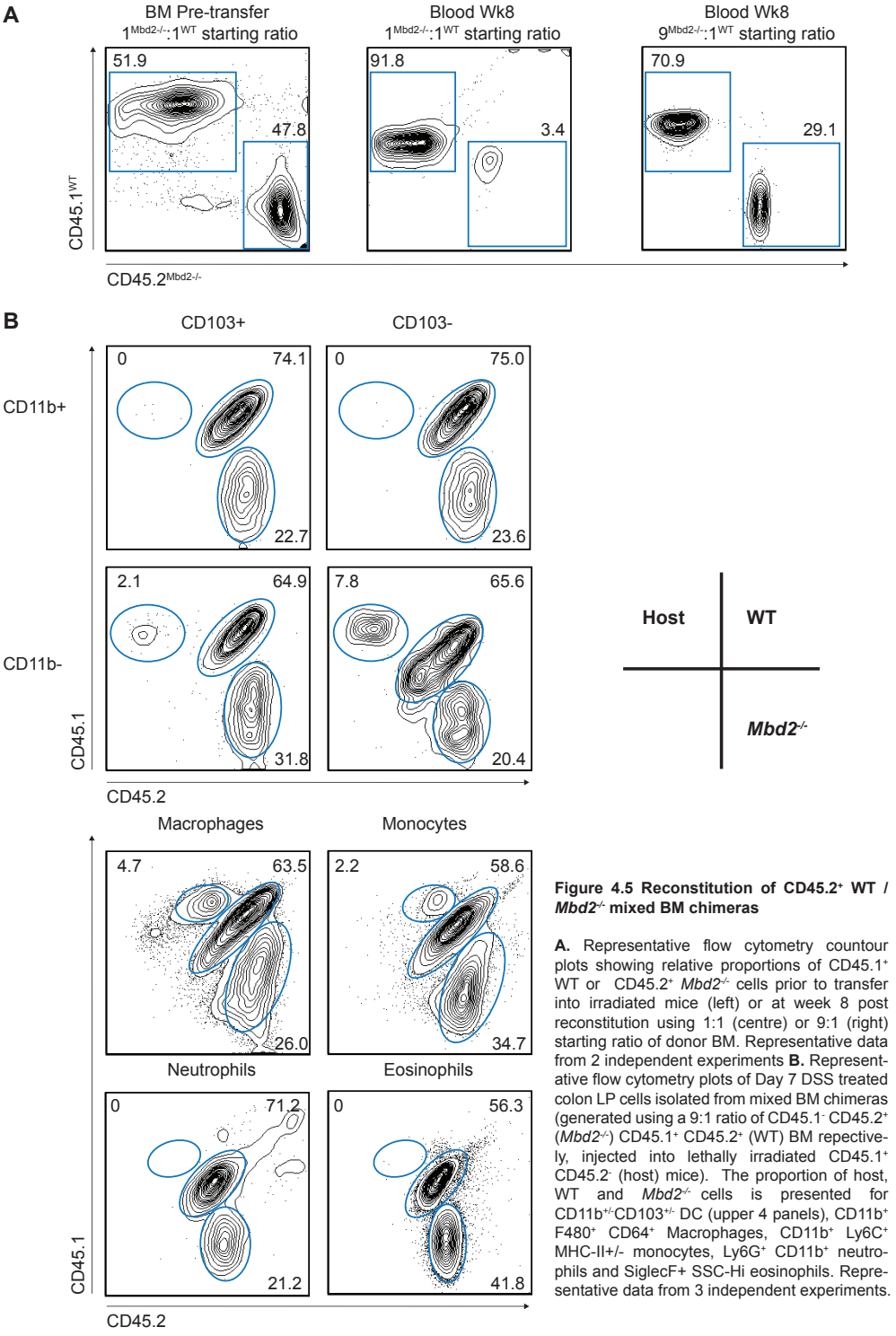

Figure 4.5 Reconstitution of CD45.2⁺ WT / *Mbd2*$^{-/-}$ mixed BM chimeras

A. Representative flow cytometry countour plots showing relative proportions of CD45.1⁺ WT or CD45.2⁺ *Mbd2*$^{-/-}$ cells prior to transfer into irradiated mice (left) or at week 8 post reconstitution using 1:1 (centre) or 9:1 (right) starting ratio of donor BM. Representative data from 2 independent experiments **B.** Representative flow cytometry plots of Day 7 DSS treated colon LP cells isolated from mixed BM chimeras (generated using a 9:1 ratio of CD45.1⁻ CD45.2⁺ (*Mbd2*$^{-/-}$) CD45.1⁺ CD45.2⁺ (WT) BM repectively, injected into lethally irradiated CD45.1⁺ CD45.2⁻ (host) mice). The proportion of host, WT and *Mbd2*$^{-/-}$ cells is presented for CD11b$^{+/-}$CD103$^{+/-}$ DC (upper 4 panels), CD11b⁺ F480⁺ CD64⁺ Macrophages, CD11b⁺ Ly6C⁺ MHC-II+/- monocytes, Ly6G⁺ CD11b⁺ neutrophils and SiglecF+ SSC-Hi eosinophils. Representative data from 3 independent experiments.

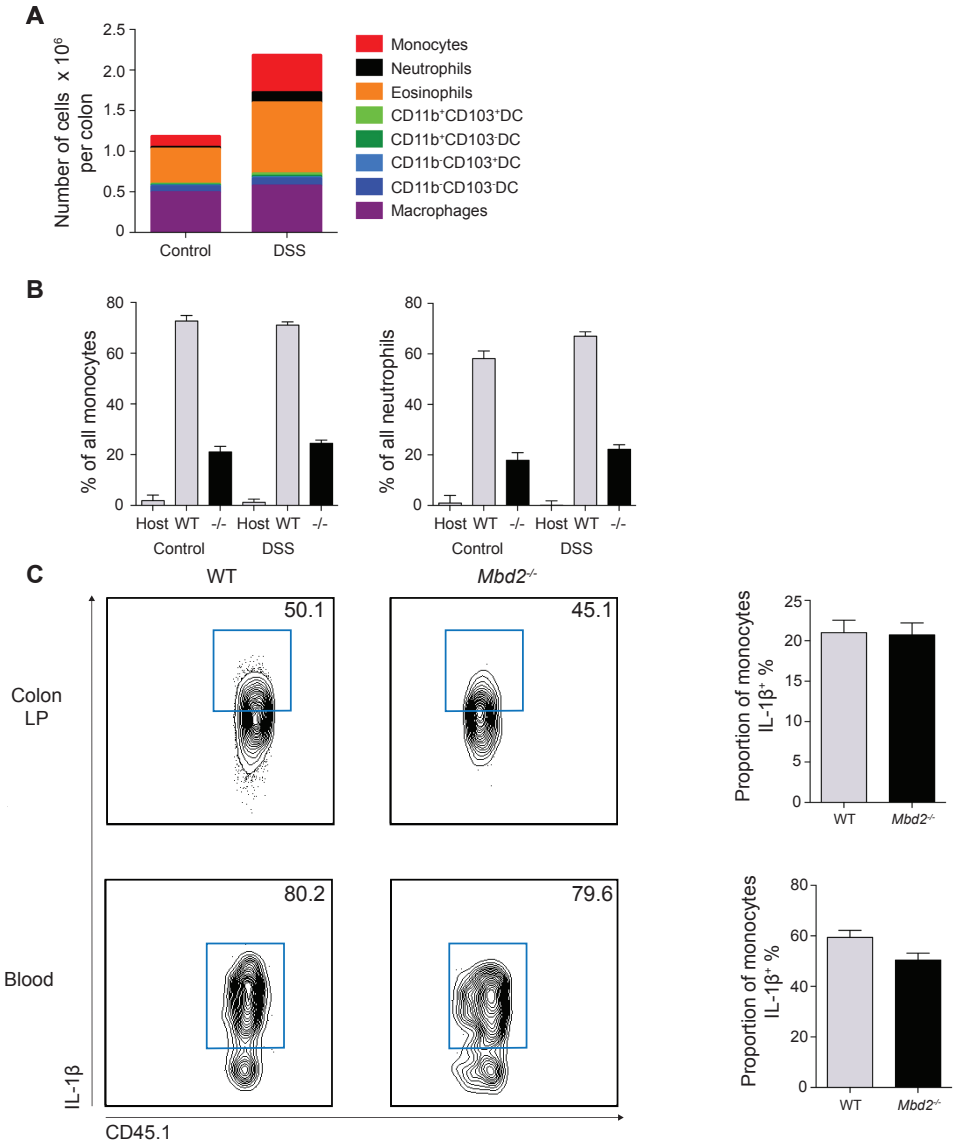

Figure 4.6 Flow Cytometry analysis of DSS treated CD45.2$^+$ WT / *Mbd2*$^{-/-}$ mixed BM chimeras

Mixed BM chimeras were generated by lethally irradiating CD45.1$^+$ CD45.2$^-$ (host) mice and reconstituted with CD45.1$^+$ CD45.2$^+$ (WT) and CD45.1$^-$ CD45.2$^+$ (*Mbd2*$^{-/-}$) BM. Chimeras were treated for 7 consecutive days with 2% DSS or normal drinking water with colon LP and blood cells isolated for analysis by flow cytometry. Cells were stained with the following antibodies (CD11b, CD45.1, CD45.2, CD11c, CD103, Ly6G, Ly6C, MHC-II, SiglecF and CD64) The least square mean total number of cells x10^6 per colon is presented for the populations outlined in Figure 3.2 **(A)**. **B.** Least mean square proportion of colon LP monocytes (left) and neutrophils (right) identified as host, WT or *Mbd2*$^{-/-}$ **C**. Representative flow cytometry contour plots of colon LP and blood CD45.2$^+$ monocytes displaying CD45.1$^+$ (*Mbd2*$^{-/-}$) or CD45.1$^-$ (WT) cells. Cells were cultured for 4 hours with 1ul/ml GolgiStop and 1ug/ml LPS (blood only) surface stained as above and in addition stained intraceullarly for IL-1β. The least square mean proprotion compared to isotype control of IL-1β$^+$ colon LP or blood monocytes is displayed, n=6-18 mice per group analysed by linear regression of 3 independent experiments.

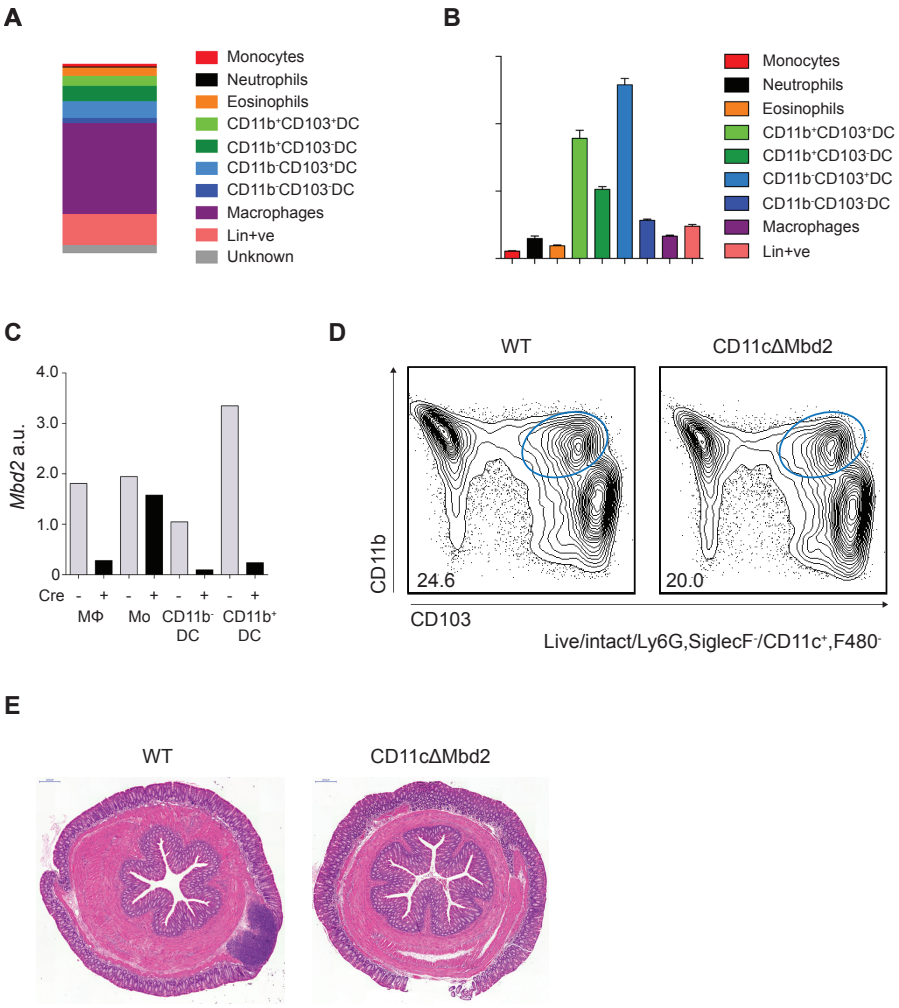

Figure 4.7 CD11c expressing populations in the Colon LP and naive phenotyping in CD11cΔMbd2 mice

Colon LP cells were isolated from WT mice and assessed by flow cytometry. Live, intact cells, $CD11c^+$ cells were subdivided into populations based on the surface expression and gating strategy outlines in Figure 3.2. Populations were then expressed as the proportion of all $CD11c^+$ cells (**A**), or by their MFI of CD11c (**B**). **C.** Colon LP cells from WT or CD11cΔMbd2 mice were FACS purified based on the sort logic in Figure 3.5, RNA was extracted and gene expression of *Mbd2* quantified by RT-qPCR normalised to GAPDH, n=5 per group analysed by linear regression of 3 independent experiments (Primer sequences in Table 2.5). **D.** Colon LP cells from WT or CD11cΔMbd2 mice were isolated and surface stained for the following antibodies (CD11b, CD45, CD11c, CD103, Ly6G, Ly6C, MHC-II, SiglecF and CD64), the proportion of $CD11b^+$ $CD103^+$ cells as a proprotion of all DCs is presented, representative of 3 independent experiments. **E**. Transverse sections of 1cm H&E stained distal colon from WT or CD11cΔ mice.

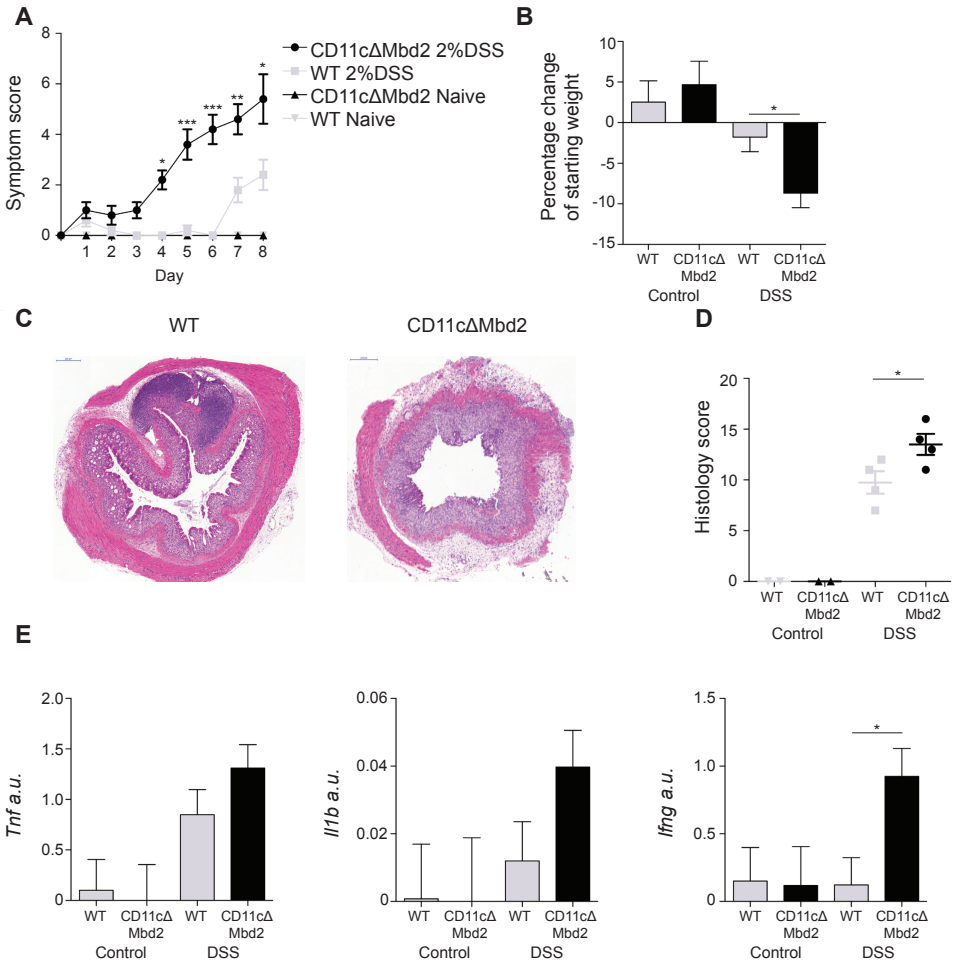

Figure 4.8 Susceptibility of CD11cΔMbd2 mice to DSS colitis

CD11cΔ or littermate WT mice recieved 2% DSS b/w in drinking water or normal drinking water for 8 consecutive days **A**. Mean symptom score per day over the duration of DSS treatment. Cumulative score as per Table 2.3 of weight loss (0-4), diarrhoea (0-4) and per rectal bleeding (0-4). n=4 per group, representative of 4 independent experiments **B**. Least square mean day 8 weight change of DSS treated and naive control, WT and CD11cΔMbd2 mice as a percentage of starting body weight, n=15-20 analysed by linear regression modelling of 3 separate experiments. **C.** H&E stained transverse sections of distal WT or CD11cΔMbd2 DSS treated colon, x10 magnification. **D.** Least square mean±SEM blinded histology score of inflammation of (**C**), as per Table 2.4, comprising inflammatory cell infiltrate (0-4, +0.5 per ulcer), Goblet cell depletion (0-4, +0.5 per crypt abscess), Muscosal thickening (0-4), submucosal cell infiltration (0-4) and architecture destruction (0-4), n=8 per group analysed by linear regression modelling of 2 separate experiments. **E**. mRNA expression of selected cytokines from 1cm sections of distal colon determined by qRT-PCR, the least square mean±SEM value relative to *Gapdh* expression is presented, n=12-18 per group, analysed by linear regression modelling of 3 separate experiments. Primer sequences are in Table 2.5. Representative data from 4 independent experiments (*p<0.05, **p<0.001, ***p<0.0005).

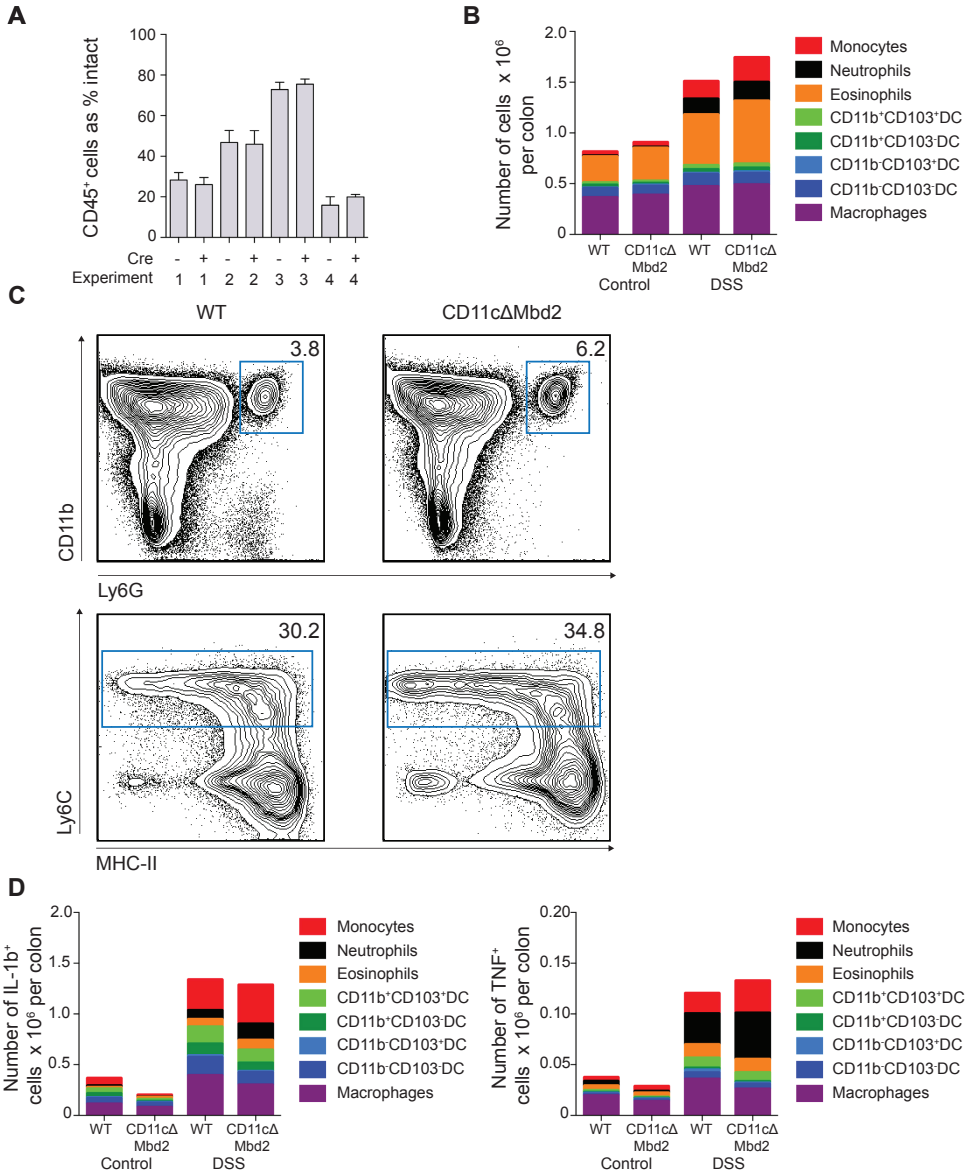

Figure 4.9 Flow cytometry analysis of CD11cΔMbd2 colon lamina propria cells in DSS colitis

CD11cΔMbd2 or littermate WT mice recieved 2% DSS b/w in drinking water or normal drinking water for 8 consecutive days, colon LP cells were isolated and assessed for the expression of SiglecF, Ly6G, CD11b, CD11c, F4/80, MertK, CD64, CD45, CD103 and Lineage markers by flow cytometry. The % of $CD45^+$ colon LP cells per experiment (**A**) and least square mean total total number of cells $x10^6$ per colon is presented for the populations outlined in Figure 3.2 **(B)** , n=15 per group, analysed by linear regression of 3 independent experiments **C**. Representative flow cytometry contour plots in Day8 DSS treated WT and CD11cΔMbd2 mice for neutrophil and monocyte populations as defined in Figure 3.2. The least square mean number of colon LP myeloid cells $x10^6$ per colon after 3 hr incubation with 1µl/ml GolgiStop expressing IL-1β **(D)** or TNF **(E)** as assesed by intracellular staining and flow cytometry compared to isotype antibody control, n=12-15 mice per group analysed by linear regression of 3 independent experiments.

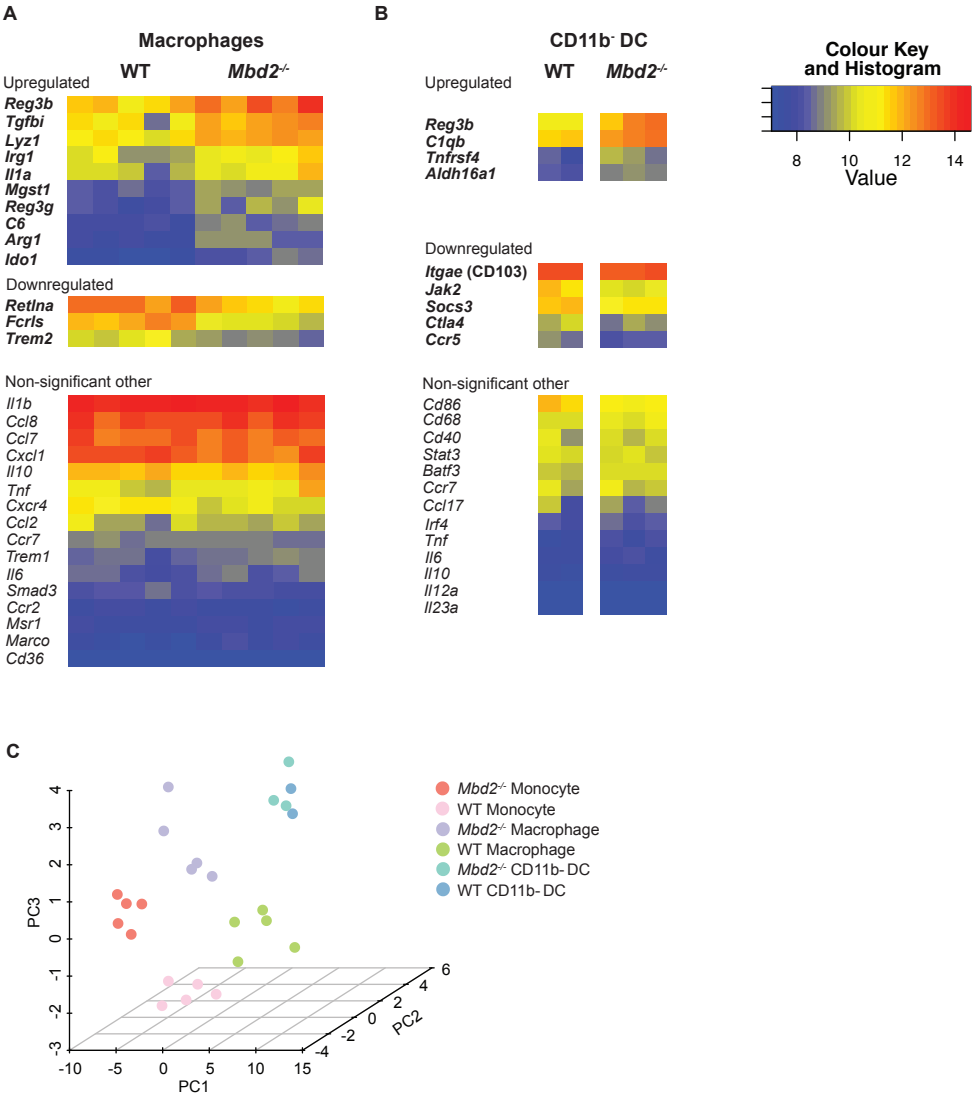

Figure 4.10 Gene expression analysis of *Mbd2*$^{-/-}$ and WT DSS treated colon LP Macrophages and DC

Day 6 2%DSS treated *Mbd2*$^{-/-}$ or littermate WT mice colon LP macrophage, monocyte and CD11b^{-} DC cells were isolated and purified by flow cytometry as described in Figure 3.5. RNA was extracted and gene expression assessed by hybridisation to IlluminaMouseRef6 microarray. Heat map of normalised gene expression from WT versus *Mbd2*$^{-/-}$ macrophages (**A**), or CD11b^{-} DC (**B**) are presented with genes significantly up (upper panel) or down (middle panel) regulated in *Mbd2*$^{-/-}$ populations presented in bold (adj p<0.01). Selected equivalently expressed, non-significant genes are prented in the lower panel. Each individual heatmap represents a biolgical replicate composed of 2-3 (macrophage) or 5 (CD11b^{-} DC) pooled mice. **C**. Principal component analysis of gene expression profiles from macrophage, monocyte and CD11b^{-} DC populations, each data point representing an individual biological replicate composed of 2-3 (macrophage and monocyte) or 5 (CD11b^{-} DC) pooled mice.

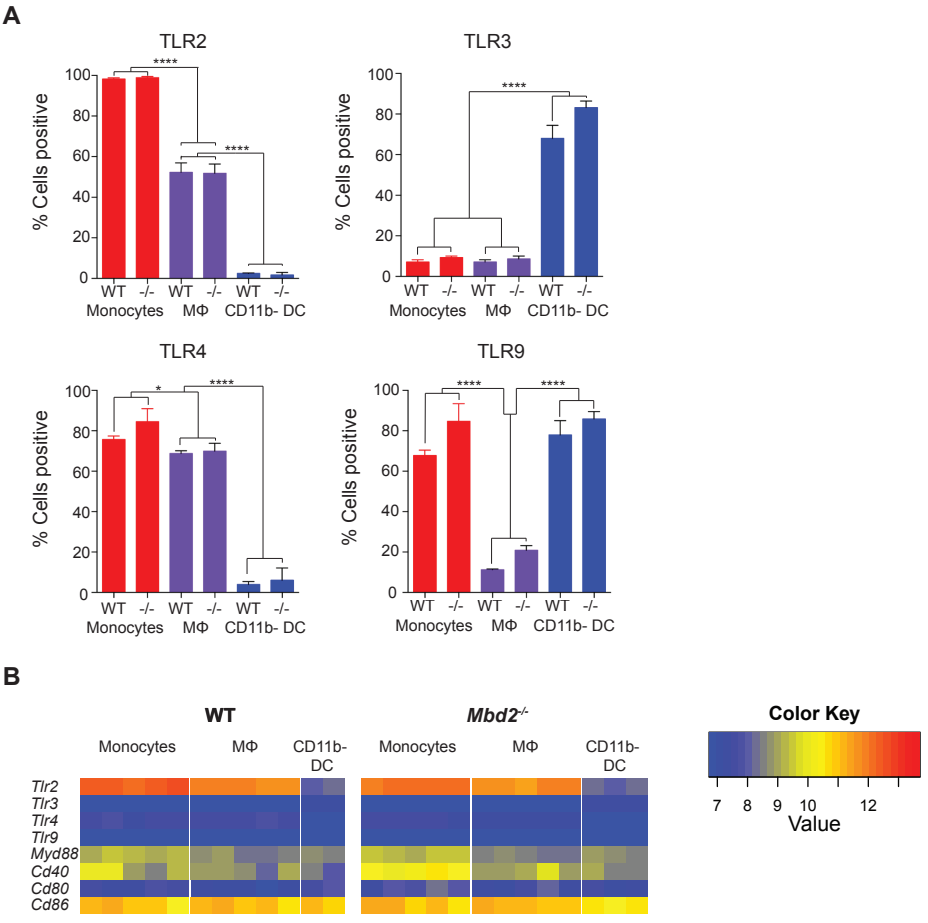

Figure 4.11 TLR production and gene expression in *Mbd2*$^{-/-}$ and WT DSS treated colon LP cells.

A. Mean percentage±SEM of TLR^{+} cells per MP population. Day 6 DSS treated *Mbd2*$^{-/-}$ or WT colon LP cells were stained for monoclonal Ab against the named TLR and analysed by flow cytometry. Monocytes, Macrophages (MΦ) and CD11b- DC are defined as per Figure 3.2. **B**. Heatmap of normalised gene expression values for TLR expression in Day 6 DSS treated *Mbd2*$^{-/-}$ versus WT MP populations purified by flow cytometry as per Figure 3.5 and hybridised to IlluminaMouseRef6 array. Significant genes are presented in bold (Adj p<0.01). Each individual heat map represents a biological replicate composed of 2-3 (Macrophage and monocyte) or 5 (CD11b- DC) pooled mice.

Population	% CD45.2$^+$				Number of cells per colon					
	Control		DSS		Control		DSS		Fold Change	
	WT	*Mbd2*$^{-/-}$	WT	*Mbd2*$^{-/-}$	WT	*Mbd2*$^{-/-}$	WT	*Mbd2*$^{-/-}$	WT	*Mbd2*$^{-/-}$
Neutrophils	92.4	91.9	98.5	97.5	0.010	0.011	0.058	0.103	5.9	9.2
CD11b+ CD103-	98.2	92.4	98.8	94.9	0.028	0.009	0.052	0.032	1.9	3.7
Monocytes	96.9	93.3	99.0	98.3	0.092	0.072	0.240	0.226	2.6	3.1
CD11b- CD103-	83.1	50.1	80.9	37.3	0.014	0.012	0.018	0.023	1.2	2.0
Eosinophils	98.7	97.9	99.2	97.2	0.460	0.230	0.515	0.364	1.1	1.6
Macrophages	96.1	95.3	97.4	96.1	0.397	0.327	0.503	0.471	1.3	1.4
CD11b+ CD103+	96.8	89.0	98.4	94.7	0.013	0.006	0.024	0.007	1.8	1.3
CD11b- CD103+	77.0	24.9	91.9	55.2	0.087	0.104	0.096	0.089	1.1	0.9

Table 4.1 Summary of colon LP myeloid population cell numbers in Naïve and DSS treated, WT and *Mbd2-/-* BM chimeras

BM chimeras were generated by lethally irraditing CD45.1 congenic mice before reconstitution with either CD45.2$^+$ *Mbd2*$^{-/-}$ or CD45.2 WT CD90- BM. 8 weeks post reconstitution mice were treated with 2%DSS or normal drinking water (control) for 8 consective days. Colon LP cells were isolated and stained for the following antibodies; CD11b, CD45.1, CD45.2, CD11c, CD103, Ly6G, Ly6C, MHC-II, SIglecF, CD64 and analysed by flow cytometry as described in Figure 3.2. The proportion of each population expressing CD45.2 (i.e. donor cells) and the total number of cells x10^6 per colon with fold change conferred by DSS treatment for each genotype is presented. Significance is denoted by grey shading of cells, $p<0.05$).

Blood - LPS 1ug/ml

Cytokine	Control		DSS	
	WT	*Mbd2*$^{-/-}$	WT	*Mbd2*$^{-/-}$
IL-1β	28.0	14.3	36.3	22.1
IL-6	4.7	4.5	11.0	7.4
IL-10	2.2	1.5	0.9	1.9
IL-12p40	16.5	12.7	19.3	21.6
TNF	81.8	81.6	73.4	80.6

Blood - Pam3Cys 1ug/ml

Cytokine	Control		DSS	
	WT	*Mbd2*$^{-/-}$	WT	*Mbd2*$^{-/-}$
IL-1β	25.4	16.2	41.5	42.2
IL-6	12.1	11.2	19.9	29
IL-10	1.9	3.1	1	1.4
IL-12p40	21.2	14.7	26.7	20.2
TNF	67.8	69.1	81.1	65.9

Blood - CpG 50mMol

Cytokine	Control		DSS	
	WT	*Mbd2*$^{-/-}$	WT	*Mbd2*$^{-/-}$
IL-1β	6.0	16.1	22.7	10.0
IL-6	19.6	20.6	35.9	33.4
IL-10	1.6	3.3	2.6	2.7
IL-12p40	2.1	5.4	5.2	0.0
TNF	39.5	56.3	60.2	37.2

Colon LP

Cytokine	Control		DSS	
	WT	*Mbd2*$^{-/-}$	WT	*Mbd2*$^{-/-}$
IL-1β	23.6	30.0	43.8	51.8
TNF	4.3	6.5	4.9	6.1

Table 4.2 Blood and colon LP cytokine production in WT and *Mbd2-/-* monocytes

WT and *Mbd2*$^{-/-}$ mice were treated for 6 consecutive days with DSS or normal drinking water (control). The cellular component of blood and colon LP cells were isolated and stimulated with either LPS 1ug/ml, Pam3Cys (1ug/ml) or CpG (50mMol) (blood) or GolgiStop 1ul/ml (colon LP) for 3 hours. Cells were analysed by flow cytometry after staining with the antibodies described in Figure 4.3 (blood) and Figure 3.2 (colon LP) to identify monocyte cells. In addition cells were stained with intracellular antibodies for IL-1β, IL-6, IL-12p40 and TNF (blood) or IL-1β and TNF (colon LP). The proportion of monocytes staining for these cytokines compared to isotype controls is presented.

FeatureID	Symbol	Description	Chromosome	logFC	Average Expression	P.Value	adj.P.Val
UP							
xlSmlWj_1oE_iJMWjA	Apoc1	apolipoprotein C-I	7	1.1	7.4	1.10E-10	9.00E-07
0A_I8SOOKr6ycO5Tvo	NA	NA	-	1.1	9.4	6.20E-05	0.013
WRUt.WF9dcJPfUJBHY	P2ry14	purinergic receptor P2Y, G-protein coupled, 14	3	1.1	9.6	0.00041	0.042
K9eOi9JJaq5Su4pfKE	C4b	complement component 4B (Childo blood group)	17	1.3	9.1	0.00018	0.026
9gVNx5flW5.e6SftCI	Reg3b	regenerating islet-derived 3 beta	6	1.4	11	0.00016	0.023
lW2Yr78iySR1M5K0gY	Vcam1	vascular cell adhesion molecule 1	3	1.5	10	4.60E-07	0.00055
ZOkieX1t3_LUI0VC14	C4a	complement component 4A (Rodgers blood group)	17	1.5	9.6	7.70E-05	0.014
ZAuCiC_CFG914kXpqU	Apoc1	apolipoprotein C-I	7	1.6	7.7	7.20E-12	1.70E-07
ceigFHiUoI3mQQvWJQ	Irg1	immunoresponsive gene 1	14	1.6	8.5	0.00039	0.04
lxwd4hIIn7FJQwUSiQ	Lyz1	lysozyme 1	10	1.8	9.6	6.70E-09	3.20E-05
DOWN							
rmQuKNExO5ep9Tesg4	Fcrls	Fc receptor-like S, scavenger receptor	3	-1	8.5	1.60E-06	0.0011
9uyQVlkkgR.f9PqPMs	Malt1	mucosa associated lymphoid tissue lymphoma translocation gene 1	18	-1	9.2	7.40E-06	0.0035

Table 4.3 Gene expression analysis in DSS treated *Mbd2-/-* and WT colon LP monocytes

Day 6 2% DSS treated colon LP cells were isolated from WT and *Mbd2*$^{-/-}$ mice. Monocyte cells were identified and purified by flow cytometry as described in Figure 3.5. RNA was isolated and hybridised to IlluminaMouseRef6 array. The details of significant (adj $p<0.05$) $>\pm1$ log FC genes are presented. Details of raw data processing and normalisation methods are presented in Chapter 2.16

Ontology	GO_ID	Goterm	Enrich_pValue	Symbol
			Up-regulated	
BP	GO:0034612	response to tumor necrosis factor	4.17E-05	1100001G20Rik, Ubd
BP	GO:0051704	multi-organism process	1.05E-04	1100001G20Rik, Bdkrb1, Ido1, Lyz1, Mst1r, Vcam1
BP	GO:0051707	response to other organism	1.51E-04	1100001G20Rik, Bdkrb1, Ido1, Lyz1, Mst1r
BP	GO:0060669	embryonic placenta morphogenesis	1.87E-04	Spint1, Vcam1
BP	GO:0032496	response to lipopolysaccharide	3.15E-04	1100001G20Rik, Bdkrb1, Ido1
BP	GO:0002532	production of molecular mediator involved in inflammatory response	3.22E-04	Ido1, Slc7a2
BP	GO:0009607	response to biotic stimulus	4.44E-04	1100001G20Rik, Bdkrb1, Ido1, Lyz1, Mst1r
BP	GO:0009617	response to bacterium	4.54E-04	1100001G20Rik, Bdkrb1, Ido1, Lyz1
BP	GO:0060713	labyrinthine layer morphogenesis	4.94E-04	Spint1, Vcam1
BP	GO:0006952	defense response	5.65E-04	Bdkrb1, C1rl, Ido1, Lyz1, Slc7a2, Ubd
			Down-regulated=None	

Table 4.4 Gene ontology analysis of DSS treated *Mbd2-/-* and WT colon LP monocytes

Day 6 2% DSS treated colon LP cells were isolated from WT and *Mbd2*$^{-/-}$ mice. Monocyte cells were identified and purified by flow cytometry as described in Figure 3.5. RNA was isolated and hybridised to IlluminaMouseRef6 array. The details of significant (adj p<0.05) pathways as assessed by gene onotology (GO) analysis. Details of raw data processing and normalisation methods are presented in Chapter 2.16 . (BP=biological process).

Population	Control			DSS		
	Host	*Mbd2*$^{-/-}$	WT	Host	*Mbd2*$^{-/-}$	WT
CD11b+ CD103+	0.6	18.5	76.2	1.5	19.9	74.8
CD11b+ CD103-	0.0	15.8	81.5	1.4	17.8	78.4
CD11b- CD103+	4.0	21.5	68.2	4.7	23.3	67.0
CD11b- CD103-	6.5	18.1	64.4	6.4	18.9	65.8
Macrophages	3.3	23.0	68.0	3.4	23.5	67.9
Monocytes	1.9	21.1	72.7	1.2	24.5	71.1
Eosinophils	0.1	32.2	58.8	0.4	36.4	58.7
Neutrophils	0.9	17.9	58.2	0.1	22.3	67.0

Table 4.5 Proportions of colon LP myeloid cells in *Mbd2-/-* : WT mixed BM chimeras

Mixed BM chimeras were generated by lethally irradiating CD45.1 mice (host) and reconstituted with CD45.1^{+} CD45.2^{+} (WT) and CD45.1^{-} CD45.2^{+} (*Mbd2*$^{-/-}$) CD90 depleted BM. 8 weeks post irradiation colon LP cells were isolated from day 8 DSS treated or normal drinking water (control) mixed BM chimeras and anlaysed by flow cytometry to identify the populations detailed in Figure 3.2. The proportion of each population is presented that was identified as host, *Mbd2*$^{-/-}$ or WT as defined by the expression of CD45.1 and CD45.2 (See Figure 4.5B).

Blood - LPS 1µg/ml

Cytokine	Control		DSS	
	WT	*Mbd2*$^{-/-}$	WT	*Mbd2*$^{-/-}$
IL-1β	54.7	44.0	59.4	50.4
IL-6	18.6	13.4	32.3	25.8
IL-12p40	25.2	20.6	29.6	26.7
TNF	74.9	69.2	80.9	79.4

Colon LP

Cytokine	Control		DSS	
	WT	*Mbd2*$^{-/-}$	WT	*Mbd2*$^{-/-}$
IL-1β	20.1	16.9	33.9	32.4
TNF	12.6	9.9	14.0	13.9

Table 4.6 Blood and colon LP cytokine production in *Mbd2-/-* : WT mixed BM chimeras

Mixed BM chimeras were generated by lethally irradiating CD45.1 mice (host) and reconstituted with CD45.1^{+} CD45.2^{+} (WT) and CD45.1^{-} CD45.2^{+} (*Mbd2*$^{-/-}$) CD90 depleted BM. Mixed BM chimeras were treated for 6 consecutive days with DSS or normal drinking water (control). The cellular component of blood and colon LP cells were isolated and stimulated with either LPS 1µg/ml (blood) or GolgiStop 1µl/ml (colon LP) for 3 hours. Cells were analysed by flow cytometry after staining with the antibodies described in Figure 4.3 (blood) and Figure 3.2 (colon LP) to identify monocyte cells. In addition cells were stained with intracellular antibodies for IL-1β, IL-6, IL-12p40 and TNF (blood) or IL-1β and TNF (colon LP). The proportion of monocytes staining for these cytokines compared to isotype controls is presented.

Population	Control		DSS		Fold change	
	WT	CD11cΔ	WT	CD11cΔ	WT	CD11cΔ
Neutrophils	0.047	0.030	0.328	0.333	7.0	11.0
Monocytes	0.066	0.045	0.414	0.423	6.2	9.4
CD11b+ CD103-	0.044	0.038	0.076	0.055	1.7	1.5
CD11b+ CD103+	0.055	0.043	0.075	0.052	1.4	1.2
CD11b+ Cells	1.832	1.917	3.062	2.707	1.7	1.4
Eosinophils	0.494	0.641	0.865	0.902	1.8	1.4
CD45+ Cells	4.237	4.322	5.487	4.247	1.3	1.0
CD11b- CD103+	0.181	0.171	0.232	0.147	1.3	0.9
CD11b- CD103-	0.011	0.015	0.019	0.019	1.7	1.3
Macrophages	0.686	0.655	0.925	0.650	1.3	1.0

Table 4.7 Summary of colon LP myeloid population cell numbers in naïve and DSS treated, CD11cΔMbd2 and control mice

WT or CD11cΔ mice were treated with 2% DSS or normal drinking water (control) for 7 consecutive days. Colon LP cells were isolated, stained and analysed by flow cytometry using the antibody cocktail and logic described in Figure 3.2. The total number of colon LP myeloid cells x10^6 per colon was identified by analyzing the proportion of $CD45^+$ cells enumerated against the total number of cells isolated per colon. Fold change in least square mean total number is presented, ordered from largest to smallest change after DSS treatment. n=8-15 per group, analysed by linear regression of 4 independent experiments.

FeatureID	Symbol	Description	Chromosome	logFC	Average Expression	P.Value	adj.P.Val
UP							
TOjpxbrtCenh6u78nQ	Lyz1	lysozyme 1	10	2.1	7.9	2.00E-04	0.018
xVSgsX2S7KY6Ih7ov4	Gm11560	CCAAT-binding protein	11	1.9	9.6	0.00072	0.035
ukj.SfXnDS5dLTDtSI	Gm10880	predicted gene 10880	6	1.8	9.5	3.00E-04	0.022
0JnQoghSVu_eCi_UgE	Il1a	interleukin 1 alpha	2	1.8	8	0.00036	0.025
ceigFHiUoI3mQQvWJQ	Irg1	immunoresponsive gene 1	14	1.7	8.5	0.00019	0.018
HiNjjVE3oN6jgNpQtQ	Rgs1	regulator of G-protein signaling 1	1	1.7	8.2	0.0013	0.045
Zj.SfXnDS7dLTDtSKE	NA	NA	-	1.5	8.4	5.80E-05	0.0094
oSfXnDS5dLTHtSKED4	LOC100047316	similar to anti-MOG Z12 variable light chain	6	1.5	8.8	0.00023	0.02
cSfXnDS5dLTDtSKED4	Gm10880	predicted gene 10880	6	1.5	8.9	5.00E-04	0.03
rojiekh3lfgN9ASm0k	Tgfbi	transforming growth factor, beta induced	13	1.5	10	0.00055	0.031
TdDt374UHGyh66EXeQ	Serpina3g	serine (or cysteine) peptidase inhibitor, clade A, member 3G	12	1.5	11	0.0012	0.043
cUSexDBLOt509_WgtM	Gde1	glycerophosphodiester phosphodiesterase 1	7	1.4	8.4	8.40E-06	0.0033
9SfXnDS59LTDtSKED4	NA	NA	-	1.4	8.2	5.50E-05	0.0092
3V0s6UF40qcXS.AUeg	Spic	Spi-C transcription factor (Spi-1/PU.1 related)	10	1.3	8.1	2.30E-09	9.20E-06
EnDS5dLTDtSqED73RU	NA	NA	-	1.3	8.2	3.90E-05	0.008
oSfXnDS5dLXDtSKED4	NA	NA	-	1.3	8.1	0.00021	0.019
9gVNx5flW5.e6SftCI	Reg3b	regenerating islet-derived 3 beta	6	1.3	11	0.00031	0.023
EClipcXoqZuTotnWSM	H2-K2	histocompatibility 2, K region locus 2	17	1.3	9.7	0.00049	0.029
0VckdcNKEiC2XBXC7c	Serpina3f	serine (or cysteine) peptidase inhibitor, clade A, member 3F	12	1.3	8.2	0.00096	0.039
HKegKHWgKUlQKa.VnY	H2afz	H2A histone family, member Z	3	1.3	11	0.0012	0.043
xi3iC26XgnhCx5aeiA	Mgl2	macrophage galactose N-acetyl-galactosamine specific lectin 2	11	1.3	9.1	0.0013	0.045
i5LnUoa3xX9S3q3q1Q	Isg15	ISG15 ubiquitin-like modifier	4	1.3	9.8	0.0013	0.046
rF6UO00jH1UVKd0H.U	Gm5560	solute carrier family 25 member 5 pseudogene	5	1.3	9.2	0.0015	0.048
xefVO3Uii.jiO1aMuo	Stat1	signal transducer and activator of transcription 1	1	1.2	8.3	1.00E-04	0.013
c_MoTh18vEyPX_kgdU	NA	NA	-	1.2	9.4	0.00012	0.014
clRI2UKlOJlv1iol4o	H2-Q8	histocompatibility 2, Q region locus 8	17	1.2	9.1	0.00023	0.02
H4uXS0w7UqhA_90VLc	NA	NA	-	1.2	8.5	0.00036	0.025
6PsHyLxXO3kD0KXIsQ	Reg3g	regenerating islet-derived 3 gamma	6	1.2	8.2	0.00039	0.027
EneSd_Y336Evw3nVHo	NA	selenoprotein	3	1.2	8.3	0.00092	0.039
xt16dROQdzQQTckF14	AI607873	expressed sequence AI607873	1	1.2	9.3	0.0014	0.047
Wife1LJ9CTES6yOUt0	Vcam1	vascular cell adhesion molecule 1	3	1.1	7.2	1.60E-10	1.90E-06
ZnfeL6Xy7JCdR9zSpE	Ido1	indoleamine 2,3-dioxygenase 1	8	1.1	7.5	2.00E-06	0.0013
EdBqKsFMJSoeHF8BRc	Arg1	arginase, liver	10	1.1	7.9	2.60E-06	0.0015
NIA9KudKMJ3O3bq6Lo	Plin2	perilipin 2	4	1.1	8.4	4.20E-05	0.008
uFxd_p96OE.OL.UIH0	Ndufs2	NADH dehydrogenase (ubiquinone) Fe-S protein 2	1	1.1	8.3	7.60E-05	0.011
iiK._I6UYied5Cchuo	Gm12844	predicted gene 12844	4	1.1	9.9	3.00E-04	0.022
xqefud6NXolPqjPuOE	NA	NA	-	1.1	8	0.00065	0.033
NnI7rseMBIFfUW7nks	Coq10b	coenzyme Q10 homolog B (S. cerevisiae)	1	1.1	8.3	0.0011	0.042
DOWN							
BYld3fkcu0lc4EjqXU	Retnla	resistin like alpha	16	-1.1	9	3.80E-05	0.0079
3VLofUh9J7p819CKHY	Fcrls	Fc receptor-like S, scavenger receptor	3	-1.4	7.8	1.70E-11	4.00E-07
rmQuKNExO5ep9Tesg4	Fcrls	Fc receptor-like S, scavenger receptor	3	-1.6	8.5	1.40E-09	6.80E-06

Table 4.8 Gene expression analysis in DSS treated *Mbd2-/-* and WT colon LP macrophages

Day 6 2% DSS treated colon LP cells were isolated from WT and *Mbd2*$^{-/-}$ mice. Macrophage cells were identified and purified by flow cytometry as described in Figure 3.5. RNA was isolated and hybridised to IlluminaMouseRef6 array. The details of significant (adj p<0.05) >±1 log FC genes are presented. Details of raw data processing and normalisation methods are presented in Chapter 2.16

Ontology	GO_ID	Goterm	Enrich_pValue	Symbol
			Up-regulated	
BP	GO:0006575	cellular amino acid derivative metabolic process	1.31E-05	Fabp3, Ido1, Mgst1, Slc1a3, Vnn3
BP	GO:0006519	cellular amino acid and derivative metabolic process	2.29E-05	Arg1, Fabp3, Ido1, Mgst1, Slc1a3, Vnn3
BP	GO:0044281	small molecule metabolic process	4.36E-04	Apoc1, Arg1, Fabp3, Gde1, Ido1, Mgst1, Mpi, Myh10, Slc1a3, Vnn3
BP	GO:0015909	long-chain fatty acid transport	5.39E-04	Fabp3, Plin2
CC	GO:0005576	extracellular region	7.63E-04	Angptl7, Apoc1, Arg1, C6, Creld2, Lyz1, Pdyn, Slc1a3, Vegfa, Vnn3
			Down-regulated	
CC	GO:0044444	cytoplasmic part	4.96E-06	Abcb1b, Agxt2l2, Akr1c18, Anxa2, Atp6v0a1, Cetn4, Chst3, Chst7, Clns1a, Ebpl, Fam3c, Ilk, Lass5, Ltc4s, Mmd, Mrpl33, Mterf, Nars, Nup210, Olfm1, Pstpip1, Rrm2b, Scoc, Sfxn3, Soat2, Spp1, Syn1, Synj2, Tmem55a, Tram1, Vamp4, Wls
CC	GO:0001725	stress fiber	5.45E-06	Anxa2, Ilk, Pdlim7, Pstpip1
CC	GO:0032432	actin filament bundle	6.99E-06	Anxa2, Ilk, Pdlim7, Pstpip1
CC	GO:0042641	actomyosin	8.83E-06	Anxa2, Ilk, Pdlim7, Pstpip1
MF	GO:0008459	chondroitin 6-sulfotransferase activity	1.45E-05	Chst3, Chst7
CC	GO:0005737	cytoplasm	1.62E-05	Abcb1b, Agxt2l2, Akr1c18, Anxa2, Arap3, Atp6v0a1, Cetn4, Chst3, Chst7, Clns1a, E2f5, Ebpl, Fam3c, Ilk, Lass5, Ltc4s, Lxn, Mmd, Mrpl33, Mterf, Nars, Nav1, Nup210, Olfm1, Pdlim7, Pid1, Pstpip1, Rrm2b, Scoc, Sfxn3, Smo, Soat2, Spp1, Syn1, Synj2, Tle1, Tmem55a, Tram1, Trib2, Ugp2, Vamp4, Wls
CC	GO:0005622	intracellular	2.55E-05	4930432O21Rik, Abcb1b, Agxt2l2, Akr1c18, Anxa2, Arap3, Arhgap18, Atp6v0a1, Bcl6, Cetn4, Chn2, Chst3, Chst7, Clns1a, E2f5, Ebpl, Fam3c, Htatsf1, Ilk, Lass5, Lbr, Ltc4s, Lxn, Matr3, Mmd, Mrpl33, Mterf, Mtf2, Nars, Nav1, Nup210, Olfm1, Pdlim7, Pid1, Pstpip1, Rrm2b, Scoc, Sfxn3, Smo, Soat2, Spp1, Srsf2, ... and others
MF	GO:0034481	chondroitin sulfotransferase activity	4.34E-05	Chst3, Chst7
CC	GO:0043226	organelle	7.55E-05	4930432O21Rik, Abcb1b, Agxt2l2, Anxa2, Arap3, Atp6v0a1, Bcl6, Cetn4, Chst3, Chst7, Clns1a, E2f5, Ebpl, Fam3c, Htatsf1, Ilk, Lass5, Lbr, Ltc4s, Matr3, Mmd, Mrpl33, Mterf, Mtf2, Nars, Nav1, Nup210, Olfm1, Pdlim7, Pstpip1, Rrm2b, Scoc, Sfxn3, Soat2, Spp1, Srsf2, Syn1, Synj2, Tle1, Tmem55a, Tram1, Trib2 ... and others
CC	GO:0044424	intracellular part	8.29E-05	4930432O21Rik, Abcb1b, Agxt2l2, Akr1c18, Anxa2, Arap3, Atp6v0a1, Bcl6, Cetn4, Chst3, Chst7, Clns1a, E2f5, Ebpl, Fam3c, Htatsf1, Ilk, Lass5, Lbr, Ltc4s, Lxn, Matr3, Mmd, Mrpl33, Mterf, Mtf2, Nars, Nav1, Nup210, Olfm1, Pdlim7, Pid1, Pstpip1, Rrm2b, Scoc, Sfxn3, Smo, Soat2, Spp1, Srsf2, Syn1, Synj2, Tl ... and others

Table 4.9 Gene ontology analysis of DSS treated *Mbd2-/-* and WT colon LP macrophages

Day 6 2% DSS treated colon LP cells were isolated from WT and *Mbd2*$^{-/-}$ mice. Macrophage cells were identified and purified by flow cytometry as described in Figure 3.5. RNA was isolated and hybridised to IlluminaMouseRef6 array. The details of significant (adj p<0.05) pathways as assessed by gene onotology (GO) analysis. Details of raw data processing and normalisation methods are presented in Chapter 2.16 . (BP=biological process, CC=cellular component, MF=molecular function).

FeatureID	Symbol	Description	Chromosome	logFC	Average Expression	P.Value	adj.P.Val
DOWN							
3N6gJl0l1e_4KFRJRM	LOC100044430	similar to Interferon activated gene 205	1	-1.7	8.9	0.0026	0.048
iVCUvn3tetOB5CPrRU	Itgae	integrin alpha E, epithelial-associated	11	-1.5	7.4	1.10E-05	0.002
6Unjno_hIeNB.7gbsU	Ifi205	interferon activated gene 205	1	-1.4	7.4	0.0014	0.034
QUJS_fe1604HkI_tFU	Itgae	integrin alpha E, epithelial-associated	11	-1.3	7.5	6.80E-05	0.0058
xaZT.3cX0uj9ff_gug	Dnajb6	DnaJ (Hsp40) homolog, subfamily B, member 6	5	-1.3	7.9	0.00046	0.019
Zqm3IX9F_KNejDepYg	Plscr1	phospholipid scramblase 1	9	-1.3	8.5	0.00081	0.025
3iKQgH4shPVAKSuIJl	Pmaip1	phorbol-12-myristate-13-acetate-induced protein 1	18	-1.3	7	0.0014	0.034
xyTpV5kKOEZA9uCb1M	Rnu6	U6 small nuclear RNA	-	-1.2	10	0.00035	0.016
Zrp.jr3RlNL7uiOzjU	Ivns1abp	influenza virus NS1A binding protein	1	-1.2	7.7	0.00038	0.017
3lx_rp0opUugsSOHSA	Rgs1	regulator of G-protein signaling 1	1	-1.2	9.6	0.00062	0.022
WJbpM.ucuGU0CiCl5l	Arl6	ADP-ribosylation factor-like 6	16	-1.1	7.3	2.30E-08	3.10E-05
clkfp1a7e98Qkly_Ml	Hhex	hematopoietically expressed homeobox	19	-1.1	8	3.80E-06	0.0011
xL0v_3tb_3tbgrt91I	NA	NA	-	-1.1	10	5.40E-06	0.0014
fn6VEsk0nPUzXQ.k9U	Samd9l	sterile alpha motif domain containing 9-like	6	-1.1	9.1	9.80E-05	0.0073
T6SGJYBU0tb8lF16ek	Slc25a20	solute carrier family 25 (mitochondrial carnitine/acylcarnitine translocase), member 20	9	-1.1	7.1	0.00028	0.014
fVIhB6S58QbrcP3Ols	Kctd12	potassium channel tetramerisation domain containing 12	14	-1.1	10	0.00033	0.016
xX700XYjvXUjN8cj3U	Nipbl	Nipped-B homolog (Drosophila)	15	-1.1	8.4	0.0016	0.036
KfM93K.l7x6CYCcEZI	Pmaip1	phorbol-12-myristate-13-acetate-induced protein 1	18	-1	6.9	0.00046	0.019
37kUUSncJLRMjLR.0M	Nab1	Ngfi-A binding protein 1	1	-0.99	8.4	5.00E-07	3.00E-04
QvSnhPl2NhLjntvRWE	H2afy	H2A histone family, member Y	13	-0.99	7.4	0.00012	0.0085
UP							
HNOd4AuwUnFJ78AXsU	Txn1	thioredoxin 1	4	0.9	9.4	0.0014	0.034
H1ImUM7n6.JXPe6EGg	NA	NA	-	0.92	6.9	3.60E-13	4.30E-09
ElX1VL3r8l.oCLsbqU	Tm4sf5	transmembrane 4 superfamily member 5	11	0.94	7.3	0.00012	0.0085
uXO3kD8evAfNISQE1Y	Reg3b	regenerating islet-derived 3 beta	6	0.94	7.4	0.0028	0.05
ck.Bu95.ESKNkW4luc	Tgm2	transglutaminase 2, C polypeptide	2	0.96	12	6.30E-07	0.00034
Z6UI3iTxxKLo.zqkaE	Tnfrsf4	tumor necrosis factor receptor superfamily, member 4	4	0.97	7.6	0.00018	0.011
0..e16B0d7IUp6XYHQ	Ctcfl	CCCTC-binding factor (zinc finger protein)-like	2	0.99	7	0.00092	0.026
NUThPlC.BeLftJQTho	Ets2	E26 avian leukemia oncogene 2, 3 domain	16	1	12	1.10E-09	2.90E-06
KhepR9Oca5dFFDizho	Blvrb	biliverdin reductase B (flavin reductase (NADPH))	7	1	10	7.30E-07	0.00036
Hd7Fx9eBEheGaFo3V0	Adcy4	adenylate cyclase 4	14	1	8	3.40E-05	0.0037
0Wlblut0kORe.zE4_4	Pacsin1	protein kinase C and casein kinase substrate in neurons 1	17	1.1	7	7.10E-08	8.00E-05
9UXk3k9Eueo8Cu5tFA	Gipc1	GIPC PDZ domain containing family, member 1	8	1.1	7.8	4.90E-05	0.0047
0K1ynnTE8RNxPElKTU	Igk-V38	immunoglobulin kappa chain variable 38(V38)	6	1.1	7.7	0.00075	0.024
rfX3d30ieU08CJSfU8	Slc4a8	solute carrier family 4 (anion exchanger), member 8	15	1.2	7.6	2.40E-06	0.00081
9eSPqxeHvh2ueR19NA	Rplp0-ps1	ribosomal protein, large, P0, pseudogene 1	3	1.2	8.7	0.00039	0.017
cqKQLRTR_QpCUITwQs	Igk-V38	immunoglobulin kappa chain variable 38(V38)	6	1.3	7.7	2.40E-05	0.0031
cRbRf.ktoo6t6QKZJ8	Hk3	hexokinase 3	13	1.3	9.4	0.00032	0.016
oF_XSi1SEr0skurSgc	LOC100046496	similar to Ig kappa V-region 24B	6	1.4	8.2	0.0014	0.034
u2RK0lQtR1R3Rbv1F8	NA	NA	-	1.6	9.1	0.0013	0.032
ldB953x57_g1Sk4zuE	Igk-V34	immunoglobulin kappa chain variable 34 (V34)	6	1.8	8	0.0015	0.035

Table 4.10 Gene expression analysis in DSS treated *Mbd2-/-* and WT colon LP CD11b- DC

Day 6 2% DSS treated colon LP cells were isolated from WT and *Mbd2*$^{-/-}$ mice. CD11b- DC cells were identified and purified by flow cytometry as described in Figure 3.5. RNA was isolated and hybridised to IlluminaMouseRef6 array. The details of significant (adj p<0.05) >±1 log FC genes are presented. Details of raw data processing and normalisation methods are presented in Chapter 2.16

Ontology	GO_ID	Goterm	Enrich_pValue	Symbol
				Up-regulated
CC	GO:0005622	intracellular	5.08E-07	3110056O03Rik, 5430437P03Rik, Abhd11, Adcy4, Ahcy, Aimp2, Akr7a5, Alg5, Ankrd54, Aprt, Avil, B3galt4, Blvrb, C030006K11Rik, Camk2b, Caskin2, Casz1, Cdk10, Cebpb, Chtf18, Cib1, Cox6a2, Cyp8b1, Dph1, Ece2, Ecsit, Edf1, Eif2b5, Eif3k, Etfb, Ets2, Exosc5, Fndc5, Gaa, Galns, Gipc1, Grhpr, Gstt2, Hip1r, H ... and others
CC	GO:0005737	cytoplasm	2.38E-06	3110056O03Rik, 5430437P03Rik, Abhd11, Ahcy, Aimp2, Akr7a5, Alg5, Ankrd54, Aprt, Avil, B3galt4, Blvrb, C030006K11Rik, Caskin2, Cebpb, Cib1, Cox6a2, Cyp8b1, Dph1, Ece2, Ecsit, Edf1, Eif2b5, Eif3k, Etfb, Fndc5, Gaa, Galns, Gipc1, Grhpr, Gstt2, Hip1r, Hn1l, Hps5, Hsdl1, Impa2, Map2k2, Mecr, Mrpl16, Mrps ... and others
CC	GO:0044424	intracellular part	2.87E-06	3110056O03Rik, 5430437P03Rik, Abhd11, Ahcy, Aimp2, Akr7a5, Alg5, Ankrd54, Aprt, Avil, B3galt4, Blvrb, C030006K11Rik, Camk2b, Caskin2, Casz1, Cdk10, Cebpb, Chtf18, Cib1, Cox6a2, Cyp8b1, Dph1, Ece2, Ecsit, Edf1, Eif2b5, Eif3k, Etfb, Ets2, Exosc5, Fndc5, Gaa, Galns, Gipc1, Grhpr, Gstt2, Hip1r, Hn1l, Hp ... and others
CC	GO:0044444	cytoplasmic part	4.04E-06	3110056O03Rik, Abhd11, Ahcy, Akr7a5, Alg5, B3galt4, C030006K11Rik, Cib1, Cox6a2, Cyp8b1, Ece2, Ecsit, Eif2b5, Eif3k, Etfb, Fndc5, Gaa, Galns, Gipc1, Grhpr, Gstt2, Hip1r, Hsdl1, Map2k2, Mecr, Mrpl16, Mrps12, Mtg1, Ndufb3, Ndufs7, Nit1, Omp, Otof, Pacsin1, Pafah1b3, Pard6a, Pdlim2, Pex16, Pkmyt1, Plin ... and others
MF	GO:0003824	catalytic activity	4.27E-05	3110056O03Rik, Abhd11, Adcy4, Ahcy, Akr7a5, Aldh3b1, Alg5, Aprt, B3galt4, Blvrb, Camk2b, Cdk10, Chtf18, Cox6a2, Cyp8b1, Ece2, Eif2b5, Epha1, Exosc5, Gaa, Galns, Gna15, Grhpr, Gstt2, Haghl, Hsdl1, Impa2, Kdm4a, Map2k2, Mecr, Mras, Mus81, N6amt2, Ndufb3, Ndufs7, Nit1, Nsun5, Nudt14, Pacsin1, Padi2, Pa ... and others
CC	GO:0043231	intracellular membrane-bounded organelle	4.97E-05	3110056O03Rik, 5430437P03Rik, Abhd11, Ahcy, Aimp2, Akr7a5, Alg5, Ankrd54, B3galt4, C030006K11Rik, Casz1, Cdk10, Cebpb, Chtf18, Cib1, Cox6a2, Cyp8b1, Dph1, Ece2, Ecsit, Edf1, Eif2b5, Eif3k, Etfb, Ets2, Exosc5, Fndc5, Gaa, Galns, Gipc1, Gstt2, Hn1l, Hsdl1, Ints1, Kdm4a, Mecr, Med18, Mrpl16, Mrps12, Mt ... and others
CC	GO:0043227	membrane-bounded organelle	5.28E-05	3110056O03Rik, 5430437P03Rik, Abhd11, Ahcy, Aimp2, Akr7a5, Alg5, Ankrd54, B3galt4, C030006K11Rik, Casz1, Cdk10, Cebpb, Chtf18, Cib1, Cox6a2, Cyp8b1, Dph1, Ece2, Ecsit, Edf1, Eif2b5, Eif3k, Etfb, Ets2, Exosc5, Fndc5, Gaa, Galns, Gipc1, Gstt2, Hn1l, Hsdl1, Ints1, Kdm4a, Mecr, Med18, Mrpl16, Mrps12, Mt ... and others
MF	GO:0004832	valine-tRNA ligase activity	5.99E-05	Vars, Vars2
BP	GO:0006438	valyl-tRNA aminoacylation	6.26E-05	Vars, Vars2
CC	GO:0043229	intracellular organelle	7.22E-05	3110056O03Rik, 5430437P03Rik, Abhd11, Ahcy, Aimp2, Akr7a5, Alg5, Ankrd54, Avil, B3galt4, C030006K11Rik, Casz1, Cdk10, Cebpb, Chtf18, Cib1, Cox6a2, Cyp8b1, Dph1, Ece2, Ecsit, Edf1, Eif2b5, Eif3k, Etfb, Ets2, Exosc5, Fndc5, Gaa, Galns, Gipc1, Gstt2, Hip1r, Hn1l, Hsdl1, Ints1, Kdm4a, Mecr, Med18, Mrpl1 ... and others
				Down-regulated
CC	GO:0005634	nucleus	1.65E-09	Adk, Ank1, Appl1, Bclaf1, Camk1d, Cdk14, Chd1, Clk1, Clk2, Clk4, Dck, Dmtf1, Dyrk3, Elf1, Ep300, Ezh2, Gcfc1, Grasp, Gtpbp4, H2afy, Hhex, Jak2, Mdm2, Mll3, Mx1, Nab1, Ndel1, Nipbl, Nop2, Nr4a2, Pbrm1, Pbx1, Prkrir, Rabgap1l, Rev3l, Rgs2, Rgs9, Rheb, Ruvbl1, Sepsecs, Sesn3, Smg1, Ss18, Stag2, Syap1, ... and others
MF	GO:0005488	binding	7.13E-08	Adk, Akap11, Akap9, Alcam, Ank1, Arl6, Arpc5, Atad1, Bclaf1, Camk1d, Car9, Cd81, Cdk14, Cetn4, Chd1, Cldn1, Clk1, Clk2, Clk4, Dck, Dmtf1, Dock10, Dyrk3, Elf1, Elmo1, Ep300, Ezh2, Fam92a, Fmnl2, G3bp2, Gcfc1, Gfod1, Gphn, Grasp, Gtpbp4, H2afy, Hhex, Il17rd, Jak2, Klri1, Klrk1, Larp1b, Larp4, Lrrk2, L ... and others
CC	GO:0043229	intracellular organelle	7.82E-07	Adk, Akap11, Akap9, Ank1, Appl1, Arpc5, Atad1, Bclaf1, Camk1d, Cdk14, Cetn4, Chd1, Clk1, Clk2, Clk4, Dck, Dmtf1, Dnalc4, Dyrk3, Elf1, Elmo1, Eml5, Ep300, Ezh2, Gcfc1, Gphn, Grasp, Gtpbp4, H2afy, Hhex, Il17rd, Jak2, Lrrk2, Mdm2, Mll3, Mtap2, Mx1, Myo9a, Nab1, Ndel1, Nipbl, Nop2, Nr4a2, Pbrm1, Pbx1, P ... and others
CC	GO:0043226	organelle	8.92E-07	Adk, Akap11, Akap9, Ank1, Appl1, Arpc5, Atad1, Bclaf1, Camk1d, Cdk14, Cetn4, Chd1, Clk1, Clk2, Clk4, Dck, Dmtf1, Dnalc4, Dyrk3, Elf1, Elmo1, Eml5, Ep300, Ezh2, Gcfc1, Gphn, Grasp, Gtpbp4, H2afy, Hhex, Il17rd, Jak2, Lrrk2, Mdm2, Mll3, Mtap2, Mx1, Myo9a, Nab1, Ndel1, Nipbl, Nop2, Nr4a2, Pbrm1, Pbx1, P ... and others
CC	GO:0005622	intracellular	9.60E-07	Adk, Akap11, Akap9, Ank1, Appl1, Arl6, Arpc5, Atad1, Bclaf1, Camk1d, Cdk14, Cetn4, Chd1, Clk1, Clk2, Clk4, Dck, Dmtf1, Dnalc4, Dyrk3, Elf1, Elmo1, Eml5, Ep300, Ezh2, Fmnl2, G3bp2, Gcfc1, Gphn, Grasp, Gtpbp4, H2afy, Hhex, Il17rd, Jak2, Larp1b, Lrrk2, Map3k8, Mdm2, Mll3, Mtap2, Mx1, Myo9a, Nab1, Ndel1 ... and others
CC	GO:0044424	intracellular part	3.28E-06	Adk, Akap11, Akap9, Ank1, Appl1, Arl6, Arpc5, Atad1, Bclaf1, Camk1d, Cdk14, Cetn4, Chd1, Clk1, Clk2, Clk4, Dck, Dmtf1, Dnalc4, Dyrk3, Elf1, Elmo1, Eml5, Ep300, Ezh2, Fmnl2, Gcfc1, Gphn, Grasp, Gtpbp4, H2afy, Hhex, Il17rd, Jak2, Larp1b, Lrrk2, Map3k8, Mdm2, Mll3, Mtap2, Mx1, Myo9a, Nab1, Ndel1, Nipbl ... and others
MF	GO:0000166	nucleotide binding	3.29E-06	Adk, Arl6, Atad1, Camk1d, Cdk14, Chd1, Clk1, Clk2, Clk4, Dck, Dock10, Dyrk3, G3bp2, Gphn, Gtpbp4, Jak2, Lrrk2, Map3k8, Mx1, Myo9a, Rab18, Rab28, Rab5a, Rala, Rbm26, Rev3l, Rheb, Riok1, Riok3, Ruvbl1, Smg1, Tnrc6a, Top2a
BP	GO:0044237	cellular metabolic process	3.94E-06	Adk, Akap11, Ank1, Arl6, Bclaf1, Camk1d, Car9, Cdk14, Chd1, Clk1, Clk2, Clk4, Dck, Dmtf1, Dyrk3, Elf1, Ep300, Ezh2, Gcfc1, Gphn, Hhex, Jak2, Klrk1, Lrrk2, Map3k8, Mdm2, Mll3, Mtap2, Mx1, Nab1, Ndel1, Nop2, Nr4a2, Pbrm1, Pbx1, Pkib, Ppap2a, Ppfibp2, Ptpn2, Ptpre, Rab18, Rab5a, Rabgap1l, Rbm26, Rev3l, ... and others
MF	GO:0032555	purine ribonucleotide binding	5.21E-06	Adk, Arl6, Atad1, Camk1d, Cdk14, Chd1, Clk1, Clk2, Clk4, Dck, Dock10, Dyrk3, Gphn, Gtpbp4, Jak2, Lrrk2, Map3k8, Mx1, Myo9a, Rab18, Rab28, Rab5a, Rala, Rheb, Riok1, Riok3, Ruvbl1, Smg1, Top2a
MF	GO:0032553	ribonucleotide binding	5.27E-06	Adk, Arl6, Atad1, Camk1d, Cdk14, Chd1, Clk1, Clk2, Clk4, Dck, Dock10, Dyrk3, Gphn, Gtpbp4, Jak2, Lrrk2, Map3k8, Mx1, Myo9a, Rab18, Rab28, Rab5a, Rala, Rheb, Riok1, Riok3,

Table 4.11 Gene ontology analysis of DSS treated *Mbd2-/-* and WT colon LP CD11b- DC

Day 6 2% DSS treated colon LP cells were isolated from WT and *Mbd2*$^{-/-}$ mice. CD11b- DC were identified and purified by flow cytometry as described in Figure 3.5. RNA was isolated and hybridised to IlluminaMouseRef6 array. The details of significant (adj p<0.05) pathways as assessed by gene onotology (GO) analysis. Details of raw data processing and normalisation methods are presented in Chapter 2.16 . (BP=biological process,

CD40 MFI

Population	Naïve		p value	DSS		p value	Naïve		p value	DSS		p value
	WT	*Mbd2-/-*		WT	*Mbd2-/-*		*CD11cCre-*	CD11cΔMbd2		*CD11cCre-*	CD11cΔMbd2	
Macrophages	802	1041	0.01	1030	1303	<0.0001	325	340	NS	722	434	NS
CD11b+ CD103-	418	641	0.02	711	1092	<0.0001	115	340	NS	250	220	NS
CD11b+ CD103+	371	568	0.0004	470	679	<0.0001	361	532	NS	170	266	NS
CD11b- CD103-	325	481	NS	440	835	<0.0001	254	490	NS	485	495	NS
CD11b- CD103+	380	534	0.0005	396	554	0.0005	344	226	NS	132	151	NS

CD80 MFI

Population	Naïve		p value	DSS		p value	Naïve		p value	DSS		p value
	WT	*Mbd2-/-*		WT	*Mbd2-/-*		*CD11cCre-*	CD11cΔMbd2		*CD11cCre-*	CD11cΔMbd2	
Macrophages	1160	1574	0.0028	1450	1964	0.0001	3383	3561	NS	4058	3589	NS
CD11b+ CD103-	1022	1434	NS	1537	2360	0.0001	2064	1899	NS	3274	2737	NS
CD11b+ CD103+	1227	1558	0.006	1230	1423	0.02	2575	2764	NS	4015	3622	NS
CD11b- CD103-	658	855	NS	751	1320	<0.0001	2103	2820	NS	2445	2756	NS
CD11b- CD103+	1076	1205	NS	822	849	NS	2578	2398	NS	1864	2086	NS

Table 4.12 CD40/CD80 expression on naïve and DSS treated, *Mbd2-/-* , CD11cΔMbd2 and WT colon LP MP cells

Colon LP cells were isolated and stained for flow cytometry markers as defined in Figure 3.2. In addition cells were stained for CD40 and CD80, with the MFI of these markers displayed above for each population. n=4-12 per group analysed by linear regression of 2-3 independent experiments. Statistical significance is presented for the difference between WT and *Mbd2-/-* or *Cd11cCre-* and CD11cΔMbd2 MFI in either naive or after 6 days of continuous DSS treatment, shaded grey for p<0.05

Chapter 5

The role of *Mbd2* on the colonic epithelium and intestinal microbiota

5.1 Introduction

In chapter 4 we observed a role for haematopoietic cells in the development of severe colonic inflammation mediated by DSS in *Mbd2*$^{-/-}$ mice. However we also observed that restricting *Mbd2* deficiency to haematopoietic cells or CD11c expressing cells alone did not reproduce the levels of disease severity seen in global *Mbd2*$^{-/-}$ mice. This led us to hypothesise that non-haematopoietic sources of MBD2 may play an important role in the control of inflammation responses in the colon. Given that the pathogenesis in DSS colitis is due to a primary breakdown of intestinal barrier function, exposing underlying tissues to the commensal microbiota, we hypothesised that colon epithelial sources of MBD2 may have important roles in epithelial-immune cell crosstalk.

The intestinal epithelium is the largest mucosal surface in the human body. This surface is a single cell thick to permit efficient ion and nutrient absorption and yet must shield the host from a diverse and sustained antigenic load, including an estimated 10^{14} commensal bacteria (100). At its most basic, IECs regulate GI tract immunity by forming a physical barrier by separating luminal contents from the underlying LP. However IECs also display innate immune function through the production of anti-microbial products, including defensins, cathelicidins and calprotectin (101). Indeed IECs are able to process and present antigen on MHC molecules enabling interaction with the adaptive immune system (102). For example, IEC MHC expression has been shown to be upregulated in the presence of intestinal inflammation supporting a role for barrier surfaces in manipulating T cell responses. Indeed IECs from IBD patients promote increased Th1 derived IFNγ when co-cultured with naïve $CD4^+$ T cells (429). Secondly, IECs express a series of PRRs, including TLRs, which are down regulated in germfree mice, with MYD88 dependent IEC signaling required to prevent translocation of mucosa-associated bacteria (430). Thus presence of intestinal microbiota is required for TLR development and host barrier function. Indeed almost all TLRs are expressed at mRNA level in the human colon (unselected populations), but our understanding of the precise spatial expression and function of PRRs is incomplete (431), (432). Thirdly, IECs secrete a number of immunoregulatory products. Co-culture of DCs with IEC supernatant favours a tolerogenic DC phenotype with lower levels of MHC II and CD86 expression, increased TGFβ and IL-10 secretion and reduced production of IL-12p70 (433). These effects are thought to be largely mediated by thymic stromal lymphopoetin (TSLP) via a NF-κB dependent mechanism (434), (435). Indeed, mice carrying an IEC specific deletion of IκB kinase, which is required for NF-κB activation, are unable to generate a protective Th2 response to the colonic parasite *T. muris*, with increased DC release of TNF and IL-12/23p40 and down-regulated TSLP expression (436). Finally, IECs are known to secrete TGFβ in response to *in vitro* models of wound injury, with TGFβ documented to reduce alloantigen presentation on epithelial-DCs (437), (438). Indeed CD11c specific deletion of

$\alpha_v\beta_8$, required for TGFβ activation, render these mice more susceptible to colitis with reduced Treg populations (439).

Further evidence for the immunomodulatory properties of IECs is observed in antibody responses. Indeed, the GI tract is the largest antibody producing organ in humans, with >80% of activated B cells residing in mucosal tissue sites (440). Secretory antibody provides crucial defence against pathogens and shapes the ecology of the microbiota (441). Class switch of differentiated B cell production of IgM to IgA occurs within PP and is dependent on secretion of APRIL and TGFβ, sources of which include IECs (Mora et al. 2006). Indeed, increased TLR signaling induces APRIL and TSLP secretion from IECs, with microbial signaling also favouring IgA2 class switch which is a more proteolytically resistant IgA (442), (443). Thus microbiota-derived signals stimulate IEC release of mediators promoting IgA class switching.

The intestinal epithelium is in close proximity to a vast array of gut-associated lymphoid cells, most notably in small intestine PP. However ILFs are present throughout the GI tract, including the colon. The IECs covering ILF include specialised antigen sampling cells (M cells) able to uptake luminal antigen directly by endocytosis (444), (445). As M cells lack lysosomes, antigen is presented intact to naïve T cells before their migration in efferent lymphatic vessels to other mucosal effector sites such as the LP. In addition, the epithelium has evolved to permit the passage of membrane extensions from DCs (dendrites) to directly sample luminal antigen without compromising barrier integrity, via the formation of tight junction (TJ) like complexes between DCs and IECs (445), and this process is induced via IEC TLR activation by microbial stimuli (444).

The luminal burden of antigen and thus daily challenge to IEC immune function is vast. Indeed the GI tract is the most heavily colonised organ in the body, with over 70% of bacteria in humans residing in the colon (446,447). Determining bacterial community structure in faecal samples through DNA sequencing is therefore an important facet of intestinal health research. Differences in intestinal microbial diversity and community structure have been implicated not only in GI tract diseases such as CD, UC and IBS but also in systemic metabolic disorders such as obesity and type II diabetes mellitus (448), (300).

Taken together, it is increasingly appreciated that IECs are critical guardians of host immunity: able to sample luminal antigen, respond and function as APCs, secrete immunomodulatory proteins including cytokines such as TGFβ and an array of chemokines, and respond to microbial signals via PRRs to augment barrier defence by facilitating

antibody and mucin production. Thus IECs represent attractive potential sources of *Mbd2* to be investigated for dysregulated function.

Chapter aims

1. Identify and extract IECs from the colon
2. Develop protocols for the purification of colon epithelial cells (CECs) by FACS
3. Characterise the surface expression phenotype of *Mbd2* deficient CECs in the steady state and in experimental colitis
4. Characterise gene expression profiles of steady state and inflamed CECs in WT and *Mbd2*$^{-/-}$ mice
5. Identify the impact of *Mbd2* deficiency on the steady state colonic microbiota

5.2 Identifying and extracting colon epithelial cells

The emerging field of epithelial-immune cell crosstalk has not yet provided a consensus on an accepted, robust extraction method for isolating CECs from murine tissue (449), (450). CEC isolation was a novel technique for the MacDonald laboratory, and thus the existing literature was interrogated for previously published methodology, as well as seeking local expertise. We therefore first sought to address this by developing a reproducible method for CEC extraction that permitted identification of a range of CEC types.

The basic premise of colon LP isolation relies upon multiple wash steps to clean the luminal surface, exposure to a chelating agent such as EDTA to remove adherent mucus before enzymatic digestion to expose underlying LP cells. We therefore hypothesised that earlier steps of our existing isolation protocol would result in the extraction of a number of CEC subtypes (goblet cells, entero-endocrine cells, stem-cell niche cells and colonocytes). We therefore attempted to identify CECs using a modified version of our isolation protocol as described in Table 5.1 (protocol #1), assessing cells by flow cytometry (See Figure 5.1).

The existing literature using flow cytometry to profile CECs is poorly described. However data suggest these cells are; epithelial cell adhesion molecule (EpCAM) positive, $CD45^{-}$, with a characteristic $SSC\text{-}A^{Hi}$, $FSC\text{-}A^{Hi}$ profile (450), (449). EpCAM is expressed uniquely by human epithelium, but the mouse homologue is also expressed by T cells and some APCs (451). Therefore to ensure CECs were not contaminated with other EpCAM expressing populations, we assessed for the presence of an array of leucocyte markers. Using this protocol we indeed identified an $EpCAM^{+}$ $CD45^{-}$ $SSC\text{-}A^{Hi}$ population (See Figure 5.1A) that was negative for a range of other leucocyte markers (See Figure 5.1B). However, we wished to compare this to two other published CEC isolation methodologies to establish differences in yield, viability and appearance by flow cytometry (See Table 5.1).

The main points of comparison were the use of Percoll to purify CECs based on size (protocol #2), and the use of dispase in preference to collagenase (protocol #3), given anecdotal reports of enhanced CEC viability when using dispase (Sheena Cruickshank, personal communication). Table 5.1 outlines the differences between the 3 protocols, while Figure 5.2A and B detail differences in CEC phenotype based on isolation protocol.

Protocol Number	#1	#2	#3
EDTA incubation steps	x1	x2	Nil
Enzyme	Liberase TM	Nil	Dispase
Enzyme Duration	40mins	N/A	120mins
DNAse	0.02mg/ml	Nil	Nil
Percoll	Nil	30% gradient	Nil

Table 5.1
Comparison of proposed CEC extraction methods

We observed a greater viability using EDTA (protocol #1 and #2) versus dispase (protocol #3) and a greater yield of CECs using Liberase (protocol #1) versus dispase (protocol#3) (See Figure 5.2A and B). In addition we observed a reduction in CECs using protocol #2, characterised by a reduction in all SSC-A^{Hi} cells, likely due to a poorly optimised Percoll gradient step (See Figure 5.2A and B). We also identified an $EpCAM^{+}$ $CD45^{mid}$ population in protocol #2 and #3. $EpCAM^{+}$ $CD45^{mid}$ cells expressed low levels of F4/80 and CD3 consistent with known EpCAM expression in both $F4/80^{+}$ and $CD3^{+}$ populations, but also expressed higher levels of viability dye Live/Dead Blue and had a greater SSC-A, FSC-A profile. Taken together we concluded that the longer incubation periods of protocol#3 led to a reduced viability of $EpCAM^{+}$ leucocytes, with resultant reduced CD45 expression (See Figure 5.2C).

Having identified that protocol #1 produced the highest yield and most discreet, viable CEC population as assessed by flow cytometry, we then sought to confirm protocol #1 $EpCAM^{+}$ $CD45^{-}$ cells displayed a mRNA profile of epithelial cells to add further evidence to our argument supporting their identification as CECs, and to confirm our isolation techniques weren't biasing towards a specific epithelial cell type. To pursue this, we optimised a FACS protocol to isolate CECs (Figure 3.3).

The colonic epithelium is maintained through a process of continual cellular renewal in which stem cells, located at the base of crypts, produce 14 to 21 intermediate cells per hour that give rise to all terminally differentiated cell types (452), (453). The three main types of differentiated CECs (colonocytes, goblet cells and enteroendocrine cells) differentiate while migrating up to the surface epithelium with a turnover period of 4 to 6 days (454). Colonocytes possess absorptive and secretory functions, aiding the transport of sodium water and short chain fatty acids whilst secreting potassium and bicarbonate (454). Goblet cells produce mucins that help protect the mucosa from injury and enteroendocrine cells secrete hormones such as secretin and cholecystekinin, that regulate intestinal function (454).

Using the sort logic in Figure 5.3, we isolated EpCAM^{+} CD45^{-} CECs from mouse colon and extracted the RNA for analysis by quantitative RT-PCR. We assessed mRNA levels of the stem cell marker, leucine-rich repeat-containing G-portein coupled receptor 5, *Lgr5*, the colonocyte marker carbonic anhydrase, *Car1,* the goblet cell markers mucin-2, *Muc2,* and Krüppel-like factor 4, *Klf4,* and the enteroendocrine marker chromogranin A, *ChgA,* compared to liver and spleen whole tissue homogenate controls (See Figure 5.4A) (454).

We observed mRNA transcript expression in CECs for colonocyte, goblet cell and enteroendocrine markers that were not seen in spleen or liver tissues. There was in addition increased expression of the stem cell marker *Lgr5* in CECs versus spleen, with equivalent levels of liver *Lgr5,* consistent with its known expression in this tissue (Figure 5.4A)(455), (456).

We then sought to compare CEC *Mbd2* expression versus other leucocyte populations we had previously identified in chapter 3. Using the sort logic in Figure 3.3 and 5.3 we identified and isolated CEC, macrophage, monocyte and CD11b$^{+/-}$ DC populations from colon LP, comparing expression of *Mbd2* transcript versus liver whole tissue control (Figure 5.4B). CECs displayed high levels of *Mbd2* transcript equivalent with monocytes and macrophages, in keeping with known data supporting constitutive expression of *Mbd2* in other epithelial sites (GeneAtlas entryU133A).

Taken together, we have identified and isolated an EpCAM^{+} CD45^{-} population from mouse colon that displays a characteristic SSC-A profile, lacks expression of other colon LP leucocyte markers, and selectively expresses gene transcripts typical of known colon epithelial cell types. We also identified CECs as constitutively expressing high levels of *Mbd2* and, given the data in Chapter 4 supporting a role for non-haematopoietic sources of *Mbd2* in pre-disposition to colonic inflammation, we now sought to compare CECs from *Mbd2*$^{-/-}$ versus. WT mice.

5.3 Characterisation of naïve CECs in *Mbd2*$^{-/-}$ and WT mice

As noted above, CECs express an array of chemokines in response to inflammatory stimuli to mobilise immune cells such as neutrophils, T cells, macrophages and DCs to sites of tissue damage. In addition, CECs also increase expression of antigen processing molecules such as MHC and the LY6 family members on their basolateral surface after the induction of colitis (*Il10*$^{-/-}$ and CD45RB^{High} T cell transfer models) (457), (458). LY6 family members are GPI anchored cell surface glycoproteins with broad distribution of cells of haematopoietic and some non-haematopoietic cells. They are widely used as differentiation markers of immune cells, though there exact functions are poorly understood. Data thus far support a role in T cell activation, olfaction and cellular adhesion (459), (460). It has recently been

demonstrated that LY6A and LY6C expression by IECs is regulated by inflammatory cytokines I including IFNγ, TNF and IL-22. Furthermore, cross-linking of LY6 family members on CECs increases cholesterol-mediated secretion of chemokines including the neutrophil attractant CXCL5 (457). Thus, in addition to forming a physical barrier between host and environment, CECs also play an important role in sensing and modulating intestinal inflammatory responses, with a suggestion that CEC LY6 molecules are upregulated during intestinal inflammation, increasing downstream signaling of leucocyte chemoattractants by currently unknown mechanism.

Using the above developed methodology, we next assessed $EpCAM^+$ $CD45^-$ cells from WT and *Mbd2*$^{-/-}$ mice using flow cytometry. To our surprise, there was a striking increase in the total number of CECs in naïve *Mbd2*$^{-/-}$ versus WT mice (23.9±1.5 versus 10.4±1.7 % of intact cells) (See Figure 5.5A). To address whether the increased frequency of CECs in *Mbd2*$^{-/-}$ was secondary to an increased proliferation of these cells we assessed intracellular expression of the cell cycle protein Ki67. However, there was no effect of genotype on the proportion of $Ki67^+$ CECs and therefore in active cell cycle (See Figure 5.5B). In addition, there was no evidence of epithelial hyperplasia on H&E stained sections of distal colon, reviewed in chapter 3 (See Figure 3.4A). We therefore hypothesised that *Mbd2*$^{-/-}$ CECs were more readily released as part of the isolation procedure, perhaps due to defective cell-cell adhesion or TJ formation.

Mbd2$^{-/-}$ mice also demonstrated a greater proportion of MHC II^+ (23.2±3.1 versus 4.9±3.3 % of MHC II^+ CECs, *Mbd2*$^{-/-}$ versus WT respectively) and $LY6A/E^+$ (66.0±3.2 versus 50.0±3.0% $Ly6A/E^+$, *Mbd2*$^{-/-}$ versus WT respectively) CECs compared to WT in keeping with a more activated epithelial phenotype (See Figure 5.5C).

Taken together, steady state *Mbd2*$^{-/-}$ mice displayed an increased number of CECs despite equivalent proliferation, which we speculate might be secondary to decreased barrier integrity. In addition *Mbd2* deficiency resulted in an activated CEC phenotype, with increased surface expression of MHC-antigen presenting, and LY6-chemoattract, molecules, consistent with a degree of indolent, sub-acute colonic inflammation.

5.4 Characterisation of *Mbd2*$^{-/-}$ and WT CECs in colonic inflammation

To address whether *Mbd2*$^{-/-}$ CECs were further dysregulated in colonic inflammation we isolated colon cells from day 6 DSS treated *Mbd2*$^{-/-}$ and WT mice (See Figure 5.5A, B and C).

In contrast to naïve mice, there was no effect of genotype on the frequency of CECs as assessed by the proportion of $EpCAM^+$ $CD45^-$ Lin^- CECs of all intact cells (See Figure 5.5A).

Similarly there was no effect of genotype on the proportion of CECs in active cell cycle, as assessed by the presence of $Ki67^+$ cells or the proportion of CECs that were MHC II^+ (See Figure 5.5C). There was however a significant increase in the proportion of *Mbd2*$^{-/-}$ CECs expressing LY6A/E (68.0±3.2 versus 54.8±3.1 % of $Ly6A/E^+$ CECs, *Mbd2*$^{-/-}$ versus WT respectively) (See Figure 5.5B).

We also assessed epithelial activation in a model of infectious colitis with the parasitic nematode *T. muris* (as described in Chapter 3.6). Day 30 High (200egg) and Low (20egg) dose *T. muris* infected *Mbd2*$^{-/-}$ or WT mice were assessed for the presence of activated, MHC II^+, CECs. Colon cells were isolated, identified and characterised as described above. There was a significantly greater proportion of activated MHC^+ CECs in high (9.6±1.6 versus 1.7±0.1 % of MHC II^+ CECs) but not low (15.0±2.1 versus 6.3±2.5 % of MHC II^+ CECs, *Mbd2*$^{-/-}$ versus WT respectively) dose infected *Mbd2*$^{-/-}$ mice.

Taken together, in the absence of *Mbd2* there was increased CEC activation in naïve *Mbd2*$^{-/-}$ compared to WT mice. This increased CEC activation was only maintained in DSS in the LY6A/E analysis of CECs. To understand whether conserved pathways existed between naïve and DSS treated *Mbd2*$^{-/-}$ CECs that predisposed to epithelial activation, and whether these putative pathways could explain the increased susceptibility to inflammation, we undertook expression analyses of these cells using WT naïve and DSS CEC controls.

5.5 Gene expression analyses of WT and *Mbd2*$^{-/-}$ CECs

Colon cells were isolated from WT or littermate *Mbd2*$^{-/-}$ day 6 DSS treated or naïve drinking water control mice. CECs were then purified by FACS as described in Figure 5.3. The RNA component of these cells was isolated, purified and its integrity quantitatively and qualitatively assessed by spectrophotometry and gel electrophoresis before hybridisation to an IlluminaMouseRef6 microarray. Data analysis of gene expression is described in Chapter 2.16 and 4.3.2. 5 biological replicates (4 for naïve analysis) of individual mice were analysed.

5.5.1 Gene expression in naïve *Mbd2*$^{-/-}$ and WT mice

In comparing *Mbd2*$^{-/-}$ to WT CECs, 351 genes were significantly different at an adjusted $p<0.01$ (191 up, 160 down), of which 61 were >logFC +1.0 and 37 >logFC-1.0 (See Table 5.2). The most up-regulated pathway by GOterm and KEGG analysis was antigen processing and presentation, with leucocyte migration (KEGG) and small metabolic process (GOterm) the most down-regulated pathways (See Table 5.3 and 5.4).

The genes below were selected from Table 5.2 as being significantly dysregulated and >logFC±1 based on literature review and known immunological function (See Figure 5.6A and B):

5.5.1.1 Genes upregulated in naïve *Mbd2*$^{-/-}$ CECs compared to WT

MHC II loci

H2-Ab1 LogFC +3.3 (MHC IIa)

H2-Dmb1 LogFC+3.0 (MHC IIb)

H2-Dmb2 LogFC +3.2 (MHC IIb)

H2-Eb1 LogFC +2.7 (MHC IIa)

H2-DMa LogFC +2.6 (MHC IIb)

H2-Aa LogFC +2.5 (MHC IIa)

MHC I loci

H2-Q8 LogFC +2.4 (MHC Ib)

H2-Q6 LogFC +1.6 (MHC Ib)

H2-Q7 LogFC +1.4 (MHC Ib)

H2-K2 LogFC +1.8 (MHC Ia)

H2-K2 LogFC +1.2 (MHC Ia)

H2-T23 LogFC +1.6 (MHC Ib)

Other MHC-related genes

Cd74 LogFC+3.8

Psmb8 Log FC +2.8

Psmb9 LogFC +2.1

Tap1 LogFC +1.6

Tap2 LogFC +1.2

There was a striking up-regulation in multiple aspects of the MHC in naïve *Mbd2*$^{-/-}$ versus WT CECs. As detailed in Table 5.4, 17 genes and 33% of the known antigen processing pathway was dysregulated in KEGG analysis with $p=1.32x10^{-19}$ significance.

Ly6A LogFC +1.7

Expression of LY6 molecules has previously focused on haematopoietic cells, used as markers of differentiation and activation. Diverse roles for LY6 molecules include T cell activation and adhesion but more recently have been described in IEC function (457).

Retnlb LogFC +2.4

RELMβ belongs to the family of resistin like cytokine molecules consisting of small, cysteine-rich secreted proteins. RELMβ is produced by goblet cells in the intestinal epithelium, where it is secreted into the intestinal lumen (461).

Reg3b +3.0, *Reg3g* +1.9

The antimicrobial peptide REG family is discussed in Chapter 4.3.2 in reference to myeloid function. Epithelial expression of REG3γ and REG3β is limited to the small intestine in steady state mouse and human, but are produced from colon enterocytes during pathogen infections or inflammatory conditions (462).

Muc1 LogFC +1.3

Mucin 1 (MUC1) is a membrane bound mucin expressed by goblet and absorptive cells which functions in promoting a cell surface protective barrier with extracellular portions cleaved with bioactive function for epithelial restitution (463).

5.5.1.2 Genes downregulated in naïve *Mbd2*$^{-/-}$ CECs compared to WT

Cldn4 LogFC-2.7

Claudin 4 (CLDN4) is a key structural protein and integral component of the TJ complex, not only in forming an intact physical barrier between the host and the lumen, but also in permitting effective paracellular transport (464).

Ceacam1 LogFC-1.2

CAECAM1 is a membrane bound, heavily glycosylated protein found on the apical surface of IECs, which has been shown to contribute to mucosal adherent mucus, directly interact with bacteria and viruses, and regulate $CD8^+$ T cell activation (465).

Tff3 LogFC -1.0

TFF3 is the second most abundant goblet cell product with important roles in promoting mucosal protection and epithelial restitution (466): TFF3 and mucin together are more effective at epithelial protection than either one alone, with TFF3 mediating epithelial restitution by blockade of apoptosis, promotion of cell migration and mediating downstream effects of TLR2 signaling (467), (468).

5.5.2 Gene expression in DSS treated *Mbd2*$^{-/-}$ and WT mice

In comparing *Mbd2*$^{-/-}$ to WT CECs; 791 genes were significant at an adjusted $p<0.01$ (366 up, 425 down), of which 83 were >logFC +1.0 and 52 >logFC-1.0 (See Table 5.5). The most up-regulated pathway by GOterm and KEGG analysis was antigen processing and presentation with leucocyte migration (KEGG) and small metabolic process (GOterm) most down-regulated (See Table 5.6 and 5.7).

The genes below have been selected from Table 5.5 being significantly dysregulated and >logFC±1 based on literature review and known immunological function (See Figure 5.7A and B):

5.5.2.1 Genes upregulated in DSS colitis, *Mbd2*$^{-/-}$ CECs compared to WT

MHC II molecules

H2-DMb1 LogFC +3.2 (MHC IIb)

H2-DMb2 LogFC +3.0 (MHC IIb)

H2-DMa LogFC +2.7 (MHC IIb)

H2-Ab1 LogFC +2.6 (MHC IIa)

H2-Aa LogFC +2.5 (MHC IIa)

H2-Eb1 LogFC+2.4 (MHC IIa)

MHC-I molecules

H2-Q8 LogFC +2.7 (MHC Ib)

H2-K2 LogFC +2.0 (MHC Ia)

H2-Q6 LogFC +2.0 (MHC Ib)

H2-Q7 LogFC +1.6 (MHC Ib)

H2-K1 LogFC +1.6 (MHC Ia)

H2-T23 LofFC +1.4 (MHC Ib)

Other MHC-related molecules

CD74 LogFC +2.8

Ciita LogFC +1.7

Psmb8 LogFC +2.2

Psmb9 LogFC +1.8

Tap2 LogFC +1.3

Tap1 LogFC +1.3

C2 LogFC +1.7

There was, as in naïve analysis, a striking upregulation in MHC expression. In pathway analysis, antigen processing and presentation pathways were significantly enriched at $p=1.9x10^{-25}$, with 25 genes and 49% of the pathways up-regulated (See Table 5.6). The same 6 MHC IIa/b, 6 MHC Ia/b, and 6 'other' MHC-molecules genes were dysregulated in both naïve and DSS treated mice.

Hspa1a LogFC +2.2

Hspa1b LogFC +2.0

Hspa8 LogFC +2.0

Following exposure to noxious stimuli, IECs respond by producing heat shock proteins (HSPs) that confer protection to stress, infection and inflammation (469). These effects are mediated by preventing the denaturation of intracellular proteins by chaperoning and re-

folding partially denatured proteins. In addition HSPs participate in protein assembly, secretion, trafficking and regulation of transcription factors and kinases (470).

Cxcl9 LogFC +1.5
Chemokine (C-X-C motif) ligand 9 is encoded by the *Cxcl9* gene, induced predominately by IFNγ, and is a T cell chemoattractant, binding to CXCR3 (471).

Reg3b LogFC +1.5
Reg3g LogFC +1.4
As described in chapter 5.2.1

Nlrc5 LogFC +1.1
NOD-like receptor, CARD domain containing protein (NLRC) 5 is part of a family of 22 known NLRs that are cytoplasmic, contributing to innate immune response by recognising microbial products and danger signals leading to inflammation and/or cell death (472).

5.5.2.2 Genes downregulated in DSS colitis, *Mbd2*$^{-/-}$ CECs compared to WT

Cldn4 LogFC -1.6
As described in chapter 5.5.1.2

Il1rn LogFC -1.3
IL-1 receptor anatagonist (*Ilrn*/ILRA*)* is part of the IL-1 family mediating susceptibility to infection and in the pathogenesis of cancers by competes with the binding of IL-1 to its receptor. Polymorphisms in *Ilrn* producing increased circulating ILRA in humans is associated with increased risk of gastric cancer and septic shock, proposed to be due to prolonged and strengthened inflammatory response (473).

Taken together, *Mbd2* deficient CECs display a striking dysregulation of MHC I / II antigen processing and presentation compared to WT intestinal epithelium. An observation strengthened by the fact that WT and *Mbd2*$^{-/-}$ mice used in the above gene expression analyses were littermates, co-housed together from birth for a minimum of 2 months to minimise inter-group variation.

There is clear evidence in the literature supporting direct and indirect crosstalk between the microbiome and host immune response, however the precise mechanism underpinning the microbial influence of disease pathogenesis remains elusive and is a current research focus (474), (150) (Chapter 1.5). Indeed many IBD susceptibility loci, notably *NOD2*, suggest an impaired response to microbes in disease (309). Gut microbiota is an essential factor in driving inflammation in IBD, exemplified by the efficacy of enterically coated antibiotics and

faecal diversion in reducing intestinal inflammation (475), (476). Many studies consistently report a reduction in biodiversity, or α diversity, a measure of the species richness and total number of species in a community in CD patients versus healthy controls (300).

We hypothesised therefore that the profound changes in antigen handling capabilities in naïve *Mbd2*$^{-/-}$ CECs may alter the composition of the intestinal microflora. To address this we performed sequencing of bacterial 16S rRNA genes from naïve WT and *Mbd2*$^{-/-}$ faeces.

5.6 Composition of the intestinal microbiota in *Mbd2* deficiency

Differences in intestinal microbial diversity and community structure have been implicated not only in GI tract diseases such as CD, UC and IBS but also in systemic metabolic disorders such as obesity and type II diabetes mellitus (448), (300).

Taken together there is strong evidence that the microbiota are implicated in the pathogenesis of IBD, with multiple bacterial handling gene polymorphisms acting as disease susceptibility loci (105). In addition, the IBD microbiota demonstrates a reduced biodiversity, with resultant changes in host inflammatory and anti-inflammatory responses (477), (478). The key question remains however, whether these observations represent a primary, disease inducing ability of the microbiota in genetically susceptible individuals, or whether a primary dysregulated immune response and subsequent inflammation causes secondary changes in the intestinal microbiota. Given identifying the requisite number of patients before the onset of IBD in a case-control study has proven thus far prohibitively large, this remains a key unanswered question in the development of IBD.

It is well documented that the environment, particularly diet, age, co-habitation all have significant effects on the human microbiome (150). Murine experiments allow us to control for all these variables, though care must still be taken. Studies which have purported effects of genotype in murine microbiome composition have been subsequently shown to be secondary to changes in the above variables, particularly co-habitation (479), (480). To control for these variables we co-housed the offspring of heterozygous, *Mbd2*$^{-/+}$, parents from birth before analysis of the microbiome at mean age 26 weeks (See Table 5.8). The colon faeces from 3 cages (total 12 mice), each cage containing *Mbd2*$^{+/+}$ (i.e. WT) and *Mbd2*$^{-/-}$ littermates, was taken, extracted and processed in tandem to control for experimental error. The methods for extraction and analysis are outlined in section 2.15.

Analysis of sequence data was performed using the Mothur software package (481). The “trim.seqs” function was performed to filter reads for quality by truncating them for average quality scores. In addition, any reads with primer or barcode sequence mismatches or reads with ambiguous “N” bases were discarded. Chimeras were removed using Perseus software

in Mothur before sequence alignment to the SILVA reference database. A distance matrix was generated before clustering into operational taxonomic units (OTU) at 97% similarity. Each OTU was assigned a taxonomic classification at all levels from phylum to genus, then using R and iTOL packages to calculate distance matrices and dendrograms using Jaccard, Yue and Clayton and Ward clustering respectively (See Figure 5.8A and B).

5.6.1 iTOL dendrogram analysis

The Jaccard calculator is used to describe the overlap in community membership between different samples and ignores the proportional abundance of each OTU, whilst in contrast the Yue and Clayton calculation takes the proportional abundance of each OTU into account when comparing similarities (482). Therefore the presence or absence of an OTU in a given sample has the same weight in Jaccard calculation, independent of the number of reads. It became apparent during the analysis there were a number of unique reads with only 1 or 2 reads in the entire dataset, therefore to prevent biasing the dataset for only a small number of reads, we present the Yue and Clayton calculation to encompass proportional data as a more robust representation of the community composition (482).

Figure 5.8A therefore shows the dendrogram of the representation of bacterial families derived from the 16S rRNA sequences within each sample clustered by Yue and Clayton distances. *Mbd2*$^{-/-}$ mice clustered together significantly independent of cage (p=0.0190). Interestingly, the microbiome isolated from sample #12 was an outlier in age (20weeks), compared to the remainder of the dataset (mean=26weeks) (Table 5.8). The length of the dendrograms in Figure 5.8A is also a representation of the Yue and Clayton similarity, therefore with the exception of the above outlier, *Mbd2*$^{-/-}$ mice separate from WT counterparts at a very early stage in the analysis, suggestive of sizeable differences in their bacterial communities.

5.6.2 Non metric multidimensional scaling analysis

To display the distance matrices in 2D form, we took advantage of non metric multidimensional scaling (NMDS). This permits collapse of multiple dimensions of distance into 2 dimensions, using rank orders (483). This method plots every rank order of OTU abundance against every OTU in the sample and then condenses that distance to compare different samples against one another (See Figure 5.8B). Once again *Mbd2*$^{-/-}$ mice clustered together independently of cage. This was a highly surprising finding, that littermate mice display significantly different bacterial communities despite the same diet, age, parents and housing.

5.6.3 Dysbiosis in *Mbd2*$^{-/-}$ mice

We then assessed whether there were organisms that were enriched or depleted in *Mbd2*$^{-/-}$ mice that accounted for the changes in Yue and Clayton distances (See Table 5.9). 4 OTU were significantly different after adjusting for multiple testing (Order, Family and Genus respectively):

Clostridiales/Peptococcaceae/Peptococcus,
Bacteriodales/Porphyromonadaceaea/Parabacteroides,
Clostridiales/Lachnospiraceae/Roseburia
Clostridiales/Lachnospiraceae/Clostrium_sp_Culture-54.

Peptococcus, Roseburia and Clostridium_sp_Culture-54 were all enriched with Parabacteroides depleted in *Mbd2*$^{-/-}$ versus WT mice.

Taken together, we have demonstrated that despite using stringent controls for assessing differences in bacterial communities, there exists a significantly altered microbiota in naïve mice in the absence of *Mbd2*. This was demonstrated by the effect of genotype on community similarity as measured by Yue and Clayton distance irrespective of co-housing.

5.7 Discussion

In this chapter we addressed the role of *Mbd2* in non-haematopoietic cells, focusing on the colonic epithelium. Firstly we have built upon previous work in identifying colon epithelial cells from existing protocols, using multi-colour flow cytometry. We compared current methodologies for CEC extraction, before assessing these cells with a variety of flow cytometry markers to ensure our isolation technique was not compromised by the presence of other cell types. We have then, for the first time to our knowledge, purified colon epithelial cells using FACS and shown sorted $EpCAM^{+}$ $CD45^{-}$ cells to express goblet cell, enterocyte, enteroenterocyte and stem cell niche specific markers (Figure 5.4A). We used these techniques to identify clear differences in surface expression of epithelial activation markers in *Mbd2*$^{-/-}$ mice. Namely we observed increased MHC II and LY6A/E molecule expression on the surface of *Mbd2* deficient CECs (Figure 5.5B).

Expression of LY6 molecules has previously focused on haematopoietic cells, used as makers of differentiation and activation (484). Diverse roles for LY6 molecules include T cell activation and adhesion but, more recently, have been described in IEC function (457). RNA and surface expression of LY6A and LY6C were increased in the IEC of colitic mice, and in a YAMC epithelial cell line after exposure to IL-22 and IFNγ (457). The ligands for LY6 molecules are not well described, but cross-linking LY6A-C using mAbs results in LY6A and LY6C up-regulation, in addition to chemokines CXCL1, 5, 10, CCL5 and 7 (485). Given IBD is viewed as an unresolved inflammatory response, it is possible that dysregulated Ly6 upregulation on IEC may cause positive feedback that propagates Ly6-mediated chemoattractant properties.

Using genome-wide profiling of naïve and inflamed CECs we were able to identify striking differences in gene expression conferred by *Mbd2* deficiency, notably up-regulated MHC I/II pathways. Key dysregulated genes that reached genome-wide adjusted significance $p<0.01$ are considered below, with the magnitude of change (LogFC) comparing *Mbd2*$^{-/-}$ to WT summarised in Table 5.13.

Function	Gene	LogFC *Mbd2*$^{-/-}$: WT Naïve	DSS
MHC-II	*Ciita*	NS	1.7
	CD74	3.8	2.8
	H2-Ab1	3.3	2.6
	H2-Dmb1	3.0	3.2
	H2-Dmb2	3.2	3.0
	H2-Eb1	2.7	2.4
	H2-Dma	2.6	2.7
	H2-Aa	2.5	2.5
MHC-I	*H2-Q8*	2.4	2.7
	H2-Q6	1.6	2.0
	H2-Q7	1.4	1.6
	H2-K1	1.2	1.6
	H2-K2	1.8	2.0
	H2-T23	1.6	1.4
	Psmb8	2.8	2.2
	Psmb9	2.1	1.8
	Tap1	1.6	1.3
	Tap2	1.2	1.3

Table 5.13
Summary of dysregulated MHC loci in *Mbd2*$^{-/-}$ CECs

CD74 also known as the invariant chain or 'Ii' is a non-polymorphic glycoprotein with diverse immunological functions (486). CD74 forms a trimeric protein on which MHC II molecules assemble, blocking the peptide cleft of class-II MHC to prevent premature binding of antigenic peptides (487). CD74 expression is increased during chronic GI tract inflammation including IBD, also acting as an accessory molecule for cell proliferation in GI tract carcinogenesis (488). However CD74 is expressed in the absence of MHC II suggesting independent function (489). CD74 is a receptor for macrophage inhibitory protein (MIF), and CXCR2 in recruiting leucocytes to site of tissue damage and promoting pro-inflammatory cytokine release (490). In addition CD74 can bind directly to GI tract pathogens, such as *Helicobacter pylori (H. pylori)* causing NF-κB mediated pro-inflammatory cytokine release including IL-8 (491). CD74 is also strongly linked to carcinogenesis, with expression and associated MIF production increased in gastric and colorectal cancers, mediated perhaps by high levels preventing tumour antigen presentation, rendering tumours less immunogenic (492). Taken together, CD74 is a versatile molecule with multifaceted roles in immune response including antigen processing, perpetuating chronic inflammation and acting as a receptor for MIF and the microbiota.

We hypothesise that increased *Mbd2*$^{-/-}$ CEC expression of CD74 may intensify inflammation by increasing free receptors for MIF +/- commensal microbiota attachment or by decreasing tolerance to the microbiota via increased epithelial MHC trafficking and presentation to LP DC and T cells. To test these hypotheses we propose to analyse sections of naive *Mbd2*$^{-/-}$ and WT colon for MIF by immunoflouresence to establish firstly expression in CECs, and then spatial localisation within areas of the crypt-cell niche in a method previously described (493). We would then seek to isolate and culture *Mbd2*$^{-/-}$ and WT CECs *ex vivo*, exposing them to MBD2 siRNA and measuring levels of MIF in supernatant ELISA. Lastly using mice

with a GFP-tagged CD74 protein crossed to our *Mbd2*$^{-/-}$ line, we would be able to visualise CD74 localisation *ex vivo* in WT and MBD2 deficient CECs and in addition using electron microscopy assess for any direct interaction with the microbiota at the epithelial-luminal interface (494).

MHC molecule expression on CECs renders them capable of activating $CD4^+$ and $CD8^+$ effector T cells under inflammatory conditions, though the exact mechanisms underpinning CEC MHC I and II up-regulation are unknown (429), (495). Both class I and II molecules are found at increased levels on IECs in active IBD, with MHC II controlled by a transcriptional complex that includes the MHC II transactivator (CIITA) (496). *Ciita* expression is tightly regulated to prevent uncontrolled immune responses. The precise mechanisms co-ordinating *Ciita* expression are not known, but factors identified that increase MHC II expression include factors that inhibit IL-10 or upregulate IFNγ signalling (497). *Ciita* was found upregulated LogFC+0.97, p=0.03 in naïve *Mbd2*$^{-/-}$ CECs compared to WT (Figure 5.6A). Interestingly in a genome wide RNAi screen of MHC control mechanisms, of 9 transcriptional regulators of *Ciita*, only 4 altered *Ciita* expression levels – i.e. up-regulated MHC II expression occurred independent of changes in *Ciita* (498). One such *Ciita* regulator was the HIV Tat-interacting protein HTATIP (aka K(lysine) acetyltransferase 5, (KAT5)), a histone acetylase with roles in regulating chromatin remodeling and signal transduction, that in turn mediates TAT control of MHC expression (498).

Increased expression of *Ciita* and multiple aspects of the MHC-II molecules in *Mbd2*$^{-/-}$ CECs may represent a primary dysregulation of *Mbd2* mediated changes in *Ciita* or its regulators, such as KAT5, or indeed a manifestation of secondary epithelial inflammation and subsequent compensatory up-regulated antigen processing capabilities. To test this hypothesis we propose to measure the level histone acetylation at the *Ciita* promoter using antibodies against H3K9/K14ac, an epigenetic marker of active gene transcription as previously described (318) assessing FACS purified *Mbd2*$^{-/-}$ and WT CECs. In addition we propose to assess spatial expression of MHC-II *ex vivo* by confocal microscopy, as previously described by (499). Hershberg et al. describe that the normal basolateral function of MHC-II presentation IECs can be augmented in the absence of inflammation by co-expressing *Ciita*, resulting in increased peptide presentation to T cells (499). Thus confocal microscopy staining for MHC-II in *ex vivo Mbd2*$^{-/-}$ CECs would assess the spatial expression of MHC-II molecules i.e. is the normal exclusive basolateral expression disturbed in the absence of MBD2. Thereafter we would assess peptide presentation using *ex vivo Mbd2*$^{-/-}$ and WT CECs in transwells cultured with T cells specific for chicken-ovalbumin (from C57Bl/6-Tg(TcraTcrb)425Cbn/Crl mice) measuring T cell proliferation as a readout of CEC-presentation. To address whether MBD2 deficient CECs display an increased activation profile in the absence of other MBD2 deficient cell types, a *Villin*^{Cre} mouse will be crossed to

our existing *Mbd2*$^{Fl/Fl}$ mouse, to allow epithelial specific deletion of *Mbd2*. Assessing epithelial activation by flow cytometry and gene expression analyses described in Chapter 5.3 and 5.4 will then aim to support or refute *Mbd2*$^{-/-}$ CECs as the primary driver for increased intestinal inflammatory responses in *Mbd2*$^{-/-}$ mice. Lastly it is well documented that CAC in IBD is strongly correlated with chronic inflammation. We hypothesise that indolent, sub-clinical inflammation in *Mbd2*$^{-/-}$ mice that is associated with basal activation of CECs will increase the incidence of colorectal cancer. To test this hypothesis we propose to age *Mbd2*$^{-/-}$ and WT littermate controls to 12months under the same housing conditions that we performed the microbiome analyses, and assess the presence of colorectal adenomas by histological analysis of intestinal sections.

MHC I antigen presentation pathways play an important role in alerting the immune system to infected, particularly virally infected, cells. MHC I molecules are expressed on the cell surface of all nucleated cells and present nucleotide fragments from intracellular proteins (497). The majority of peptides presented by MHC I molecules are derived from defective ribosomal translation products degraded by the proteasome, as opposed to the turnover of mature proteins (497). Peptides are then translocated into the ER lumen by the transporter associated with antigen processing (TAP), which also functions as a scaffold for the final stage of MHC I assembly. Thereafter loaded MHC I molecules dissociate from TAP and are selectively transported in vesicles through the Golgi apparatus to the plasma membrane (497). This process has evolved therefore to permit rapid sampling of proteins immediately after their synthesis, rapidly alerting leucocytes to infected cells. IFNγ induces the expression of 3 additional subunits (PSMB/9 and LMP7), which replace constitutively expressed counterparts and are then termed the immunoproteasome (500). It has been suggested that enhanced proteasome activity in IBD accelerates NF-κB activation that may propagate sustained progressive inflammation (501). Indeed PSMB8 has a significant role in autoimmune diseases and inflammatory reactions: patients with a homozygous miss sense mutation (G197V) suffered from autoinflammatory responses characterised by increased assembly intermediates of immunoproteasomes from resultant reduced PSMB8 and increased IL-6 (500). Both *Psmb8* (LogFC+2.8 and +2.2 in naive and inflamed CECs, *Mbd2*$^{-/-}$ versus WT respectively) and *Psmb9* (LogFC+2.1 and +1.8 in naive and inflamed CECs, *Mbd2*$^{-/-}$ versus WT respectively) were upregulated in *Mbd2*$^{-/-}$ CECs.

Thus we hypothesise that pro-inflammatory signals to *Mbd2*$^{-/-}$ CECs mediate replacement of constitutive proteasome with immunoproteasome subunits which permit an increased ability of inflamed epithelium to process and present antigen to cytotoxic T cells. To test this hypothesis we propose to measure T cell responses using an OT-I transwell system described above, in WT and *Mbd2*$^{-/-}$ CECs cultured with a selective inhibitor of the immunoprotesome subunit LMP-7 of PSMB8. We would hypothesise that negating the

increased immunoproteasome:protesome ratio in *Mbd2*$^{-/-}$ CECs using selective inhibitors would ameliorate T-cell responses to WT levels.

In contrast, only MHC II molecules were upregulated in WT DSS versus WT naïve CECs (See Table 5.10). There were no MHC I molecules up regulated LogFC>1, with fewer MHC II genes upregulated (4; *H2-DMa, H2-Aa, H2-Eb1* and *H2-Ab1*), and those upregulated had lower FC difference (LogFC range 1.1-1.8). The most up-regulated pathways when comparing WT DSS versus WT naïve CDCs were instead cytokine-cytokine receptor interaction and chemokine signaling pathway, with antigen processing not featuring in any of the top 10 most enriched pathways (See Table 5.11 and 5.12). Similarly there was no effect of treatment on WT expression of any TJ complex proteins (See Table 5.10). Taken together, these data are consistent with the hypothesis that *Mbd2*$^{-/-}$ predisposition to colonic inflammation is dependent on up-regulated CEC pathways out with the normal WT inflammatory response. We also observed a number of dysregulated cellular structural proteins involved in cell adhesion and epithelial barrier integrity, and these are considered below, comparing LogFC *Mbd2*$^{-/-}$ and WT.

IECs are required to be selectively permeable to permit the passage of nutrients whilst maintaining a physical barrier. This selective permeability is underwritten by transcellular and paracellular capabilities (464). The paracellular pathway is regulated by an apical junctional complex, which is composed of TJ and adherence junctions (AJ) (502), (503). TJ barrier disruption and increased paracellular permeability, followed by increased translocation of luminal pro-inflammatory molecules, can induce activation of the mucosal immune system (504). TJs are comprised of 4 transmembrane proteins; occludins, claudins, JAM and tricellulin, the intracellular domains of which anchor to cytosolic scaffold proteins (464). Numerous studies have now identified claudins as the key component and backbone of TJs (505), (506). *Cldn1*$^{-/-}$ mice (*Cldn1* naïve NS, inflamed LogFC -1.0) die within 24hours of birth because of dramatic fluid and electrolyte loss from an impaired epidermal barrier (505). Claudin 4 (*Cldn4* naïve LogFC-2.7, inflamed LogFC-1.6) is a barrier forming claudin and as such decreases paracellular permeability (507). Phosphorylation processes are key in dictating claudin localisation and permeability function. Claudin 4 phosphorylation by ephrin receptor tyrosine kinase, largely expressed on various tumour cells, increases paracellular permeability by reducing interaction with the occluding protein, ZO-1 (508). It is well known that IFNγ alone, or in conjunction with other cytokines (particularly TNF) disrupts the barrier function of TJs across culture epithelial monolayers (509). Emerging evidence suggests this may be mediated by internalization of TJ proteins, decreased expression of occludin proteins or altered distribution of junctional proteins (510). Thus reduced CEC expression of *Cldn1* and *4*, key barrier forming TJ components, would be hypothesised to increase paracellular permeability and therefore luminal antigen uptake leading to mucosal inflammation.

We would therefore propose *Mbd2* as a key regulator of CEC function. It is not currently clear whether there is a primary defect in epithelial TJ formation caused by *Mbd2* mediated dysregulation of CLDN4, leading to a greater influx of luminal antigen or indeed a primary dysregulation in antigen processing of the intestinal microbiota, predisposing to an inappropriate activation and a resultant inflamed microenvironment.

In a further layer of complexity, we observed the selection of *Clostridia* and depletion of *Parabacteroides* communities in the *Mbd2*$^{-/-}$ microbiome. 4 OTU were significantly altered including the enrichment of 3 *Clostridiales* organisms. Interestingly reduced *Clostridia* species in man have been found in patients with IBD and atopy, with a recent study using the administration of a mixture of 17 human *Clostridiales* organisms to mice induced increased colon LP Treg numbers and protected against TNBS colitis (147). This mix of bacteria did not include any of the significant OTU in our dataset, however. Further, another study found an accumulation of *Clostridiales* species in a Chinese cohort with active UC or CD, underlining the difficulties in comparing human microbiota cohorts from different geographical areas, with all the resultant ethnic and dietary variation therein (511). *Parabacteroides*, a member of the *Bacteroidetes* phyla which is the most numerically abundant in the human gut and has been shown to predominate at the mucosal surface, is by contrast reduced in IBD patients and in *Mbd2*$^{-/-}$ mice (150). *Parabacteroides distasonsis* has been shown to be more common in healthy controls versus IBD patients, isolated from the colon mucosa by endoscopic biopsy (512). Similarly oral treatment of mice with *P. distasonis* significantly reduced the severity of intestinal inflammation mediated by DSS thought to be mediated by induction of anti-*P. distasonis* antibody responses and stabilisation of other members of the intestinal microbiota by negating DSS mediated changes in a Treg independent manner (513).

An interesting observation was the presence of an outlier in the *Mbd2*$^{-/-}$ microbiota analyses (Figure 5.8A). *Mbd2*$^{-/-}$ microbiota associated together independent of cage, but whilst efforts were made to age-match all mice, 1 mouse was significantly younger and this mouse was an outlier in analysis (Table 5.8 and Figure 5.8A). Whilst this may represent outlying data based on unknown methodological issues or biological variation, it opens the possibility of epigenetic modification of the microbiome during the ageing process. The composition of intestinal bacteria changes in the elderly, with a decrease in anaerobes (e.g. *Bifidobacteria*) in both abundance and species diversity, and in increase in facultative anaerobes including streptococci, staphylococci and enterobacteria, a balance that is associated with IBD (514), (515).

We speculate this may be a product of increased susceptibility to intestinal *Clostridia* due to inappropriate CEC antigen processing or that these organisms may have been selected due to inappropriate host-driven steady state inflammation. This parallels the same key question of dysbiosis in IBD pathogenesis, namely whether this is a cause or an effect of inflammation. To address the hypothesis of a primary dysbiosis in MBD2 deficiency we propose to re-derive *Mbd2*$^{-/-}$ mice into germ-free conditions, assessing basal epithelial activation and response to DSS colitis. To supplement this, we propose to repeat our DSS experiments in WT and *Mbd2*$^{-/-}$ mice that have been pre-treated with broad spectrum antibiotics (amplicillin 1g/L, vancomycin 500mg/L, neomycin 1g/L and metronidazole 1g/L in drinking water for 4 weeks) to remove the commensal microbiome, as described by Rakoff-Nahoum et al. (162). Lastly we propose to perform faecal transplantation of *Mbd2*$^{-/-}$ microflora into WT mice, to assess if this microbiome is capable of inducing aberrant CEC responses in an *Mbd2* sufficient environment.

We would therefore expect that if *Mbd2* is controlling intestinal dysbiosis that is required the pro-inflammatory phenotype of *Mbd2*$^{-/-}$ then abrogating this as described above will ameliorate intestinal damage to that seen in WT animals.

A significant limitation in our microbiota analyses is the assumption that non-bacterial members of the microbiome, namely viruses and fungi amongst others, do not contribute to IBD pathogenesis. It is likely this will become a key research focus of unbiased sequencing work in the future. Specific taxonomic shifts have been reported in IBD. *Enterobacteriaceae* are increased in relative abundance in both patients with IBD and animal models (152), while adherent invasive *E. coli* strains in particular have been isolated from ileal CD biopsies and in are enriched in patients with UC (153). This may simply represent an increased preference of these organisms to survive in an inflammatory environment, with administration of anti-inflammatory treatments, such as mesalazine, reducing their frequency (154). In contrast some bacteria have demonstrated protective effects on host immunity. *Bacteroiodes* and *Clostridium* species have been shown to induce the expansion of Tregs, reducing intestinal inflammation, with other organisms shown to attenuate inflammation by regulating NF-κB activation (156). Similarly the *Bifidobacterium, Lactobacillus* and *Faecalibacterium* genera may protect the host from inflammation by down-regulating inflammatory cytokine or augmenting IL-10 production (157). *F. prausnitzii* has received much attention in recent years, underrepresented in IBD patients, with lower levels of mucosa associated *F. prausnitzii* associated with higher risk of recurrent CD after surgery (158). In addition to immunomodualtory effects, the *Faecalibacterium* genus is also responsible for the fermentation of dietary fibre to produce SCFA, which are the primary energy source for CECs (161). SCFAs have been shown to modify leucocyte recruitment, chemotaxis and effector mechanisms (516). SCFAs activate the G protein coupled receptor

GPR43 that in turn activates mitogen-activated protein kinases and protein kinase C that induce directional migration of neutrophils (517). In addition SCFAs modulate the expression of IL-8, CCL2, and CXCL-1 by IEC in response to response to microbial-derived molecules such as peptidoglycan (518). Lastly SCFAs, mainly butyrate, have been shown to suppress LPS and cytokine stimulated production of pro-inflammatory mediators such as TNF, IL-6 and NO from macrophages and monocytes (519). The main mechanism for this effect is the attenuation of HDAC activity. By directly inhibiting HDAC activity, SCFAs increase histone acetylation and therefore modulate gene expression (520). SCFAs may also increase prostaglandin E_2 (PGE_2), production by inflammatory monocytes in response to commensals in acute gastrointestinal infection that inhibits neutrophil activation, suggesting dual anti- and pro- inflammatory roles for SCFAs and their downstream effectors (46).

Therefore in addition to direct interaction of the microbiota with CECs, metabolism of luminal foodstuffs such as SCFAs may directly modulate host response. To assess this further we propose the analysis of SCFA content such as acetate, propionate and butyrate in faeces of *Mbd2*$^{-/-}$ and WT mice and thereafter culture of *Mbd2* deficient and sufficient CECs *ex vivo* with SCFAs assessing release of chemokines (e.g. CCL2 and CXCL1) and pro-inflammatory cytokines (e.g. IL-1β) by ELISA to characterise potential meta-genomic interactions.

Given the gene expression data is taken from *Mbd2*$^{-/-}$ mice, we also consider an additional explanation, that a non-epithelial *Mbd2* deficient cell type is facilitating an activated epithelial phenotype. *Mbd2*$^{-/-}$ naïve splenic T cells are known to possess the potential to produce more IFNγ than WT when stimulated with PMA/iomomycin *in vitro* (319). However it is not clear whether *Mbd2*$^{-/-}$ T cells constitutively express IFNγ without such stimulation. This is particularly relevant in the colon LP given TJ function; antigen processing and barrier defense mechanisms are all upregulated in an IFNγ rich environment (521). Whilst we cannot discount this possibility, given the level of whole colon *Ifng* transcript was equivalent between *Mbd2*$^{-/-}$ and WT mice, we suggest this explanation is less likely than the others considered (Figure 3.5).

Epigenetic regulation of IECs has been described elsewhere in the literature. Alenghat et al. documented the role of histone deacteylase 3 (HDAC3) in exacerbating colonic inflammation, altering basal gene expression profiles and altering the intestinal microflora (449). IECs with an epithelial specific deletion of HDAC3 (HDAC3$^{\Delta IEC}$) displayed up-regulated PPAR signaling and lipid synthesis with associated increased H3K9 acetylation and down-regulated antigen processing genes (including *H2-Ab1*) (449). However, there was no difference in acetylation at downregulated gene sites. HDAC3$^{\Delta IEC}$ mice were more susceptible to chemical (DSS) and infectious (*L. monocytogenes*) colitis, had increased barrier permeability, reduced Paneth cells and increased levels of Proteobacteria. However

these differences were abrogated when HDAC3$^{\Delta IEC}$ mice were re-derived into germ free conditions, suggesting that commensal-bacteria derived signals are required for HDAC3-induced dysregulation (449). Similarly Turgeon et al. reported HDAC1/2$^{\Delta IEC}$ but not HDAC2$^{\Delta IEC}$ displayed increased susceptibility to DSS colitis and decreased barrier function suggesting not only differing roles for HDACs in IEC function, and also the combination of HDACs is important in determining the overall pre-disposition to intestinal pathology (522). Lastly, Marjoram et al. showed loss of the epigenetic regulator ubiquitin-like protein containing PHD and RING finger domains (UHRF1), itself an IBD risk susceptibility loci, predisoposes to intestinal inflammation in zebrafish (523). Mutant *Uhrf1* zebrafish demonstrated reduced *Tnfa* promoter methylation and increased *Tnfa* IEC expression. This increase was microbe dependent and resulted in IEC shedding, immune cell recruitment and barrier dysfunction and was restored by *Tnfa* knockdown.

We hypothesise that in a combined model in naïve *Mbd2*$^{-/-}$, given the overwhelming upregulation of antigen processing and defence pathways, that the most likely primary candidate for *Mbd2*-mediated dysregulation are *Cd74* and/or MHC II molecules. We speculate this results in inappropriate CEC activation and creation of an inflamed microenvironment at the mucosal surface with subsequent TJ breakdown and increased barrier permeability mediated by reduced *Cldn4*. This inflamed microenvironment thereafter selects out *Clostridia* and depletes protective *Parabacteroides* species in the commensal microbiome.

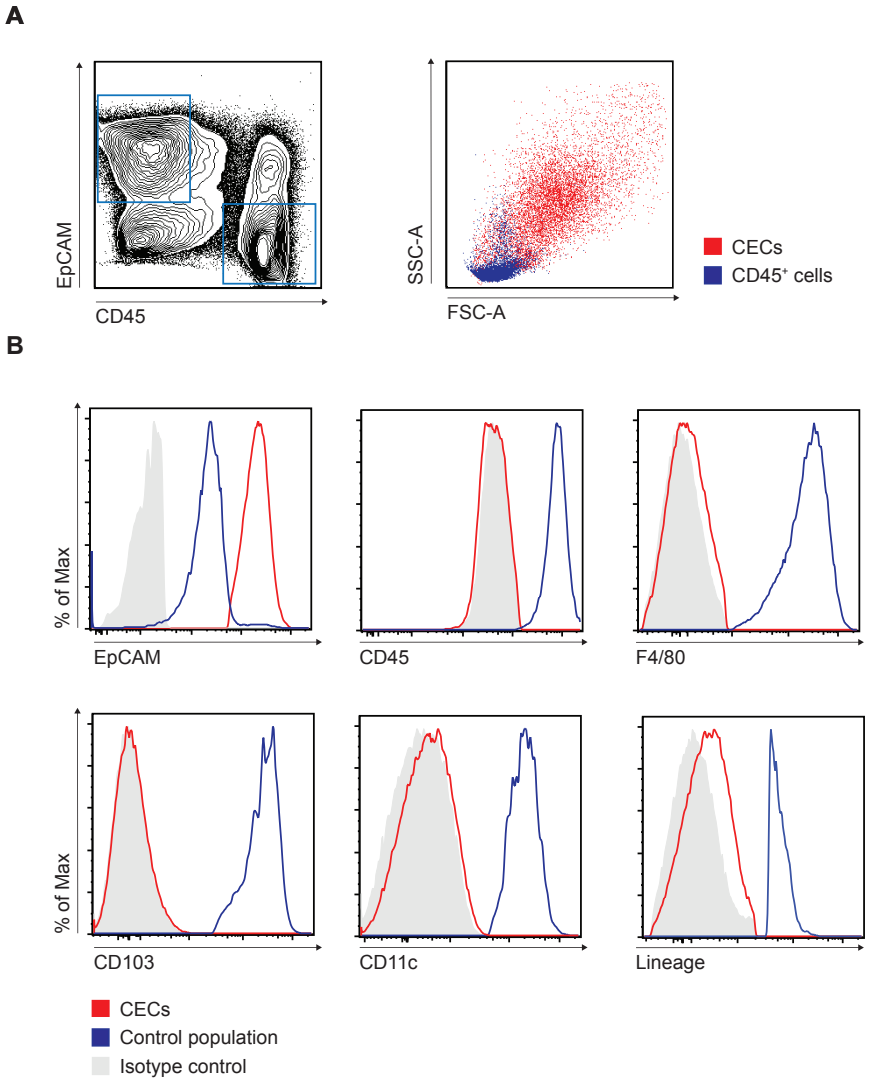

Figure 5.1 Flow cytometry analysis of CECs

Colon cells were isolated and stained with Live Dead (Blue) and thereafter an antibody cocktail consisting of SiglecF, Ly6G, CD11b, CD11c, F4/80, CD64, CD45, CD103 and Lineage markers (CD3, NK1.1 and CD19) and analysed by flow cytometry. **A**. Flow cytometry contour plot of $EpCAM^+$, $CD45^-$ CECs after exclusion of $CD3^+$ $F4/80^+$ $EpCAM^+$ cells, with SSC and FSC profile of CEC and $CD45^+$ populations for comparison. **B**. Histogram of selected surface marker expression comparing $CD45^+$ and CEC populations compared to isotype antibody control. Representative of 3 independent experiments, n=5 mice per experiment.

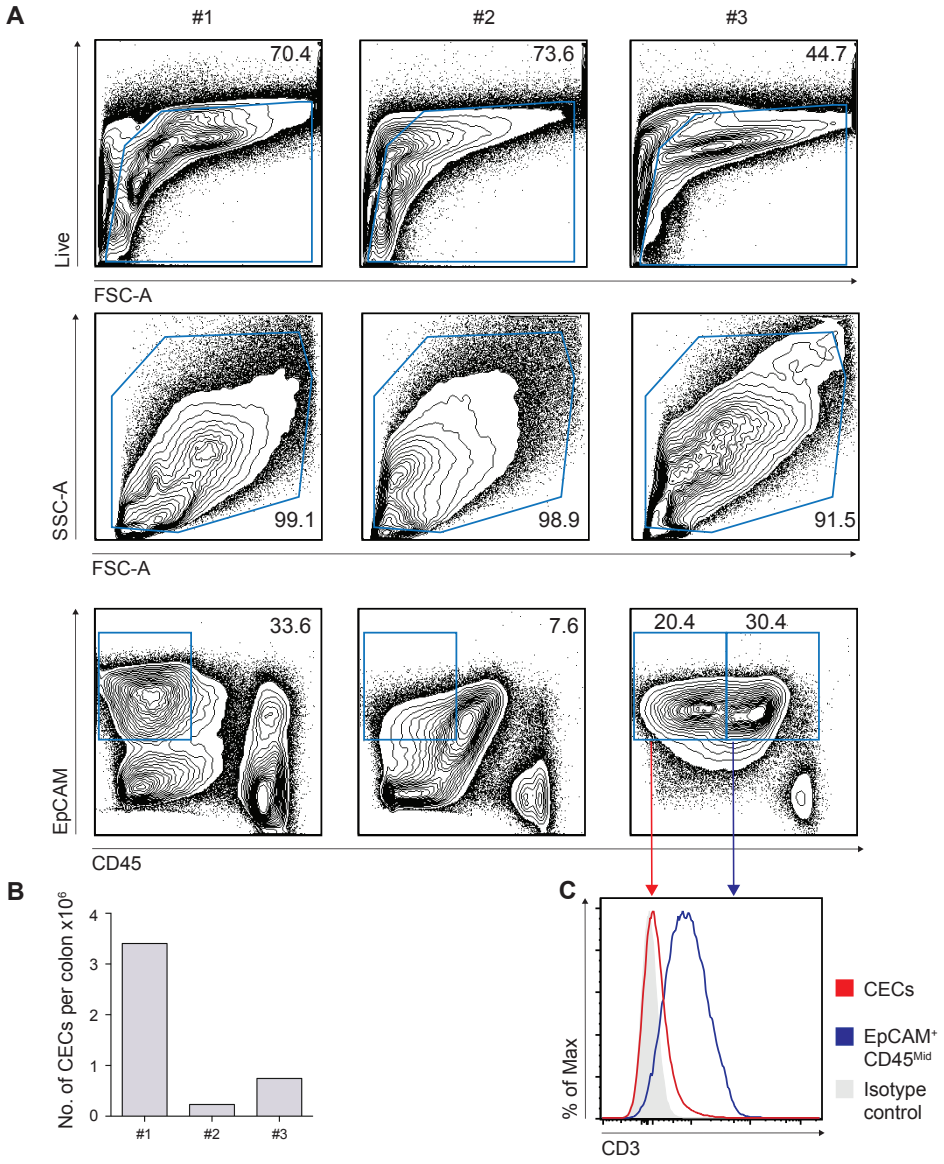

Figure 5.2 Optimising CEC isolation by comparison of 3 established extraction protocols

Colon cells were isolated using 3 different protocols described in chapter 5.2 and table 5.1. Protocol #1 was our exisiting colon cell isolation protocol described in chapter 2.3, protocol #2 utilised a percoll gradient to enrich for CECs, protocol #3 involved a longer incubation period (90 versus 45 mins) with dispase instead of colangenase. Cells were stained for LiveDead(Blue) and thereafter surface stained with an antibody cocktail consisting of EpCAM, CD45, CD3 and F4/80 and analysed by flow cytometry. **A**. sequential vertical gating comparing protocols, gating live and intact cells before identifying EpCAM^{+}, CD45^{-} CECs. **B** The number of CECs was enumerated per colon comparing isolation method. **C** Histogram comparison of CD3 expression on CECs and EpCAM^{+} CD45^{mid} cells compared to isotype antibody controls.

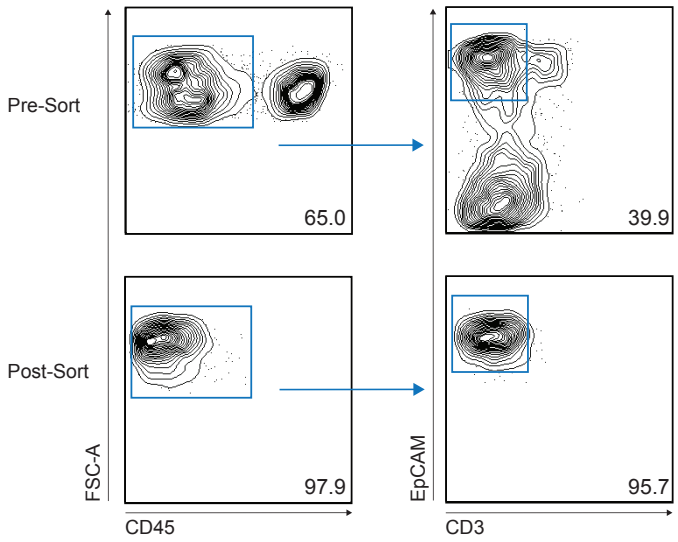

Figure 5.3 Pre and post FACS purification analysis of CECs
A. Contour plots of naive WT colon cells stained for expression of Live Dead Blue, CD45, EpCAM, F4/80 and CD3 surface markers and then purified by FACS. Cells are pre-gated on Live and intact cells. Representative pre- and post-sort purity is presented for $EpCAM^{+}$, $CD45^{-}$ $CD3^{-}$ $F4/80^{-}$ CECs from 1 individual mouse and from 5 independent experiments

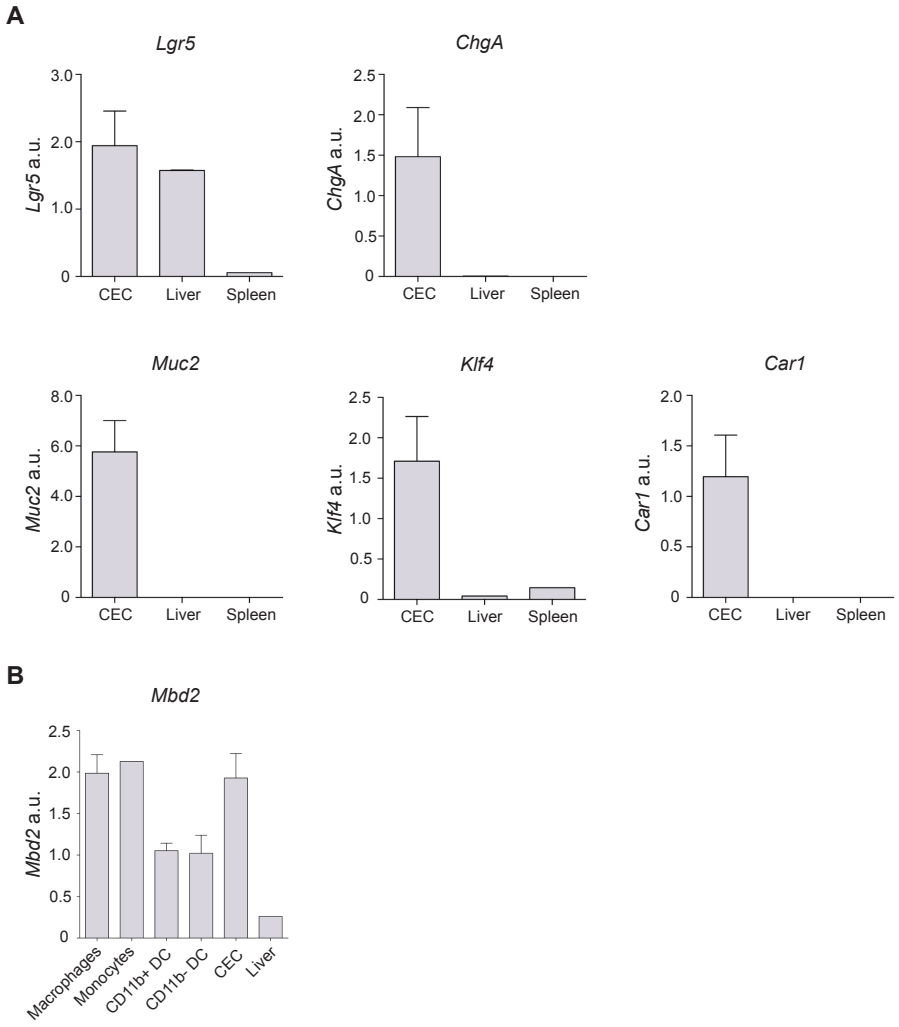

Figure 5.4 mRNA expression of epithelial cell markers and *Mbd2* in CECs

Colon cells were isolated and stained for the following antibody cocktail (CD3, CD45, EpcAM, F4/80) before purification of CECs using the sort logic presented in Figure 5.3. mRNA expression of the above epithelial cell markers (**A**) and *Mbd2* (**B**) was determined by qRT-PCR, the mean value relative to *Gapdh* expression is presented. Mean values were obtained from 3 independent experiments using 3 individual mice. Primer sequences are in Table 2.5. For the other presented populations in **B**, mice were pooled 3 mice per biological replicate, and 3 biological replicates presented, with whole tissue homogenate presented as a control.

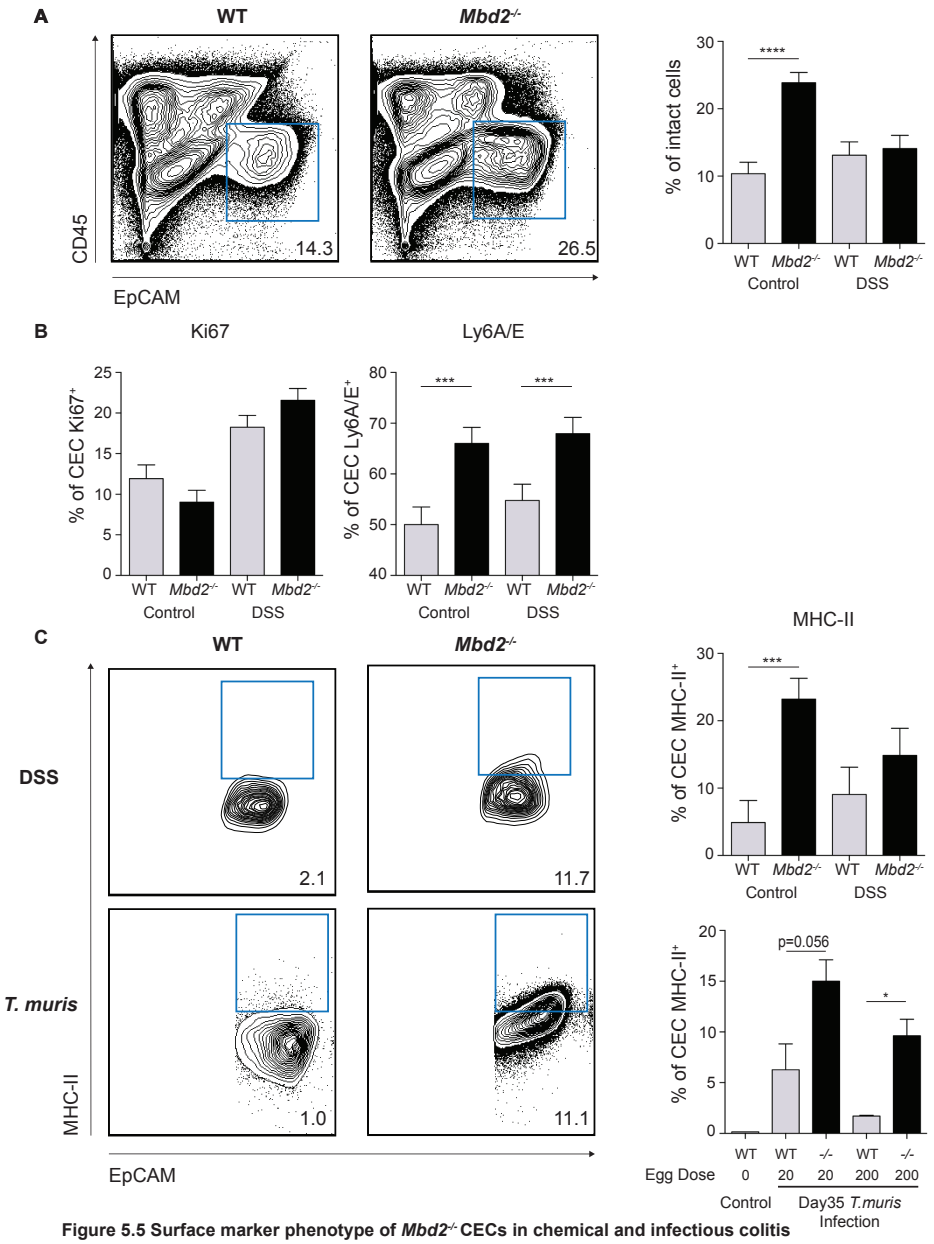

Figure 5.5 Surface marker phenotype of *Mbd2*$^{-/-}$ CECs in chemical and infectious colitis

WT or *Mbd2*$^{-/-}$ mice were treated with 2% DSS or normal drinking water for 6 days (**A,B,C**) or 20 or 200 T. muris eggs for 35days (**C**). Colon cells were then isolated surface stained for the following antibody cocktail (CD3, F4/80, EpCAM, CD45, MHC-II and Ly6A/E) and then permeabilised and stained for intracellular Ki67 and analysed by flow cytometry. A. EpCAM^{+} CD45^{-} CECs were identified and enumerated as the proportion of intact cells. **B**. CECs were analysed for the proportion of total CECs that expressed Ly6A/E or Ki67.**C**. Flow cytometry contour plots of low dose (20eggs) T. muris infected or Day6 DSS treated WT and *Mbd2*$^{-/-}$ CECs at day35 post infection, with the proportion of CECs expressing MHC-II presented. 1 T. muris experiment and 3 independent DSS experiments, n=1-5 per group are presented. *p<0.05, ***p<0.001, ****p<0.0001, analysed by linear regression modelling.

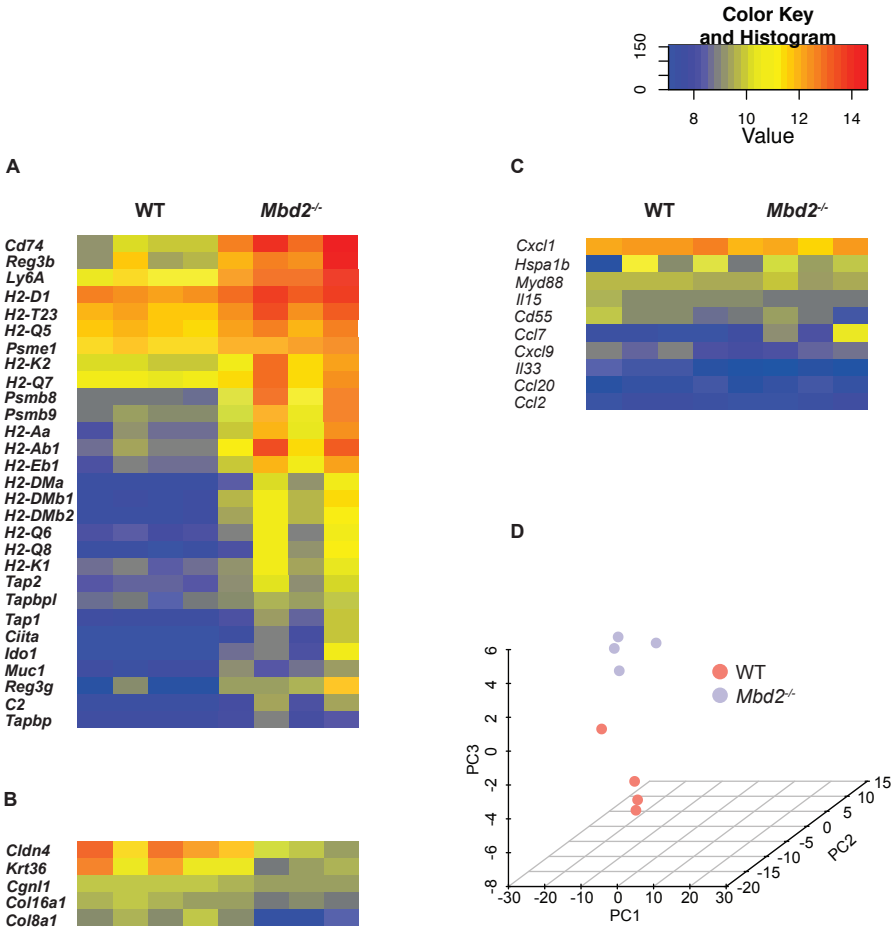

Figure 5.6 Gene expression analysis of naive WT versus *Mbd2*$^{-/-}$ CEC

Naive *Mbd2*$^{-/-}$ or littermate WT mice CECs were isolated and purified by flow cytometry as detailed in Figure 5.3. RNA was extracted and gene expression assessed by hybridisation to IlluminaMouseRef6 microarray. Heatmap of normalised gene expression from WT versus *Mbd2*$^{-/-}$ CECs are presented with genes significantly upregulated (**A**), downregulated (**B**) presented in bold (adj p<0.01). Selected non significant genes are presented based on literature review for pertient loci (**C**). Each individual heatmap represents a biological replicate composed of 1 individual mouse. (**D**) Principal component analysis of gene expression profiles from CECs each data point representing individual biological replicate composed of 1 individual mouse.

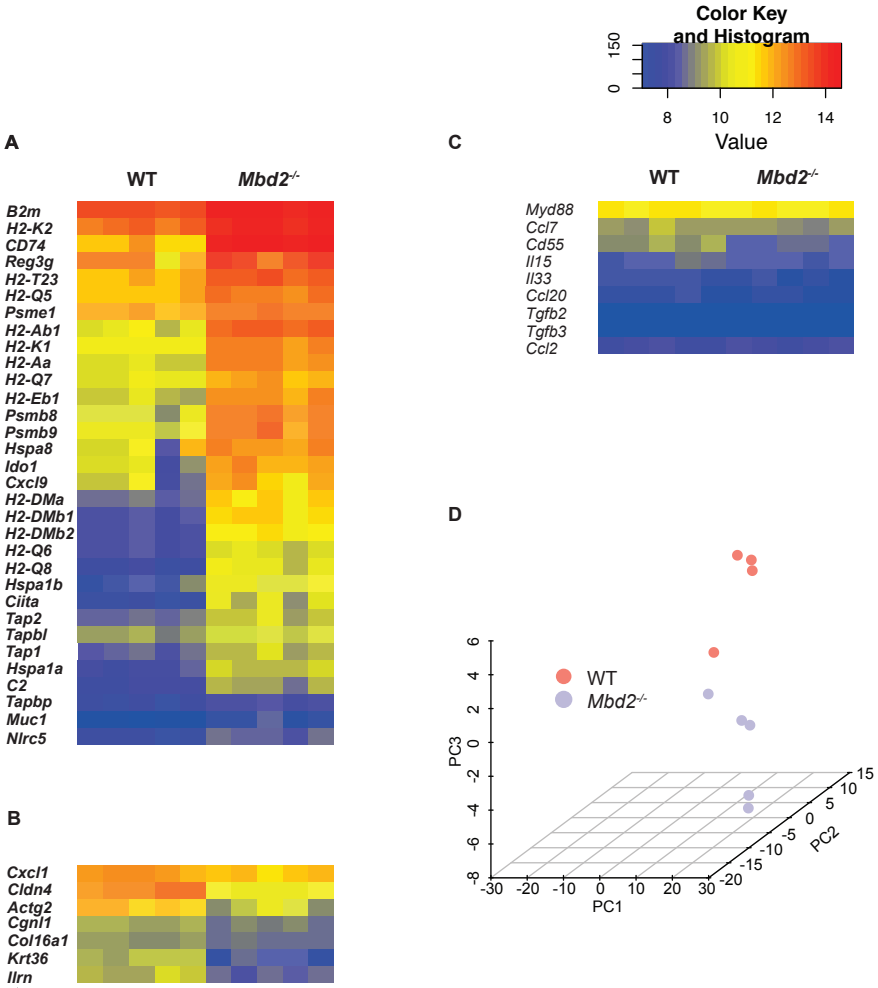

Figure 5.7 Gene expression analysis of DSS treated WT versus *Mbd2*$^{-/-}$ CEC

Day 6 DSS treated *Mbd2*$^{-/-}$ or littermate WT mice CECs were isolated and purified by flow cytometry as detailed in Figure 5.3. RNA was extracted and gene expression assessed by hybridisation to IlluminaMouseRef6 microarray. Heatmap of normalised gene expression from WT versus *Mbd2*$^{-/-}$ CECs are presented with genes significantly upregulated (**A**), downregulated (**B**) presented in bold (adj p<0.01). Selected non significant genes are presented based on literature review for pertient loci (**C**). Each individual heatmap represents a biological replicate composed of 1 individual mouse. (**D**) Principal component analysis of gene expression profiles from CECs each data point representing individual biological replicate composed of 1 individual mouse.

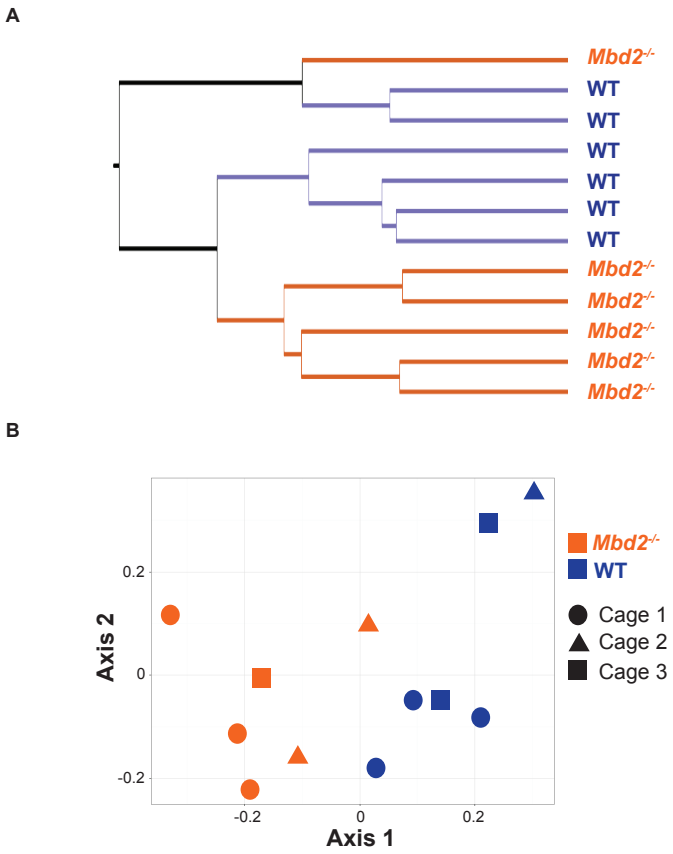

Figure 5.8 Analysis of the colonic microbiota in naive WT and *Mbd2*$^{-/-}$ mice

The colonic contents from co-housed, age and sex matched naive WT and *Mbd2*$^{-/-}$ mice were obtained, and DNA extracted (There was one non-age matched *Mbd2*$^{-/-}$ sample in the analysis, this is discussed in chapter 5.6.1 and Table 5.8 and is the outlier at the top of the dendrogram). The 16S region was amplified using primers overlapping the V3 V4 region (See Chapter 2.15 for primer sequence) and assessed for 550bp product using gel electrophoresis. DNA was then sequenced using the IlluminaMiSeq platform and FASTQ files exported to the mothur software for analysis. OTUs were identified as described in Chapter 5.6 and analysed for differences in microbial populations by Yue and Clayton metrics. (**A**) Dendrograms were produced using iTOL dendrogram software analysing differences in OTU and by non linear multi dimensional modelling (NMDS) (**B**).

FeatureID - UP	Symbol	Description	Chromosome	logFC	Average Expression	P.Value	adj.P.Val
9EgooZ6Kl_enFnNwKg	Cd74	CD74 antigen (invariant polypeptide of major histocompatibility complex, class II antigen-associated)	18	3.8	12	2.80E-09	2.90E-05
B_Ieu3v021ShGkDgtI	Cd74	CD74 antigen (invariant polypeptide of major histocompatibility complex, class II antigen-associated)	18	3.8	12	4.50E-09	3.10E-05
EefYPXh5S3F5R1h0i0	LOC64124 0	similar to H-2 class II histocompatibility antigen, A-D beta chain precursor	Un	3.3	11	4.30E-07	0.00068
6UvTqYucfRQahkmTGM	H2-Ab1	histocompatibility 2, class II antigen A, beta 1	17	3.3	11	9.60E-07	0.001
r3SHsIXg7d51g9eHII	H2-Ab1	histocompatibility 2, class II antigen A, beta 1	17	3.2	12	7.00E-07	9.00E-04
6eLeXokA74mk2qnm58	H2-Ab1	histocompatibility 2, class II antigen A, beta 1	17	3.2	11	7.40E-07	9.00E-04
cfShFUf37tMeXc9K1U	H2-DMb1	histocompatibility 2, class II, locus Mb1	17	3	9.5	4.60E-08	0.00014
9gVNx5fIW5.e6SftCI	Reg3b	regenerating islet-derived 3 beta	6	3	13	1.70E-05	0.0033
x1xqhtxF5uvSRJqF3g	H2-DMb2	histocompatibility 2, class II, locus Mb2	17	2.8	9.4	8.60E-08	2.00E-04
lN9qlC606bx6N7muWc	Psmb8	proteasome (prosome, macropain) subunit, beta type 8 (large multifunctional peptidase 7)	17	2.8	11	2.80E-06	0.0013
Z9bVC5hiBrBz_UdS5Q	Cd74	CD74 antigen (invariant polypeptide of major histocompatibility complex, class II antigen-associated)	18	2.7	9.5	7.30E-07	9.00E-04
Kt1OU4ATtefpUTV1Ig	H2-Eb1	histocompatibility 2, class II antigen E beta	17	2.7	11	1.90E-06	0.0011
r313nVlhbnSuHj33Qo	H2-DMa	histocompatibility 2, class II, locus DMa	17	2.6	9.6	1.10E-06	0.001
oeD.v97TfULxNx5Id0	H2-Aa	histocompatibility 2, class II antigen A, alpha	17	2.5	11	8.30E-06	0.0022
clRI2UKlOJlv1iol4o	H2-Q8	histocompatibility 2, Q region locus 8	17	2.4	8.8	6.50E-05	0.0063
uVHjLVKgZkOdf4t.ro	Retnlb	resistin like beta	16	2.4	13	0.00089	0.025
WQnn9QTjnksWqjqXdQ	Psmb8	proteasome (prosome, macropain) subunit, beta type 8 (large multifunctional peptidase 7)	17	2.3	8.9	1.90E-06	0.0011
fX_l2u5ykU06k_3310	H2-DMa	histocompatibility 2, class II, locus DMa	17	2.3	9.2	3.80E-06	0.0015
cB.egUgpa5jqQK4DO4	Psmb9	proteasome (prosome, macropain) subunit, beta type 9 (large multifunctional peptidase 2)	17	2.1	11	4.20E-05	0.0051
ZnfeL6Xy7JCdR9zSpE	Ido1	indoleamine 2,3-dioxygenase 1	8	2.1	9.7	9.00E-04	0.025
Q1F9V4onUoAQJRHbu0	NA	NA	-	2	8.8	0.00094	0.025

FeatureID - UP	Symbol	Description	Chromosome	logFC	Average Expression	P.Value	adj.P.Val
caE6KRI0VhkLqJKes8	H2-Q8	histocompatibility 2, Q region locus 8	17	1.9	8.9	0.00016	0.0096
xFuCOirpCuuki9VBzQ	Fabp6	fatty acid binding protein 6, ileal (gastrotropin)	11	1.9	9.7	0.00023	0.012
rKeXSrf.nyJXJy0cgI	Igtp	interferon gamma induced GTPase	11	1.9	9.7	0.00077	0.023
6PsHyLxXO3kD0KXIsQ	Reg3g	regenerating islet-derived 3 gamma	6	1.9	11	0.0015	0.031
EClipcXoqZuTotnWSM	H2-K2	histocompatibility 2, K region locus 2	17	1.8	11	1.80E-05	0.0033
BEa9fuN1P6uFYq.v4o	Ppic	peptidylprolyl isomerase C	18	1.7	9.5	2.30E-08	7.90E-05
6nThXopESUkS4IpIPU	Ly6a	lymphocyte antigen 6 complex, locus A	15	1.7	13	8.20E-06	0.0022
3wBQxudRhB1XAuRKpI	2210407C 18Rik	RIKEN cDNA 2210407C18 gene	11	1.7	11	1.10E-05	0.0026
TV3IjxxTk4Pv.50xXs	Ifi47	interferon gamma inducible protein 47	11	1.7	9	7.30E-05	0.0067
35J04IiirnFqU6yKd8	Tap1	transporter 1, ATP-binding cassette, sub-family B (MDR/TAP)	17	1.6	8.8	5.90E-05	0.006
Ng8ROU7gU4qnl4l3RU	H2-Q6	histocompatibility 2, Q region locus 6	17	1.6	9.1	0.00016	0.0098
xwCdl4r7O760SrN0Xo	Irgm2	immunity-related GTPase family M member 2	11	1.6	9.6	0.00039	0.016
u2RK0lQtR1R3Rbv1F8	NA	NA	-	1.6	9.1	0.0029	0.044
lru5F44j_0IhnnnTlY	Cd177	CD177 antigen	7	1.4	11	2.80E-05	0.0042
Hac2l6O8qc2nfdJ3_w	Cd177	CD177 antigen	7	1.4	12	3.20E-05	0.0044
0xXiOqiOol11MR7dQQ	H2-Q7	histocompatibility 2, Q region locus 7	17	1.4	11	7.10E-05	0.0066
QP0ijsae4XqtoamXXU	Gm8909	predicted gene 8909	17	1.4	10	0.00055	0.019
EslXOKK.aSsOkskt3c	Muc1	mucin 1, transmembrane	3	1.3	8.2	1.40E-05	0.0029
cUo_5ahd7lF7gkLd3c	C2	complement component 2 (within H-2S)	17	1.3	8.4	0.00021	0.011
W1ePrhlDpoISgER6ek	Ppic	peptidylprolyl isomerase C	18	1.2	8.2	1.10E-08	5.40E-05
rnp3oMfFTdCqMrTp50	Igfals	insulin-like growth factor binding protein, acid labile subunit	17	1.2	7.9	1.30E-08	5.40E-05
KpPleeuet7P_vn_nNs	Muc1	mucin 1, transmembrane	3	1.2	8.2	1.30E-06	0.001
BShOifuiFKXkqjoF9Q	LOC67413 5	similar to RT1 class I histocompatibility antigen, AA alpha chain precursor	17	1.2	13	6.40E-06	0.0019
HQupJ7brl36goks8RM	H2-T23	histocompatibility 2, T region locus 23	17	1.2	13	4.80E-05	0.0055

FeatureID - UP	Symbol	Description	Chromosome	logFC	Average Expression	P.Value	adj.P.Val
NW5aKKcq0owI_oW.6E	Tap2	transporter 2, ATP-binding cassette, sub-family B (MDR/TAP)	17	1.2	9.3	0.00043	0.017
xIJUDngCJTdeARWhOY	Pla2g2a	phospholipase A2, group IIA (platelets, synovial fluid)	4	1.2	9.2	0.0019	0.036
39FVHiHjExI5IvCTII	B2m	beta-2 microglobulin	2	1.1	14	1.50E-06	0.0011
3Cvp1fJdIqDeXRxedQ	Irf1	interferon regulatory factor 1	11	1.1	11	3.10E-06	0.0013
30VUeIeMTGXki8JOUs	B2m	beta-2 microglobulin	2	1.1	14	5.50E-06	0.0017
rSC6knuuuXfqCiSDxE	H2-K2	histocompatibility 2, K region locus 2	17	1.1	14	9.60E-06	0.0024
EuSCf0ruJwCrEh9cOE	LOC677317	similar to NADP-dependent malic enzyme (NADP-ME) (Malic enzyme 1)	9	1.1	8.3	0.00012	0.0083
6pfudyDrFDUs0OzhC4	Oasl2	2-5 oligoadenylate synthetase-like 2	5	1.1	8.7	0.0021	0.038
Wp1uusg2Huv9airH.I	Muc1	mucin 1, transmembrane	3	1	7.9	2.00E-06	0.0011
E.C_hFilAp5dJfVJU0	Lpo	lactoperoxidase	11	1	8	2.80E-06	0.0013
iPiRVRYl7kiJ6W8WP4	Psmb10	proteasome (prosome, macropain) subunit, beta type 10	8	1	12	1.90E-05	0.0034
WV53QFX40Z93.PN6hI	Cpn1	carboxypeptidase N, polypeptide 1	19	1	8.1	8.80E-05	0.0073
cUQupJ7brl36goks8Q	H2-T23	histocompatibility 2, T region locus 23	17	1	12	1.00E-04	0.0079
ZI_IX6ee7cLoekiHuk	Parp14	poly (ADP-ribose) polymerase family, member 14	16	1	9.5	0.00011	0.008
FeatureID - DOWN	**Symbol**	**Description**	**Chromosome**	**logFC**	**Average Expression**	**P.Value**	**adj.P.Val**
EFQJikGeiMgFcoKI3o	NA	NA	-	-2.7	8.9	1.00E-06	0.001
fhAFC9EQzf1GDUlfQo	NA	NA	-	-2.2	8.5	3.80E-06	0.0015
HEAUL0RDN.UYNSV9Ao	Gm4415	predicted gene 4415	2	-2.1	8.3	4.90E-06	0.0016
3VAmKQZ6IyAVyiI3oE	NA	NA	-	-2.1	8.2	7.20E-06	0.0021
f3i9XV.IT9ChFpS3mg	Cldn4	claudin 4	5	-2	11	6.20E-05	0.0061
Nwe5F9XgloifI5Ih50	NA	NA	-	-1.9	9.5	1.60E-05	0.0031
iMoFCFHRTTSBUkdUfY	NA	NA	-	-1.9	10	0.00025	0.012
ZvREM3dRg1JX0CjDJI	NA	NA	-	-1.8	8.5	8.50E-06	0.0022
3ZUfZUNShFcEReAKyE	NA	NA	-	-1.8	8.6	2.30E-05	0.0038

FeatureID - DOWN	Symbol	Description	Chromosome	logFC	Average Expression	P.Value	adj.P.Val
xet8Huf.GU5AFK9V6A	Krt36	keratin 36	11	-1.8	10	3.00E-04	0.014
rpxH.Tp0o9N4Kq4oul	Sprr1a	small proline-rich protein 1A	3	-1.7	9.8	1.00E-05	0.0025
iOCfnrnuuNdqnleddc	NA	NA	-	-1.6	8	0.00015	0.0095
oyruyspXqhyohXojdA	Arc	activity regulated cytoskeletal-associated protein	15	-1.5	11	5.20E-05	0.0058
fnp4j2_4XomkgU4s0o	NA	NA	-	-1.5	9.1	0.0022	0.039
3U4QBQPREM39Rg1JX0	NA	NA	-	-1.4	7.9	2.70E-05	0.0042
B5SVKcdxUlAd0PFMTo	NA	NA	-	-1.4	9.2	0.00011	0.008
igFCFHRTTSBUsdcfS0	NA	NA	-	-1.4	8.7	0.00048	0.018
ul5J6ij4._ip17k2eg	Fxyd4	FXYD domain-containing ion transport regulator 4	6	-1.4	8.5	0.0012	0.028
Z5FUnXQtJFSNaFNFig	Krt36	keratin 36	11	-1.4	9	0.0013	0.03
iRwiBEDlJUpxzFSUB0	Gm3308	predicted gene 3308	2	-1.3	11	0.00039	0.016
oQngF3r41AoTYThVQE	Cyp2c67	cytochrome P450, family 2, subfamily c, polypeptide 67	19	-1.3	8.8	0.00096	0.025
Hu6DqgO4ICeweSvrZE	Neat1	nuclear paraspeckle assembly transcript 1 (non-protein coding)	19	-1.2	12	9.00E-05	0.0074
BiJeSeoo_P.oqde5Nk	Fxyd4	FXYD domain-containing ion transport regulator 4	6	-1.2	8.1	0.00089	0.025
HnCTpF.DVJEUyo3eL0	Ceacam1	carcinoembryonic antigen-related cell adhesion molecule 1	7	-1.2	10	0.0026	0.042
TfncwFu8knSgjluCT0	Ttr	transthyretin	18	-1.1	11	0.00015	0.0095
ihawfn4vVODI.iHg6Q	Col8a1	collagen, type VIII, alpha 1	16	-1.1	8.2	0.00017	0.0099
iUEe0XSUtepFUExUAI	NA	NA	-	-1.1	7.9	0.00046	0.017
Ere3vD3o.tqhOQ.x94	Fosb	FBJ osteosarcoma oncogene B	7	-1.1	12	0.0015	0.032
HtJL.V6BqM8rz1QNBc	Csad	cysteine sulfinic acid decarboxylase	15	-1	8.8	1.60E-06	0.0011
uKJSi14IMCF0SUEQp4	Tff3	trefoil factor 3, intestinal	17	-1	13	0.0023	0.04

Table 5.2 Gene expression analysis of naïve *Mbd2-/-* and WT CECs
Naive colon cells were isolated from WT and *Mbd2*$^{-/-}$ mice. CECs were identified and purified by flow cytometry as described in Figure 5.3. RNA was isolated and hybridised to IlluminaMouseRef6 array. The details of significant (adj $p<0.05$) $>\pm1$ log FC genes are presented. Details of raw data processing and normalisation methods are presented in Chapter 2.16

Ontology	GO_ID	GOterm	Enrich_pValue	Symbol
Up -regulated				
BP	GO:0019882	antigen processing and presentation	8.42E-26	B2m, Cd74, H2-Aa, H2-Ab1, H2-D1, H2-DMa, H2-DMb1, H2-DMb2, H2-Eb1, H2-Q6, H2-T23, Psmb8, Psmb9, Psme1, Tapbp, Tapbpl, Traf6
BP	GO:0048002	antigen processing and presentation of peptide antigen	2.59E-23	B2m, Cd74, H2-Aa, H2-Ab1, H2-D1, H2-DMa, H2-DMb1, H2-DMb2, H2-Eb1, H2-Q6, H2-T23, Tapbp, Tapbpl, Traf6
BP	GO:0019884	antigen processing and presentation of exogenous antigen	9.72E-18	B2m, Cd74, H2-Aa, H2-Ab1, H2-DMa, H2-DMb1, H2-DMb2, H2-Eb1, Psme1, Tapbp, Traf6
BP	GO:0002478	antigen processing and presentation of exogenous peptide antigen	6.96E-17	B2m, Cd74, H2-Aa, H2-Ab1, H2-DMa, H2-DMb1, H2-DMb2, H2-Eb1, Tapbp, Traf6
CC	GO:0042611	MHC protein complex	4.08E-15	B2m, H2-Aa, H2-Ab1, H2-D1, H2-DMa, H2-DMb1, H2-DMb2, H2-Eb1, H2-Q6
BP	GO:0002495	antigen processing and presentation of peptide antigen via MHC class II	1.40E-14	Cd74, H2-Aa, H2-Ab1, H2-DMa, H2-DMb1, H2-DMb2, H2-Eb1, Traf6
BP	GO:0019886	antigen processing and presentation of exogenous peptide antigen via MHC class II	1.40E-14	Cd74, H2-Aa, H2-Ab1, H2-DMa, H2-DMb1, H2-DMb2, H2-Eb1, Traf6
BP	GO:0002504	antigen processing and presentation of peptide or polysaccharide antigen via MHC class II	1.12E-13	Cd74, H2-Aa, H2-Ab1, H2-DMa, H2-DMb1, H2-DMb2, H2-Eb1, Traf6
CC	GO:0042613	MHC class II protein complex	1.92E-11	H2-Aa, H2-Ab1, H2-DMa, H2-DMb1, H2-DMb2, H2-Eb1
BP	GO:0002376	immune system process	6.55E-10	Adora2b, B2m, Cd74, Csk, H2-Aa, H2-Ab1, H2-D1, H2-DMa, H2-DMb1, H2-DMb2, H2-Eb1, H2-Q6, H2-T23, Irf1, Irf7, Lrrc8a, Psmb8, Psmb9, Psme1, Tap1, Tapbp, Tapbpl, Tnf, Traf6, Vav1
Down-regulated				
BP	GO:0044281	small molecule metabolic process	1.07E-04	Atp5f1, Btg2, Csad, Cyp11a1, Ddc, Fhit, Gde1, Ghr, Glul, Gnai1, Grtp1, Igf2, Kdm6b, Mecr, Mlxipl, Ndel1, Pde1b, Prkar2b, Soat1, Upb1
BP	GO:0019530	taurine metabolic process	2.71E-04	Csad, Ghr
BP	GO:0031589	cell-substrate adhesion	2.76E-04	Col8a1, Ctnnb1, Hsd17b12, Itga6, Tsc1
BP	GO:0045785	positive regulation of cell adhesion	2.99E-04	Col8a1, Hsd17b12, Itga6, Selp
MF	GO:0016831	carboxy-lyase activity	3.53E-04	Csad, Ddc, Glul
CC	GO:0000267	cell fraction	3.87E-04	Ace2, Anxa7, Ctnnb1, Cyp2f2, Glul, Gnai1, Gstm2, Lin7c, Prkar2b, Rasd1, Selp, Soat1, Tsc1, Upb1
MF	GO:0005515	protein binding	4.26E-04	Abcd3, Anxa7, Arc, Ascc1, Atl2, Bckdha, Btg2, Camk1, Camk2n2, Cldn4, Ctnnb1, Cul1, Eef2k, Ghr, Glul, Gnai1, Gstm2, Hsd17b12, Id2, Igf2, Il33, Itga6, Klk1b4, Lin7c, Mecr, Mlxipl, Ndel1, Neat1, Nov, Pde1b, Pdgfa, Pmaip1, Prkar2b, Reep6, Selp, Socs2, Sun2, Tceal1, Thrap3, Timp3, Tsc1, Ttr, Wwc2
BP	GO:0030155	regulation of cell adhesion	4.64E-04	Col8a1, Hsd17b12, Itga6, Selp, Tsc1
BP	GO:0044238	primary metabolic process	6.71E-04	Ace2, Afg3l2, Ascc1, Atp5f1, Btg2, C4bp, Camk1, Csad, Ctnnb1, Cul1, Cyp11a1, Ddc, Eef2k, Fhit, Gde1, Ghr, Glul, Gnai1, Grtp1, Hsd17b12, Id2, Igf2, Itgb3bp, Kdm6b, Klf16, Klf9, Klk1b24, Klk1b4, Klk1b5, Klk1b9, Mecr, Mlxipl, Mocs1, Ndel1, Pde1b, Pdgfa, Pou6f1, Prkar2b, Prss53, Ptp4a2, Rasd1, Sik3, Soa ... and others
BP	GO:0008152	metabolic process	6.83E-04	Ace2, Afg3l2, Ascc1, Atp5f1, Bckdha, Btg2, C4bp, Camk1, Csad, Ctnnb1, Cul1, Cyp11a1, Cyp2f2, Ddc, Eef2k, Fhit, Gde1, Ghr, Glul, Gnai1, Grtp1, Gstm2, Hsd17b12, Id2, Igf2, Itgb3bp, Kdm6b, Klf16, Klf9, Klk1b24, Klk1b4, Klk1b5, Klk1b9, Mecr, Mlxipl, Mocs1, Ndel1, Nudt11, Pde1b, Pdgfa, Pou6f1, Prkar2b, P ... and others

Table 5.3 Gene ontology analysis of naïve Mbd2-/- and WT CECs

Naive colon cells were isolated from WT and *Mbd2*$^{-/-}$ mice. CECs were identified and purified by flow cytometry as described in Figure 5.3. RNA was isolated and hybridised to IlluminaMouseRef6 array. The details of significant (adj p<0.05) pathways by GOterm analysis are presented. Details of raw data processing and normalisation methods are presented in Chapter 2.16

PathID	PathDescr.	pValue	Symbol	Number of significant genes	% of pathway significant
Up-regulated					
4612	Antigen processing and presentation	1.32E-19	B2m, Cd74, H2-Aa, H2-Ab1, H2-D1, H2-DMa, H2-DMb1, H2-DMb2, H2-Eb1, H2-Q6, H2-Q7, H2-Q8, H2-T23, Psme1, Tap1, Tapbp, Tnf	17	33
5330	Allograft rejection	6.05E-14	H2-Aa, H2-Ab1, H2-D1, H2-DMa, H2-DMb1, H2-DMb2, H2-Eb1, H2-Q6, H2-Q7, H2-Q8, H2-T23, Tnf	12	47
5332	Graft-versus-host disease	9.45E-14	H2-Aa, H2-Ab1, H2-D1, H2-DMa, H2-DMb1, H2-DMb2, H2-Eb1, H2-Q6, H2-Q7, H2-Q8, H2-T23, Tnf	12	45
4940	Type I diabetes mellitus	2.68E-13	H2-Aa, H2-Ab1, H2-D1, H2-DMa, H2-DMb1, H2-DMb2, H2-Eb1, H2-Q6, H2-Q7, H2-Q8, H2-T23, Tnf	12	43
5320	Autoimmune thyroid disease	3.08E-11	H2-Aa, H2-Ab1, H2-D1, H2-DMa, H2-DMb1, H2-DMb2, H2-Eb1, H2-Q6, H2-Q7, H2-Q8, H2-T23	11	38
4145	Phagosome	1.90E-10	Atp6v0a2, H2-Aa, H2-Ab1, H2-D1, H2-DMa, H2-DMb1, H2-DMb2, H2-Eb1, H2-Q6, H2-Q7, H2-Q8, H2-T23, Stx18, Tap1	14	13
5416	Viral myocarditis	4.23E-10	H2-Aa, H2-Ab1, H2-D1, H2-DMa, H2-DMb1, H2-DMb2, H2-Eb1, H2-Q6, H2-Q7, H2-Q8, H2-T23	11	23
5310	Asthma	4.10E-09	H2-Aa, H2-Ab1, H2-DMa, H2-DMb1, H2-DMb2, H2-Eb1, Tnf	7	47
5140	Leishmaniasis	5.61E-09	H2-Aa, H2-Ab1, H2-DMa, H2-DMb1, H2-DMb2, H2-Eb1, Irak4, Tnf, Traf6	9	18
4514	Cell adhesion molecules (CAMs)	9.46E-08	H2-Aa, H2-Ab1, H2-D1, H2-DMa, H2-DMb1, H2-DMb2, H2-Eb1, H2-Q6, H2-Q7, H2-Q8, H2-T23	11	
Down-regulated					
4670	Leukocyte transendothelial migration	2.54E-02	Cldn4, Ctnnb1, Gnai1	3	4
140	Steroid hormone biosynthesis	3.24E-02	Cyp11a1, Hsd17b12	2	8
4530	Tight junction	3.53E-02	Cldn4, Ctnnb1, Gnai1	3	3
4910	Insulin signaling pathway	3.87E-02	Prkar2b, Socs2, Tsc1	3	3
62	Fatty acid elongation in mitochondria	4.29E-02	Mecr	1	13
4514	Cell adhesion molecules (CAMs)	4.85E-02	Cldn4, Itga6, Selp	3	4

Table 5.4 Gene pathway analysis of naïve *Mbd2-/-* and WT CECs

Naive colon cells were isolated from WT and *Mbd2*$^{-/-}$ mice. CECs were identified and purified by flow cytometry as described in Figure 5.3. RNA was isolated and hybridised to IlluminaMouseRef6 array. The details of significant (adj $p<0.05$) pathways by KEGG analysis are presented. Details of raw data processing and normalisation methods are presented in Chapter 2.16

FeatureID - UP	Symbol	Description	Chromosome	LogFC	Average expression	P.value	Adj. P.value
cfShFUf37tMeXc9K1U	H2-DMb1	histocompatibility 2, class II, locus Mb1	17	3.2	9.5	2.90E-09	5.10E-05
x1xqhtxF5uvSRJqF3g	H2-DMb2	histocompatibility 2, class II, locus Mb2	17	3	9.4	8.70E-09	5.10E-05
B_Ieu3v021ShGkDgtI	Cd74	CD74 antigen (invariant polypeptide of major histocompatibility complex, class II antigen-associated)	18	2.8	12	8.90E-08	0.00014
ZnfeL6Xy7JCdR9zSpE	Ido1	indoleamine 2,3-dioxygenase 1	8	2.8	9.7	1.80E-05	0.0017
9EgooZ6KI_enFnNwKg	Cd74	CD74 antigen (invariant polypeptide of major histocompatibility complex, class II antigen-associated)	18	2.7	12	9.20E-08	0.00014
r313nVIhbnSuHj33Qo	H2-DMa	histocompatibility 2, class II, locus DMa	17	2.7	9.6	1.30E-07	0.00015
xFuCOirpCuuki9VBzQ	Fabp6	fatty acid binding protein 6, ileal (gastrotropin)	11	2.7	9.7	7.30E-07	0.00036
cIRI2UKIOJIv1iol4o	H2-Q8	histocompatibility 2, Q region locus 8	17	2.7	8.8	7.50E-06	0.001
fX_I2u5ykU06k_3310	H2-DMa	histocompatibility 2, class II, locus DMa	17	2.6	9.2	1.20E-07	0.00015
EefYPXh5S3F5R1h0i0	LOC641240	similar to H-2 class II histocompatibility antigen, A-D beta chain precursor	Un	2.6	11	1.50E-06	0.00045
6UvTqYucfRQahkmTGM	H2-Ab1	histocompatibility 2, class II antigen A, beta 1	17	2.6	11	4.30E-06	0.00081
oeD.v97TfULxNx5Id0	H2-Aa	histocompatibility 2, class II antigen A, alpha	17	2.5	11	2.00E-06	0.00052
r3SHsIXg7d51g9eHII	H2-Ab1	histocompatibility 2, class II antigen A, beta 1	17	2.5	12	4.10E-06	0.00078
6eLeXokA74mk2qnm58	H2-Ab1	histocompatibility 2, class II antigen A, beta 1	17	2.5	11	5.20E-06	0.00087
xhZEiMcQUiQqad0RHU	NA	NA	-	2.4	9.1	1.30E-06	0.00045
Kt1OU4ATtefpUTV1Ig	H2-Eb1	histocompatibility 2, class II antigen E beta	17	2.4	11	1.80E-06	0.00049
iqjhRqjmuOIJ0CWP10	Ubd	ubiquitin D	17	2.3	8.4	8.70E-07	0.00039

FeatureID - UP	Symbol	Description	Chromosome	LogFC	Average expression	P.value	Adj. P.value
caE6KRI0VhkLqJKes8	H2-Q8	histocompatibility 2, Q region locus 8	17	2.3	8.9	4.40E-06	0.00081
lN9qlC606bx6N7muWc	Psmb8	proteasome (prosome, macropain) subunit, beta type 8 (large multifunctional peptidase 7)	17	2.2	11	1.40E-05	0.0014
TaY2k2F6kUXHbm6m70	Hspa1b	heat shock protein 1B	17	2.2	9.5	0.00015	0.0059
3wBQxudRhB1XAuRKpI	2210407C18Rik	RIKEN cDNA 2210407C18 gene	11	2.1	11	2.90E-07	0.00023
Q1F9V4onUoAQJRHbu0	NA	NA	-	2.1	8.8	0.00025	0.008
EClipcXoqZuTotnWSM	H2-K2	histocompatibility 2, K region locus 2	17	2	11	1.20E-06	0.00045
WQnn9QTjnksWqjqXdQ	Psmb8	proteasome (prosome, macropain) subunit, beta type 8 (large multifunctional peptidase 7)	17	2	8.9	3.00E-06	0.00069
Ng8ROU7gU4qnl4l3RU	H2-Q6	histocompatibility 2, Q region locus 6	17	2	9.1	5.80E-06	0.00091
KeWaJkF9Uok1eWaJkE	Hspa1a	heat shock protein 1A	17	2	9.1	0.00015	0.0059
rKeXSrf.nyJXJy0cgI	Igtp	interferon gamma induced GTPase	11	2	9.7	0.00018	0.0065
fpClt6OmV3nXESICEA	Upp1	uridine phosphorylase 1	11	2	9.4	0.00019	0.0068
95LnXSF4OL1U6_6kEU	Upp1	uridine phosphorylase 1	11	2	9.8	0.00041	0.01
9SOoAB9VkX3lJ016FU	Eef2	eukaryotic translation elongation factor 2	10	2	10	0.00047	0.011
WoW3kKlUjQR1UY7n7o	Upp1	uridine phosphorylase 1	11	2	11	0.00086	0.016
T5ek.u63bbSZJ6lxEQ	Hspa8	heat shock protein 8	9	2	12	0.00087	0.016
QP0ijsae4XqtoamXXU	Gm8909	predicted gene 8909	17	1.9	10	1.20E-05	0.0013
HAfVZF95SdNehVN9Cs	Eef2	eukaryotic translation elongation factor 2	10	1.9	11	0.0013	0.021
cB.egUgpa5jqQK4DO4	Psmb9	proteasome (prosome, macropain) subunit, beta type 9 (large multifunctional peptidase 2)	17	1.8	11	4.90E-05	0.003

FeatureID - UP	Symbol	Description	Chromosome	LogFC	Average expression	P.value	Adj. P.value
6gKSN7NnZ5f63t6A5Q	Ciita	class II transactivator	16	1.7	7.8	9.10E-07	0.00039
cUo_5ahd7lF7gkLd3c	C2	complement component 2 (within H-2S)	17	1.7	8.4	5.60E-06	0.00089
TV3IjxxTk4Pv.50xXs	Ifi47	interferon gamma inducible protein 47	11	1.7	9	1.40E-05	0.0014
6enl5KoZXXkjjRTUfE	Eef2	eukaryotic translation elongation factor 2	10	1.7	10	0.0013	0.02
0xXiOqiOol11MR7dQQ	H2-Q7	histocompatibility 2, Q region locus 7	17	1.6	11	3.90E-06	0.00077
EeQddH1EeIMMP4OwX4	H2-K1	histocompatibility 2, K1, K region	17	1.6	12	1.70E-05	0.0016
3TSSXkl4IT5R8ce0Eo	Igk-V32	immunoglobulin kappa chain variable 32 (V32)	6	1.6	8.3	0.0012	0.019
u2RK0lQtR1R3Rbv1F8	NA	NA	-	1.6	9.1	0.0013	0.02
lO5FMKp5eJd0V4joJ8	H2-K1	histocompatibility 2, K1, K region	17	1.5	9.2	1.20E-05	0.0013
TUi_l9IF1Rsn9iFOo8	Cxcl9	chemokine (C-X-C motif) ligand 9	5	1.5	8.7	0.00074	0.015
uXO3kD8evAfNISQE1Y	Reg3b	regenerating islet-derived 3 beta	6	1.5	9.5	0.0017	0.024
BtF7vMrHdpfTTlSUxs	Gbp2	guanylate binding protein 2	3	1.5	9.6	0.0025	0.03
cUQupJ7brl36goks8Q	H2-T23	histocompatibility 2, T region locus 23	17	1.4	12	1.40E-06	0.00045
60yG19JV42SJFKVhkI	Wars	tryptophanyl-tRNA synthetase	12	1.4	9.2	1.80E-06	0.00049
3rolfp6Cn_SOpx4n30	Gm4951	predicted gene 4951	18	1.4	7.6	8.70E-06	0.0011
Tih0InhS.IDi6paLpA	Saa3	serum amyloid A 3	7	1.4	8.4	0.0021	0.027
6PsHyLxXO3kD0KXIsQ	Reg3g	regenerating islet-derived 3 gamma	6	1.4	11	0.006	0.05
BShOifuiFKXkqjoF9Q	LOC674135	similar to RT1 class I histocompatibility antigen, AA alpha chain precursor	17	1.3	13	7.10E-07	0.00036
HQupJ7brl36goks8RM	H2-T23	histocompatibility 2, T region locus 23	17	1.3	13	5.40E-06	0.00087
ZRJFVQuXUvfRSv9ERI	Batf2	basic leucine zipper transcription factor, ATF-like 2	19	1.3	8.9	2.50E-05	0.002
NW5aKKcq0owI_oW.6E	Tap2	transporter 2, ATP-binding cassette, sub-family B (MDR/TAP)	17	1.3	9.3	6.40E-05	0.0035

FeatureID - UP	Symbol	Description	Chromosome	LogFC	Average expression	P.value	Adj. P.value
HsA.rmhnYl8OfQrshc	Hspd1	heat shock protein 1 (chaperonin)	1	1.3	8.5	0.00011	0.0047
35J04IiirnFqU6yKd8	Tap1	transporter 1, ATP-binding cassette, sub-family B (MDR/TAP)	17	1.3	8.8	0.00011	0.0047
lJr0oU0fUnHNmqdOk0	Rab1b	RAB1B, member RAS oncogene family	19	1.3	9.1	0.00014	0.0056
6wkaeoTQQo5e3vWieo	Irf1	interferon regulatory factor 1	11	1.3	9	0.00016	0.0062
KcJGnqE0EKOXt71ono	Irf1	interferon regulatory factor 1	11	1.3	9.1	0.00023	0.0077
xwCdl4r7O760SrN0Xo	Irgm2	immunity-related GTPase family M member 2	11	1.3	9.6	0.00075	0.015
rSC6knuuuXfqCiSDxE	H2-K2	histocompatibility 2, K region locus 2	17	1.2	14	1.10E-06	0.00045
ft3UI_wJuCEnI6HkeI	NA	NA	-	1.2	10	4.90E-06	0.00086
fuHsoAIgOLjTXunHJI	1600029 D21Rik	RIKEN cDNA 1600029D21 gene	9	1.2	9.1	5.40E-06	0.00087
N1IGJElsKkNFFn00WI	St6galna c6	ST6 (alpha-N-acetyl-neuraminyl-2,3-beta-galactosyl-1,3)-N-acetylgalactosaminide alpha-2,6-sialyltransferase 6	2	1.2	8.4	0.00085	0.016
ikq50hQji5S4VQddTc	Wars	tryptophanyl-tRNA synthetase	12	1.1	8.3	1.50E-06	0.00045
foohEyuwCjnOdO9ykk	H2-T23	histocompatibility 2, T region locus 23	17	1.1	11	6.40E-06	0.00092
6Nu99QofUlSnyi8F4U	Nlrc5	NLR family, CARD domain containing 5	8	1.1	7.7	9.40E-06	0.0011
3IaUhYHSn.WJih5uG4	Rbbp7	retinoblastoma binding protein 7	X	1.1	9.1	0.00082	0.016
uoniNGO9Z9OKhuiXig	Mlf2	myeloid leukemia factor 2	6	1.1	9.5	0.0019	0.026
3S0y7cOiA_50VLdQUU	NA	NA	-	1.1	7.6	0.0037	0.039
KkJ0O5IIkHqKSgMf0U	NA	NA	-	1	7.5	8.80E-06	0.0011
Hac2l6O8qc2nfdJ3_w	Cd177	CD177 antigen	7	1	12	0.00018	0.0066
coo5BZ16r.4kJ9ziJY	Vsig2	V-set and immunoglobulin domain containing 2	9	1	11	0.00019	0.0067
lru5F44j_0IhnnnTIY	Cd177	CD177 antigen	7	1	11	0.00023	0.0075

FeatureID - UP	Symbol	Description	Chromosome	LogFC	Average expression	P.value	Adj. P.value
HR5BSUnVnYN457oOfA	Hnrnpk	heterogeneous nuclear ribonucleoprotein K	13	1	8.7	0.0012	0.019
rtfnS.fk9__f6.UrkI	NA	NA	-	1	7.8	0.0015	0.022
BqpFU7I.nciDo.dKIE	Duoxa2	dual oxidase maturation factor 2	2	1	10	0.0029	0.033
FeatureID - DOWN	**Symbol**	**Description**	**Chromosome**	**LogFC**	**Average expression**	**P.value**	**Adj. P.value**
NgKfggqMR7qq45DjR0	1810030J14Rik	RIKEN cDNA 1810030J14 gene	1	-2.6	12	0.006	0.05
xet8Huf.GU5AFK9V6A	Krt36	keratin 36	11	-1.9	10	7.00E-05	0.0037
W1UQh57RSUSNPAF9CU	Actg2	actin, gamma 2, smooth muscle, enteric	6	-1.7	11	8.10E-06	0.0011
r4He86cWw7_kLq9vgw	Spink3	serine peptidase inhibitor, Kazal type 3	18	-1.7	12	0.0024	0.029
f3i9XV.IT9ChFpS3mg	Cldn4	claudin 4	5	-1.6	11	0.00021	0.0071
oWJXZSQ0_ztLTv_77A	Atp12a	ATPase, H+/K+ transporting, nongastric, alpha polypeptide	14	-1.6	8.9	0.0016	0.023
TfncwFu8knSgjluCT0	Ttr	transthyretin	18	-1.5	11	1.50E-06	0.00045
ul5J6ij4._ip17k2eg	Fxyd4	FXYD domain-containing ion transport regulator 4	6	-1.5	8.5	0.00019	0.0067
Z5FUnXQtJFSNaFNFig	Krt36	keratin 36	11	-1.5	9	0.00041	0.01
iMoFCFHRTTSBUkdUfY	NA	NA	-	-1.5	10	0.00075	0.015
iohWMQGvTB5.TFycp4	Pmp22	peripheral myelin protein 22	11	-1.4	11	0.00011	0.0047
Nwe5F9XgIoifI5Ih50	NA	NA	-	-1.4	9.5	0.00014	0.0056
cCS4jRkvJ6vMX33f3U	Clps	colipase, pancreatic	17	-1.4	10	0.00026	0.0081
TO5oJW4G5I5.3UFV6E	Tgm3	transglutaminase 3, E polypeptide	2	-1.4	8.5	0.00029	0.0086
fnp4j2_4XomkgU4s0o	NA	NA	-	-1.4	9.1	0.0011	0.018
N5Tu50o4njwJ33Sq9I	Il1rn	interleukin 1 receptor antagonist	2	-1.3	9.1	4.90E-06	0.00086

FeatureID - DOWN	Symbol	Description	Chromosome	LogFC	Average expression	P.value	Adj. P.value
oyruyspXqhyohXojdA	Arc	activity regulated cytoskeletal-associated protein	15	-1.3	11	6.70E-05	0.0036
9VSF3u1.lKJ3_oTx6I	Gprc5a	G protein-coupled receptor, family C, group 5, member A	6	-1.3	11	0.00034	0.0094
3UKlE.01Q2XUB0eUFU	Gprc5a	G protein-coupled receptor, family C, group 5, member A	6	-1.3	11	0.00068	0.014
EFQJikGeiMgFcoKI3o	NA	NA	-	-1.3	8.9	0.00082	0.016
lR_7U9vdC0SA0dRV0U	Myh11	myosin, heavy polypeptide 11, smooth muscle	16	-1.2	9.1	1.70E-06	0.00048
TOCqEffeel_euHoieo	Abpb	androgen binding protein beta	7	-1.2	8.5	1.00E-05	0.0012
BE4SHVJJWoX57fdh30	Sparc	secreted acidic cysteine rich glycoprotein	11	-1.2	9.2	1.50E-05	0.0015
u_6NJl1L1.UDT15UCc	Acta2	actin, alpha 2, smooth muscle, aorta	19	-1.2	11	6.20E-05	0.0034
rpxH.Tp0o9N4Kq4oul	Sprr1a	small proline-rich protein 1A	3	-1.2	9.8	9.70E-05	0.0044
redeot5Toq..0.vRik	Saa1	serum amyloid A 1	7	-1.2	11	0.00011	0.0047
fa.v5RJjovur4Hm0QU	Hist1h1c	histone cluster 1, H1c	13	-1.2	12	0.00013	0.0052
ljpCMDFREXeXStEFTU	Ctse	cathepsin E	1	-1.2	9.4	0.00026	0.0081
3ZUfZUNShFcEReAKyE	NA	NA	-	-1.2	8.6	4.00E-04	0.01
cSzkuwiSOeUE4RTXqQ	Clps	colipase, pancreatic	17	-1.2	9.4	0.00085	0.016
oQngF3r41AoTYThVQE	Cyp2c67	cytochrome P450, family 2, subfamily c, polypeptide 67	19	-1.2	8.8	0.00097	0.017
6heJwSi0U4SSeFyl6c	Aqp8	aquaporin 8	7	-1.2	9	0.0014	0.022
TCl5D5edeCtBSNp1uE	Eno3	enolase 3, beta muscle	11	-1.2	9.5	0.0033	0.036
67bSf7w6YXsrtAfuFE	Gde1	glycerophosphodiester phosphodiesterase 1	7	-1.1	11	1.80E-07	0.00018
ou9QhO3vdXIx0v8xC0	Cav1	caveolin 1, caveolae protein	6	-1.1	8.7	2.10E-06	0.00054

FeatureID - DOWN	Symbol	Description	Chromosome	LogFC	Average expression	P.value	Adj. P.value
fMrp4JTj1dTvx3Wvro	2210023 G05Rik	RIKEN cDNA 2210023G05 gene	8	-1.1	8.5	1.20E-05	0.0013
EkhUEuIODOKlKAF7m A	Dpt	dermatopontin	1	-1.1	9	2.00E-05	0.0017
9XSfVgmfn8xu7ttHgg	Hist1h1c	histone cluster 1, H1c	13	-1.1	13	4.70E-05	0.003
TpX7u2_NV_T2DArbvU	Spon2	spondin 2, extracellular matrix protein	5	-1.1	10	0.00025	0.008
oTVeKcC9RQhbYzYYq E	Epha2	Eph receptor A2	4	-1.1	8.9	0.00074	0.015
BiJeSeoo_P.oqde5Nk	Fxyd4	FXYD domain-containing ion transport regulator 4	6	-1.1	8.1	0.00089	0.016
0Z7N7bUo.nVGTSUTR 4	Ltbp4	latent transforming growth factor beta binding protein 4	7	-1	8.7	1.00E-05	0.0012
Et618unLX1HeAkCuc0	Col6a1	collagen, type VI, alpha 1	10	-1	9.1	4.20E-05	0.0028
oSE7nFfB_yV6XJBHj0	Acta2	actin, alpha 2, smooth muscle, aorta	19	-1	9.2	4.30E-05	0.0028
EyCA0hd.Xu5PnqEDl0	NA	NA	-	-1	8.9	6.10E-05	0.0034
ur.RVfd4Bko_XXwex0	Fhl1	four and a half LIM domains 1	X	-1	11	0.00068	0.014
9QNvcaVUDc16FLU.Vc	Sult1c2	sulfotransferase family, cytosolic, 1C, member 2	17	-1	10	0.002	0.026
igFCFHRTTSBUsdcfS0	NA	NA	-	-1	8.7	0.0021	0.028
0X_hee46enHqH1Po3E	Aqp8	aquaporin 8	7	-1	8.8	0.0032	0.035
iOCfnrnuuNdqnleddc	NA	NA	-	-1	8	0.0032	0.035

Table 5.5 Gene expression analysis of *Mbd2-/-* and WT CECs in colitis
Colon cells were isolated from Day6 2% DSS treated WT and *Mbd2*$^{-/-}$ mice. CECs were identified and purified by flow cytometry as described in Figure 5.3. RNA was isolated and hybridised to IlluminaMouseRef6 array. The details of significant (adj $p<0.05$) $>\pm1$ log FC genes are presented. Details of raw data processing and normalisation methods are presented in Chapter 2.16

Ontology	GO_ID	Goterm	Enrich_pValue	Symbol
Up-regulated				
BP	GO:0019882	antigen processing and presentation	2.36E-28	B2m, Cd74, H2-Aa, H2-Ab1, H2-D1, H2-DMa, H2-DMb1, H2-DMb2, H2-Eb1, H2-Eb2, H2-K1, H2-M3, H2-Q6, H2-T23, Psmb8, Psmb9, Psme1, Tap2, Tapbp, Tapbpl, Unc93b1
BP	GO:0048002	antigen processing and presentation of peptide antigen	1.84E-25	B2m, Cd74, H2-Aa, H2-Ab1, H2-D1, H2-DMa, H2-DMb1, H2-DMb2, H2-Eb1, H2-K1, H2-M3, H2-Q6, H2-T23, Tap2, Tapbp, Tapbpl, Unc93b1
BP	GO:0019884	antigen processing and presentation of exogenous antigen	1.94E-20	B2m, Cd74, H2-Aa, H2-Ab1, H2-DMa, H2-DMb1, H2-DMb2, H2-Eb1, H2-K1, H2-M3, Psme1, Tap2, Tapbp, Unc93b1
BP	GO:0002478	antigen processing and presentation of exogenous peptide antigen	3.51E-20	B2m, Cd74, H2-Aa, H2-Ab1, H2-DMa, H2-DMb1, H2-DMb2, H2-Eb1, H2-K1, H2-M3, Tap2, Tapbp, Unc93b1
CC	GO:0042611	MHC protein complex	1.78E-18	B2m, H2-Aa, H2-Ab1, H2-D1, H2-DMa, H2-DMb1, H2-DMb2, H2-Eb1, H2-Eb2, H2-K1, H2-M3, H2-Q6
BP	GO:0002376	immune system process	5.81E-18	Adora2b, B2m, Bak1, C1s, C4b, Cd274, Cd38, Cd74, Cebpa, Cfb, Ciita, Cnn2, Fcgr4, H2-Aa, H2-Ab1, H2-D1, H2-DMa, H2-DMb1, H2-DMb2, H2-Eb1, H2-Eb2, H2-K1, H2-M3, H2-Q6, H2-T23, Hspa1b, Hspd1, Ido1, Irf1, Irf7, Irf8, Irgm1, Ly6d, Oasl2, Prg2, Psmb8, Psmb9, Psme1, Ptpn6, Samhd1, Tap1, Tap2, Tapbp, Tapbpl ... and others
BP	GO:0006955	immune response	2.24E-14	Adora2b, B2m, C1s, C4b, Cd74, Cfb, Ciita, H2-Aa, H2-Ab1, H2-D1, H2-DMa, H2-DMb1, H2-Eb1, H2-K1, H2-M3, H2-Q6, H2-T23, Hspa1b, Ido1, Irf7, Irf8, Irgm1, Oasl2, Prg2, Ptpn6, Samhd1, Tap1, Tap2, Tnfsf13b, Ubd, Unc93b1
BP	GO:0002483	antigen processing and presentation of endogenous peptide antigen	5.29E-14	H2-D1, H2-K1, H2-M3, H2-T23, Tap2, Tapbp, Tapbpl
BP	GO:0019883	antigen processing and presentation of endogenous antigen	5.29E-14	H2-D1, H2-K1, H2-M3, H2-T23, Tap2, Tapbp, Tapbpl
BP	GO:0002504	antigen processing and presentation of peptide or polysaccharide antigen via MHC class II	1.83E-13	Cd74, H2-Aa, H2-Ab1, H2-DMa, H2-DMb1, H2-DMb2, H2-Eb1, H2-Eb2, Unc93b1
Down-regulated				
MF	GO:0005515	protein binding	7.10E-23	1200009O22Rik, Acta2, Actb, Actg2, Adcy4, Akap12, Aldh1a7, Amfr, Amigo3, Aoc3, Arap3, Arc, Arhgap23, Arhgdig, Baiap2, Bcl10, Bmp1, Bsdc1, Btbd7, Btc, Cav1, Ccl17, Cdh5, Cish, Cldn4, Cldn5, Clic6, Col6a1, Csrp2, Ctse, Cul3, Cxcl12, Cxcl14, Ddr1, Dennd5a, Des, Dusp6, Dysf, Ednra, Ednrb, Ehd4, Eltd1, E ... and others
CC	GO:0044421	extracellular region part	2.69E-19	Adamts2, Adamts4, Aoc3, Bmp1, Ccl17, Col12a1, Col14a1, Col16a1, Col4a2, Col4a5, Col6a1, Col6a2, Cxcl12, Cxcl14, Dkk3, Dpt, Emilin2, Entpd6, Fbln2, Fbn1, Fn1, Gdnf, Ghr, Gpc1, Hdlbp, Igf2, Igfbp7, Ihh, Il1rn, Il7, Lama2, Lamc1, Lgi4, Loxl1, Ltbp3, Ltbp4, Lum, Masp1, Mfap5, Mmrn2, Ogn, Pros1, Saa1, Se ... and others
MF	GO:0005488	binding	2.72E-16	1200009O22Rik, Acpp, Acss2, Acta2, Actb, Actg2, Adam23, Adamts2, Adamts4, Adcy4, Afg3l2, Akap12, Aldh1a7, Amfr, Amigo3, Antxr1, Anxa3, Aoc3, Arap3, Arc, Arhgap23, Arhgdig, Armcx2, Atp13a3, Atp2a3, Baiap2, Bcl10, Bmp1, Bsdc1, Btbd7, Btc, Capsl, Cav1, Ccbl1, Ccl17, Cdh5, Cish, Cldn4, Cldn5, Clic6, Col ... and others
CC	GO:0005578	proteinaceous extracellular matrix	6.72E-16	Adamts2, Adamts4, Col12a1, Col14a1, Col16a1, Col4a2, Col4a5, Col6a1, Col6a2, Dpt, Emilin2, Fbln2, Fbn1, Fn1, Gpc1, Lama2, Lamc1, Loxl1, Ltbp3, Ltbp4, Lum, Mfap5, Mmrn2, Ogn, Sparc, Spon2, Timp2, Tnc, Tnxb, Vwf
CC	GO:0031012	extracellular matrix	1.40E-15	Adamts2, Adamts4, Col12a1, Col14a1, Col16a1, Col4a2, Col4a5, Col6a1, Col6a2, Dpt, Emilin2, Fbln2, Fbn1, Fn1, Gpc1, Ihh, Lama2, Lamc1, Loxl1, Ltbp3, Ltbp4, Lum, Mfap5, Mmrn2, Ogn, Sparc, Spon2, Timp2, Tnc, Tnxb, Vwf
BP	GO:0007155	cell adhesion	1.18E-13	Adam23, Amigo3, Aoc3, Cdh5, Cldn5, Col12a1, Col14a1, Col16a1, Col6a1, Col6a2, Ddr1, Dpt, Emilin2, Eng, Esam, Fbln2, Fermt2, Fn1, Igfbp7, Ihh, Itga11, Itga5, Lama2, Lamc1, Mcam, Pcdh1, Pecam1, Rapgef1, Ror2, Sdk1, Selp, Spon2, Svep1, Tek, Thy1, Tnc, Tnxb, Vav3, Vcl, Vwf
BP	GO:0022610	biological adhesion	1.18E-13	Adam23, Amigo3, Aoc3, Cdh5, Cldn5, Col12a1, Col14a1, Col16a1, Col6a1, Col6a2, Ddr1, Dpt, Emilin2, Eng, Esam, Fbln2, Fermt2, Fn1, Igfbp7, Ihh, Itga11, Itga5, Lama2, Lamc1, Mcam, Pcdh1, Pecam1, Rapgef1, Ror2, Sdk1, Selp, Spon2, Svep1, Tek, Thy1, Tnc, Tnxb, Vav3, Vcl, Vwf
CC	GO:0005576	extracellular region	1.78E-13	Abpb, Acpp, Adam23, Adamts2, Adamts4, Aoc3, Bmp1, Btc, C4bp, Ccl17, Clps, Col12a1, Col14a1, Col16a1, Col4a2, Col4a5, Col6a1, Col6a2, Cxcl12, Cxcl14, Dkk3, Dpt, Emilin2, Enho, Entpd6, Esm1, Fbln2, Fbn1, Fn1, Fstl1, Gdnf, Ghr, Gpc1, Hdlbp, Htra1, Igf2, Igfbp7, Igsf10, Ihh, Il1rn, Il7, Lama2, Lamc1, Lg ... and others
BP	GO:0007275	multicellular organismal development	1.08E-12	Actb, Adamts2, Afg3l2, Amigo3, Ano1, Arc, Bcl10, Bmp1, Cav1, Cdh5, Cldn5, Col4a2, Csrp2, Cul3, Cxcl12, Ddr1, Des, Dkk3, Dusp6, Ednra, Ednrb, Eif2ak3, Eng, Evx1, F2r, Fbn1, Fhl2, Flt1, Fn1, Foxq1, Fzd8, Gdnf, Gja1, Hey1, Igf2, Igsf10, Ihh, Il7, Irx3, Jph2, Klf9, Krt36, Lama2, Lamc1, Lgi4, Lmna, Lor, ... and others
BP	GO:0048731	system development	1.53E-12	Actb, Adamts2, Afg3l2, Amigo3, Ano1, Arc, Bcl10, Bmp1, Cav1, Cdh5, Cldn5, Col4a2, Cxcl12, Ddr1, Des, Dusp6, Ednra, Ednrb, Eif2ak3, Eng, Evx1, F2r, Fbn1, Fhl2, Flt1, Fn1, Foxq1, Fzd8, Gdnf, Gja1, Hey1, Igf2, Igsf10, Ihh, Il7, Irx3, Krt36, Lamc1, Lgi4, Lmna, Lor, Ltbp3, Meis1, Napa, Ndn, Nefm, Nos3, N ... and others

Table 5.6 Gene ontology analysis of *Mbd2-/-* and WT CECs in colitis

Colon cells were isolated from Day6 2% DSS treated WT and *Mbd2*$^{-/-}$ mice. CECs were identified and purified by flow cytometry as described in Figure 5.3. RNA was isolated and hybridised to IlluminaMouseRef6 array. The details of significant (adj p<0.05) pathways by GOterm analysis are presented. Details of raw data processing and normalisation methods are presented in Chapter 2.16

PathID	PathDescr.	pValue	Symbol	Number of significant genes	% of pathway significant
Up-regulated					
4612	Antigen processing and presentation	1.87E-25	B2m, Calr, Cd74, Ciita, H2-Aa, H2-Ab1, H2-D1, H2-DMa, H2-DMb1, H2-DMb2, H2-Eb1, H2-K1, H2-M3, H2-Q2, H2-Q6, H2-Q7, H2-Q8, H2-T10, H2-T23, Hspa1a, Hspa1b, Psme1, Tap1, Tap2, Tapbp	25	49
4940	Type I diabetes mellitus	8.56E-15	H2-Aa, H2-Ab1, H2-D1, H2-DMa, H2-DMb1, H2-DMb2, H2-Eb1, H2-K1, H2-M3, H2-Q2, H2-Q6, H2-Q7, H2-Q8, H2-T10, H2-T23, Hspd1	16	58
5330	Allograft rejection	2.72E-14	H2-Aa, H2-Ab1, H2-D1, H2-DMa, H2-DMb1, H2-DMb2, H2-Eb1, H2-K1, H2-M3, H2-Q2, H2-Q6, H2-Q7, H2-Q8, H2-T10, H2-T23	15	58
5332	Graft-versus-host disease	4.77E-14	H2-Aa, H2-Ab1, H2-D1, H2-DMa, H2-DMb1, H2-DMb2, H2-Eb1, H2-K1, H2-M3, H2-Q2, H2-Q6, H2-Q7, H2-Q8, H2-T10, H2-T23	15	56
5416	Viral myocarditis	2.12E-13	Ccnd1, H2-Aa, H2-Ab1, H2-D1, H2-DMa, H2-DMb1, H2-DMb2, H2-Eb1, H2-K1, H2-M3, H2-Q2, H2-Q6, H2-Q7, H2-Q8, H2-T10, H2-T23, Rac3	17	36
5320	Autoimmune thyroid disease	1.14E-12	H2-Aa, H2-Ab1, H2-D1, H2-DMa, H2-DMb1, H2-DMb2, H2-Eb1, H2-K1, H2-M3, H2-Q2, H2-Q6, H2-Q7, H2-Q8, H2-T10, H2-T23	15	52
4145	Phagosome	8.03E-12	Calr, Cyba, Fcgr4, H2-Aa, H2-Ab1, H2-D1, H2-DMa, H2-DMb1, H2-DMb2, H2-Eb1, H2-K1, H2-M3, H2-Q2, H2-Q6, H2-Q7, H2-Q8, H2-T10, H2-T23, Tap1, Tap2	20	19
4514	Cell adhesion molecules (CAMs)	9.39E-10	Cd274, Cldn10a, H2-Aa, H2-Ab1, H2-D1, H2-DMa, H2-DMb1, H2-DMb2, H2-Eb1, H2-K1, H2-M3, H2-Q2, H2-Q6, H2-Q7, H2-Q8, H2-T10, H2-T23	17	21
5140	Leishmaniasis	1.44E-08	Cyba, Fcgr4, H2-Aa, H2-Ab1, H2-DMa, H2-DMb1, H2-DMb2, H2-Eb1, Nos2, Ptpn6, Stat1	11	22
5310	Asthma	4.21E-07	H2-Aa, H2-Ab1, H2-DMa, H2-DMb1, H2-DMb2, H2-Eb1, Prg2	7	47
Down-regulated					
4510	Focal adhesion	2.03E-09	Actb, Cav1, Col4a2, Col6a1, Col6a2, Flna, Flnc, Flt1, Fn1, Itga11, Itga5, Lama2, Lamc1, Pik3r3, Rapgef1, Tnc, Tnxb, Vav3, Vcl, Vwf	20	14
4512	ECM-receptor interaction	8.15E-08	Col4a2, Col6a1, Col6a2, Fn1, Itga11, Itga5, Lama2, Lamc1, Sdc2, Tnc, Tnxb, Vwf	12	24
4670	Leukocyte transendothelial migration	4.10E-06	Actb, Cdh5, Cldn4, Cldn5, Cxcl12, Esam, Msn, Pecam1, Pik3r3, Thy1, Vav3, Vcl	12	14
5412	Arrhythmogenic right ventricular cardiomyopathy (ARVC)	6.91E-04	Actb, Des, Gja1, Itga11, Itga5, Lama2, Lmna	7	17
4270	Vascular smooth muscle contraction	8.45E-04	Acta2, Actg2, Adcy4, Ednra, Gucy1a3, Gucy1b3, Mrvi1, Myh11, Prkg1	9	12
5222	Small cell lung cancer	1.96E-03	Col4a2, Fn1, Lama2, Lamc1, Pias3, Pik3r3, Traf4	7	10
5414	Dilated cardiomyopathy	2.23E-03	Actb, Adcy4, Des, Itga11, Itga5, Lama2, Lmna	7	14
5100	Bacterial invasion of epithelial cells	2.78E-03	Actb, Cav1, Fn1, Itga5, Pik3r3, Vcl	6	11
360	Phenylalanine metabolism	3.90E-03	Aoc3, Ddc, Maob	3	25
4610	Complement and coagulation cascades	4.22E-03	C4bp, F2r, Masp1, Pros1, Thbd, Vwf	6	15

Table 5.7 Gene pathway analysis of *Mbd2*$^{-/-}$ and WT CECs in colitis

Colon cells were isolated from Day6 2% DSS treated WT and *Mbd2*$^{-/-}$ mice. CECs were identified and purified by flow cytometry as described in Figure 5.3. RNA was isolated and hybridised to IlluminaMouseRef6 array. The details of significant (adj p<0.05) pathways by KEGG analysis are presented. Details of raw data processing and normalisation methods are presented in Chapter 2.16

	Cage 1						Cage 2			Cage 3		
Age / weeks	26	24	26	26	26	24	30	30	20	27	27	27
Genotype	WT	WT	WT	*Mbd2*$^{-/-}$	*Mbd2*$^{-/-}$	*Mbd2*$^{-/-}$	WT	*Mbd2*$^{-/-}$	*Mbd2*$^{-/-}$	WT	WT	*Mbd2*$^{-/-}$
Sample Number	1	2	3	7	8	9	4	10	11	5	6	12

Table 5.8 Co-housing and age of mice used in 16S analysis

Mice details for samples submitted for 16S sequencing detailing co-habitation and age.

ID	Difference from Mean as in Square root of Proportion	Mean as in Square root of proportion in WT	t	P.Value	adj.P.Value	B
Clostridiales|Peptococcaceae|Peptococcus	0.008934	0.0149686	7.303	1.77E-05	0.002992	1.1
Bacteroidales|Porphyromonadaceae|Parabacteroides	-0.027589	0.0368588	-4.95	4.70E-04	0.039727	-2.405
Clostridiales|Lachnospiraceae|Roseburia	0.051624	0.0586216	4.621	7.91E-04	0.040244	-2.954
Clostridiales|Lachnospiraceae|Clostridium_sp._Culture-54	0.007591	0.0135731	4.505	9.53E-04	0.040244	-3.15
Clostridiales|Lachnospiraceae|Clostridium_sp._Culture-27	0.02823	0.0564603	3.734	3.45E-03	0.097824	-4.492
Gastranaerophilales|uncultured_bacterium|unclassified	-0.052159	0.1332211	-3.73	3.47E-03	0.097824	-4.501
Bacteroidales|S24-7|unidentified	0.020429	0.0342675	2.906	1.47E-02	0.353854	-5.971
Pasteurellales|Pasteurellaceae|unclassified	-0.003031	0.0015157	-2.663	2.25E-02	0.452307	-6.399
Clostridiales|Lachnospiraceae|uncultured_bacterium	0.028368	0.0556957	2.595	2.54E-02	0.452307	-6.518
Bacteroidales|Rikenellaceae|RC9_gut_group	-0.050238	0.1173271	-2.558	2.71E-02	0.452307	-6.584
Bacteroidales|Prevotellaceae|unclassified	-0.003761	0.0045975	-2.477	3.13E-02	0.452307	-6.724
Caulobacterales|Caulobacteraceae|Brevundimonas	0.001638	0.0012987	2.426	3.42E-02	0.452307	-6.811
Bacteroidales|Rikenellaceae|Rikenella	-0.042419	0.0910912	-2.416	3.48E-02	0.452307	-6.828
Clostridiales|Lachnospiraceae|mouse_gut_metagenome	0.011745	0.0393168	2.333	4.02E-02	0.485639	-6.969
Bacteroidales|Prevotellaceae|uncultured_Bacteroidales_bacterium	-0.059068	0.146154	-2.197	5.09E-02	0.556815	-7.196
Gastranaerophilales|unclassified|unclassified	-0.003479	0.0178269	-2.159	5.44E-02	0.556815	-7.259
Bacteroidales|S24-7|mouse_gut_metagenome	0.004141	0.0208741	2.142	5.60E-02	0.556815	-7.287
Erysipelotrichales|Erysipelotrichaceae|uncultured_bacterium	0.001158	0.0005791	2.072	6.32E-02	0.579426	-7.401
Erysipelotrichales|Erysipelotrichaceae|unidentified	-0.005837	0.0059058	-2.054	6.51E-02	0.579426	-7.43
Clostridiales|Defluviitaleaceae|uncultured_bacterium	0.024739	0.0444072	1.975	7.46E-02	0.610289	-7.557
Sphingomonadales|Sphingomonadaceae|Sphingomonas	-0.001357	0.0006785	-1.965	7.58E-02	0.610289	-7.572
Bacillales|Staphylococcaceae|Staphylococcus	-0.006608	0.0036432	-1.927	8.09E-02	0.621482	-7.632
Clostridiales|vadinBB60|Clostridiales_bacterium_enrichment_culture_clone_06-1235251-76	-0.002483	0.0021681	-1.898	8.50E-02	0.624366	-7.678
Clostridiales|Family_XIII|Incertae_Sedis	-0.001411	0.0075553	-1.837	9.41E-02	0.662242	-7.771
Bacteroidales|Bacteroidaceae|Bacteroides	-0.042867	0.0958886	-1.754	1.08E-01	0.66459	-7.896
Clostridiales|Lachnospiraceae|unclassified	0.041704	0.236057	1.731	1.12E-01	0.66459	-7.93
Verrucomicrobiales|Verrucomicrobiaceae|Akkermansia	-0.02142	0.0142595	-1.727	1.13E-01	0.66459	-7.936
Clostridiales|vadinBB60|uncultured_bacterium	-0.063125	0.2081455	-1.72	1.14E-01	0.66459	-7.946
Enterobacteriales|Enterobacteriaceae|Escherichia-Shigella	-0.025335	0.0151389	-1.72	1.14E-01	0.66459	-7.946
Anaeroplasmatales|Anaeroplasmataceae|Anaeroplasma	0.071428	0.053763	1.67	1.24E-01	0.697641	-8.02

Table 5.9 OTU classification of 16S sequencing in *Mbd2-/-* and WT microbiome

OTU classification of bacteria identified from 16S sequencing of naïve WT and *Mbd2*$^{-/-}$ colon faeces. Order, family and genus data are detailed above for the top 30 most significant organisms that were differentially present. Those organisms that reached statistical signficance ($p<0.05$) after adjustment for multiple testing are shaded in grey.

FeatureID - UP	Symbol	Description	Chromosome	logFC	Average Expression	P.Value	adj.P.Val
9gVNx5flW5.e6SftCI	Reg3b	regenerating islet-derived 3 beta	6	4.3	13	8.50E-08	1.00E-04
6PsHyLxXO3kD0KXIsQ	Reg3g	regenerating islet-derived 3 gamma	6	3.9	11	3.20E-07	0.00017
uXO3kD8evAfNISQE1Y	Reg3b	regenerating islet-derived 3 beta	6	2.8	9.5	6.30E-06	7.00E-04
uVHjLVKgZkOdf4t.ro	Retnlb	resistin like beta	16	2.7	13	0.00019	0.0051
ZnfeL6Xy7JCdR9zSpE	Ido1	indoleamine 2,3-dioxygenase 1	8	2.6	9.7	8.70E-05	0.0031
6lQuzX65.5cUyV93cU	NA	NA	-	2.5	12	0.0023	0.023
Wb00ovLP3HPue3uup0	AI747448	expressed sequence AI747448	3	2.2	8.9	5.50E-07	0.00024
WVekdcflECyX9.y9Uk	Serpina3n	serine (or cysteine) peptidase inhibitor, clade A, member 3N	12	2.2	9.1	2.40E-06	0.00044
NsTpyScXhXhJCJOoCk	NA	NA	-	2.2	10	0.0043	0.034
6nThXopESUkS4IpIPU	Ly6a	lymphocyte antigen 6 complex, locus A	15	2.1	13	1.80E-07	0.00012
xNbt9cCzqeh79w5fVQ	Il1b	interleukin 1 beta	2	2.1	9.3	8.20E-07	0.00028
BtF7vMrHdpfTTlSUxs	Gbp2	guanylate binding protein 2	3	2.1	9.6	0.00019	0.0051
B_Ieu3v021ShGkDgtI	Cd74	CD74 antigen (invariant polypeptide of major histocompatibility complex, class II antigen-associated)	18	2	12	1.60E-05	0.0012
9VUpRfu.N6f4Rt79Ko	Lrg1	leucine-rich alpha-2-glycoprotein 1	17	2	9	0.00011	0.0037
9EgooZ6KI_enFnNwKg	Cd74	CD74 antigen (invariant polypeptide of major histocompatibility complex, class II antigen-associated)	18	1.9	12	1.00E-05	0.00092
r3SHsIXg7d51g9eHII	H2-Ab1	histocompatibility 2, class II antigen A, beta 1	17	1.8	12	0.00037	0.0074
rKeXSrf.nyJXJy0cgI	Igtp	interferon gamma induced GTPase	11	1.8	9.7	0.00088	0.013
WSiA5QRfztV0kiumJw	Mgp	matrix Gla protein	6	1.7	9.5	8.70E-07	0.00029
ivVLtOKT0oocuJ7l7U	Lyz1	lysozyme 1	10	1.7	11	1.90E-06	0.00039
Heee6fErII7hNSOHS0	NA	NA	-	1.7	9.3	0.0051	0.038
HqENS6t697hDu5zjIM	Col18a1	collagen, type XVIII, alpha 1	10	1.6	9.1	2.10E-06	0.00041

FeatureID - UP	Symbol	Description	Chromosome	logFC	Average Expression	P.Value	adj.P.Val
BqpFU7l.nciDo.dKlE	Duoxa2	dual oxidase maturation factor 2	2	1.6	10	8.30E-05	0.0031
fEUuCulnqhCJBiANE4	Lgals2	lectin, galactose-binding, soluble 2	15	1.6	9.4	0.00044	0.0084
Bid7Ewz7q321rb3t78	Osr2	odd-skipped related 2 (Drosophila)	15	1.5	11	3.70E-07	0.00019
ruyFURILq0uLE6I1_E	Ccl8	chemokine (C-C motif) ligand 8	11	1.5	8.2	5.70E-07	0.00024
ERRMThZ0RsFBEqD7Ko	Sulf2	sulfatase 2	2	1.5	9.2	5.20E-06	0.00063
BvVHsXu0_fuzh_ggqU	Laptm5	lysosomal-associated protein transmembrane 5	4	1.5	9.5	6.90E-06	0.00074
BaU2202_3uU8jjuI7c	Ifitm1	interferon induced transmembrane protein 1	7	1.5	9.2	9.30E-06	0.00088
QJOz4gwIRe2XQgeVGU	Defb37	defensin beta 37	8	1.5	9.4	1.50E-05	0.0011
xjhH3NJ0HQJexIcZKI	Ifi27l2a	interferon, alpha-inducible protein 27 like 2A	12	1.5	9.1	1.90E-05	0.0013
E_oQxIgjybpV5kKOEY	Med23	mediator complex subunit 23	10	1.5	11	0.00012	0.0039
Q6dJPRY38qA576IkDA	Slpi	secretory leukocyte peptidase inhibitor	2	1.5	9.1	0.00012	0.0039
Hleeu5Q0qNcE0qIofU	Ly6c1	lymphocyte antigen 6 complex, locus C1	15	1.5	9.7	0.00019	0.005
ffRHwyKPWH1rXgufRU	Ifitm3	interferon induced transmembrane protein 3	7	1.5	11	2.00E-04	0.0051
TUi_l9IF1Rsn9iFOo8	Cxcl9	chemokine (C-X-C motif) ligand 9	5	1.5	8.7	0.0011	0.014
EefYPXh5S3F5R1h0i0	LOC641240	similar to H-2 class II histocompatibility antigen, A-D beta chain precursor	Un	1.5	11	0.0011	0.015
K6d3nSiUvVKe_4dKDc	NA	NA	-	1.5	9.2	0.0043	0.034
WoKLuTvRNP._wkWKIs	Cxcl2	chemokine (C-X-C motif) ligand 2	5	1.4	8.6	1.00E-07	0.00011
BFFI4IH5KM0EdyC6as	Lgals9	lectin, galactose binding, soluble 9	11	1.4	9.9	4.30E-07	0.00021
ct6oCNE6tir93HrSjk	Icam1	intercellular adhesion molecule 1	9	1.4	9.5	2.50E-06	0.00046
EqEqVN.rSrPa01hDl8	Igfbp4	insulin-like growth factor binding protein 4	11	1.4	9.1	2.80E-06	0.00046
Kqk9Eg3Ouvzr7VB4cQ	C3	complement component 3	17	1.4	9.4	9.20E-06	0.00088
Kt1OU4ATtefpUTV1Ig	H2-Eb1	histocompatibility 2, class II antigen E beta	17	1.4	11	0.0012	0.015
cB.egUgpa5jqQK4DO4	Psmb9	proteasome (prosome, macropain) subunit, beta type 9 (large multifunctional peptidase 2)	17	1.4	11	0.0014	0.017
6eLeXokA74mk2qnm58	H2-Ab1	histocompatibility 2, class II antigen A, beta 1	17	1.4	11	0.0026	0.025
IN9qlC606bx6N7muWc	Psmb8	proteasome (prosome, macropain) subunit, beta type 8 (large multifunctional peptidase 7)	17	1.4	11	0.0028	0.026

FeatureID - UP	Symbol	Description	Chromosome	logFC	Average Expression	P.Value	adj.P.Val
07p8SOUjuE1I4dLdSU	NA	NA	-	1.4	8.8	0.0049	0.037
Ie.det23Z2oSIb0Ch4	Cxcl1	chemokine (C-X-C motif) ligand 1	5	1.3	11	1.60E-07	0.00012
ZOkieX1t3_LUI0VC14	C4a	complement component 4A (Rodgers blood group)	17	1.3	8.8	6.10E-07	0.00024
IW2Yr78iySR1M5K0gY	Vcam1	vascular cell adhesion molecule 1	3	1.3	8.5	1.40E-06	0.00034
ZSBIbn6eT3.VH3D3dY	Fcer1g	Fc receptor, IgE, high affinity I, gamma polypeptide	1	1.3	8.2	3.90E-06	0.00054
QdyAlERxVfUBSTucjU	Osr2	odd-skipped related 2 (Drosophila)	15	1.3	11	4.50E-06	0.00058
BE4SHVJJWoX57fdh30	Sparc	secreted acidic cysteine rich glycoprotein	11	1.3	9.2	7.20E-06	0.00076
uOnpxzotJelh6u78nQ	Lyz2	lysozyme 2	10	1.3	8.9	2.40E-05	0.0014
xQnq69GtQdEpAionIA	Ccl21c	chemokine (C-C motif) ligand 21C (leucine)	4	1.3	10	1.00E-04	0.0035
iNE3kaU1f3xemieX1c	Ccl21a	chemokine (C-C motif) ligand 21A (serine)	4	1.3	9.9	0.00013	0.0039
oeD.v97TfULxNx5Id0	H2-Aa	histocompatibility 2, class II antigen A, alpha	17	1.3	11	0.0024	0.023
Tih0InhS.IDi6paLpA	Saa3	serum amyloid A 3	7	1.3	8.4	0.0067	0.044
xUX6XTSnd64gelNodE	Hoxb6	homeobox B6	11	1.2	9	1.80E-08	9.80E-05
3Xo_KI5fSBA7kIkVlM	C4a	complement component 4A (Rodgers blood group)	17	1.2	8.7	6.80E-07	0.00026
f1F4FVv0OlOe_1gEdI	Lgals9	lectin, galactose binding, soluble 9	11	1.2	9.5	1.00E-06	3.00E-04
I15UCh2r7eE2eTjk3Q	Mmp2	matrix metallopeptidase 2	8	1.2	8.8	1.10E-06	3.00E-04
raaDor6gjp9MCC.gVA	Bcl2a1d	B-cell leukemia/lymphoma 2 related protein A1d	9	1.2	8.4	1.20E-06	0.00031
3SROHnFKKewVH1kRHk	Lgmn	legumain	12	1.2	9.9	9.20E-06	0.00088
HnElNcHl0g0dC99R2s	Ccl9	chemokine (C-C motif) ligand 9	11	1.2	11	2.40E-05	0.0014
Z1tRFflefQU8TeRpTU	LOC100041504	similar to beta chemokine Exodus-2	Un	1.2	9.3	6.60E-05	0.0027
Z9bVC5hiBrBz_UdS5Q	Cd74	CD74 antigen (invariant polypeptide of major histocompatibility complex, class II antigen-associated)	18	1.2	9.5	0.0024	0.024
xwCdl4r7O760SrN0Xo	Irgm2	immunity-related GTPase family M member 2	11	1.2	9.6	0.0034	0.029
QRKIOjGmg6K_oI6fTA	Bcl2a1b	B-cell leukemia/lymphoma 2 related protein A1b	9	1.1	8.3	2.20E-07	0.00014
xoLeZ4JU0gurYopzJM	Ccl7	chemokine (C-C motif) ligand 7	11	1.1	8.7	7.50E-07	0.00027
3Cvp1fJdIqDeXRxedQ	Irf1	interferon regulatory factor 1	11	1.1	11	1.30E-06	0.00033

FeatureID - UP	Symbol	Description	Chromosome	logFC	Average Expression	P.Value	adj.P.Val
uoJ_A01eYlzXlRu_l0	Cxcl10	chemokine (C-X-C motif) ligand 10	5	1.1	9.2	7.10E-06	0.00075
Zd76F9Mlobr0l7nUgk	Sfrp1	secreted frizzled-related protein 1	8	1.1	8.5	1.40E-05	0.0011
TFB6nf7v0L46eeyLpk	Fbln1	fibulin 1	15	1.1	9.8	5.10E-05	0.0024
KRHB3iEjiXs0kDBRKl	Lyz2	lysozyme 2	10	1.1	8.7	8.20E-05	0.0031
ck.Bu95.ESKNkW4luc	Tgm2	transglutaminase 2, C polypeptide	2	1.1	11	9.20E-05	0.0033
cqKQLRTR_QpCUlTwQs	Igk-V38	immunoglobulin kappa chain variable 38(V38)	6	1.1	7.8	0.00019	0.0051
9LJWXolSiNVRgfQnq4	Ccl21c	chemokine (C-C motif) ligand 21C (leucine)	4	1.1	9.5	0.00041	0.008
3wBQxudRhB1XAuRKpI	2210407C18 Rik	RIKEN cDNA 2210407C18 gene	11	1.1	11	6.00E-04	0.01
ioyxL0hCHX0j1iGXFo	Igfbp5	insulin-like growth factor binding protein 5	1	1.1	9.1	0.00063	0.01
6pfudyDrFDUs0OzhC4	Oasl2	2-5 oligoadenylate synthetase-like 2	5	1.1	8.7	0.0012	0.015
TV3ljxxTk4Pv.50xXs	Ifi47	interferon gamma inducible protein 47	11	1.1	9	0.002	0.021
r313nVlhbnSuHj33Qo	H2-DMa	histocompatibility 2, class II, locus DMa	17	1.1	9.6	0.003	0.027
3GtcKjKJ7eyg7gEtGU	Ccl7	chemokine (C-C motif) ligand 7	11	1	8.4	8.30E-08	1.00E-04
coleKNRyfebeuT.p54	Hoxb7	homeobox B7	11	1	9.9	4.90E-06	0.00061
QVxXzF1zVlN3FVepP8	Igfbp4	insulin-like growth factor binding protein 4	11	1	9	1.30E-05	0.001
BjJ4nR4VP1FQo5OS7k	Col4a2	collagen, type IV, alpha 2	8	1	8.6	1.30E-05	0.0011
6IIz9S324Rqh0u_eoQ	Pdpn	podoplanin	4	1	8.6	1.60E-05	0.0012
KVOiOtRT5793nPujOE	Ccl4	chemokine (C-C motif) ligand 4	11	1	8	2.20E-05	0.0014
lVfl9XFpT9fydXQp34	Gpx2	glutathione peroxidase 2	12	1	14	2.40E-05	0.0014
THnlFNLJilTVBUagq8	Cd52	CD52 antigen	4	1	8.3	4.80E-05	0.0023
EkhUEuIODOKlKAF7mA	Dpt	dermatopontin	1	1	9	9.50E-05	0.0033
ih4OHh9WxhJQpf7yXU	Col4a1	collagen, type IV, alpha 1	8	1	9.2	8.00E-04	0.012
TetXvQxHfTgfeeXqfY	Ifitm1	interferon induced transmembrane protein 1	7	1	12	0.001	0.014
xPHsndzLvG9IRbJ3tc	Igfbp5	insulin-like growth factor binding protein 5	1	1	9.4	0.0017	0.019
35J04IiirnFqU6yKd8	Tap1	transporter 1, ATP-binding cassette, sub-family B (MDR/TAP)	17	1	8.8	0.0021	0.022

ZVY7oInadd.JP_sfCg	Igfbp5	insulin-like growth factor binding protein 5	1	1	9.6	0.0036	0.03
FeatureID - DOWN	**Symbol**	**Description**	**Chromosome**	**logFC**	**Average Expression**	**P.Value**	**adj.P.Val**
9SOoAB9VkX3lJ016FU	Eef2	eukaryotic translation elongation factor 2	10	-1.9	10	0.00086	0.013
HAfVZF95SdNehVN9Cs	Eef2	eukaryotic translation elongation factor 2	10	-1.9	11	0.0023	0.023
6tTWtCdx5ehd7sRzQ8	Rasd2	RASD family, member 2	8	-1.7	9.1	1.50E-07	0.00012
6enl5KoZXXkjjRTUfE	Eef2	eukaryotic translation elongation factor 2	10	-1.7	10	0.0022	0.023
ihawfn4vVODI.iHg6Q	Col8a1	collagen, type VIII, alpha 1	16	-1.6	8.2	1.00E-06	3.00E-04
K0diUkUW90ZXieSEnI	Tsc22d1	TSC22 domain family, member 1	14	-1.6	9.9	0.00015	0.0043
N1IGJElsKkNFFn00WI	St6galnac6	ST6 (alpha-N-acetyl-neuraminyl-2,3-beta-galactosyl-1,3)-N-acetylgalactosaminide alpha-2,6-sialyltransferase 6	2	-1.6	8.4	0.00016	0.0046
EFQJikGeiMgFcoKI3o	NA	NA	-	-1.6	8.9	0.00032	0.0068
oQngF3r41AoTYThVQE	Cyp2c67	cytochrome P450, family 2, subfamily c, polypeptide 67	19	-1.5	8.8	0.00016	0.0045
TfncwFu8knSgjluCT0	Ttr	transthyretin	18	-1.4	11	3.60E-06	0.00052
iTXoYS6cbi5cQAZKRc	Tppp3	tubulin polymerization-promoting protein family member 3	8	-1.4	9.2	6.70E-05	0.0027
lJr0oU0fUnHNmqdOk0	Rab1b	RAB1B, member RAS oncogene family	19	-1.4	9.1	0.00014	0.0041
HEAUL0RDN.UYNSV9Ao	Gm4415	predicted gene 4415	2	-1.4	8.3	0.00031	0.0067
fhAFC9EQzf1GDUlfQo	NA	NA	-	-1.4	8.5	0.00041	0.008
ZOpRruKB66ImylyJYQ	Muc3	mucin 3, intestinal	5	-1.4	11	0.0023	0.023
31arccf58070eQqKQY	Col8a1	collagen, type VIII, alpha 1	16	-1.2	7.8	1.20E-06	0.00031
HXcU0UY4CC97cy30ec	Ctse	cathepsin E	1	-1.2	8.9	8.80E-05	0.0032
HyC4SG3Ek9Sc407494	Hexb	hexosaminidase B	13	-1.2	10	0.00011	0.0036
iUeo9LJRLUC1EB0e7g	Fam55b	family with sequence similarity 55, member B	9	-1.2	9.7	0.00021	0.0053
BVdLuiDko.kJFaAkH8	Adh1	alcohol dehydrogenase 1 (class I)	3	-1.2	12	0.00089	0.013
rJ0tKx6QhJRP5z9TXk	Eif4a2	eukaryotic translation initiation factor 4A2	16	-1.2	9.9	0.00099	0.014
3VAmKQZ6IyAVyiI3oE	NA	NA	-	-1.2	8.2	0.001	0.014
iOCfnrnuuNdqnIeddc	NA	NA	-	-1.2	8	0.0017	0.019

FeatureID - DOWN	Symbol	Description	Chromosome	logFC	Average Expression	P.Value	adj.P.Val
3Lh3rPL.u80vw578eA	Nov	nephroblastoma overexpressed gene	15	-1.1	7.8	4.50E-08	9.80E-05
K27KzVK44qPqgU6lyU	Ramp1	receptor (calcitonin) activity modifying protein 1	1	-1.1	11	1.70E-07	0.00012
WCgvoIO7ngt0.ndI.s	NA	NA	-	-1.1	8	9.80E-07	3.00E-04
KTMxMe67XC58qnv7As	Fam134b	family with sequence similarity 134, member B	15	-1.1	10	1.20E-06	0.00031
6lUEtfxHHGoOUU7f44	St3gal6	ST3 beta-galactoside alpha-2,3-sialyltransferase 6	16	-1.1	11	1.50E-05	0.0011
iPCh1ehhSjhddodjl0	Cyr61	cysteine rich protein 61	3	-1.1	10	2.40E-05	0.0014
cJIQ9KC1CqAe1N5Xk4	Gm1123	predicted gene 1123	9	-1.1	11	3.50E-05	0.0018
Nj3O4VCCzzEot3UAF0	Fam55b	family with sequence similarity 55, member B	9	-1.1	8.1	4.30E-05	0.0021
96A_lzFKl2DVIbJ5Hs	Atp6ap2	ATPase, H+ transporting, lysosomal accessory protein 2	X	-1.1	9.2	0.00011	0.0037
9VdLh1xI_NS.R.R6p0	Car2	carbonic anhydrase 2	3	-1.1	11	0.00022	0.0054
crVPTDIL8JXcV0APiE	Hao2	hydroxyacid oxidase 2	3	-1.1	11	0.00078	0.012
r02ll_EU4feV54nlOQ	Adh1	alcohol dehydrogenase 1 (class I)	3	-1.1	13	0.0023	0.023
Q5SVKccxWlBd0PNMjo	NA	NA	-	-1.1	9.7	0.0026	0.025
ul5J6ij4._ip17k2eg	Fxyd4	FXYD domain-containing ion transport regulator 4	6	-1.1	8.5	0.0033	0.029
fgdoF.6XE6qJuT.tMl	Ugt1a7c	UDP glucuronosyltransferase 1 family, polypeptide A7C	1	-1.1	9.6	0.0038	0.031

Table 5.10 Gene expression analysis of naïve versus colitic WT CECs

Naive or day 6 2% DSS treated colon cells were isolated from WT mice. CECs were identified and purified by flow cytometry as described in Figure 5.3. RNA was isolated and hybridised to IlluminaMouseRef6 array. The details of significant (adj $p<0.05$) $>\pm1$ log FC genes are presented comparing DSS treated to non treated samples. Details of raw data processing and normalisation methods are presented in Chapter 2.16

PathID	PathDescr.	pValue	Symbol	Number of significant genes
Up-regulated				
4060	Cytokine-cytokine receptor interaction	2.37E-11	Ccl11, Ccl17, Ccl2, Ccl21a, Ccl21c, Ccl3, Ccl4, Ccl7, Ccl8, Ccl9, Ccr7, Cd40, Csf1, Csf1r, Csf2rb2, Cxcl1, Cxcl10, Cxcl14, Cxcl2, Flt1, Ifnar2, Il10, Il11, Il1b, Il1r2, Il4ra, Il6, Il6st, Lif, Osmr, Pdgfb, Pdgfra, Tgfb1, Tnf, Tnfrsf1b	35
4062	Chemokine signaling pathway	4.34E-08	Adcy4, Arrb2, Ccl11, Ccl17, Ccl2, Ccl21a, Ccl21c, Ccl3, Ccl4, Ccl7, Ccl8, Ccl9, Ccr7, Cxcl1, Cxcl10, Cxcl14, Cxcl2, Gnai2, Itk, Jak3, Nfkb1, Prex1, Stat3, Vav2, Was	25
5322	Systemic lupus erythematosus	2.19E-06	C1qa, C1qb, C1qc, C3, C4b, Cd40, Cd86, Fcgr2b, Fcgr4, H2-Ab1, Hist1h2ab, Hist1h3a, Hist1h3c, Hist1h3d, Hist1h3e, Hist1h3h, Hist2h4, Il10, Tnf	19
4620	Toll-like receptor signaling pathway	2.78E-06	Ccl3, Ccl4, Cd40, Cd86, Ctsk, Cxcl10, Ifnar2, Il1b, Il6, Irf5, Lbp, Map2k4, Nfkb1, Tlr4, Tnf, Traf3	16
4512	ECM-receptor interaction	4.25E-06	Cd44, Col4a2, Col5a1, Col6a1, Col6a2, Fn1, Gp1bb, Hspg2, Itga5, Itgav, Itgb7, Lama2, Lamc1, Tnc	14
Down-regulated				
4142	Lysosome	1.97E-06	Acp5, Ap1s3, Cln3, Clta, Ctse, Ctsh, Gaa, Glb1, Hexb, Laptm4b, Naglu, Npc2	12
1100	Metabolic pathways	2.78E-06	Abat, Acsl1, Acss2, Asah2, Atp5f1, Atp6v0e2, Ccbl1, Chka, Chpt1, Csad, Ddc, Dtymk, Gaa, Ganc, Glb1, Glul, Hadh, Hexb, Hpd, Hsd3b2, Man2a1, Mat2a, Mccc1, Mdh1, Mecr, Naglu, Nme7, Papss1, Pcca, Pck1, Pdhb, Pfkm, Ppap2a, Sdhb, Smpd2, St3gal6, St6galnac4, St6galnac6, Suclg1, Trit1, Upb1	41
604	Glycosphingolipid biosynthesis - ganglio series	1.27E-04	Glb1, Hexb, St6galnac4, St6galnac6	4
20	Citrate cycle (TCA cycle)	2.23E-04	Mdh1, Pck1, Pdhb, Sdhb, Suclg1	5
600	Sphingolipid metabolism	7.58E-04	Asah2, Glb1, Neu2, Ppap2a, Smpd2	5

Table 5.11 Gene ontology analysis of naïve versus colitic WT CECs

Colon cells were isolated from Day6 Naive or 2% DSS treated WT mice. CECs were identified and purified by flow cytometry as described in Figure 5.3. RNA was isolated and hybridised to IlluminaMouseRef6 array. The details of significant (adj $p<0.05$) pathways by KEGG analysis are presented. Details of raw data processing and normalisation methods are presented in Chapter 2.16

Ontology	GO_ID	Goterm	Enrich_pValue	Symbol
Up-regulated				
CC	GO:0044421	extracellular region part	2.90E-32	Abi3bp, Adamts2, Adamts4, Alpl, Anxa2, Apoe, Bgn, Bmp1, C1qb, C3, Ccdc80, Ccl11, Ccl17, Ccl2, Ccl3, Ccl4, Ccl7, Ccl8, Ccl9, Col14a1, Col18a1, Col4a2, Col4a5, Col5a1, Col6a1, Col6a2, Cpxm1, Crispld2, Csf1, Ctsk, Cxcl1, Cxcl10, Cxcl14, Cxcl2, Dcn, Dkk3, Dpt, Ecm1, Efemp2, Emilin2, Entpd6, Fbln1, Fbln2 ... and others
CC	GO:0005576	extracellular region	2.04E-31	Abi3bp, Adam23, Adamts2, Adamts4, Aebp1, Alpl, Anxa2, Apoe, BC028528, Bgn, Bmp1, C1qa, C1qb, C1qc, C3, C4b, Capg, Ccdc80, Ccl11, Ccl17, Ccl2, Ccl3, Ccl4, Ccl7, Ccl8, Ccl9, Cd40, Cfp, Col14a1, Col18a1, Col4a2, Col4a5, Col5a1, Col6a1, Col6a2, Cpxm1, Crispld2, Csf1, Ctsk, Cxcl1, Cxcl10, Cxcl14, Cxcl2, ... and others
BP	GO:0009611	response to wounding	4.80E-29	Adora2b, Anxa2, Apoe, C1qa, C1qb, C1qc, C3, C4b, Ccl11, Ccl2, Ccl3, Ccl4, Ccl7, Cd8, Cd44, Cfp, Chst1, Clec7a, Crcp, Cxcl1, Cxcl10, Cxcl2, Ednra, Efemp2, F2r, Fcer1g, Fcgr2b, Fgf7, Fn1, Gdnf, Gja1, Gp1bb, Gpx2, Hdac7, Ido1, Ifnar2, Il10, Il1b, Il6, Lbp, Ly86, Masp1, Mif, Mmp2, Nlrc4, Pdpn, Plau, Pl ... and others
BP	GO:0006954	inflammatory response	7.99E-29	Adora2b, C1qa, C1qb, C1qc, C3, C4b, Ccl11, Ccl2, Ccl3, Ccl4, Ccl7, Ccl8, Cd44, Cfp, Chst1, Clec7a, Crcp, Cxcl1, Cxcl10, Cxcl2, Ednra, F2r, Fcer1g, Fcgr2b, Fn1, Gpx2, Hdac7, Ido1, Il10, Il1b, Il6, Lbp, Ly86, Masp1, Mif, Nlrc4, Reg3a, Reg3b, Reg3g, Sbno2, Serpina3n, Serpinf1, Serping1, Slc11a1, Sphk1, ... and others
MF	GO:0005488	binding	5.29E-28	2310014H01Rik, Abcc8, Abi3bp, Acox2, Actb, Adam23, Adamts2, Adamts4, Adar, Adcy4, Aebp1, Aif1, Akap12, Aldh1a3, Alpl, Antxr1, Anxa2, Aoc2, Apoe, Arap3, Arhgap23, Arhgdib, Arhgdig, Arid5a, Arih1, Arrb2, Asns, Atp13a1, Atp2a2, AU040829, Axl, Baz1a, Bdh2, Bgn, Bicc1, Bmp1, Brp16, C1qb, C3, Capg, Ccdc80 ... and others
BP	GO:0002376	immune system process	2.73E-27	Adora2b, Arrb2, Bcl2a1d, C1qa, C1qb, C1qc, C3, C4b, Ccl11, Ccl2, Ccl21a, Ccl3, Ccl4, Ccl7, Ccl8, Ccl9, Ccr7, Cd274, Cd40, Cd44, Cd74, Cd86, Cfp, Clec4n, Clec7a, Coro1a, Crcp, Csf1, Csf1r, Cxcl1, Cxcl10, Cxcl14, Cxcl2, Dnaja3, Fcer1g, Fcgr2b, Fcgr4, Gpx2, Grem1, H2-Ab1, Hcls1, Hdac7, Hmox1, Hoxb7, Ic ... and others
BP	GO:0006952	defense response	2.47E-25	Adora2b, C1qa, C1qb, C1qc, C3, C4b, Ccl11, Ccl17, Ccl2, Ccl3, Ccl4, Ccl7, Ccl8, Cd44, Cd74, Cd86, Cfp, Chst1, Clec4n, Clec7a, Crcp, Cxcl1, Cxcl10, Cxcl2, Defb37, Ednra, F2r, Fcer1g, Fcgr2b, Fn1, Gpx2, Hdac7, Ido1, Il10, Il1b, Il1rl1, Il6, Irf8, Lbp, Ly86, Lyz1, Lyz2, Masp1, Mif, Mx2, Nlrc4, Reg3a, R ... and others
BP	GO:0006955	immune response	2.43E-24	Adora2b, Bcl2a1d, C1qa, C1qb, C1qc, C3, C4b, Ccl11, Ccl2, Ccl3, Ccl4, Ccl7, Ccl8, Ccl9, Ccr7, Cd40, Cd74, Cd86, Cfp, Clec4n, Clec7a, Crcp, Cxcl1, Cxcl10, Cxcl14, Cxcl2, Fcer1g, Fcgr2b, Gpx2, H2-Ab1, Hmox1, Icam1, Ido1, Il10, Il1b, Il1rl1, Il4ra, Il6, Irf8, Jak3, Lat2, Lbp, Lif, Ly86, Masp1, Mif, Mx2 ... and others
MF	GO:0005515	protein binding	7.06E-24	2310014H01Rik, Abcc8, Abi3bp, Actb, Adcy4, Aebp1, Aif1, Akap12, Anxa2, Apoe, Arap3, Arhgap23, Arhgdib, Arhgdig, Arih1, Arrb2, Asns, Atp2a2, AU040829, Axl, Baz1a, Bgn, Bmp1, C1qb, C3, Capg, Ccdc80, Ccl11, Ccl17, Ccl2, Ccl3, Ccl4, Ccl7, Ccl8, Ccl9, Ccnd1, Ccne1, Ccr7, Cd200, Cd274, Cd40, Cd44, Cd74, C ... and others
BP	GO:0048518	positive regulation of biological process	2.39E-21	Abcc8, Abi3bp, Adora2b, Aif1, Aldh1a3, Apoe, Arrb2, Bcl2a1d, Bmp1, C1qa, C1qb, C1qc, C3, C4b, Ccdc80, Ccl11, Ccl2, Ccl21a, Ccl3, Ccnd1, Ccne1, Cd40, Cd44, Cd74, Cd86, Cebpb, Cfp, Clec7a, Col18a1, Coro1a, Csf1, Csf1r, Cxcl10, Cyp7b1, Ddah1, Dnaja3, Dnmt3b, Ednra, Ednrb, Ets1, F2r, Fbln2, Fcer1g, Fcgr ... and others
Down-regulated				
MF	GO:0003824	catalytic activity	3.25E-10	Abat, Abhd14b, Ace2, Acp1, Acp5, Acpl2, Acsl1, Acss2, Acvr1b, Afg3l2, Akr1c14, Ang, Araf, Asah2, Atp2c2, Atp6v0e2, Camk1, Camk1d, Car2, Ccbl1, Ccdc111, Cdk10, Chid1, Chka, Chpt1, Cpm, Csad, Ctse, Ctsh, Cybasc3, Cyp2c67, Cyp2d40, Cyp2f2, Ddc, Ddx6, Dhrs7, Dio1, Dtymk, Entpd5, Eri3, Fads6, Fkbp9, Gaa, ... and others
CC	GO:0005737	cytoplasm	9.43E-09	1810049H13Rik, 2410091C18Rik, Abat, Abhd14b, Acp1, Acp5, Acsl1, Acss2, Afg3l2, Ano1, Ap1s3, Appl2, Araf, Asah2, Atp5f1, Atp5s, Bfar, Camk1, Camk1d, Camta1, Capsl, Car2, Ccbl1, Cdh1, Chid1, Chka, Chmp2a, Chpt1, Clic6, Cln3, Clta, Csda, Ctse, Ctsh, Cybasc3, Cyp2f2, Ddx6, Dio1, Dram2, Eif3h, Entpd5, Es ... and others
BP	GO:0008152	metabolic process	2.01E-08	Abat, Ace2, Acp1, Acp5, Acsl1, Acss2, Acvr1b, Afg3l2, Akr1c14, Ang, Appl2, Araf, Asah2, Atp2c2, Atp5f1, Atp5s, Atp6v0e2, Btg2, C4bp, Camk1, Camk1d, Camta1, Car2, Cbx3, Ccbl1, Ccdc111, Cdh1, Cdk10, Cfb, Chid1, Chka, Chpt1, Cln3, Cpm, Csad, Csda, Ctse, Ctsh, Cybasc3, Cyp2c67, Cyp2d40, Cyp2f2, Ddc, Dhr ... and others
BP	GO:0044281	small molecule metabolic process	3.55E-08	Abat, Acsl1, Acss2, Atp2c2, Atp5f1, Atp5s, Atp6v0e2, Btg2, Car2, Chka, Cln3, Csad, Ddc, Dtymk, Edn2, Fads6, Gaa, Ganc, Gdi1, Gdpd1, Glb1, Glul, Gmpr, Gnai1, Gnas, Grtp1, Gstt3, Hadh, Hexb, Hpd, Hpgd, Insig1, Man2a1, Map2k1, Mat2a, Mdh1, Mecr, Mlxipl, Myh14, Ndel1, Nme7, Npy1r, Papss1, Pck1, Pdhb, Pf ... and others
CC	GO:0044444	cytoplasmic part	1.04E-07	1810049H13Rik, 2410091C18Rik, Abat, Acp5, Acsl1, Afg3l2, Ap1s3, Appl2, Araf, Asah2, Atp5f1, Atp5s, Bfar, Car2, Chid1, Chmp2a, Chpt1, Cln3, Clta, Ctse, Ctsh, Cybasc3, Cyp2f2, Dio1, Dram2, Eif3h, Entpd5, Esr2, Exoc4, Fam134b, Fkbp9, Fndc5, Gaa, Gbas, Ggnbp1, Glb1, Glul, Gnas, Golga4, Golph3l, Gper, Ha ... and others
BP	GO:0006665	sphingolipid metabolic process	1.17E-05	Asah2, Hexb, Kit, Lass5, Mtap7, Ppap2a, Smpd2, St6galnac6
MF	GO:0004553	hydrolase activity, hydrolyzing O-glycosyl compounds	1.28E-05	Chid1, Gaa, Ganc, Glb1, Hexb, Klb, Man2a1, Naglu, Neu2
BP	GO:0006643	membrane lipid metabolic process	1.65E-05	Asah2, Hexb, Kit, Lass5, Mtap7, Ppap2a, Smpd2, St6galnac6
BP	GO:0044238	primary metabolic process	2.19E-05	Abat, Ace2, Acp1, Acsl1, Acvr1b, Afg3l2, Ang, Araf, Asah2, Atp2c2, Atp5f1, Atp5s, Atp6v0e2, Btg2, C4bp, Camk1, Camk1d, Camta1, Cbx3, Ccdc111, Cdh1, Cdk10, Cfb, Chid1, Chka, Chpt1, Cln3, Cpm, Csad, Csda, Ctse, Ctsh, Ddc, Dtymk, Edn2, Eif3h, Esr2, Esrrg, Fads6, Fbxo32, Fgf1, Fkbp9, Foxk1, Foxn3, Gaa, ... and others
BP	GO:0006091	generation of precursor metabolites and energy	2.91E-05	Atp5f1, Atp6v0e2, Cybasc3, Gaa, Gnas, Mdh1, Mlxipl, Pck1, Pdhb, Pfkm, Ppp1r3b, Sdhb, Slc25a12, Suclg1, Tmx4

Table 5.12 Gene pathway analysis of naïve versus colitic WT CECs

Naive or Day6 2%DSS treated colon cells were isolated from WT mice. CECs were identified and purified by flow cytometry as described in Figure 5.3. RNA was isolated and hybridised to IlluminaMouseRef6 array. The details of significant (adj p<0.05) pathways by KEGG analysis are presented. Details of raw data processing and normalisation methods are presented in Chapter 2.16

Concluding Remarks

6.1 Introduction

The human GI tract has evolved to simultaneously promote efficient nutrient absorption and negate pathogen entry. This is achieved by finger-like epithelial projections, villi, to produce a vast surface area, co-existing with a highly sophisticated network of specialised immune cells. Both innate and adaptive arms of the immune response are located at intestinal mucosal surfaces, operating the dichotomous roles of tolerance to the commensal microbiota and brisk response to luminal pathogens. Inappropriate, overactive response to the former would not only be a wasteful use of resources by the host, but may instigate a cascade of damaging inflammation that has the potential to disrupt normal physiological function, in particular, nutrient absorption. The components of the intestinal immune system therefore demonstrate phenotypes unique to this tissue site. For example intestinal macrophages exhibit 'immune inertia', poorly responsive to TLR stimuli and secreting large quantities of the regulatory cytokine IL-10 (43). IECs also display antigen-processing capabilities, with expression of such machinery tightly regulated and spatially expressed exclusively on their baso-lateral surface (499). These cells are also able to sense and respond to luminal pathogens via PRR, able to secrete a vast array of immune regulatory and recruitment products that shape the local immune response and micro-environment (100).

These keys facets of intestinal immune response are perturbed in IBD. IBD is thought to be the result of a dysregulated immune system in genetically predisposed individuals with susceptibility variants described in autophagy, IL-23/Th17 and TGFβ pathways (104). Whilst recent studies have also identified intestinal monocytes and monocyte-derived precursors as critical perpetrators in driving IBD (113), (43), the immune mechanisms underpinning the dysregulated immune response in IBD pathogenesis are not well described. Previous work has therefore utilised animal models of IBD to describe the immune response in WT and transgenic animals to shed new light on existing control mechanisms, and uncover novel areas for therapeutic investigation in man.

Despite large strides forward in our understanding of the genetic contribution to common, polygenic conditions such as IBD, we can currently only account for <30% of IBD heritability using GWAS disease susceptibility loci (Anderson et al. 2011). Heritable changes in gene expression not encoded in DNA sequence and thus not accounted for using existing techniques therefore represent an attractive hypothesis for explaining part of this heritable component to disease susceptibility. Epigenetic processes such as DNA methylation, histone modification and nucleosome remodelling have all been shown to influence the regulation of key cell functions, including immune response, and require the presence of MBD proteins to exert these effects efficiently (242). MBD2 binds preferentially, though not

exclusively, to methylated DNA recruiting a large nucleosome re-modelling complex, exerting alterations in chromatin folding and histone motifs that confer significant gene expression changes (280). As such MBD2 has been shown to be critical in both innate and adaptive immune response; in mediating appropriate T cell differentiation and DC activation and function in response to Th2 pathogens and allergens (318), (321), (319).

Previous indications therefore suggest that *Mbd2* may play an important role in immune cells and in the GI tract in response to infection and predisposition to colorectal malignancy ((321), (325). However the immune mechanisms and cell types underlying these observations has not been explored in the GI tract.

The aims of this project were therefore to delineate, for the first time, the role of *Mbd2* in the intestinal immune response, specifically in animal models of colonic inflammation. We also sought to complement this with assessments of monocyte-like / macrophage populations in a homogenous colonic IBD dataset. This necessitated the optimisation and in some cases development of novel techniques to simultaneously assess multiple colon LP innate populations and in addition extract, identify and phenotype CECs by flow cytometry.

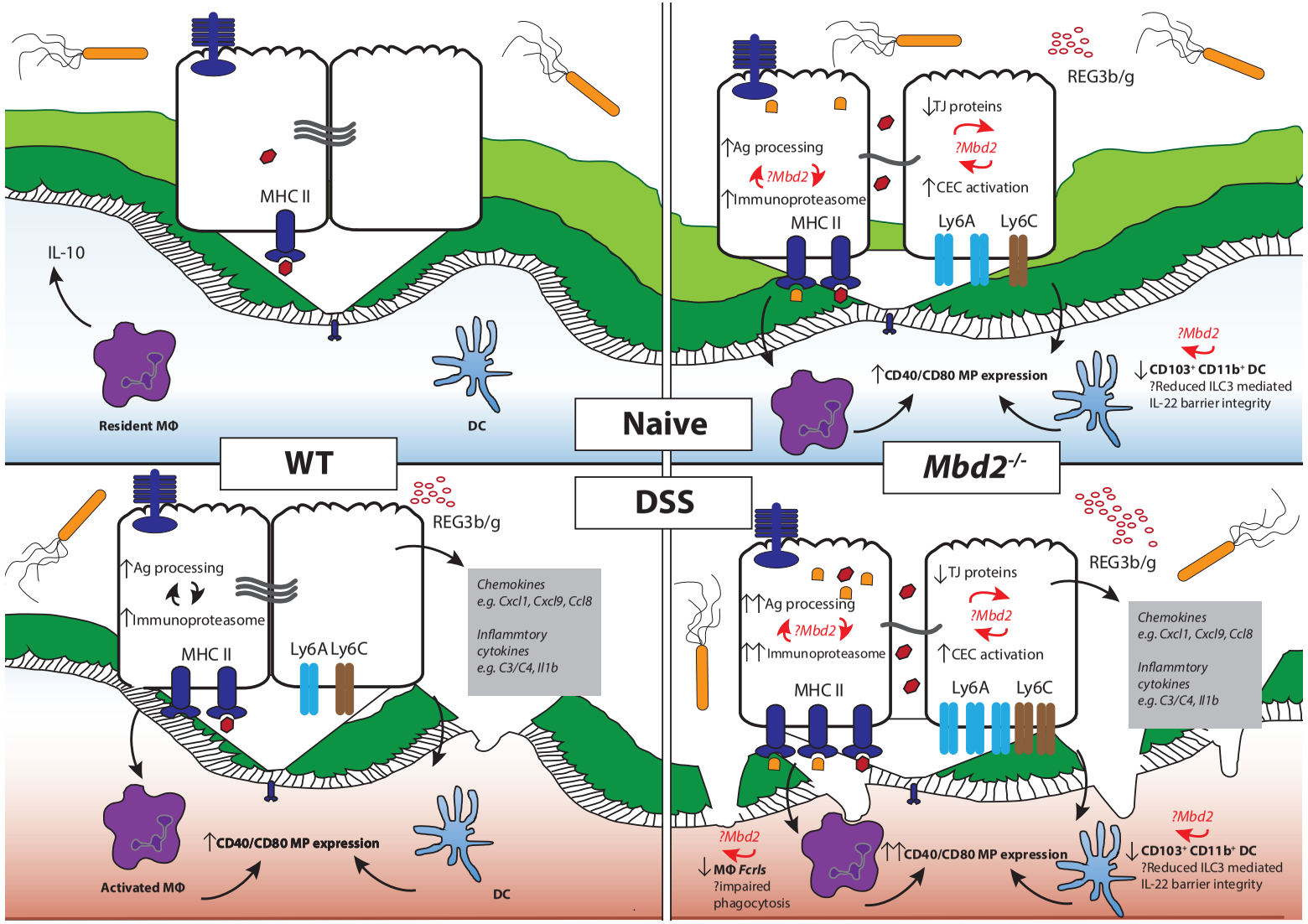
WT
Mbd2-/-
Naive
DSS
MHC II
IL-10
Resident MΦ
DC
REG3b/g
↓TJ proteins
?Mbd2
↑Ag processing
?Mbd2
↑Immunoproteasome
↑CEC activation
Ly6A
Ly6C
↑CD40/CD80 MP expression
?Mbd2
↓CD103+ CD11b+ DC
?Reduced ILC3 mediated
IL-22 barrier integrity
Chemokines
e.g. Cxcl1, Cxcl9, Ccl8
Inflammtory
cytokines
e.g. C3/C4, Il1b
Activated MΦ
↓MΦ FcrIs
?impaired
phagocytosis

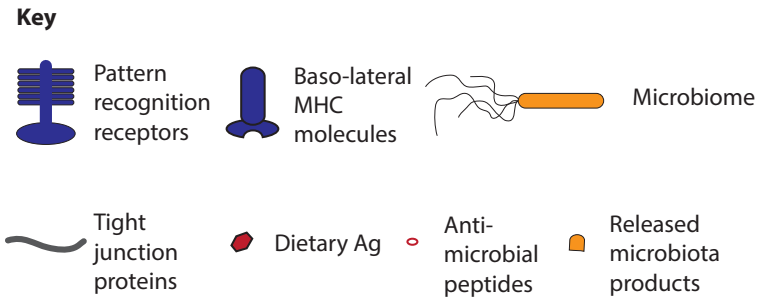

Figure 6.1 Proposed mechanisms for *Mbd2* mediated changes in colon homeostasis
Naïve
1. Absence of *Mbd2* may increase Ag processing and presentation gene expression in naive *Mbd2*$^{-/-}$ CEC (versus naive WT)
2. Absence of *Mbd2* may reduce tight junction protein gene expression in naive *Mbd2*$^{-/-}$ CEC (versus naive WT), though this may be a secondary phenomena (e.g. due to increased local IFNγ)
3. Absence of *Mbd2* may increase LY6C A/E/*Ly6c* expression in naive *Mbd2*$^{-/-}$ CEC (versus naive WT)
4. *Mbd2* is required to prevent the observed reduced number of CD11b^{+} CD103^{+} DCs in naïve *Mbd2*$^{-/-}$ LP, the reasons for which are not clear but may include a role for *Mbd2* in local DC survival or appropriate differentiation
5. Result of 1-4 yields altered interactions with the steady state microbiota, leading to dysbiosis

DSS
1. The same process of dysregulated Ag processing, MHC-II, LY6A/E and AMPs (CECs) CD40, CD80 expression (CD11c^{+} cells) seen in naïve *Mbd2*$^{-/-}$ now occurs in WT, but this is less than the increases in the already activated *Mbd2* deficient system
2. The same chemokine/proinflammatory response elements are upregulated independent of *Mbd2* deficiency in DSS
3. Decreased *Mbd2*$^{-/-}$ MΦ *Fcrls* expression may impair phagocytosis and therefore response to invading pathogens, further exacerbating host inflammatory response

6.2 Concluding remarks

We suggest that *Mbd2* acts to limit damaging inflammation in the mouse colon by preventing excessive monocyte and neutrophil accumulation. This end-result of colonic inflammation is lessened by the action of *Mbd2* in a multitude of cell types, underlining its functional importance. Firstly, *Mbd2*-mediated changes in CD11c expressing cells limits colonic inflammation (Figure 4.8), and we hypothesise this is due to its promotion of efficient phagocytosis in colon macrophages. Secondly, we have identified monocyte-like cells as increased in patients with endoscopic evidence of active IBD, irrespective of symptoms (Figure 3.12). This may have important implications for IBD management and we speculate that in the future phenotyping the proportion of immune cells at inflamed tissue sites may provide insight into disease activity, prognosis and disease natural history. Thirdly, our data strongly indicate that *Mbd2*-mediated changes in CECs prevents inappropriate antigen processing of luminal contents and promotes epithelial barrier integrity via TJ protein expression (Figure 5.6). Lastly, *Mbd2* regulation of colonic immune and epithelial cells alters the local microbial environment, maintaining species of bacteria that promote intestinal health.

One of the key unanswered questions of dysbiosis pathogenesis is whether observed dysbiosis in human IBD, or indeed in *Mbd2*$^{-/-}$, is a primary or secondary phenomenon. Therefore future work, will seek to address whether the microbiota in *Mbd2*$^{-/-}$ are inherently colitogenic, or indeed if by abrogating dysbiosis under germ-free or antibiotic treated conditions *Mbd2*$^{-/-}$ mice continue to demonstrate impaired inflammatory responses.

We foresee the main limitation in generalising these results is understanding the precise nature of *Mbd2* action. Namely demonstrating that dysregulated gene expression in the absence of *Mbd2* correlates to local binding of *Mbd2* at these loci and subsequent NuRD complex mediated changes in epigenetic motifs, altering the binding of transcriptional apparatus and ultimately gene expression. *Mbd2* chromatin immune precipitation has in our experience proved technically challenging due to poor antibody affinity, thus we are currently generating transgenic mice wherein a his-tagged *Mbd2* protein will permit investigation of its binding sites to answer these important questions.

Another limitation is that we have undertaken our gene expression analyses using mice globally deficient in *Mbd2*. At this point, we are therefore not able to exclude the possibility that other *Mbd2*$^{-/-}$ cell types may influence gene expression in our reported cells of investigation. For example, whether MBD2 deficient colon LP ILCs, neutrophils or eosinophils are directly influencing the gene expression profiles of MBD2 deficient macrophages, DCs or epithelial cells. To address this we are seeking to validate *Mbd2*-

mediated gene expression changes in animals where *Mbd2* deficiency is restricted to specific cell types, e.g. epithelial cells (*Villin-CreMbd2*$^{Fl/Fl}$) and T cells (*Vav-CreMbd2*$^{Fl/Fl}$).

Whilst the gene expression data in chapters 4 and 5 have permitted the use of hypothesis-free strategies to identify putative genes under the control of *Mbd2*, one of the most striking features in the DC, macrophage and monocyte expression data was the absence of a single, consistently dysregulated locus. This is perhaps re-inforces the multitude of small *Mbd2* mediated gene expression changes occurring within multiple different cell types. This further underlines simultaneously the importance of *Mbd2* in a spectrum of immune cells, but also the difficultly in identifying the presence of a primary regulatory pathway. The second most striking feature was the complicated balance of pro- and anti-inflammatory feedback mechanisms (See Diagram 4.2). Despite a more severe disease phenotype in response to chemical colitis, *Mbd2*$^{-/-}$ cells displayed both enhanced inflammatory and regulatory pathways. We therefore speculate that the biological kinetics of macrophage and monocyte responses to inflammatory challenge change over time, with pro-inflammatory pathways predominating early in the response, with a tipping-point whereby inflammation is no longer physiological but pathological, with a rise in anti-inflammatory mechanisms to limit further tissue damage. Evidence for this hypothesis is seen in the upregulation of anti-inflammatory pathways in active IBD and adult respiratory distress syndrome (ARDS), both characterized by aberrant inflammation and failure of anti-inflammatory control mechanisms (524), (525).

The data presented herein suggest that heritable changes in mucosal immune function may not be encoded in an organisms DNA sequence. 'Epigenetic stress', defined here as the perturbation on the host epigenome caused by environmental pressure, may explain the limitations of existing genetic techniques to explain common heritable disease susceptibility (250). We hypothesise therefore that environmental pressures at mucosal surfaces may lead to alterations in the epigenome, which is inherently more plastic than the genome, leading to altered expression of key regulatory immune processes and thus disposition to diseases characterised by aberrant inflammatory responses.

Rather than suggesting that MBD2 is the 'smoking gun' for IBD pathogenesis, we speculate that our data support the principle of epigenetic processes forming a fundamental control mechanism for host defence and appropriate mucosal responses. This may in turn provide a plausible hypothesis for the observation that most *NOD2* mutants, the largest genetic risk factor identified for CD, do not develop IBD (107). Indeed perhaps in a multi-hit hypothesis of heritable contribution to common disease, genetically susceptible individuals require either an inherited or environmentally-disturbed mutant epigenome that impairs host responses. Just as there is no one cell type that is dysregulated in IBD, our work using *Mbd2*$^{-/-}$ animals strongly suggests that *Mbd2* regulation of gene expression impacts a network of mucosal

cell types that together are key for limiting excessive intestinal inflammation, underlining the importance of these mechanisms in controlling appropriate immune responses.

Biblography

1. Kararli TT. Comparison of the gastrointestinal anatomy, physiology, and biochemistry of humans and commonly used laboratory animals. Biopharm Drug Dispos. 1995 Jul;16(5):351–80.

2. Turnbaugh PJ, Ley RE, Hamady M, Fraser-Liggett CM, Knight R, Gordon JI. The Human Microbiome Project. Nature. 2007 Oct 18;449(7164):804–10.

3. Worbs T, Bode U, Yan S, Hoffmann MW, Hintzen G, Bernhardt G, et al. Oral tolerance originates in the intestinal immune system and relies on antigen carriage by dendritic cells. Journal of Experimental Medicine. Rockefeller Univ Press; 2006 Mar 20;203(3):519–27.

4. Stange EF, TRAVIS SPL, Vermeire S, Beglinger C, Kupcinkas L, Geboes K, et al. European evidence based consensus on the diagnosis and management of Crohn's disease: definitions and diagnosis. 2006. pp. i1–15.

5. Stange EF, TRAVIS SPL, Vermeire S, Reinisch W, Geboes K, Barakauskiene A, et al. European evidence-based Consensus on the diagnosis and management of ulcerative colitis: Definitions and diagnosis. Journal of Crohn's and Colitis. 2008 Mar;2(1):1–23.

6. Rubin GP, Hungin APS, Kelly PJ, Ling J. Inflammatory bowel disease: epidemiology and management in an English general practice population. Aliment Pharmacol Ther. Blackwell Science Ltd; 2000 Dec 27;14(12):1553–9.

7. Armitage E, Drummond H, Ghosh S, Ferguson A. Incidence of juvenile-onset Crohn's disease in Scotland. The Lancet. 1999 May;353(9163):1496–7.

8. Langholz E, Munkholm P, Nielsen OH, Kreiner S, Binder V. Incidence and Prevalence of Ulcerative Colitis in Copenhagen County from 1962 to 1987. Scand J Gastroenterol. Taylor & Francis; 2009 Jul 8;26(12):1247–56.

9. Solberg IC, Vatn MH, Høie O, Stray N, Sauar J, Jahnsen J, et al. Clinical Course in Crohn's Disease: Results of a Norwegian Population-Based Ten-Year Follow-Up Study. Clinical Gastroenterology and Hepatology. 2007 Dec;5(12):1430–8.

10. Bernell O, Lapidus A, Hellers G. Risk factors for surgery and postoperative recurrence in Crohn's disease. Ann Surg. 2000 Jan;231(1):38–45.

11. Ramadas AV, Gunesh S, Thomas GAO, Williams GT, Hawthorne AB. Natural history of Crohn's disease in a population-based cohort from Cardiff (1986-2003): a study of changes in medical treatment and surgical resection rates. Gut. 2010 Aug 26;59(9):1200–6.

12. Olaison G, Smedh K, Sjödahl R. Natural course of Crohn's disease after ileocolic resection: endoscopically visualised ileal ulcers preceding symptoms. Gut. BMJ Publishing Group Ltd and British Society of Gastroenterology; 1992 Mar 1;33(3):331–5.

13. Rutgeerts P, Geboes K, Vantrappen G, Kerremans R, Coenegrachts JL, Coremans G. Natural-History of Recurrent Crohns-Disease at the Ileocolonic Anastomosis After Curative Surgery. Gut. 1984;25(6):665–72.

14. WILLIAMS JG, WONG WD, ROTHENBERGER DA, GOLDBERG SM. Recurrence of Crohns-Disease After Resection. Br J Surg. 1991 Jan;78(1):10–9.

15. Abraham C, Medzhitov R. Interactions Between the Host Innate Immune System and Microbes in Inflammatory Bowel Disease. Gastroenterology. Elsevier Inc; 2011 May 1;140(6):1729–37.

16. Murphy KP. Janeways Immunobiology 8th Edition. Janeways Immunobiology, ed. K. Murphy

.

17. Banchereau J, Steinman RM. Dendritic cells and the control of immunity. Nature. 1998;392(6673):245–52.

18. Steinman RM. Dendritic cells: Understanding immunogenicity. Eur J Immunol. 2007 Nov;37(S1):S53–S60.

19. Agace WW. T-cell recruitment to the intestinal mucosa. Trends in Immunology. 2008 Nov;29(11):514–22.

20. CAMERINI V, PANWALA C, KRONENBERG M. Regional Specialization of the Mucosal Immune-System - Intraepithelial Lymphocytes of the Large-Intestine Have a Different Phenotype and Function Than Those of the Small-Intestine. The Journal of Immunology. American Association of Immunologists; 1993;151(4):1765–76.

21. Fournier BM, Parkos CA. The role of neutrophils during intestinal inflammation. Nature Publishing Group; 2012 Apr 11;5(4):354–66.

22. Daley JM, Thomay AA, Connolly MD, Reichner JS, Albina JE. Use of Ly6G-specific monoclonal antibody to deplete neutrophils in mice. J Leukoc Biol. 2007 Sep 17;83(1):64–70.

23. Maloy KJ, Powrie F. Intestinal homeostasis and its breakdown in inflammatory bowel disease. Nature. 2011 Jun 15;474(7351):298–306.

24. Tester AM, Cox JH, Connor AR, Starr AE, Dean RA, Puente XS, et al. LPS responsiveness and neutrophil chemotaxis in vivo require PMN MMP-8 activity. Unutmaz D, editor. PLoS ONE. Public Library of Science; 2007;2(3):e312.

25. Rosenberg HF, Dyer KD, Foster PS. Eosinophils: changing perspectives in health and disease. Nat Rev Immunol. Nature Publishing Group; 2012 Nov 16;13(1):9–22.

26. Rothenberg ME, Hogan SP. THE EOSINOPHIL. Annu Rev Immunol. 2006 Apr;24(1):147–74.

27. Carlens J, Wahl B, Ballmaier M, Bulfone-Paus S, Forster R, Pabst O. Common -Chain-Dependent Signals Confer Selective Survival of Eosinophils in the Murine Small Intestine. The Journal of Immunology. 2009 Oct 20;183(9):5600–7.

28. Ziegler SF, Roan F, Bell BD, Stoklasek TA, Kitajima M, Han H. The biology of thymic stromal lymphopoietin (TSLP). Adv Pharmacol. Elsevier; 2013;66:129–55.

29. Ahrens R, Waddell A, Seidu L, Blanchard C, Carey R, Forbes E, et al. Intestinal Macrophage/Epithelial Cell-Derived CCL11/Eotaxin-1 Mediates Eosinophil Recruitment and Function in Pediatric Ulcerative Colitis. The Journal of Immunology. American Association of Immunologists; 2008 Nov 15;181(10):7390–9.

30. Lampinen M. Eosinophil granulocytes are activated during the remission phase of ulcerative colitis. Gut. 2005 May 28;54(12):1714–20.

31. Akuthota P, Wang H, Weller PF. Eosinophils as antigen-presenting cells in allergic upper airway disease. Current Opinion in Allergy and Clinical Immunology. 2010 Feb;10(1):14–9.

32. Wang Y-H, Angkasekwinai P, Lu N, Voo KS, Arima K, Hanabuchi S, et al. IL-25 augments type 2 immune responses by enhancing the expansion and functions of TSLP-DC-activated Th2 memory cells. Journal of Experimental Medicine. Rockefeller Univ Press; 2007 Aug 6;204(8):1837–47.

33. Masterson JC, McNamee EN, Fillon SA, Hosford L, Harris R, Fernando SD, et al. Eosinophil-mediated signalling attenuates inflammatory responses in experimental colitis. Gut. BMJ Publishing Group Ltd and British Society of Gastroenterology; 2014 Sep 10;64(8):1–13.

34. Griseri T, Arnold IC, Pearson C, Krausgruber T, Schiering C, Franchini F, et al. Granulocyte Macrophage Colony-Stimulating Factor-Activated Eosinophils Promote Interleukin- 23 Driven Chronic Colitis. Immunity. The Authors; 2015 Jul 21;43(1):187–99.

35. Palframan RT, Jung S, Cheng CY, Weninger W, Luo Y, Dorf M, et al. Inflammatory chemokine transport and presentation in HEV: A remote control mechanism for monocyte recruitment to lymph nodes in inflamed tissues. Journal of Experimental Medicine. Rockefeller Univ Press; 2001;194(9):1361–73.

36. Geissmann F, Gordon S, Hume DA, Mowat AM, Randolph GJ. PeRSPeCtiveS. Nature Publishing Group. Nature Publishing Group; 2010 May 14;10(6):453–60.

37. Serbina NV, Jia T, Hohl TM, Pamer EG. Monocyte-Mediated Defense Against Microbial Pathogens. Annu Rev Immunol. 2008 Apr;26(1):421–52.

38. Ziegler-Heitbrock L. The CD14+ CD16+ blood monocytes: their role in infection and inflammation. J Leukoc Biol. Society for Leukocyte Biology; 2007 Mar;81(3):584–92.

39. Ziegler-Heitbrock L, Ancuta P, Crowe S, Dalod M, Grau V, Hart DN, et al. Nomenclature of monocytes and dendritic cells in blood. Blood. American Society of Hematology; 2010 Oct 21;116(16):e74–80.

40. Cros J, Cagnard N, Woollard K, Patey N, Zhang S-Y, Senechal B, et al. Human CD14dim Monocytes Patrol and Sense Nucleic Acids and Viruses via TLR7 and TLR8 Receptors. Immunity. Elsevier Inc; 2010 Sep 24;33(3):375–86.

41. Ingersoll MA, Spanbroek R, Lottaz C, Gautier EL. Comparison of gene expression profiles between human and mouse monocyte subsets. Blood. 2010.

42. Bain CC, Bravo-Blas A, Scott CL, Perdiguero EG, Geissmann F, Henri S, et al. Constant replenishment from circulating monocytes maintains the macrophage

pool in the intestine of adult mice. Nature Immunology. 2014 Aug 24.

43. Bain CC, Scott CL, Uronen-Hansson H, Gudjonsson S, Jansson O, Grip O, et al. Resident and pro-inflammatory macrophages in the colon represent alternative context-dependent fates of the same Ly6Chi monocyte precursors. Mucosal Immunology. 2013 May;6(3):498–510.

44. Kurihara T, Warr G, Loy J, Bravo R. Defects in macrophage recruitment and host defense in mice lacking the CCR2 chemokine receptor. Journal of Experimental Medicine. Rockefeller Univ Press; 1997;186(10):1757–62.

45. Serbina NV, Kuziel W, Flavell R, Akira S, Rollins B, Pamer EG. Sequential MyD88-independent and -dependent activation of innate immune responses to intracellular bacterial infection. Immunity. 2003 Dec;19(6):891–901.

46. Grainger JR, Wohlfert EA, Fuss IJ, Bouladoux N, Askenase MH, Legrand F, et al. Inflammatory monocytes regulate pathologic responses to commensals during acute gastrointestinal infection. Nature Medicine. Nature Publishing Group; 2013 May 26;19(6):713–21.

47. Zigmond E, Varol C, Farache J, Elmaliah E, Satpathy AT, Friedlander G, et al. Monocytes in the Inflamed Colon Give Rise to Proinflammatory Effector Cellsand Migratory Antigen-Presenting Cells. Immunity. Elsevier Inc; 2012 Dec 14;37(6):1076–90.

48. Hume DA. The mononuclear phagocyte system. Current Opinion in Immunology. 2006 Feb;18(1):49–53.

49. Murray PJ, Wynn TA. Protective and pathogenic functions of macrophage subsets. Nat Rev Immunol. Nature Publishing Group; 2011 Oct 14;11(11):723–37.

50. Rogler G, Hausmann M, Vogl D, Aschenbrenner E, Andus T, Falk W, et al. Isolation and phenotypic characterization of colonic macrophages. Clinical & Experimental Immunology. Blackwell Science Ltd; 1998 May;112(2):205–15.

51. Platt AM, Bain CC, Bordon Y, Sester DP, Mowat AM. An Independent Subset of TLR Expressing CCR2-Dependent Macrophages Promotes Colonic Inflammation. The Journal of Immunology. 2010 Jun 3;184(12):6843–54.

52. Denning TL, Wang Y-C, Patel SR, Williams IR, Pulendran B. Lamina propria macrophages and dendritic cells differentially induce regulatory and interleukin 17–producing T cell responses. Nature Immunology. 2007 Sep 16;8(10):1086–94.

53. Murai M, Turovskaya O, Kim G, Madan R, Karp CL, Cheroutre H, et al. Interleukin 10 acts on regulatory T cells to maintain expression of the transcription factor Foxp3 and suppressive function in mice with colitis. Nature Immunology. Nature Publishing Group; 2009 Sep 27;10(11):1178–84.

54. Kamada N, Hisamatsu T, Okamoto S, Sato T, Matsuoka K, Arai K, et al. Abnormally differentiated subsets of intestinal macrophage play a key role in Th1-dominant chronic colitis through excess production of IL-12 and IL-23 in response to bacteria. The Journal of Immunology. American Association of Immunologists; 2005 Nov 15;175(10):6900–8.

55. Hadis U, Wahl B, Schulz O, Hardtke-Wolenski M, Schippers A, Wagner N, et al.

Intestinal Tolerance Requires Gut Homing and Expansion of FoxP3+ Regulatory T Cells in the Lamina Propria. Immunity. Elsevier Inc; 2011 Feb 25;34(2):237–46.

56. Smythies LE, Sellers M, Clements RH, Mosteller-Barnum M, Meng G, Benjamin WH, et al. Human intestinal macrophages display profound inflammatory anergy despite avid phagocytic and bacteriocidal activity. J Clin Invest. 2005 Jan 3;115(1):66–75.

57. Rugtveit J, Nilsen EM, Bakka A, Carlsen H, Brandtzaeg P, Scott H. Cytokine profiles differ in newly recruited and resident subsets of mucosal macrophages from inflammatory bowel disease. YGAST. 1997 May;112(5):1493–505.

58. Hausmann M, OBERMEIER F, SCHREITER K, SPOTTL T, Falk W, Schölmerich J, et al. Cathepsin D is up-regulated in inflammatory bowel disease macrophages. Clinical & Experimental Immunology. 2004 Apr;136(1):157–67.

59. Milling S, Yrlid U, Cerovic V, MacPherson G. Subsets of migrating intestinal dendritic cells. Immunological Reviews. Blackwell Publishing Ltd; 2010;234(1):259–67.

60. Cepek KL, Shaw SK, Parker CM, Russell GJ. Adhesion between epithelial cells and T lymphocytes mediated by E-cadherin and the αEβ7 integrin. Nature. 1994;372(6502):190–3.

61. Schon MP, Arya A, Murphy EA, Adams CM, Strauch UG, Agace WW, et al. Mucosal T lymphocyte numbers are selectively reduced in integrin alpha(E) (CD103)-deficient mice. The Journal of Immunology. 1999;162(11):6641–9.

62. Bachem A, Hartung E, Güttler S, Mora A, Zhou X, Hegemann A, et al. Expression of XCR1 Characterizes the Batf3-Dependent Lineage of Dendritic Cells Capable of Antigen Cross-Presentation. Front Immunol. 2012;3:214.

63. Crozat K, Tamoutounour S, Vu Manh T-P, Fossum E, Luche H, Ardouin L, et al. Cutting edge: expression of XCR1 defines mouse lymphoid-tissue resident and migratory dendritic cells of the CD8α+ type. J Immunol. American Association of Immunologists; 2011 Nov 1;187(9):4411–5.

64. Edelson BT, KC W, Juang R, Kohyama M, Benoit LA, Klekotka PA, et al. Peripheral CD103+ dendritic cells form a unified subset developmentally related to CD8α+ conventional dendritic cells. Journal of Experimental Medicine. Rockefeller Univ Press; 2010 Apr 12;207(4):823–36.

65. Persson EK, Uronen-Hansson H, Semmrich M, Rivollier A, Hägerbrand K, Marsal J, et al. IRF4 Transcription-Factor-Dependent CD103. Immunity. Elsevier; 2013 May 23;38(5):958–69.

66. Watchmaker PB, Lahl K, Lee M, Baumjohann D, Morton J, Kim SJ, et al. Comparative transcriptional and functional profiling defines conserved programs of intestinal DC differentiation in humans and mice. Nature Immunology. 2013 Dec 1;15(1):98–108.

67. Uematsu S, Fujimoto K, Jang M-H, Yang B-G, Jung Y-J, Nishiyama M, et al. Regulation of humoral and cellular gut immunity by lamina propria dendritic cells expressing Toll-like receptor 5. Nature Immunology. 2008 May 30;9(7):769–76.

68. Satpathy AT, o CGBN, Lee JS, Ng D, Manieri NA, KC W, et al. Notch2-

dependent classical dendritic cells orchestrate intestinal immunity to attaching-and-effacing bacterial pathogens. Nature Immunology [Internet]. Nature Publishing Group; 2013 Aug 4;14(9):937–48. Available from: http://www.nature.com/doifinder/10.1038/ni.2679

69. Cerovic V, Houston SA, Scott CL, Aumeunier A, Yrlid U, Mowat AM, et al. Intestinal CD103(-) dendritic cells migrate in lymph and prime effector T cells. Mucosal Immunology. 2013 Jan;6(1):104–13.

70. Bogunovic M, Ginhoux F, Helft J, Shang L, Hashimoto D, Greter M, et al. Origin of the Lamina Propria Dendritic Cell Network. Immunity. 2009 Sep;31(3):513–25.

71. Varol C, Vallon-Eberhard A, Elinav E, Aychek T, Shapira Y, Luche H, et al. Intestinal Lamina Propria Dendritic Cell Subsets Have Different Origin and Functions. Immunity. Elsevier Ltd; 2009 Sep 18;31(3):502–12.

72. Tamoutounour S, Henri S, Lelouard H, de Bovis B, de Haar C, van der Woude CJ, et al. CD64 distinguishes macrophages from dendritic cells in the gut and reveals the Th1-inducing role of mesenteric lymph node macrophages during colitis. Eur J Immunol. 2012 Oct 17;42(12):3150–66.

73. Schreiber HA, Loschko J, Karssemeijer RA, Escolano A, Meredith MM, Mucida D, et al. Intestinal monocytes and macrophages are required for T cell polarization in response to Citrobacter rodentium. Journal of Experimental Medicine. 2013 Sep 23;210(10):2025–39.

74. Poulin LF, Salio M, Griessinger E, Anjos-Afonso F, Craciun L, Chen JL, et al. Characterization of human DNGR-1+ BDCA3+ leukocytes as putative equivalents of mouse CD8 + dendritic cells. Journal of Experimental Medicine. 2010 Jun 7;207(6):1261–71.

75. Jongbloed SL, Kassianos AJ, McDonald KJ, Clark GJ, Ju X, Angel CE, et al. Human CD141+ (BDCA-3)+ dendritic cells (DCs) represent a unique myeloid DC subset that cross-presents necrotic cell antigens. Journal of Experimental Medicine. 2010 Jun 7;207(6):1247–60.

76. Poulin LF, Reyal Y, Uronen-Hansson H, Schraml BU, Sancho D, Murphy KM, et al. DNGR-1 is a specific and universal marker of mouse and human Batf3-dependent dendritic cells in lymphoid and nonlymphoid tissues. Blood. 2012 Jun 22;119(25):6052–62.

77. Cheroutre H. IELs: enforcing law and order in the court of the intestinal epithelium. Immunological Reviews. Munksgaard International Publishers; 2005 Aug;206(1):114–31.

78. Kunisawa J, Takahashi I, Kiyono H. Intraepithelial lymphocytes: their shared and divergent immunological behaviors in the small and large intestine. Immunological Reviews. 2007 Feb;215(1):136–53.

79. Cheroutre H, Lambolez F, Mucida D. The light and dark sides of intestinal intraepithelial lymphocytes. Nature Publishing Group. Nature Publishing Group; 2011 Jun 17;11(7):445–56.

80. Boismenu R, Havran WL. Modulation of epithelial cell growth by intraepithelial gamma delta T cells. Science. 1994 Nov 18;266(5188):1253–5.

81. Inagaki-Ohara K. Suppressor of cytokine signalling 1 in lymphocytes regulates the development of intestinal inflammation in mice. Gut. 2006 Feb 1;55(2):212–9.

82. Ismail AS, Behrendt CL, Hooper LV. Reciprocal Interactions between Commensal Bacteria and Intraepithelial Lymphocytes during Mucosal Injury. The Journal of Immunology. 2009 Mar 1;182(5):3047–54.

83. ROMAGNANI S. Lymphokine Production by Human T-Cells in Disease States. Annu Rev Immunol. 1994;12(1):227–57.

84. Zhou L, Lopes JE, Chong MMW, Ivanov II, Min R, Victora GD, et al. TGF-β-induced Foxp3 inhibits TH17 cell differentiation by antagonizing RORγt function. Nature. 2008 Mar 26;453(7192):236–40.

85. Ivanov II, McKenzie BS, Zhou L, Tadokoro CE, Lepelley A, Lafaille JJ, et al. The Orphan Nuclear Receptor RORγt Directs the Differentiation Program of Proinflammatory IL-17+ T Helper Cells. Cell. 2006 Sep;126(6):1121–33.

86. Yang XO, Pappu BP, Nurieva R, Akimzhanov A, Kang HS, Chung Y, et al. T Helper 17 Lineage Differentiation Is Programmed by Orphan Nuclear Receptors RORα and RORγ. Immunity. 2008 Jan;28(1):29–39.

87. O'Garra A, Vieira P. Regulatory T cells and mechanisms of immune system control. Nature Medicine. 2004 Aug;10(8):801–5.

88. Asseman C, Mauze S, Leach MW, Coffman RL, Powrie F. An essential role for interleukin 10 in the function of regulatory T cells that inhibit intestinal inflammation. Journal of Experimental Medicine. 1999;190(7):995–1003.

89. Wildin RS, Ramsdell F, Peake J, Faravelli F, Casanova JL, Buist N, et al. X-linked neonatal diabetes mellitus, enteropathy and endocrinopathy syndrome is the human equivalent of mouse scurfy. Nat Genet. 2001 Jan;27(1):18–20.

90. Valencia X, Stephens G, Goldbach-Mansky R. TNF downmodulates the function of human CD4+ CD25hi T-regulatory cells. Blood. 2006.

91. Spits H, Cupedo T. Innate Lymphoid Cells: Emerging Insights in Development, Lineage Relationships, and Function. Annu Rev Immunol. 2012 Apr 23;30(1):647–75.

92. Spits H, Di Santo JP. The expanding family of innate lymphoidcells: regulators and effectors of immunityand tissue remodeling. Nature Publishing Group. Nature Publishing Group; 2010 Nov 28;12(1):21–7.

93. Fort MM, Cheung J, Yen D, Li J, Zurawski SM, Lo S, et al. IL-25 induces IL-4 IL-5, and IL-13 and Th2-associated pathologies in vivo. Immunity. 2001 Dec;15(6):985–95.

94. Price AE, Liang H-E, Sullivan BM, Reinhardt RL, Eisley CJ, Erle DJ, et al. Systemically dispersed innate IL-13-expressing cells in type 2 immunity. Proc Natl Acad Sci USA. National Acad Sciences; 2010 Jun 22;107(25):11489–94.

95. Takatori H, Kanno Y, Watford WT, Tato CM, Weiss G, Ivanov II, et al. Lymphoid tissue inducer-like cells are an innate source of IL-17 and IL-22. Journal of Experimental Medicine. 2009 Jan 19;206(1):35–41.

96. Buonocore S, Ahern PP, Uhlig HH, Ivanov II, Littman DR, Maloy KJ, et al. Innate lymphoid cells drive interleukin-23-dependent innate intestinal pathology. Nature. Nature Publishing Group; 2010 Apr 21;464(7293):1371–5.

97. Takayama T, Kamada N, Chinen H, Okamoto S, Kitazume MT, Chang J, et al. Imbalance of NKp44+NKp46− and NKp44−NKp46+ Natural Killer Cells in the Intestinal Mucosa of Patients With Crohn's Disease. YGAST. Elsevier Inc; 2010 Sep 1;139(3):882–3.

98. Eken A, Singh AK, Treuting PM, Oukka M. IL-23R+ innate lymphoid cells induce colitis via interleukin-22-dependent mechanism. Mucosal Immunology. 2014 Jan;7(1):143–54.

99. Geremia A, Arancibia-Carcamo CV, Fleming MPP, Rust N, Singh B, Mortensen NJ, et al. IL-23-responsive innate lymphoid cells are increased in inflammatory bowel disease. Journal of Experimental Medicine. 2011 Jun 6;208(6):1127–33.

100. Shale M, Ghosh S. How intestinal epithelial cells tolerise dendritic cells and its relevance to inflammatory bowel disease. Gut. 2009 Aug 11;58(9):1291–9.

101. Ganz T. Defensins: antimicrobial peptides of innate immunity. Nat Rev Immunol. 2003 Sep;3(9):710–20.

102. Mayer L, EISENHARDT D, SALOMON P, BAUER W, PLOUS R, PICCININI L. Expression of Class-Ii Molecules on Intestinal Epithelial-Cells in Humans - Differences Between Normal and Inflammatory Bowel-Disease. YGAST. 1991 Jan;100(1):3–12.

103. Niess JH, Brand S, Gu X, Landsman L, Jung S. CX3CR1-mediated dendritic cell access to the intestinal lumen and bacterial clearance. Science. 2005;307(5706):121–3.

104. Anderson CA, Boucher G, Lees CW, Franke A, D'Amato M, Taylor KD, et al. Meta-analysis identifies 29 additional ulcerative colitis risk loci, increasing the number of confirmed associations to 47. Nat Genet. 2011 Feb 6;43(3):246–52.

105. Franke A, McGovern DPB, Barrett JC, Wang K, Radford-Smith GL, Ahmad T, et al. Genome-wide meta-analysis increases to 71 the number of confirmed Crohn's disease susceptibility loci. Nature Publishing Group. Nature Publishing Group; 2010 Nov 21;42(12):1118–25.

106. Hampe J, Franke A, Rosenstiel P, Till A, Teuber M, Huse K, et al. A genome-wide association scan of nonsynonymous SNPs identifies a susceptibility variant for Crohn disease in ATG16L1. Nat Genet. 2006 Dec 31;39(2):207–11.

107. Hugot JP, Chamaillard M, Zouali H, Lesage S, Cézard JP, Belaiche J, et al. Association of NOD2 leucine-rich repeat variants with susceptibility to Crohn's disease. Nature. 2001 May 31;411(6837):599–603.

108. Ogura Y, Bonen DK, Inohara N, Nicolae DL, Chen FF, Ramos R, et al. A frameshift mutation in NOD2 associated with susceptibility to Crohn's disease. Nature. 2001 May 31;411(6837):603–6.

109. Adler J, Rangwalla SC, Dwamena BA, Higgins PD. The Prognostic Power of the NOD2 Genotype for Complicated Crohn's Disease: A Meta-Analysis. The American Journal of Gastroenterology. 2011 Feb 22;106(4):699–712.

110. Wallace KL. Immunopathology of inflammatory bowel disease. WJG. 2014;20(1):6–17.

111. Cadwell K, Liu JY, Brown SL, Miyoshi H, Loh J, Lennerz JK, et al. A key role for autophagy and the autophagy gene Atg16l1 in mouse and human intestinal Paneth cells. Nature. 2008 Oct 5;456(7219):259–63.

112. Cooney R, Baker J, Brain O, Danis B, Pichulik T, Allan P, et al. NOD2 stimulation induces autophagy in dendritic cells influencing bacterial handling and antigen presentation. Nature Medicine. Nature Publishing Group; 2009 Dec 6;16(1):90–7.

113. Kamada N, Hisamatsu T, Okamoto S, Chinen H, Kobayashi T, Sato T, et al. Unique CD14+ intestinal macrophages contribute to the pathogenesis of Crohn disease via IL-23/IFN-γ axis. J Clin Invest. 2008 May 1;:1–12.

114. Schulz O, Jaensson E, Persson EK, Liu X, Worbs T, Agace WW, et al. Intestinal CD103+, but not CX3CR1+, antigen sampling cells migrate in lymph and serve classical dendritic cell functions. Journal of Experimental Medicine. 2009 Dec 21;206(13):3101–14.

115. McDole JR, Wheeler LW, McDonald KG, Wang B, Konjufca V, Knoop KA, et al. Goblet cells deliver luminal antigen to CD103. Nature. Nature Publishing Group; 2013 Apr 9;483(7389):345–9.

116. Medina-Contreras O, Geem D, Laur O, Williams IR, Lira SA, Nusrat A, et al. CX3CR1 regulates intestinal macrophage homeostasis, bacterial translocation, and colitogenic Th17 responses in mice. J Clin Invest. 2011 Dec 1;121(12):4787–95.

117. Mowat AM, Bain CC. Mucosal Macrophages in Intestinal Homeostasis and Inflammation. J Innate Immun. 2011;3(6):550–64.

118. Lee SH, Starkey PM, Gordon S. Quantitative analysis of total macrophage content in adult mouse tissues. Immunochemical studies with monoclonal antibody F4/80. Journal of Experimental Medicine. Rockefeller Univ Press; 1985 Mar 1;161(3):475–89.

119. Smythies LE, Shen R, Bimczok D, Novak L, Clements RH, Eckhoff DE, et al. Inflammation Anergy in Human Intestinal Macrophages Is Due to Smad-induced IκBα Expression and NF-κB Inactivation. Journal of Biological Chemistry. American Society for Biochemistry and Molecular Biology; 2010 Jun 18;285(25):19593–604.

120. Thiesen S, Janciauskiene S, Uronen-Hansson H, Agace W, Hogerkorp CM, Spee P, et al. CD14hiHLA-DRdim macrophages, with a resemblance to classical blood monocytes, dominate inflamed mucosa in Crohn's disease. J Leukoc Biol. 2014 Feb 28;95(3):531–41.

121. GRIMM MC, PULLMAN WE, BENNETT GM, SULLIVAN PJ, PAVLI P, DOE WF. Direct evidence of monocyte recruitment to inflammatory bowel disease mucosa. Journal of Gastroenterology and Hepatology. Blackwell Publishing Ltd; 1995 Aug 1;10(4):387–95.

122. Hammer GE, Turer EE, Taylor KE, Fang CJ, Advincula R, Oshima S, et al. Expression of A20 by dendritic cells preserves immune homeostasis and prevents colitis and spondyloarthritis. Nature Immunology. 2011 Oct

23;12(12):1184–93.

123. Siddiqui KRR, Laffont S, Powrie F. E-Cadherin Marks a Subset of Inflammatory Dendritic Cells that Promote T Cell-Mediated Colitis. Immunity. Elsevier Ltd; 2010 Apr 23;32(4):557–67.

124. Powell N, Walker AW, Stolarczyk E, Canavan JB, Gökmen MR, Marks E, et al. The Transcription Factor T-bet Regulates Intestinal Inflammation Mediated by Interleukin-7 Receptor. Immunity. Elsevier Inc; 2012 Oct 19;37(4):674–84.

125. McGovern DPB, Gardet A, Törkvist L, Goyette P, Essers J, Taylor KD, et al. Genome-wide association identifies multiple ulcerative colitis susceptibility loci. Nat Genet. 2010 Mar 14;42(4):332–7.

126. Rovedatti L, Kudo T, Biancheri P, Sarra M, Knowles CH, Rampton DS, et al. Differential regulation of interleukin 17 and interferon production in inflammatory bowel disease. Gut. 2009 Nov 18;58(12):1629–36.

127. Fujino S, Andoh A, Bamba S, Ogawa A, Hata K, Araki Y, et al. Increased expression of interleukin 17 in inflammatory bowel disease. Gut. 2003 Jan;52(1):65–70.

128. Sugihara T, Kobori A, Imaeda H, Tsujikawa T, Amagase K, Takeuchi K, et al. The increased mucosal mRNA expressions of complement C3 and interleukin-17 in inflammatory bowel disease. Clinical & Experimental Immunology. 2010 Jan 19;160(3):386–93.

129. Zhang Z, Zheng M, Bindas J, Schwarzenberger P, Kolls JK. Critical role of IL-17 receptor signaling in acute TNBS-induced colitis. Inflammatory Bowel Diseases. 2006 May;12(5):382–8.

130. Bush KA, Farmer KM, Walker JS, Kirkham BW. Reduction of joint inflammation and bone erosion in rat adjuvant arthritis by treatment with interleukin-17 receptor IgG1 Fc fusion protein. Arthritis & Rheumatism. 2002 Mar 7;46(3):802–5.

131. Komiyama Y, Nakae S, Matsuki T, Nambu A, Ishigame H, Kakuta S, et al. IL-17 Plays an Important Role in the Development of Experimental Autoimmune Encephalomyelitis. The Journal of Immunology. 2006 Jun 19;177(1):566–73.

132. O'Connor W Jr, Kamanaka M, Booth CJ, Town T, Nakae S, Iwakura Y, et al. A protective function for interleukin 17A in T cell–mediated intestinal inflammation. Nature Immunology. 2009 May 17;10(6):603–9.

133. Sarra M, Pallone F, MacDonald TT, Monteleone G. IL-23/IL-17 axis in IBD. Inflammatory Bowel Diseases. 2010 Oct;16(10):1808–13.

134. Geremia A, Biancheri P, Allan P, Corazza GR, Di Sabatino A. Innate and adaptive immunity in inflammatory bowel disease. Autoimmunity Reviews. Elsevier B.V; 2014 Jan 1;13(1):3–10.

135. Fantini MC. Transforming growth factor induced FoxP3+ regulatory T cells suppress Th1 mediated experimental colitis. Gut. 2006 May 1;55(5):671–80.

136. Singh B, Read S, Asseman C, Malmström V, Mottet C, Stephens LA, et al. Control of intestinal inflammation by regulatory T cells. Immunological Reviews. 2001 Aug;182(11):190–200.

137. Chamouard P, Monneaux F, Richert Z, Voegeli A-C, Lavaux T, Gaub MP, et al. Diminution of Circulating CD4+CD25high T Cells in Naïve Crohn's Disease. Dig Dis Sci. 2008 Dec 3;54(10):2084–93.

138. Maul J, Loddenkemper C, Mundt P, Berg E, Giese T, Stallmach A, et al. Peripheral and Intestinal Regulatory CD4+CD25high T Cells in Inflammatory Bowel Disease. Gastroenterology. 2005 Jun;128(7):1868–78.

139. Eastaff-Leung N, Mabarrack N, Barbour A, Cummins A, Barry S. Foxp3+ Regulatory T Cells, Th17 Effector Cells, and Cytokine Environment in Inflammatory Bowel Disease. J Clin Immunol. 2009 Nov 20;30(1):80–9.

140. Chen W, Jin W, Hardegen N, Lei K-J, Li L, Marinos N, et al. Conversion of Peripheral CD4+CD25− Naive T Cells to CD4+CD25+ Regulatory T Cells by TGF-β Induction of Transcription Factor Foxp3. Journal of Experimental Medicine. Rockefeller Univ Press; 2003 Dec 15;198(12):1875–86.

141. Allan SE, Crome SQ, Crellin NK, Passerini L, Steiner TS, Bacchetta R, et al. Activation-induced FOXP3 in human T effector cells does not suppress proliferation or cytokine production. International Immunology. 2007 Feb 20;19(4):345–54.

142. Hovhannisyan Z, Treatman J, Littman DR, Mayer L. Characterization of Interleukin-17–Producing Regulatory T Cells in Inflamed Intestinal Mucosa From Patients With Inflammatory Bowel Diseases. YGAST. Elsevier Inc; 2011 Mar 1;140(3):957–65.

143. Kryczek I, Wu K, Zhao E, Wei S, Vatan L, Szeliga W, et al. IL-17+ Regulatory T Cells in the Microenvironments of Chronic Inflammation and Cancer. The Journal of Immunology. 2011 Mar 21;186(7):4388–95.

144. Eckburg PB, Bik EM, Bernstein CN, Purdom E, Dethlefsen L, Sargent M, et al. Diversity of the human intestinal microbial flora. Science. American Association for the Advancement of Science; 2005;308(5728):1635–8.

145. Qin J, Li R, Raes J, Arumugam M, Burgdorf KS, Manichanh C, et al. A human gut microbial gene catalogue established by metagenomic sequencing. Nature. 2010 Mar 4;464(7285):59–65.

146. Iliev ID, Funari VA, Taylor KD, Nguyen Q, Reyes CN, Strom SP, et al. Interactions Between Commensal Fungi and the C-Type Lectin Receptor Dectin-1 Influence Colitis. Science. 2012 Jun 7;336(6086):1314–7.

147. Atarashi K, Tanoue T, Oshima K, Suda W, Nagano Y, Nishikawa H, et al. Treg induction by a rationally selected mixture of Clostridia strains from the human microbiota. Nature. 2013 Aug 8;500(7461):232–6.

148. Smith PM, Howitt MR, Panikov N, Michaud M, Gallini CA, Bohlooly-Y M, et al. The Microbial Metabolites, Short-Chain Fatty Acids, Regulate Colonic T-reg Cell Homeostasis. Science. 2013;341(6145):569–73.

149. Blaser MJ, Falkow S. What are the consequences of the disappearing human microbiota? Nature Reviews Microbiology. Nature Publishing Group; 2009 Nov 9;7(12):887–94.

150. Kostic AD, Xavier RJ, Gevers D. The Microbiome in Inflammatory Bowel Disease: Current Status and the Future Ahead. YGAST. Elsevier, Inc; 2014 May

1;146(6):1489–99.

151. D'Haens GR, Geboes K, Peeters M, Baert F. Early lesions of recurrent Crohn's disease caused by infusion of intestinal contents in excluded ileum. Gastroenterology. 1998.

152. Lupp C, Robertson ML, Wickham ME, Sekirov I, Champion OL, Gaynor EC, et al. Host-Mediated Inflammation Disrupts the Intestinal Microbiota and Promotes the Overgrowth of Enterobacteriaceae. Cell Host & Microbe. 2007 Aug;2(2):119–29.

153. Martinez-Medina M, Aldeguer X, Lopez-Siles M, González-Huix F, López-Oliu C, Dahbi G, et al. Molecular diversity of Escherichia coli in the human gut: New ecological evidence supporting the role of adherent-invasive E. coli (AIEC) in Crohn's disease. Inflammatory Bowel Diseases. 2009 Jun;15(6):872–82.

154. Morgan XC, Tickle TL, Sokol H, Gevers D, Devaney KL, Ward DV, et al. Dysfunction of the intestinal microbiome in inflammatory bowel disease and treatment. Genome Biology. BioMed Central Ltd; 2012 Sep 26;13(9):R79.

155. Benjamin JL, Hedin CRH, Koutsoumpas A, Ng SC, McCarthy NE, Prescott NJ, et al. Smokers with active Crohn's disease have a clinically relevant dysbiosis of the gastrointestinal microbiota*. Inflammatory Bowel Diseases. 2012 Jun;18(6):1092–100.

156. Medellin-Pena MJ, Wang H, Johnson R, Anand S, Griffiths MW. Probiotics Affect Virulence-Related Gene Expression in Escherichia coli O157:H7. Applied and Environmental Microbiology. 2007 Jun 27;73(13):4259–67.

157. Llopis M, Antolin M, Carol M, Borruel N, Casellas F, Martinez C, et al. Lactobacillus casei downregulates commensals' inflammatory signals in Crohn's disease mucosa. Inflammatory Bowel Diseases. 2009 Feb;15(2):275–83.

158. Sokol H, Pigneur B, Watterlot L, Lakhdari O, Bermudez-Humaran LG, Gratadoux J-J, et al. Faecalibacterium prausnitzii is an anti-inflammatory commensal bacterium identified by gut microbiota analysis of Crohn disease patients. PNAS. National Acad Sciences; 2008;105(43):16731–6.

159. Sokol H, Seksik P, Furet JP, Firmesse O, Nion-Larmurier I, Beaugerie L, et al. Low counts of Faecalibacterium prausnitzii in colitis microbiota. Inflammatory Bowel Diseases. 2009 Aug;15(8):1183–9.

160. Varela E, Manichanh C, Gallart M, Torrejón A, Borruel N, Casellas F, et al. Colonisation by Faecalibacterium prausnitziiand maintenance of clinical remission in patients with ulcerative colitis. Aliment Pharmacol Ther. 2013 Jun 3;38(2):151–61.

161. Ahmad MS, Krishnan S, Ramakrishna BS, Mathan M, Pulimood AB, Murthy SN. Butyrate and glucose metabolism by colonocytes in experimental colitis in mice. Gut. BMJ Group; 2000 Apr;46(4):493–9.

162. Rakoff-Nahoum S, Paglino J, Eslami-Varzaneh F. Recognition of commensal microflora by toll-like receptors is required for intestinal homeostasis. Cell. 2004;118(2):229–41.

163. Peterson LW, Artis D. Intestinal epithelial cells: regulators of barrier function and immune homeostasis. Nature Publishing Group. Nature Publishing Group; 2014

Mar 1;14(3):141–53.

164. Okayasu I, Hatakeyama S, Yamada M, Ohkusa T, INAGAKI Y, NAKAYA R. A Novel Method in the Induction of Reliable Experimental Acute and Chronic Ulcerative-Colitis in Mice. YGAST. 1990 Mar;98(3):694–702.

165. Cooper HS, Murthy SN, Shah RS, Sedergran DJ. Clinicopathologic study of dextran sulfate sodium experimental murine colitis. Lab Invest. 1993 Aug;69(2):238–49.

166. Dieleman LA, Ridwan BU, TENNYSON GS, Beagley KW, BUCY RP, Elson CO. Dextran Sulfate Sodium-Induced Colitis Occurs in Severe Combined Immunodeficient Mice. YGAST. 1994 Dec;107(6):1643–52.

167. Perše M, Cerar A. Dextran Sodium Sulphate Colitis Mouse Model: Traps and Tricks. Journal of Biomedicine and Biotechnology. 2012;2012(1):1–13.

168. Kiesler P, Fuss IJ, Strober W. Experimental Models of Inflammatory Bowel Diseases. Cellular and Molecular Gastroenterology and Hepatology. Elsevier Inc; 2015 Mar 1;1(2):154–70.

169. Mankertz J, Schulzke J-D. Altered permeability in inflammatory bowel disease: pathophysiology and clinical implications. Current Opinion in Gastroenterology. 2007 Jul;23(4):379–83.

170. HERMISTON ML, GORDON JI. Inflammatory Bowel-Disease and Adenomas in Mice Expressing a Dominant-Negative N-Cadherin. Science. American Association for the Advancement of Science; 1995;270(5239):1203–7.

171. Peltekova VD, Wintle RF, Rubin LA, Amos CI, Huang Q, Gu X, et al. Functional variants of OCTN cation transporter genes are associated with Crohn disease. Nat Genet. 2004 Apr 11;36(5):471–5.

172. Tanaka T, Kohno H, Suzuki R, Yamada Y, Sugie S, Mori H. A novel inflammation-related mouse colon carcinogenesis model induced by azoxymethane and dextran sodium sulfate. Cancer Science. 2003 Nov;94(11):965–73.

173. Wirtz S, Neufert C, Weigmann B, Neurath MF. Chemically induced mouse models of intestinal inflammation. Nat Protoc. 2007 Mar;2(3):541–6.

174. Morris GP, Beck PL, Herridge MS, Depew WT, Szewczuk MR, Wallace JL. Hapten-induced model of chronic inflammation and ulceration in the rat colon. YGAST. 1989 Mar;96(3):795–803.

175. Neurath MF, Fuss I, Kelsall BL, Stüber E, Strober W. Antibodies to interleukin 12 abrogate established experimental colitis in mice. Journal of Experimental Medicine. Rockefeller Univ Press; 1995 Nov 1;182(5):1281–90.

176. Khanna R, Preiss JC, MacDonald JK, Timmer A. Anti-IL-12/23p40 antibodies for induction of remission in Crohn's disease. Timmer A, editor. Cochrane Database Syst Rev. Chichester, UK: John Wiley & Sons, Ltd; 2015;5:CD007572.

177. Neurath MF, Fuss I, Kelsall BL, Presky DH, Waegell W, Strober W. Experimental granulomatous colitis in mice is abrogated by induction of TGF-beta-mediated oral tolerance. Journal of Experimental Medicine. Rockefeller

Univ Press; 1996 Jun 1;183(6):2605–16.

178. Fuss IJ, Boirivant M, Lacy B, Strober W. The interrelated roles of TGF-beta and IL-10 in the regulation of experimental colitis. The Journal of Immunology. American Association of Immunologists; 2002 Jan 15;168(2):900–8.

179. Dohi T, Fujihashi K, Rennert PD, Iwatani K, Kiyono H, McGhee JR. Hapten-induced Colitis Is Associated with Colonic Patch Hypertrophy and T Helper Cell 2–Type Responses. Journal of Experimental Medicine. Rockefeller Univ Press; 1999 Apr 19;189(8):1169–80.

180. Dohi T, Fujihashi K, Kiyono H, Elson CO, McGhee JR. Mice deficient in Th1- and Th2-type cytokines develop distinct forms of hapten-induced colitis. Gastroenterology. 2000 Sep;119(3):724–33.

181. Fichtner-Feigl S. Treatment of murine Th1- and Th2-mediated inflammatory bowel disease with NF- B decoy oligonucleotides. J Clin Invest. 2005 Nov 1;115(11):3057–71.

182. Boirivant M, Strober W, Fuss IJ. Regulatory cells induced by feeding TNP-Haptenated colonic protein cross-protect mice from colitis induced by an unrelated hapten. Inflammatory Bowel Diseases. 2005 Jan;11(1):48–55.

183. Heller F, Fuss IJ, Nieuwenhuis EE, Blumberg RS, Strober W. Oxazolone colitis, a Th2 colitis model resembling ulcerative colitis, is mediated by IL-13-producing NK-T cells. Immunity. 2002 Nov;17(5):629–38.

184. Olszak T, An D, Zeissig S, Vera MP, Richter J, Franke A, et al. Microbial Exposure During Early Life Has Persistent Effects on Natural Killer T Cell Function. Science. 2012 Apr 26;336(6080):489–93.

185. Camelo A, Barlow JL, Drynan LF, Neill DR, Ballantyne SJ, Wong SH, et al. Blocking IL-25 signalling protects against gut inflammation in a type-2 model of colitis by suppressing nuocyte and NKT derived IL-13. J Gastroenterol. 2012 Apr 27;47(11):1198–211.

186. Gerlach K, Hwang Y, Nikolaev A, Atreya R, Dornhoff H, Steiner S, et al. TH9 cells that express the transcription factor PU.1 drive T cell–mediated colitis via IL-9 receptor signaling in intestinal epithelial cells. Nature Immunology. 2014 Jun 8;15(7):676–86.

187. Fuss IJ, Joshi B, Yang Z, Degheidy H, Fichtner-Feigl S, de Souza H, et al. IL-13Rα2-bearing, type II NKT cells reactive to sulfatide self-antigen populate the mucosa of ulcerative colitis. Gut. BMJ Publishing Group Ltd and British Society of Gastroenterology; 2014 Nov 1;63(11):1728–36.

188. Powrie F, Leach MW, Mauze S, CADDLE LB, Coffman RL. Phenotypically Distinct Subsets of Cd4(+) T-Cells Induce or Protect From Chronic Intestinal Inflammation in C - B-17 Scid Mice. International Immunology. 1993 Nov;5(11):1461–71.

189. Powrie F, Leach MW, Mauze S, Menon S, CADDLE LB. Inhibition of Thl responses prevents inflammatory bowel disease in scid mice reconstituted with CD45RB hi CD4+ T cells. Immunity. 1994;1(7):553–62.

190. Leach MW, Bean AG, Mauze S, Coffman RL, Powrie F. Inflammatory bowel disease in C.B-17 scid mice reconstituted with the CD45RBhigh subset of CD4+

T cells. AJPA. American Society for Investigative Pathology; 1996 May;148(5):1503–15.

191. Read S, Malmström V, Powrie F. Cytotoxic T lymphocyte-associated antigen 4 plays an essential role in the function of CD25(+)CD4(+) regulatory cells that control intestinal inflammation. Journal of Experimental Medicine. Rockefeller Univ Press; 2000;192(2):295–302.

192. Nakamura K, Kitani A, Strober W. Cell contact-dependent immunosuppression by CD4(+)CD25(+) regulatory T cells is mediated by cell surface-bound transforming growth factor beta. Journal of Experimental Medicine. 2001;194(5):629–44.

193. Fahlén L, Read S, Gorelik L, Hurst SD, Coffman RL, Flavell RA, et al. T cells that cannot respond to TGF-beta escape control by CD4(+)CD25(+) regulatory T cells. Journal of Experimental Medicine. 2005 Mar 7;201(5):737–46.

194. Neurath MF, Weigmann B, Finotto S, Glickman J, Nieuwenhuis E, Iijima H, et al. The transcription factor T-bet regulates mucosal T cell activation in experimental colitis and Crohn's disease. Journal of Experimental Medicine. Rockefeller Univ Press; 2002 May 6;195(9):1129–43.

195. Hue S, Ahern P, Buonocore S, Kullberg MC, Cua DJ, McKenzie BS, et al. Interleukin-23 drives innate and T cell-mediated intestinal inflammation. Journal of Experimental Medicine. 2006 Oct 16;203(11):2473–83.

196. Ahern PP, Schiering C, Buonocore S, McGeachy MJ, Cua DJ, Maloy KJ, et al. Interleukin-23 Drives Intestinal Inflammation through Direct Activity on T Cells. Immunity. Elsevier Ltd; 2010 Aug 27;33(2):279–88.

197. Sujino T, Kanai T, Ono Y, Mikami Y, Hayashi A, Doi T, et al. Regulatory T Cells Suppress Development of Colitis, Blocking Differentiation of T-Helper 17 Into Alternative T-Helper 1 Cells. YGAST. Elsevier Inc; 2011 Sep 1;141(3):1014–23.

198. Kühn R, Löhler J, Rennick D, Rajewsky K, Müller W. Interleukin-10-deficient mice develop chronic enterocolitis. Cell. 1993;75(2):263–74.

199. Groux H, O'Garra A, Bigler M, Rouleau M, Antonenko S, deVries JE, et al. A CD4(+) T-cell subset inhibits antigen-specific T-cell responses and prevents colitis. Nature. 1997;389(6652):737–42.

200. Glocker E-O, Kotlarz D, Boztug K, Gertz EM, Schäffer AA, Noyan F, et al. Inflammatory Bowel Disease and Mutations Affecting the Interleukin-10 Receptor. N Engl J Med. 2009 Nov 19;361(21):2033–45.

201. Berg DJ, Davidson N, Kühn R, Müller W, Menon S, Holland G, et al. Enterocolitis and colon cancer in interleukin-10-deficient mice are associated with aberrant cytokine production and CD4(+) TH1-like responses. J Clin Invest. American Society for Clinical Investigation; 1996 Aug 15;98(4):1010–20.

202. Roers A, Siewe L, Strittmatter E, Deckert M, Schlüter D, Stenzel W, et al. T cell-specific inactivation of the interleukin 10 gene in mice results in enhanced T cell responses but normal innate responses to lipopolysaccharide or skin irritation. Journal of Experimental Medicine. 2004 Nov 15;200(10):1289–97.

203. Rubtsov YP, Rasmussen JP, Chi EY, Fontenot J, Castelli L, Ye X, et al. Regulatory T Cell-Derived Interleukin-10 Limits Inflammation at Environmental

Interfaces. Immunity. 2008 Apr;28(4):546–58.

204. Zigmond E, Bernshtein B, Friedlander G, Walker CR, Yona S, Kim K-W, et al. Macrophage-Restricted Interleukin-10 Receptor Deficiency, but Not IL-10 Deficiency, Causes Severe Spontaneous Colitis. Immunity. Elsevier Inc; 2014 May 15;40(5):720–33.

205. Kullberg MC, Jankovic D, Feng CG, Hue S, Gorelick PL, McKenzie BS, et al. IL-23 plays a key role in Helicobacter hepaticus-induced T cell-dependent colitis. Journal of Experimental Medicine. Rockefeller Univ Press; 2006 Oct 30;203(11):2485–94.

206. Shouval DS, Biswas A, Goettel JA, McCann K, Conaway E, Redhu NS, et al. Interleukin-10 Receptor Signaling in Innate Immune Cells Regulates Mucosal Immune Tolerance and Anti-Inflammatory Macrophage Function. Immunity. Elsevier; 2014 May 15;40(5):706–19.

207. Garrett WS, Lord GM, Punit S, Lugo-Villarino G, Mazmanian SK, Ito S, et al. Communicable Ulcerative Colitis Induced by T-bet Deficiency in the Innate Immune System. Cell. 2007 Oct;131(1):33–45.

208. Velcich A, Yang WC, Heyer J, Fragale A, Nicholas C, Viani S, et al. Colorectal cancer in mice genetically deficient in the mucin Muc2. Science. American Association for the Advancement of Science; 2002;295(5560):1726–9.

209. Van der Sluis M, De Koning BAE, De Bruijn ACJM, Velcich A, Meijerink JPP, Van Goudoever JB, et al. Muc2-Deficient Mice Spontaneously Develop Colitis, Indicating That MUC2 Is Critical for Colonic Protection. Gastroenterology. 2006 Jul;131(1):117–29.

210. Nenci A, Becker C, Wullaert A, Gareus R, van Loo G, Danese S, et al. Epithelial NEMO links innate immunity to chronic intestinal inflammation. Nature. 2007 Mar 14;446(7135):557–61.

211. Matsumoto S, Okabe Y, Setoyama H, Takayama K, Ohtsuka J, Funahashi H, et al. Inflammatory bowel disease-like enteritis and caecitis in a senescence accelerated mouse P1/Yit strain. Gut. BMJ Publishing Group Ltd and British Society of Gastroenterology; 1998 Jul;43(1):71–8.

212. Pizarro TT, Pastorelli L, Bamias G, Garg RR, Reuter BK, Mercado JR, et al. SAMP1/YitFc mouse strain: A spontaneous model of Crohn's disease-like ileitis. Inflammatory Bowel Diseases. 2011 Dec;17(12):2566–84.

213. Klementowicz JE, Travis MA, Grencis RK. Trichuris muris: a model of gastrointestinal parasite infection. Semin Immunopathol. Springer-Verlag; 2012 Oct 11;34(6):815–28.

214. HURST RJM, Else KJ. Trichuris muris research revisited: a journey through time. Parasitology. 2013 Aug 21;140(11):1325–39.

215. Else KJ, Hültner L, Grencis RK. Modulation of Cytokine Production and Response Phenotypes in Murine Trichuriasis. Parasite Immunology. 1992 Jul;14(4):441–9.

216. BANCROFT AJ, Else KJ, Grencis RK. Low-level infection with Trichuris muris significantly affects the polarization of the CD4 response. Eur J Immunol. 1994 Dec;24(12):3113–8.

217. BANCROFT AJ, Else KJ, Humphreys NE, Grencis RK. The effect of challenge and trickle Trichuris muris infections on the polarisation of the immune response. International Journal for Parasitology. 2001 Dec;31(14):1627–37.

218. Behnke JM, Wakelin D. The survival of Trichuris muris in wild populations of its natural hosts. Parasitology. 1973 Oct;67(2):157–64.

219. Weinstock JV, Elliott DE. Helminths and the IBD hygiene hypothesis. Inflammatory Bowel Diseases. 2009 Jan;15(1):128–33.

220. Hunter MM, McKay DM. Helminths as therapeutic agents for inflammatory bowel disease. Aliment Pharmacol Ther. 2004 Jan;19(2):167–77.

221. KOYAMA K. NK1.1(+) cell depletion in vivo fails to prevent protection against infection with the murine nematode parasite Trichuris muris. Parasite Immunology. Blackwell Science Ltd; 2002 Nov;24(11-12):527–33.

222. KOYAMA K, TAMAUCHI H, ITO Y. The role of CD4+ and CD8+ T cells in protective immunity to the murine nematode parasite Trichuris muris. Parasite Immunology. Blackwell Publishing Ltd; 1995 Mar 1;17(3):161–5.

223. Humphreys NE, Worthington JJ, Little MC, Rice EJ, Grencis RK. The role of CD8(+) cells in the establishment and maintenance of a Trichuris muris infection. Parasite Immunology. Blackwell Science Ltd; 2004 Apr;26(4):187–96.

224. Perrigoue JG, Saenz SA, Siracusa MC, Allenspach EJ, Taylor BC, Giacomin PR, et al. MHC class II–dependent basophil–CD4+ T cell interactions promote TH2 cytokine–dependent immunity. Nature Publishing Group. Nature Publishing Group; 2009 May 24;10(7):697–705.

225. Blackwell NM, Else KJ. B Cells and Antibodies Are Required for Resistance to the Parasitic Gastrointestinal Nematode Trichuris muris. Infection and Immunity. 2001 Jun 1;69(6):3860–8.

226. Cliffe LJ, Humphreys NE, Lane TE, Potten CS, Booth C, Grencis RK. Accelerated intestinal epithelial cell turnover: A new mechanism of parasite expulsion. Science. American Association for the Advancement of Science; 2005;308(5727):1463–5.

227. Hasnain SZ, Evans CM, Roy M, Gallagher AL, Kindrachuk KN, Barron L, et al. Muc5ac: a critical component mediating the rejection of enteric nematodes. Journal of Experimental Medicine. 2011 May 9;208(5):893–900.

228. Schauer DB, Falkow S. The eae gene of Citrobacter freundii biotype 4280 is necessary for colonization in transmissible murine colonic hyperplasia. Infection and Immunity. American Society for Microbiology; 1993 Nov 1;61(11):4654–61.

229. Deng WY, Vallance BA, Li YL, Puente JL, Finlay BB. Citrobacter rodentium translocated intimin receptor (Tir) is an essential virulence factor needed for actin condensation, intestinal colonization and colonic hyperplasia in mice. Mol Microbiol. Blackwell Science Ltd; 2003 Apr;48(1):95–115.

230. Luperchio SA, Schauer DB. Molecular pathogenesis of Citrobacter rodentium and transmissible murine colonic hyperplasia. Microbes Infect. 2001 Apr;3(4):333–40.

231. Wiles S, Clare S, Harker J, Huett A, Young D, Dougan G, et al. Organ

specificity, colonization and clearance dynamics in vivo following oral challenges with the murine pathogen Citrobacter rodentium. Cell Microbiol. 2004 Oct;6(10):963–72.

232. Gibson DL, Ma C, Bergstrom KSB, Huang JT, Man C, Vallance BA. MyD88 signalling plays a critical role in host defence by controlling pathogen burden and promoting epithelial cell homeostasis during Citrobacter rodentium-induced colitis. Cell Microbiol. 2008 Mar;10(3):618–31.

233. Lebeis SL, Bommarius B, Parkos CA, Sherman MA, Kalman D. TLR Signaling Mediated by MyD88 Is Required for a Protective Innate Immune Response by Neutrophils to Citrobacter rodentium. The Journal of Immunology. 2007 Jun 19;179(1):566–77.

234. Rathinam VAK, Vanaja SK, Fitzgerald KA. Regulation of inflammasome signaling. Nature Immunology. 2012 Mar 19;13(4):333–332.

235. Kayagaki N, Warming S, Lamkanfi M, Walle LV, Louie S, Dong J, et al. Non-canonical inflammasome activation targets caspase-11. Nature. Nature Publishing Group; 2011 Oct 24;479(7371):117–21.

236. Torchinsky MB, Garaude J, Martin AP, Blander JM. Innate immune recognition of infected apoptotic cells directs TH17 cell differentiation. Nature. Nature Publishing Group; 2009 Feb 23;457(7234):78–82.

237. Geddes K, Rubino SJ, Magalhaes JG, Streutker C, Le Bourhis L, Cho JH, et al. Identification of an innate T helper type 17 response to intestinal bacterial pathogens. Nature Medicine. Nature Publishing Group; 2011 Jun 12;17(7):837–44.

238. Zheng Y, Valdez PA, Danilenko DM, Hu Y, Sa SM, Gong Q, et al. Retinoic acid expression associates with enhanced IL-22 production by T cells and innate lymphoid cells and attenuation of intestinal inflammation. Nature Medicine [Internet]. 2008 Feb 10;210(10):2025–39. Available from: http://www.jem.org/cgi/doi/10.1084/jem.20130903

239. Willing BP, Vacharaksa A, Croxen M, Thanachayanont T, Finlay BB. Altering Host Resistance to Infections through Microbial Transplantation. Bereswill S, editor. PLoS ONE. 2011 Oct 28;6(10):e26988–9.

240. Ghosh S, Dai C, Brown K, Rajendiran E, Makarenko S, Baker J, et al. Colonic microbiota alters host susceptibility to infectious colitis by modulating inflammation, redox status, and ion transporter gene expression. AJP: Gastrointestinal and Liver Physiology. 2011 Jun 28;301(1):G39–G49.

241. Waddington CH. The Epigenotype. Int J Epidemiol. 2012 Mar 14;41(1):10–3.

242. Däbritz J, Menheniott TR. Linking Immunity, Epigenetics, and Cancer in Inflammatory Bowel Disease. Inflammatory Bowel Diseases. 2014 Sep;20(9):1638–54.

243. Sauvageau M, Sauvageau G. Polycomb Group Proteins: Multi-Faceted Regulators of Somatic Stem Cells and Cancer. Stem Cell. Elsevier Inc; 2010 Sep 3;7(3):299–313.

244. Chuang JC, Jones PA. Epigenetics and MicroRNAs. Pediatr Res. 2007 May;61(5 Part 2):24R–29R.

245. Eccleston A, Cesari F, Skipper M. Transcription and epigenetics. Nature. 2013;502(7472):461–1.

246. Bell AC, Felsenfeld G. Methylation of a CTCF-dependent boundary controls imprinted expression of the Igf2 gene. Nature. 2000;405(6785):482–5.

247. Fraga MF, Ballestar E, Paz MF, Ropero S, Setien F, Ballestart ML, et al. Epigenetic differences arise during the lifetime of monozygotic twins. PNAS. National Acad Sciences; 2005;102(30):10604–9.

248. Kaminsky ZA, Tang T, Wang S-C, Ptak C, Oh GHT, Wong AHC, et al. DNA methylation profiles in monozygotic and dizygotic twins. Nat Genet. 2009 Jan 18;41(2):240–5.

249. Renz H, Mutius von E, Brandtzaeg P, Cookson WO, Autenrieth IB, Haller D. Gene-environment interactions in chronic inflammatory disease. Nature Publishing Group. Nature Publishing Group; 2011 Apr 1;12(4):273–7.

250. Satsangi J, Kennedy NA, Henderson P, Wilson DC, Nimmo ER. Exploring the hidden heritability of inflammatory bowel disease. Gut. 2011 Sep 30;60(11):1447–8.

251. Painter RC, Osmond C, Gluckman P, Hanson M, Phillips D, Roseboom TJ. Transgenerational effects of prenatal exposure to the Dutch famine on neonatal adiposity and health in later life. BJOG: An International Journal of Obstetrics & Gynaecology. 2008 Sep;115(10):1243–9.

252. Morgan HD, Sutherland H, Martin D, Whitelaw E. Epigenetic inheritance at the agouti locus in the mouse. Nat Genet. 1999 Nov;23(3):314–8.

253. Cooper DN, Gerber-Huber S. DNA methylation and CpG suppression. Cell differentiation. 1985.

254. Jones PA. Functions of DNA methylation: islands, start sites, gene bodies and beyond. Nature Reviews Genetics. Nature Publishing Group; 2012 May 29;13(7):484–92.

255. Bird AP, Wolffe AP. Methylation-induced repression—belts, braces, and chromatin. Cell. 1999;99(5):451–4.

256. Young JI, Hong EP, Castle JC, Crespo-Barreto J, Bowman AB, Rose MF, et al. Regulation of RNA splicing by the methylation-dependent transcriptional repressor methyl-CpG binding protein 2. PNAS. National Acad Sciences; 2005 Dec 6;102(49):17551–8.

257. Sproul D, Nestor C, Culley J, Dickson JH, Dixon JM, Harrison DJ, et al. Transcriptionally repressed genes become aberrantly methylated and distinguish tumors of different lineages in breast cancer. PNAS. National Acad Sciences; 2011;108(11):4364–9.

258. Keshet I, Schlesinger Y, Farkash S, Rand E, Hecht M, Segal E, et al. Evidence for an instructive mechanism of de novo methylation in cancer cells. Nat Genet. 2006 Feb;38(2):149–53.

259. Bestor TH. The DNA methyltransferases of mammals. Human Molecular Genetics. Oxford University Press; 2000 Oct;9(16):2395–402.

260. LI E, Bestor TH, JAENISCH R. Targeted Mutation of the Dna Methyltransferase Gene Results in Embryonic Lethality. Cell. 1992;69(6):915–26.

261. Biniszkiewicz D, Gribnau J, Ramsahoye B, Gaudet F, Eggan K, Humpherys D, et al. Dnmt1 overexpression causes genomic hypermethylation, loss of imprinting, and embryonic lethality. Molecular and Cellular Biology. American Society for Microbiology; 2002 Apr;22(7):2124–35.

262. Harris AR, Nagy-Szakal D, Pedersen N, Opekun A, Bronsky J, Munkholm P, et al. Genome-wide peripheral blood leukocyte DNA methylation microarrays identified a single association with inflammatory bowel diseases. Inflammatory Bowel Diseases. 2012 Dec;18(12):2334–41.

263. Nimmo ER, Prendergast JG, Aldhous MC, Kennedy NA, Henderson P, Drummond HE, et al. Genome-wide methylation profiling in Crohn's disease identifies altered epigenetic regulation of key host defense mechanisms including the Th17 pathway. Inflammatory Bowel Diseases. 2012 May;18(5):889–99.

264. Cooke J, Zhang H, Greger L, Silva A-L, Massey D, Dawson C, et al. Mucosal genome-wide methylation changes in inflammatory bowel disease. Inflammatory Bowel Diseases. 2012 Nov;18(11):2128–37.

265. Kouzarides T. Chromatin Modifications and Their Function. Cell. 2007 Feb;128(4):693–705.

266. Jenuwein T, Allis CD. Translating the histone code. Science. American Association for the Advancement of Science; 2001;293(5532):1074–80.

267. Zentner GE, Henikoff S. Regulation of nucleosome dynamics by histone modifications. Nature Publishing Group. Nature Publishing Group; 2013 Mar 1;20(3):259–66.

268. Henikoff S, Shilatifard A. Histone modification: cause or cog? Trends in Genetics. Elsevier Ltd; 2011 Oct 1;27(10):389–96.

269. Szerlong HJ, Hansen JC. Nucleosome distribution and linker DNA: connecting nuclear function to dynamic chromatin structure. Biochem Cell Biol. 2011 Feb;89(1):24–34.

270. Parmar JJ, Marko JF, Padinhateeri R. Nucleosome positioning and kinetics near transcription-start-site barriers are controlled by interplay between active remodeling and DNA sequence. Nucleic Acids Research. 2013 Dec 28;42(1):128–36.

271. Ho L, Crabtree GR. Chromatin remodelling during development. Nature. 2010 Jan 28;463(7280):474–84.

272. Bowen NJ, Fujita N, Kajita M, Wade PA. Mi-2/NuRD: multiple complexes for many purposes. Biochimica et Biophysica Acta (BBA) - Gene Structure and Expression. 2004 Mar;1677(1-3):52–7.

273. Denslow SA, Wade PA. The human Mi-2/NuRD complex and gene regulation. Oncogene. 2007 Aug 13;26(37):5433–8.

274. Deaton AM, Bird A. CpG islands and the regulation of transcription. Genes & Development. 2011 May 16;25(10):1010–22.

275. Robertson KD, Jones PA. DNA methylation: past, present and future directions. Carcinogenesis. Oxford University Press; 2000 Mar;21(3):461–7.

276. Bird AP. Cpg-Rich Islands and the Function of Dna Methylation. Nature. 1986;321(6067):209–13.

277. Mohn F, Weber M, Rebhan M, Roloff TC, Richter J, Stadler MB, et al. Lineage-Specific Polycomb Targets and De Novo DNA Methylation Define Restriction and Potential of Neuronal Progenitors. Molecular Cell. 2008 Jun;30(6):755–66.

278. Klose RJ, Bird AP. Genomic DNA methylation: the mark and its mediators. Trends in Biochemical Sciences. 2006 Feb;31(2):89–97.

279. Menafra R, Brinkman AB, Matarese F, Franci G, Bartels SJJ, Nguyen L, et al. Genome-Wide Binding of MBD2 Reveals Strong Preference for Highly Methylated Loci. Tora L, editor. PLoS ONE. 2014 Jun 13;9(6):e99603.

280. Baubec T, Ivánek R, Lienert F, Schübeler D. Methylation-Dependent and -Independent Genomic Targeting Principlesof the MBD Protein Family. Cell. Elsevier Inc; 2013 Apr 11;153(2):480–92.

281. Zhang Y, Ng HH, Erdjument-Bromage H. Analysis of the NuRD subunits reveals a histone deacetylase core complex and a connection with DNA methylation. Genes Development. 1999.

282. Stefanska B, Suderman M, Machnes Z, Bhattacharyya B, Hallett M, Szyf M. Transcription onset of genes critical in liver carcinogenesis is epigenetically regulated by methylated DNA-binding protein MBD2. Carcinogenesis. Oxford University Press; 2013 Dec;34(12):2738–49.

283. Gunther K, Rust M, Leers J, Boettger T, Scharfe M, Jarek M, et al. Differential roles for MBD2 and MBD3 at methylated CpG islands, active promoters and binding to exon sequences. Nucleic Acids Research. 2013 Mar 12;41(5):3010–21.

284. Scarpa M, Stylianou E. Epigenetics: Concepts and relevance to IBD pathogenesis. Inflammatory Bowel Diseases. 2012 Oct;18(10):1982–96.

285. Ivashkiv LB. Epigenetic regulation of macrophage polarization and function. Trends in Immunology. Elsevier Ltd; 2013 May 1;34(5):216–23.

286. Sica A, Mantovani A. Macrophage plasticity and polarization: in vivo veritas. J Clin Invest. 2012 Mar 1;122(3):787–95.

287. Kleinnijenhuis J, Quintin J, Preijers F. Bacille Calmette-Guerin induces NOD2-dependent nonspecific protection from reinfection via epigenetic reprogramming of monocytes. 2012.

288. Zhang Z, Maurer K, Perin JC, Song L, Sullivan KE. Cytokine-Induced Monocyte Characteristics in SLE. Journal of Biomedicine and Biotechnology. 2010;2010(6):1–13.

289. Zanette DL, van Eggermond MCJA, Haasnoot G, van den Elsen PJ. Simvastatin reduces CCL2 expression in monocyte-derived cells by induction of a repressive CCL2 chromatin state. Human Immunology. American Society for Histocompatibility and Immunogenetics; 2014 Jan 1;75(1):10–4.

290. Wen H, Dou Y, Hogaboam CM, Kunkel SL. Epigenetic regulation of dendritic cell-derived interleukin-12 facilitates immunosuppression after a severe innate immune response. Blood. American Society of Hematology; 2008;111(4):1797–804.

291. Kim H-P, Lee Y-S, Park JH, Kim Y-J. Transcriptional and epigenetic networks in the development and maturation of dendritic cells. Epigenomics. 2013 Apr;5(2):195–204.

292. Ishii M, Asano K, Namkoong H, Tasaka S, Mizoguchi K, Asami T, et al. CRTH2 Is A Critical Regulator of Neutrophil Migration and Resistance to Polymicrobial Sepsis. The Journal of Immunology. 2012 May 18;188(11):5655–64.

293. Zhu J, Yamane H, Paul WE. Differentiation of Effector CD4 T Cell Populations *. Annu Rev Immunol. 2010 Mar;28(1):445–89.

294. Wilson CB, Rowell E, Sekimata M. Epigenetic control of T-helper-cell differentiation. Nat Rev Immunol. 2009 Feb;9(2):91–105.

295. Allan RS, Zueva E, Cammas F, Schreiber HA, Masson V, Belz GT, et al. An epigenetic silencing pathway controlling T helper 2 cell lineage commitment. Nature. 2012 Jul 4;487(7406):249–53.

296. Janson PCJ, Winerdal ME, Winqvist O. At the crossroads of T helper lineage commitment—Epigenetics points the way. BBA - General Subjects. Elsevier B.V; 2009 Sep 1;1790(9):906–19.

297. Kanno Y, Vahedi G, Hirahara K, Singleton K, O'Shea JJ. Transcriptional and Epigenetic Control of T Helper Cell Specification: Molecular Mechanisms Underlying Commitment and Plasticity *. Annu Rev Immunol. 2012 Apr 23;30(1):707–31.

298. Katoh H, Qin ZS, Liu R, Wang L, Li W, Li X, et al. FOXP3 Orchestrates H4K16 Acetylation and H3K4 Trimethylation for Activation of Multiple Genes by Recruiting MOF and Causing Displacement of PLU-1. Molecular Cell. Elsevier Inc; 2011 Dec 9;44(5):770–84.

299. Zheng Y, Josefowicz SZ, Kas A, Chu T-T, Gavin MA, Rudensky AY. Genome-wide analysis of Foxp3 target genes in developing and mature regulatory T cells. Nature. 2007 Jan 21;445(7130):936–40.

300. Manichanh C, Borruel N, Casellas F, Guarner F. The gut microbiota in IBD. Nat Rev Gastroenterol Hepatol. Nature Publishing Group; 2012 Aug 21;9(10):599–608.

301. Leung C-H, Lam W, Ma D-L, Gullen EA, Cheng Y-C. Butyrate mediates nucleotide-binding and oligomerisation domain (NOD) 2-dependent mucosal immune responses against peptidoglycan. Eur J Immunol. 2009 Oct 14;39(12):3529–37.

302. Ghadimi D, Helwig U, Schrezenmeir J, Heller KJ, de Vrese M. Epigenetic imprinting by commensal probiotics inhibits the IL-23/IL-17 axis in an in vitro model of the intestinal mucosal immune system. J Leukoc Biol. 2012 Oct 1;92(4):895–911.

303. Takahashi K, Sugi Y, Hosono A, Kaminogawa S. Epigenetic Regulation of TLR4 Gene Expression in Intestinal Epithelial Cells for the Maintenance of Intestinal

Homeostasis. The Journal of Immunology. 2009 Nov 4;183(10):6522–9.

304. Takahashi K, Sugi Y, Nakano K, Tsuda M, Kurihara K, Hosono A, et al. Epigenetic Control of the Host Gene by Commensal Bacteria in Large Intestinal Epithelial Cells. Journal of Biological Chemistry. 2011 Oct 7;286(41):35755–62.

305. Lin Z, Hegarty JP, Cappel JA, Yu W, Chen X, Faber P, et al. Identification of disease-associated DNA methylation in intestinal tissues from patients with inflammatory bowel disease. Clinical Genetics. 2010 Oct 18;80(1):59–67.

306. Wright KL, Ting JP-Y. Epigenetic regulation of MHC-II and CIITA genes. Trends in Immunology. 2006 Sep;27(9):405–12.

307. Zika E, Ting JP-Y. Epigenetic control of MHC-II: interplay between CIITA and histone-modifying enzymes. Current Opinion in Immunology. 2005 Feb;17(1):58–64.

308. Barrett JC, Hansoul S, Nicolae DL, Cho JH, Duerr RH, Rioux JD, et al. Genome-wide association defines more than 30 distinct susceptibility loci for Crohn's disease. Nat Genet. 2008 Jun 29;40(8):955–62.

309. Jostins L, Barrett JC. Genetic risk prediction in complex disease. Human Molecular Genetics. 2011 Sep 23;20(R2):R182–8.

310. Nimmo ER, Stevens C, Phillips AM, Smith A, Drummond HE, Noble CL, et al. TLE1 Modifies the Effects of NOD2 in the Pathogenesis of Crohn'sDisease. Gastroenterology. Elsevier Inc; 2011 Sep 1;141(3):972–2.

311. Wellcome Trust Case Control Consortium, Craddock N, Hurles ME, Cardin N, Pearson RD, Plagnol V, et al. Genome-wide association study of CNVs in 16,000 cases of eight common diseases and 3,000 shared controls. Nature. 2010 Apr 1;464(7289):713–20.

312. Phythian-Adams AT, Cook PC, Lundie RJ, Jones LH, Smith KA, Barr TA, et al. CD11c depletion severely disrupts Th2 induction and development in vivo. J Exp Med. Rockefeller Univ Press; 2010 Sep 27;207(10):2089–96.

313. Worthington JJ, Czajkowska BI, Melton AC, Travis MA. Intestinal Dendritic Cells Specialize to Activate Transforming Growth Factor. Gastroenterology. Elsevier Inc; 2011 Nov 1;141(5):1802–12.

314. Peña-Llopis S, Brugarolas J. Simultaneous isolation of high-quality DNA, RNA, miRNA and proteins from tissues for genomic applications. Nat Protoc. 2013 Oct 17;8(11):2240–55.

315. Antwis RE, Haworth RL, Engelmoer DJP, Ogilvy V, Fidgett AL, Preziosi RF. Ex situ diet influences the bacterial community associated with the skin of red-eyed tree frogs (Agalychnis callidryas). PLoS ONE. 2014;9(1):e85563.

316. Abe K, Nguyen KP, Fine SD, Mo J-H, Shen C, Shenouda S, et al. Conventional dendritic cells regulate the outcome of colonic inflammation independently of T cells. PNAS. 2007 Oct 23;104(43):17022–7.

317. Kaser A, Zeissig S, Blumberg RS. Inflammatory Bowel Disease. Annu Rev Immunol. 2010 Mar;28(1):573–621.

318. Cook PC, Owen H, Deaton AEEM, Borger JG, Brown SL, Clouaire T, et al. A

dominant role for the methyl-CpG-binding protein Mbd2 in controlling Th2 induction by dendritic cells. Nature Communications. Nature Publishing Group; 2015 Apr 17;6:1–11.

319. Hutchins AS, Mullen AC, Lee HW, Sykes KJ, High FA, Hendrich BD, et al. Gene silencing quantitatively controls the function of a developmental trans-activator. Molecular Cell. 2002 Jul;10(1):81–91.

320. Berger J, Sansom O, Clarke A, Bird A. MBD2 Is Required for Correct Spatial Gene Expression in the Gut. Molecular and Cellular Biology. 2007 May 15;27(11):4049–57.

321. Hutchins AS, Artis D, Hendrich BD, Bird AP, Scott P, Reiner SL. Cutting edge: a critical role for gene silencing in preventing excessive type 1 immunity. The Journal of Immunology. 2005 Nov 1;175(9):5606–10.

322. Eads CA, Nickel AE, Laird PW. Complete genetic suppression of polyp formation and reduction of CpG-island hypermethylation in Apc(Min/+) Dnmt1-hypomorphic Mice. Cancer Research. 2002 Mar 1;62(5):1296–9.

323. Laird PW, Jackson-Grusby L, Fazeli A, Dickinson SL. Suppression of intestinal neoplasia by DNA hypomethylation. Cell. 1995;81(2):197–205.

324. Su LK, Kinzler KW, Vogelstein B, Preisinger AC, Moser AR, Luongo C, et al. Multiple intestinal neoplasia caused by a mutation in the murine homolog of the APC gene. Science. American Association for the Advancement of Science; 1992 May 1;256(5057):668–70.

325. Sansom OJ, Berger J, Bishop SM, Hendrich B, Bird A, Clarke AR. Deficiency of Mbd2 suppresses intestinal tumorigenesis. Nat Genet. 2003 Jun;34(2):145–7.

326. Noble CL, Abbas AR, Cornelius J, Lees CW, Ho G-T, Toy K, et al. Regional variation in gene expression in the healthy colon is dysregulated in ulcerative colitis. Gut. 2008 Apr 29;57(10):1398–405.

327. Schulz O, Pabst O. Antigen sampling in the small intestine. Trends in Immunology. Elsevier Ltd; 2013 Apr 1;34(4):155–61.

328. Pabst O. New concepts in the generation and functions of IgA. Nature Publishing Group. Nature Publishing Group; 2012 Oct 29;12(12):821–32.

329. Mantis NJ, Forbes SJ. Secretory IgA: Arresting Microbial Pathogens at Epithelial Borders. Immunol Invest. 2010 Jan;39(4-5):383–406.

330. Mizoguchi A, Mizoguchi E, Takedatsu H, Blumberg RS, Bhan AK. Chronic intestinal inflammatory condition generates IL-10-producing regulatory B cell subset characterized by CD1d upregulation. Immunity. 2002 Feb;16(2):219–30.

331. Lee JH, Noh J, Noh G, Choi WS, Cho S, Lee SS. Allergen-specific transforming growth factor-β-producing CD19+CD5+ regulatory B-cell (Br3) responses in human late eczematous allergic reactions to cow's milk. J Interferon Cytokine Res. 2011 May;31(5):441–9.

332. Schoenberger SP. CD69 guides CD4+ T cells to the seat of memory. Proc Natl Acad Sci USA. National Acad Sciences; 2012 May 29;109(22):8358–9.

333. NAOR D, NEDVETZKI S, WALMSLEY M, YAYON A, TURLEY EA, GOLAN I, et

al. CD44 Involvement in Autoimmune Inflammations: The Lesson to be Learned from CD44-Targeting by Antibody or from Knockout Mice. Annals of the New York Academy of Sciences. Blackwell Publishing Inc; 2007 Sep 1;1110(1):233–47.

334. Bonder CS. Use of CD44 by CD4+ Th1 and Th2 lymphocytes to roll and adhere. Blood. 2006 Jun 15;107(12):4798–806.

335. Curtsinger JM, Lins DC, Mescher MF. CD8+ memory T cells (CD44high, Ly-6C+) are more sensitive than naive cells to (CD44low, Ly-6C-) to TCR/CD8 signaling in response to antigen. The Journal of Immunology. 1998 Apr 1;160(7):3236–43.

336. Pender SL, Lionetti P, Murch SH, Wathan N, MacDonald TT. Proteolytic degradation of intestinal mucosal extracellular matrix after lamina propria T cell activation. Gut. BMJ Publishing Group Ltd and British Society of Gastroenterology; 1996 Aug 1;39(2):284–90.

337. Di Sabatino A, Rovedatti L, Kaur R, Spencer JP, Brown JT, Morisset VD, et al. Targeting Gut T Cell Ca2+ Release-Activated Ca2+ Channels Inhibits T Cell Cytokine Production and T-Box Transcription Factor T-Bet in Inflammatory Bowel Disease. The Journal of Immunology. 2009 Aug 20;183(5):3454–62.

338. Sandborn WJ, Feagan BG, Rutgeerts P, Hanauer S, Colombel J-F, Sands BE, et al. Vedolizumab as Induction and Maintenance Therapy for Crohn's Disease. N Engl J Med. 2013 Aug 22;369(8):711–21.

339. Hall LJ, Faivre E, Quinlan A, Shanahan F, Nally K, Melgar S. Induction and Activation of Adaptive Immune Populations During Acute and Chronic Phases of a Murine Model of Experimental Colitis. Dig Dis Sci. 2010 May 14;56(1):79–89.

340. Grencis RK. Cytokine regulation of resistance and susceptibility to intestinal nematode infection—from host to parasite. Veterinary parasitology. 2001.

341. HAYES KS, BANCROFT AJ, Grencis RK. The role of TNF-α in Trichuris muris infection I: influence of TNF-α receptor usage, gender and IL-13. Parasite Immunology. 2007 Nov;29(11):575–82.

342. BANCROFT AJ, McKenzie A, Grencis RK. A critical role for IL-13 in resistance to intestinal nematode infection. The Journal of Immunology. American Association of Immunologists; 1998;160(7):3453–61.

343. Else KJ, Grencis RK. Antibody-independent effector mechanisms in resistance to the intestinal nematode parasite Trichuris muris. Infection and Immunity. American Society for Microbiology; 1996 Aug;64(8):2950–4.

344. Buisson A, Chevaux JB, Allen PB, Bommelaer G, Peyrin-Biroulet L. Review article: the natural history of postoperative Crohn's disease recurrence. Aliment Pharmacol Ther. 2012 Feb 7;35(6):625–33.

345. Bogdanović O, Veenstra GJC. DNA methylation and methyl-CpG binding proteins: developmental requirements and function. Chromosoma. 2009 Jun 9;118(5):549–65.

346. Kinnebrew MA, Buffie CG, Diehl GE, Zenewicz LA, Leiner I, Hohl TM, et al. Interleukin 23 Production by Intestinal CD103. Immunity. Elsevier Inc; 2012 Feb 24;36(2):276–87.

347. Rugtveit J, Nilsen EM, Bakka A, Carlsen H, Brandtzaeg P, Scott H. Cytokine profiles differ in newly recruited and resident subsets of mucosal macrophages from inflammatory bowel disease. YGAST. 1997 May;112(5):1493–505.

348. Jones GR, Kennedy NA, Lees CW, Arnott ID, Satsangi J. Systematic review: The use of thiopurines or anti-TNF in post-operative Crohn's disease maintenance--progress and prospects. Aliment Pharmacol Ther. 2014 Jun;39(11):1253–65.

349. Robben PM. Recruitment of Gr-1+ monocytes is essential for control of acute toxoplasmosis. Journal of Experimental Medicine. 2005 Jun 6;201(11):1761–9.

350. Dunay IR, DaMatta RA, Fux B, Presti R, Greco S, Colonna M, et al. Gr1+ Inflammatory Monocytes Are Required for Mucosal Resistance to the Pathogen Toxoplasma gondii. Immunity. 2008 Aug;29(2):306–17.

351. Dunay IR, Fuchs A, Sibley LD. Inflammatory Monocytes but Not Neutrophils Are Necessary To Control Infection with Toxoplasma gondii in Mice. Infection and Immunity. 2010 Mar 16;78(4):1564–70.

352. Foti M, Granucci F, Ricciardi-Castagnoli P. A central role for tissue-resident dendritic cells in innate responses. Trends in Immunology. 2004 Dec;25(12):650–4.

353. Economou M, Trikalinos TA, Loizou KT, Tsianos EV, Ioannidis JPA. Differential Effects of NOD2 Variants on Crohn's Disease Risk and Phenotype in Diverse Populations: A Metaanalysis. The American Journal of Gastroenterology. 2004 Dec;99(12):2393–404.

354. Berndt BE, Zhang M, Chen GH, Huffnagle GB, Kao JY. The Role of Dendritic Cells in the Development of Acute Dextran Sulfate Sodium Colitis. The Journal of Immunology. American Association of Immunologists; 2007 Oct 18;179(9):6255–62.

355. Abe K, Nguyen KP, Fine SD, Mo J-H, Shen C, Shenouda S, et al. Conventional dendritic cells regulate the outcome of colonic inflammation independently of T cells. PNAS. National Acad Sciences; 2007 Oct 23;104(43):17022–7.

356. Hans W, Schölmerich J, Gross V, Falk W. The role of the resident intestinal flora in acute and chronic dextran sulfate sodium-induced colitis in mice. European Journal of Gastroenterology & Hepatology. 2000 Mar 1;12(3):267&hyhen; 273–3.

357. Rubio C. The Natural Antimicrobial Enzyme Lysozyme is Up-Regulated in Gastrointestinal Inflammatory Conditions. Pathogens. 2014 Mar;3(1):73–92.

358. Rubio CA. Lysozyme expression in microscopic colitis. Journal of Clinical Pathology. BMJ Publishing Group Ltd and Association of Clinical Pathologists; 2011 Jun;64(6):510–5.

359. Rubio CA. Lysozyme-rich mucus metaplasia in duodenal crypts supersedes Paneth cells in celiac disease. Virchows Arch. 2011 Jul 18;459(3):339–46.

360. Hashimoto S, Suzuki T, Dong HY, Yamazaki N, Matsushima K. Serial analysis of gene expression in human monocytes and macrophages. Blood. 1999;94(3):837–44.

361. Lee CG, Jenkins NA, Gilbert DJ, Copeland NG, O'Brien WE. Cloning and analysis of gene regulation of a novel LPS-inducible cDNA. Immunogenetics. 1995;41(5):263–70.

362. Degrandi D, Hoffmann R, Beuter-Gunia C, Pfeffer K. The proinflammatory cytokine-induced IRG1 protein associates with mitochondria. J Interferon Cytokine Res. 2009 Jan;29(1):55–67.

363. Gironella M, Calvo C, Fernández A, Closa D, Iovanna JL, Rosello-Catafau J, et al. Reg3β deficiency impairs pancreatic tumor growth by skewing macrophage polarization. Cancer Research. 2013 Sep 15;73(18):5682–94.

364. Sarma JV, Ward PA. The complement system. Cell Tissue Res. 2010 Sep 14;343(1):227–35.

365. HODGSON H, POTTER BJ, Jewell DP. Humoral Immune System in Inflammatory Bowel-Disease .1. Complement Levels. Gut. BMJ Publishing Group Ltd and British Society of Gastroenterology; 1977;18(9):749–53.

366. Dong W, Liu Y, Peng J, Chen L, Zou T, Xiao H, et al. The IRAK-1-BCL10-MALT1-TRAF6-TAK1 cascade mediates signaling to NF-kappaB from Toll-like receptor 4. Journal of Biological Chemistry. 2006 Sep 8;281(36):26029–40.

367. Jeltsch KM, Hu D, Brenner S, Iler JZO, Heinz GA, Nagel D, et al. Cleavage of roquin and regnase-1 by the paracaspase MALT1 releases their cooperatively repressed targets to promote TH17 differentiation. Nature Immunology. Nature Publishing Group; 2014 Oct 5;:1–13.

368. Biswas SK, Gangi L, Paul S, Schioppa T, Saccani A, Sironi M, et al. A distinct and unique transcriptional program expressed by tumor-associated macrophages (defective NF-kappa B and enhanced IRF-3/STAT1 activation). Blood. American Society of Hematology; 2006;107(5):2112–22.

369. Sims JE, Smith DE. The IL-1 family: regulators of immunity. Nature Publishing Group. Nature Publishing Group; 2010 Jan 18;10(2):89–102.

370. Bauer C, Duewell P, Mayer C, Lehr HA, Fitzgerald KA, Dauer M, et al. Colitis induced in mice with dextran sulfate sodium (DSS) is mediated by the NLRP3 inflammasome. Gut. 2010 Aug 26;59(9):1192–9.

371. Pastorelli L, Garg RR, Hoang SB, Spina L, Mattioli B, Scarpa M, et al. Epithelial-derived IL-33 and its receptor ST2 are dysregulated in ulcerative colitis and in experimental Th1/Th2 driven enteritis. Proc Natl Acad Sci USA. National Acad Sciences; 2010 Apr 27;107(17):8017–22.

372. Monteleone G, Boirivant M, Pallone F, MacDonald TT. TGF-β1 and Smad7 in the regulation of IBD. Mucosal Immunology. 2008 Nov;1(1s):S50–3.

373. Babyatsky MW, Rossiter G, Podolsky DK. Expression of transforming growth factors alpha and beta in colonic mucosa in inflammatory bowel disease. Gastroenterology. 1996;110(4):975–84.

374. Nacu N, Luzina IG, Highsmith K, Lockatell V, Pochetuhen K, Cooper ZA, et al. Macrophages produce TGF-beta-induced (beta-ig-h3) following ingestion of apoptotic cells and regulate MMP14 levels and collagen turnover in fibroblasts. The Journal of Immunology. American Association of Immunologists; 2008;180(7):5036–44.

375. Ball HJ, Sanchez-Perez A, Weiser S, Austin CJD, Astelbauer F, Miu J, et al. Characterization of an indoleamine 2,3-dioxygenase-like protein found in humans and mice. Gene. 2007 Jul;396(1):203–13.

376. Barcelo-Batllori S, Andre M, Servis C, Levy N, Takikawa O, Michetti P, et al. Proteomic analysis of cytokine induced proteins in human intestinal epithelial cells: Implications for inflammatory bowel diseases. Proteomics. 2002 May;2(5):551–60.

377. Wolf AM, Wolf D, Rumpold H, Moschen AR, Kaser A, Obrist P, et al. Overexpression of indoleamine 2,3-dioxygenase in human inflammatory bowel disease. Clinical Immunology. 2004 Oct;113(1):47–55.

378. Holcomb IN, Kabakoff RC, Chan B, Baker TW, Gurney A, Henzel W, et al. FIZZ1, a novel cysteine-rich secreted protein associated with pulmonary inflammation, defines a new gene family. The EMBO Journal. EMBO Press; 2000 Aug 1;19(15):4046–55.

379. Munitz A, Waddell A, Seidu L, Cole ET, Ahrens R, Hogan SP, et al. Resistin-like molecule α enhances myeloid cell activation and promotes colitis. Journal of Allergy and Clinical Immunology. 2008 Dec;122(6):1200–1.

380. Osborne LC, Joyce KL, Alenghat T, Sonnenberg GF, Giacomin PR, Du Y, et al. Resistin-like molecule α promotes pathogenic Th17 cell responses and bacterial-induced intestinal inflammation. J Immunol. American Association of Immunologists; 2013 Mar 1;190(5):2292–300.

381. N'Diaye E-N, Branda CS, Branda SS, Nevarez L, Colonna M, Lowell C, et al. TREM-2 (triggering receptor expressed on myeloid cells 2) is a phagocytic receptor for bacteria. J Cell Biol. 2009 Jan 26;184(2):215–23.

382. Correale C, Genua M, Vetrano S, Mazzini E, Martinoli C, Spinelli A, et al. Bacterial Sensor Triggering Receptor Expressed on Myeloid Cells-2 Regulates the Mucosal Inflammatory Response. YGAST. Elsevier Inc; 2013 Feb 1;144(2):346–356.e3.

383. Botto M, Dell'Agnola C, Bygrave AE, Thompson EM, Cook HT, Petry F, et al. Homozygous C1q deficiency causes glomerulonephritis associated with multiple apoptotic bodies. Nat Genet. 1998 May;19(1):56–9.

384. Castellano G, Woltman AM, Nauta AJ, Roos A, Trouw LA, Seelen MA, et al. Maturation of dendritic cells abrogates C1q production in vivo and in vitro. Blood. 2004;103(10):3813–20.

385. Teh BK, Yeo JG, Chern LM, Lu J. C1q regulation of dendritic cell development from monocytes with distinct cytokine production and T cell stimulation. Molecular Immunology. Elsevier Ltd; 2011 May 1;48(9-10):1128–38.

386. del Rio M-L, Bernhardt G, Rodriguez-Barbosa J-I, Foerster R. Development and functional specialization of CD103+dendritic cells. Immunological Reviews. Blackwell Publishing Ltd; 2010 Mar;234(1):268–81.

387. Schlickum S, Sennefelder H, Friedrich M, Harms G, Lohse MJ, Kilshaw P, et al. Integrin alpha E(CD103)beta 7 influences cellular shape and motility in a ligand-dependent fashion. Blood. American Society of Hematology; 2008 Aug 1;112(3):619–25.

388. Watford WT, Hissong BD, Bream JH, Kanno Y, Muul L, O'Shea JJ. Signaling by IL-12 and IL-23 and the immunoregulatory roles of STAT4. Immunological Reviews. 2004 Dec;202(1):139–56.

389. de Beaucoudrey L, Puel A, Filipe-Santos O, Cobat A, Ghandil P, Chrabieh M, et al. Mutations in STAT3 and IL12RB1 impair the development of human IL-17-producing T cells. J Exp Med. Rockefeller Univ Press; 2008 Jul 7;205(7):1543–50.

390. Gilsbach BK, Kortholt A. Structural biology of the LRRK2 GTPase and kinase domains: implications for regulation. Frontiers in Molecular Neuroscience. Frontiers; 2014;7(e8463).

391. Gómez-Suaga P, Hilfiker S. LRRK2 as a modulator of lysosomal calcium homeostasis with downstream effects on autophagy. Autophagy. 2014 Nov 3;8(4):692–3.

392. Gardet A, Benita Y, Li C, Sands BE, Ballester I, Stevens C, et al. LRRK2 is involved in the IFN-gamma response and host response to pathogens. J Immunol. 2010 Nov 1;185(9):5577–85.

393. Liu Z, Lee J, Krummey S, Lu W, Cai H, Lenardo MJ. The kinase LRRK2 is a regulator of the transcription factor NFAT that modulates the severity of inflammatory bowel disease. Nature Immunology. 2011 Nov;12(11):1063–70.

394. Ma DY, Clark EA. The role of CD40 and CD154/CD40L in dendritic cells. Seminars in Immunology. 2009 Oct;21(5):265–72.

395. Philpott A, Winton DJ. Lineage selection and plasticity in the intestinal crypt. Curr Opin Cell Biol. 2014 Dec;31:39–45.

396. Leibowitz BJ, Qiu W, Liu H, Cheng T, Zhang L, Yu J. Uncoupling p53 functions in radiation-induced intestinal damage via PUMA and p21. Mol Cancer Res. 2011 May;9(5):616–25.

397. Jia T, Leiner I, Dorothee G, Brandl K, Pamer EG. MyD88 and Type I Interferon Receptor-Mediated Chemokine Induction and Monocyte Recruitment during Listeria monocytogenes Infection. The Journal of Immunology. 2009 Jul 6;183(2):1271–8.

398. Askenase MH, Han S-J, Byrd AL, da Fonseca DM, Bouladoux N, Wilhelm C, et al. Bone-Marrow-Resident NK Cells Prime Monocytes for Regulatory Function during Infection. Immunity. Elsevier Inc; 2015 Jun 16;42(6):1130–42.

399. Fleming A. On a remarkable bacteriolytic element found in tissues and secretions. Proceedings of the Royal Society of London Series B-Containing Papers of a Biological Character. 1922 May;93(653):306–17.

400. Torsteinsdottir I, Hakansson L, Hallgren R, Gudbjornsson B, Arvidson NG, Venge P. Serum lysozyme: a potential marker of monocyte/macrophage activity in rheumatoid arthritis. Rheumatology (Oxford). Oxford University Press; 1999 Dec;38(12):1249–54.

401. Dong C, Zhao G, Zhong M, Yue Y, Wu L, Xiong S. RNA sequencing and transcriptomal analysis of human monocyte to macrophage differentiation. Gene. Elsevier B.V; 2013 May 1;519(2):279–87.

402. Hall CJ, Boyle RH, Astin JW, Flores MV, Oehlers SH, Sanderson LE, et al. Immunoresponsive Gene 1 Augments Bactericidal Activity of Macrophage-Lineage Cells by Regulating β-Oxidation-Dependent Mitochondrial ROS Production. Cell Metabolism. Elsevier Inc; 2013 Aug 6;18(2):265–78.

403. DRICKAMER K. Increasing Diversity of Animal Lectin Structures. Current Opinion in Structural Biology. 1995 Oct;5(5):612–6.

404. Gironella M, Iovanna JL, Sans M, Gil F, Peñalva M, Closa D, et al. Anti-inflammatory effects of pancreatitis associated protein in inflammatory bowel disease. Gut. 2005 Sep;54(9):1244–53.

405. Mc Guire C, Wieghofer P, Elton L, Muylaert D, Prinz M, Beyaert R, et al. Paracaspase MALT1 deficiency protects mice from autoimmune-mediated demyelination. J Immunol. American Association of Immunologists; 2013 Mar 15;190(6):2896–903.

406. Kobayashi Y, Miyaji C, Watanabe H, Umezu H, Hasegawa G, Abo T, et al. Role of macrophage scavenger receptor in endotoxin shock. J Pathol. 2000 Oct;192(2):263–72.

407. Thomas CA, Li YM, Kodama T, Suzuki H, Silverstein SC, Khoury El J. Protection from lethal gram-positive infection by macrophage scavenger receptor-dependent phagocytosis. Journal of Experimental Medicine. Rockefeller Univ Press; 2000;191(1):147–55.

408. Álvarez-Errico D, Vento-Tormo R, Sieweke M, Ballestar E. Epigenetic control of myeloid cell differentiation, identity and function. Nat Rev Immunol. Nature Publishing Group; 2015 Jan 1;15(1):7–17.

409. Wilting RH, Yanover E, Heideman MR, Jacobs H, Horner J, van der Torre J, et al. Overlapping functions of Hdac1 and Hdac2 in cell cycle regulation and haematopoiesis. The EMBO Journal. Nature Publishing Group; 2010 Jun 22;29(15):2586–97.

410. Bröske A-M, Vockentanz L, Kharazi S, Huska MR, Mancini E, Scheller M, et al. DNA methylation protects hematopoietic stem cell multipotency from myeloerythroid restriction. Nat Genet. Nature Publishing Group; 2009 Oct 4;41(11):1207–15.

411. Dinarello CA, van der Meer JWM. Treating inflammation by blocking interleukin-1 in humans. Seminars in Immunology. Elsevier Ltd; 2013 Dec 15;25(6):469–84.

412. Bersudsky M, Luski L, Fishman D, White RM, Ziv-Sokolovskaya N, Dotan S, et al. Non-redundant properties of IL-1 and IL-1 during acute colon inflammation in mice. Gut. 2014 Feb 27;63(4):598–609.

413. Pallotta MT, Orabona C, Volpi C, Vacca C, Belladonna ML, Bianchi R, et al. Indoleamine 2,3-dioxygenase is a signaling protein in long-term tolerance by dendritic cells. Nature Immunology. 2011 Jul 31;12(9):870–8.

414. Matteoli G, Mazzini E, Iliev ID, Mileti E, Fallarino F, Puccetti P, et al. Gut CD103+ dendritic cells express indoleamine 2,3-dioxygenase which influences T regulatory/T effector cell balance and oral tolerance induction. Gut. 2010 Apr 28;59(5):595–604.

415. Jasperson LK, Bucher C, Panoskaltsis-Mortari A. Inducing the tryptophan catabolic pathway, indoleamine 2, 3-dioxygenase (IDO), for suppression of graft-versus-host disease (GVHD) lethality. Blood. 2009.

416. Banerjee RR, Lazar MA. Dimerization of Resistin and Resistin-like Molecules Is Determined by a Single Cysteine. Journal of Biological Chemistry. American Society for Biochemistry and Molecular Biology; 2001 Jul 13;276(28):25970–3.

417. Charles JF, Humphrey MB, Zhao X, Quarles E, Nakamura MC, Aderem A, et al. The innate immune response to Salmonella enterica serovar Typhimurium by macrophages is dependent on TREM2-DAP12. Infection and Immunity. American Society for Microbiology; 2008 Jun;76(6):2439–47.

418. Schenk M, Bouchon A, Seibold F, Mueller C. TREM-1--expressing intestinal macrophages crucially amplify chronic inflammation in experimental colitis and inflammatory bowel diseases. J Clin Invest. 2007 Oct;117(10):3097–106.

419. Hsieh CL, Koike M, Spusta SC, Niemi EC, Yenari M, Nakamura MC, et al. A role for TREM2 ligands in the phagocytosis of apoptotic neuronal cells by microglia. Journal of Neurochemistry. 2009 May;109(4):1144–56.

420. Seno H, Miyoshi H, Brown SL, Geske MJ, Colonna M, Stappenbeck TS. Efficient colonic mucosal wound repair requires Trem2 signaling. PNAS. National Acad Sciences; 2009;106(1):256–61.

421. Fullerton JN, O'Brien AJ, Gilroy DW. Lipid mediators in immune dysfunction after severe inflammation. Trends in Immunology. Elsevier Ltd; 2014 Jan 1;35(1):12–21.

422. Dulhunty JM, Lipman J, Finfer S, the Sepsis Study Investigators for the ANZICS Clinical Trials Group. Does severe non-infectious SIRS differ from severe sepsis? Intensive Care Med. 2008 May 27;34(9):1654–61.

423. Wunsch H, Angus DC, Harrison DA, Linde-Zwirble WT, Rowan KM. Comparison of Medical Admissions to Intensive Care Units in the United States and United Kingdom. Am J Respir Crit Care Med. 2011 Jun 15;183(12):1666–73.

424. Serhan CN, Chiang N, Van Dyke TE. Resolving inflammation: dual anti-inflammatory and pro-resolution lipid mediators. Nat Rev Immunol. 2008 May;8(5):349–61.

425. Li J-Q, Tan L, Yu J-T. The role of the LRRK2 gene in Parkinsonism. Mol Neurodegeneration. 2014;9(1):47–17.

426. Vowinkel T, Anthoni C, Wood KC, Stokes KY, Russell J, Gray L, et al. CD40–CD40 Ligand Mediates the Recruitment of Leukocytes and Platelets in the Inflamed Murine Colon. Gastroenterology. 2007 Mar;132(3):955–65.

427. Shapiro E, Biezuner T, Linnarsson S. Single-cell sequencing-based technologies will revolutionize whole-organism science. Nature Publishing Group. Nature Publishing Group; 2013 Jul 30;14(9):618–30.

428. del Hoyo GM, Martin P, Arias CF, Marin AR, Ardavin C. CD8 alpha(+) dendritic cells originate from the CD8 alpha(-) dendritic cell subset by a maturation process involving CD8 alpha, DEC-205, and CD24 up-regulation. Blood. American Society of Hematology; 2002;99(3):999–1004.

429. Dotan I, Allez M, Nakazawa A, Brimnes J, Schulder-Katz M, Mayer L. Intestinal epithelial cells from inflammatory bowel disease patients preferentially stimulate CD4+ T cells to proliferate and secrete interferon-gamma. AJP: Gastrointestinal and Liver Physiology. 2007 Jun;292(6):G1630–40.

430. Frantz AL, Rogier EW, Weber CR, Shen L, Cohen DA, Fenton LA, et al. Targeted deletion of MyD88 in intestinal epithelial cells results in compromised antibacterial immunity associated with downregulation of polymeric immunoglobulin receptor, mucin-2, and antibacterial peptides. Mucosal Immunology. Nature Publishing Group; 2012 Apr 11;:1–12.

431. Abreu MT. Toll-like receptor signalling in the intestinal epithelium: how bacterial recognition shapes intestinal function. Nature Publishing Group. Nature Publishing Group; 2010 Feb 1;10(2):131–44.

432. Wells JM, Loonen LMP, Karczewski JM. The role of innate signaling in the homeostasis of tolerance and immunity in the intestine. Int J Med Microbiol. 2010 Jan;300(1):41–8.

433. Butler M, Ng C-Y, van Heel DA, Lombardi G, Lechler R, Playford RJ, et al. Modulation of dendritic cell phenotype and functionin anin vitromodel of the intestinal epithelium. Eur J Immunol. 2006 Apr;36(4):864–74.

434. Zhou B, Comeau MR, Smedt TD, Liggitt HD, Dahl ME, Lewis DB, et al. Thymic stromal lymphopoietin as a key initiator of allergic airway inflammation in mice. Nature Immunology. 2005 Sep 4;6(10):1047–53.

435. Al-Shami A. A role for TSLP in the development of inflammation in an asthma model. Journal of Experimental Medicine. 2005 Sep 12;202(6):829–39.

436. Zaph C, Troy AE, Taylor BC, Berman-Booty LD, Guild KJ, Du Y, et al. Epithelial-cell-intrinsic IKK-β expression regulates intestinal immune homeostasis. Nature. 2007 Feb 25;446(7135):552–6.

437. Strobl H, Knapp W. TGF-beta 1 regulation of dendritic cells. Microbes Infect. 1999 Dec;1(15):1283–90.

438. Yoshimura A. Negative regulation of cytokine signaling influences inflammation. Current Opinion in Immunology. 2003 Dec;15(6):704–8.

439. Travis MA, Reizis B, Melton AC, Masteller E, Tang Q, Proctor JM, et al. Loss of integrin αvβ8 on dendritic cells causes autoimmunity and colitis in mice. Nature. 2007 Aug 12;449(7160):361–5.

440. Brandtzaeg P, Farstad IN, Johansen FE, Morton HC, Norderhaug IN, Yamanaka T. The B-cell system of human mucosae and exocrine glands. Immunological Reviews. 1999 Oct;171:45–87.

441. Owens WE, Berg RD. Bacterial translocation from the gastrointestinal tract of athymic (nu/nu) mice. Infection and Immunity. American Society for Microbiology; 1980 Feb 1;27(2):461–7.

442. Shang L, Fukata M, Thirunarayanan N, Martin AP, Arnaboldi P, Maussang D, et al. Toll-Like Receptor Signaling in Small Intestinal Epithelium Promotes B-Cell Recruitment and IgA Production in Lamina Propria. Gastroenterology. 2008 Aug;135(2):529–538.e1.

443. He B, Xu W, Santini PA, Polydorides AD, Chiu A, Estrella J, et al. Intestinal Bacteria Trigger T Cell-Independent Immunoglobulin A2 Class Switching by Inducing Epithelial-Cell Secretion of the Cytokine APRIL. Immunity. 2007 Jun;26(6):812–26.

444. Chieppa M, Rescigno M, Huang AYC, Germain RN. Dynamic imaging of dendritic cell extension into the small bowel lumen in response to epithelial cell TLR engagement. Journal of Experimental Medicine. Rockefeller Univ Press; 2006 Dec 25;203(13):2841–52.

445. Rescigno M. Dendritic Cells Shuttle Microbes Across Gut Epithelial Monolayers. Immunobiology. 2001;204(5):572–81.

446. Ley RE, Peterson DA, Gordon JI. Ecological and Evolutionary Forces Shaping Microbial Diversity in the Human Intestine. Cell. 2006 Feb;124(4):837–48.

447. Whitman WB, Coleman DC, Wiebe WJ. Prokaryotes: The unseen majority. PNAS. 1998;95(12):6578–83.

448. Simrén M, Barbara G, Flint HJ, Spiegel BMR, Spiller RC, Vanner S, et al. Intestinal microbiota in functional bowel disorders: a Rome foundation report. BMJ Publishing Group Ltd and British Society of Gastroenterology; 2013. pp. 159–76.

449. Alenghat T, Osborne LC, Saenz SA, Kobuley D, Ziegler CGK, Mullican SE, et al. Histone deacetylase 3 coordinates commensal- bacteria-dependent intestinal homeostasis. Nature. Nature Publishing Group; 2013 Nov 3;:1–17.

450. Cruickshank SM, McVay LD, Baumgart DC, Felsburg PJ, Carding SR. Colonic epithelial cell mediated suppression of CD4 T cell activation. Gut. BMJ Publishing Group Ltd and British Society of Gastroenterology; 2004 May;53(5):678–84.

451. Trzpis M, McLaughlin PMJ, de Leij LMFH, Harmsen MC. Epithelial cell adhesion molecule: more than a carcinoma marker and adhesion molecule. AJPA. 2007 Aug;171(2):386–95.

452. Karam SM. Lineage commitment and maturation of epithelial cells in the gut. Front Biosci. 1999 Mar 15;4:D286–98.

453. Barker N, van Es JH, Kuipers J, Kujala P, van den Born M, Cozijnsen M, et al. Identification of stem cells in small intestine and colon by marker gene Lgr5. Nature. 2007 Oct 14;449(7165):1003–7.

454. Beuling E, Aronson BE, Tran LMD, Stapleton KA, Horst ter EN, Vissers LATM, et al. GATA6 is required for proliferation, migration, secretory cell maturation, and gene expression in the mature mouse colon. Molecular and Cellular Biology. American Society for Microbiology; 2012 Sep;32(17):3392–402.

455. Huch M, Dorrell C, Boj SF, van Es JH, Li VSW, van de Wetering M, et al. In vitro expansion of single Lgr5+ liver stem cells induced by Wnt-driven regeneration. Nature. Nature Publishing Group; 2013 Feb 6;494(7436):247–50.

456. Khan Z, Orr A, Michalopoulos G, Ranganathan S. Immunohistochemical Analysis of LGR5 Expression in Pediatric Liver Disease. The FASEB Journal. 2015 Apr;29.

457. Flanagan K, Modrusan Z, Cornelius J, Chavali A, Kasman I, Komuves L, et al. Intestinal epithelial cell up-regulation of LY6 molecules during colitis results in enhanced chemokine secretion. The Journal of Immunology. American Association of Immunologists; 2008 Mar 15;180(6):3874–81.

458. Thelemann C, Eren RO, Coutaz M, Brasseit J, Bouzourene H, Rosa M, et al. Interferon-γ induces expression of MHC class II on intestinal epithelial cells and protects mice from colitis. PLoS ONE. 2014;9(1):e86844.

459. Zhang ZX, Stanford WL, Zhang L. Ly-6A is critical for the function of double negative regulatory T cells. Eur J Immunol. 2002 Jun;32(6):1584–92.

460. Henderson SC, Kamdar MM, Bamezai A. Ly-6A.2 Expression Regulates Antigen-Specific CD4+ T Cell Proliferation and Cytokine Production. The Journal of Immunology. 2002 Jan 1;168(1):118–26.

461. Artis D, Wang ML, Keilbaugh SA, He W, Brenes M, Swain GP, et al. RELMβ/FIZZ2 is a goblet cell-specific immune-effector molecule in the gastrointestinal tract. PNAS. National Acad Sciences; 2004 Sep 14;101(37):13596–600.

462. Ogawa H, Fukushima K, Naito H, Funayama Y, Unno M, Takahashi K, et al. Increased expression of HIP/PAP and regenerating gene III in human inflammatory bowel disease and a murine bacterial reconstitution model. Inflammatory Bowel Diseases. 2003 May;9(3):162–70.

463. Hattrup CL, Gendler SJ. Structure and Function of the Cell Surface (Tethered) Mucins. Annu Rev Physiol. 2008 Mar;70(1):431–57.

464. Suzuki T. Regulation of intestinal epithelial permeability by tight junctions. Cell Mol Life Sci. SP Birkhäuser Verlag Basel; 2012 Jul 11;70(4):631–59.

465. Gray-Owen SD, Blumberg RS. CEACAM1: contact-dependent control of immunity. Nat Rev Immunol. 2006 Jun;6(6):433–46.

466. Kim YS, Ho SB. Intestinal Goblet Cells and Mucins in Health and Disease: Recent Insights and Progress. Curr Gastroenterol Rep. 2010 Aug 13;12(5):319–30.

467. Kindon H, Pothoulakis C, Thim L, Lynch-Devaney K. Trefoil peptide protection of intestinal epithelial barrier function: cooperative interaction with mucin glycoprotein. Gastroenterology. 1995;109(2):516–23.

468. Podolsky DK, Gerken G, Eyking A, Cario E. Colitis-Associated Variant of TLR2 Causes Impaired Mucosal Repair Because of TFF3 Deficiency. YGAST. AGA Institute American Gastroenterological Association; 2009 Jul 1;137(1):209–20.

469. Malago JJ, Koninkx J, van Dijk JE. The heat shock response and cytoprotection of the intestinal epithelium. Cell Stress Chaperones. 2002 Apr;7(2):191–9.

470. Adachi T, Sakurai T, Kashida H, Mine H, Hagiwara S, Matsui S, et al. Involvement of Heat Shock Protein A4/Apg-2 in Refractory Inflammatory Bowel Disease. Inflammatory Bowel Diseases. 2015 Jan;21(1):31–9.

471. Griffith JW, Sokol CL, Luster AD. Chemokines and Chemokine Receptors: Positioning Cells for Host Defense and Immunity. Annu Rev Immunol. 2014 Mar 21;32(1):659–702.

472. Meissner TB, Li A, Biswas A, Lee K-H, Liu Y-J, Bayir E, et al. NLR family member NLRC5 is a transcriptional regulator of MHC class I genes. Proc Natl Acad Sci USA. National Acad Sciences; 2010 Aug 3;107(31):13794–9.

473. Zhang Y, Liu C, Peng H, Zhang J, Feng Q. IL1 Receptor Antagonist Gene IL1-RN Variable Number of Tandem Repeats Polymorphism and Cancer Risk: A Literature Review and Meta-Analysis. Katoh M, editor. PLoS ONE. 2012 Sep 25;7(9):e46017–7.

474. Kennedy NA, Walker AW, Berry SH, Duncan SH, Farquarson FM, Louis P, et al. The Impact of Different DNA Extraction Kits and Laboratories upon the Assessment of Human Gut Microbiota Composition by 16S rRNA Gene Sequencing. Sanz Y, editor. PLoS ONE. 2014 Feb 24;9(2):e88982.

475. Swidsinski A, Ladhoff A, Pernthaler A, Swidsinski S, Loening Baucke V, Ortner M, et al. Mucosal flora in inflammatory bowel disease. Gastroenterology. 2002 Jan;122(1):44–54.

476. Sartor RB. Microbial Influences in Inflammatory Bowel Diseases. Gastroenterology. 2008 Feb;134(2):577–94.

477. Frank DN, Amand ALS, Feldman RA, Boedeker EC, Harpaz N, Pace NR. Molecular-phylogenetic characterization of microbial community imbalances in human inflammatory bowel diseases. PNAS. National Acad Sciences; 2007;104(34):13780–5.

478. Manichanh C, Rigottier-Gois L, Bonnaud E, Gloux K, Pelletier E, Frangeul L, et al. Reduced diversity of faecal microbiota in Crohn's disease revealed by a metagenomic approach. Gut. 2006 Feb;55(2):205–11.

479. Hildebrand F, Nguyen TLA, Brinkman B, Yunta RG, Cauwe B, Vandenabeele P, et al. Inflammation-associated enterotypes, host genotype, cage and inter-individual effects drive gut microbiota variation in common laboratory mice. Genome Biology. BioMed Central Ltd; 2013 Jan 24;14(1):R4.

480. Campbell JH, Foster CM, Vishnivetskaya T, Campbell AG, Yang ZK, Wymore A, et al. Host genetic and environmental effects on mouse intestinal microbiota. ISME J. Nature Publishing Group; 2012 Jun 14;6(11):2033–44.

481. Schloss PD, Westcott SL, Ryabin T, Hall JR, Hartmann M, Hollister EB, et al. Introducing mothur: Open-Source, Platform-Independent, Community-Supported Software for Describing and Comparing Microbial Communities. Applied and Environmental Microbiology. 2009 Nov 18;75(23):7537–41.

482. Yue JC, Clayton MK, Lin FC. A nonparametric estimator of species overlap. Biometrics. Blackwell Publishing Ltd; 2001 Sep;57(3):743–9.

483. MINCHIN PR. An Evaluation of the Relative Robustness of Techniques for Ecological Ordination. Vegetatio. Dordrecht: Springer Netherlands; 1987;69(1-3):89–107.

484. Sunderkötter C, Nikolic T, Dillon MJ, van Rooijen N, Stehling M, Drevets DA, et al. Subpopulations of mouse blood monocytes differ in maturation stage and inflammatory response. The Journal of Immunology. American Association of Immunologists; 2004 Apr 1;172(7):4410–7.

485. Classon BJ. Ly-6 ligands remain elusive. Trends in Immunology. 2001

Mar;22(3):126–6.

486. Beswick EJ. CD74 in antigen presentation, inflammation, and cancers of the gastrointestinal tract. WJG. 2009;15(23):2855–7.

487. Barrera CA. Polarized Expression of CD74 by Gastric Epithelial Cells. Journal of Histochemistry and Cytochemistry. 2005 Jun 27;53(12):1481–9.

488. Leng L, Metz CN, Fang Y, Xu J, Donnelly S, Baugh J, et al. MIF Signal Transduction Initiated by Binding to CD74. Journal of Experimental Medicine. 2003 Jun 2;197(11):1467–76.

489. HENNE C, SCHWENK F, KOCH N, Möller P. Surface Expression of the Invariant Chain (Cd74) Is Independent of Concomitant Expression of Major Histocompatibility Complex Class-Ii Antigens. Immunology. Wiley-Blackwell; 1995 Feb;84(2):177–82.

490. Bernhagen J, Krohn R, Lue H, Gregory JL, Zernecke A, Koenen RR, et al. MIF is a noncognate ligand of CXC chemokine receptors in inflammatory and atherogenic cell recruitment. Nature Medicine. 2007 Apr 15;13(5):587–96.

491. Beswick EJ, Pinchuk IV, Minch K, Suarez G, Sierra JC, Yamaoka Y, et al. The Helicobacter pylori Urease B Subunit Binds to CD74 on Gastric Epithelial Cells and Induces NF- B Activation and Interleukin-8 Production. Infection and Immunity. 2006 Jan 20;74(2):1148–55.

492. Jiang Z, Xu M, Savas L, LeClair P, Banner BF. Invariant chain expression in colon neoplasms. Virchows Arch. Springer-Verlag; 1999;435(1):32–6.

493. Lo J, Leung A, Huang XR, Lie A, Metz C, Bucala R, et al. Macrophage migratory inhibitory factor (MIF) expression in acute graft-versus-host disease (GVHD) in allogeneic hemopoietic stem cell transplant recipients. Bone Marrow Transplant. 2002 Sep;30(6):375–80.

494. Becker-Herman S, Arie G, Medvedovsky H, Kerem A, Shachar I. CD74 is a member of the regulated intramembrane proteolysis-processed protein family. Mol Biol Cell. American Society for Cell Biology; 2005 Nov;16(11):5061–9.

495. Bisping G, Lügering N, Lütke Brintrup S, Pauels HG, Schürmann G, Domschke W, et al. Patients with inflammatory bowel disease (IBD) reveal increased induction capacity of intracellular interferon-gamma (IFN-γ) in peripheral CD8+ lymphocytes co-cultured with intestinal epithelial cells. Clinical & Experimental Immunology. Blackwell Publishing Ltd; 2001 Jan 1;123(1):15–22.

496. Bär F, Sina C, Hundorfean G, Pagel R, Lehnert H, Fellermann K, et al. Inflammatory bowel diseases influence major histocompatibility complex class I (MHC I) and II compartments in intestinal epithelial cells. Clinical & Experimental Immunology. 2013 Apr 10;172(2):280–9.

497. Neefjes J, Jongsma MLM, Paul P, Bakke O. Towards a systems understanding of MHC class I and MHC class II antigen presentation. Nat Rev Immunol. Nature Publishing Group; 2011 Nov 11;11(12):823–36.

498. Paul P, van den Hoorn T, Jongsma MLM, Bakker MJ, Hengeveld R, Janssen L, et al. A Genome-wide Multidimensional RNAi Screen Reveals Pathways Controlling MHC Class II Antigen Presentation. Cell. Elsevier Inc; 2011 Apr 15;145(2):268–83.

499. Hershberg RM, Cho DH, Youakim A, Bradley MB, Lee JS, Framson PE, et al. Highly polarized HLA class II antigen processing and presentation by human intestinal epithelial cells. J Clin Invest. American Society for Clinical Investigation; 1998;102(4):792–803.

500. Kitamura A, Maekawa Y, Uehara H, Izumi K, Kawachi I, Nishizawa M, et al. A mutation in the immunoproteasome subunit PSMB8 causes autoinflammation and lipodystrophy in humans. J Clin Invest. 2011 Oct 3;121(10):4150–60.

501. Visekruna A, Joeris T, Seidel D, Kroesen A, Loddenkemper C, Zeitz M, et al. Proteasome-mediated degradation of IκBα and processing of p105 in Crohn disease and ulcerative colitis. J Clin Invest. 2006 Dec 1;116(12):3195–203.

502. Tsukita S, Furuse M, Itoh M. Multifunctional strands in tight junctions. Nat Rev Mol Cell Biol. 2001 Apr;2(4):285–93.

503. Van Itallie CM, Anderson JM. CLAUDINS AND EPITHELIAL PARACELLULAR TRANSPORT. Annu Rev Physiol. 2006 Jan;68(1):403–29.

504. Turner JR. Intestinal mucosal barrier function in health and disease. Nature Publishing Group. 2009 Nov;9(11):799–809.

505. Furuse M, Hata M, Furuse K, Yoshida Y, Haratake A, Sugitani Y, et al. Claudin-based tight junctions are crucial for the mammalian epidermal barrier: a lesson from claudin-1-deficient mice. J Cell Biol. 2002 Mar 18;156(6):1099–111.

506. Tamura A, Hayashi H, Imasato M, Yamazaki Y, Hagiwara A, Wada M, et al. Loss of claudin-15, but not claudin-2, causes Na+ deficiency and glucose malabsorption in mouse small intestine. Gastroenterology. 2011 Mar;140(3):913–23.

507. Hou J, Gomes AS, Paul DL, Goodenough DA. Study of Claudin Function by RNA Interference. Journal of Biological Chemistry. American Society for Biochemistry and Molecular Biology; 2006 Nov 24;281(47):36117–23.

508. Tanaka M, Kamata R, Sakai R. EphA2 Phosphorylates the Cytoplasmic Tail of Claudin-4 and Mediates Paracellular Permeability. Journal of Biological Chemistry. American Society for Biochemistry and Molecular Biology; 2005 Dec 23;280(51):42375–82.

509. Clayburgh DR, Shen L, Turner JR. A porous defense: the leaky epithelial barrier in intestinal disease. Lab Invest. 2004 Mar;84(3):282–91.

510. Chiba H, Kojima T, Osanai M, Sawada N. The significance of interferon-gamma-triggered internalization of tight-junction proteins in inflammatory bowel disease. Sci STKE. Science Signaling; 2006 Jan 3;2006(316):pe1–pe1.

511. Zhang T, Chen Y, Wang Z, Zhou Y, Zhang S. [Changes of fecal flora and its correlation with inflammatory indicators in patients with inflammatory bowel disease]. Nan fang yi ke da xue …. 2013.

512. Zitomersky NL, Atkinson BJ, Franklin SW, Mitchell PD, Snapper SB, Comstock LE, et al. Characterization of Adherent Bacteroidales from Intestinal Biopsies of Children and Young Adults with Inflammatory Bowel Disease. Sanz Y, editor. PLoS ONE. Public Library of Science; 2013 Jun 11;8(6):e63686–11.

513. Kverka M, Zakostelska Z, Klimesova K, Sokol D, Hudcovic T, Hrncir T, et al.

Oral administration of Parabacteroides distasonis antigens attenuates experimental murine colitis through modulation of immunity and microbiota composition. Clinical & Experimental Immunology. 2011 Feb;163(2):250–9.

514. Hopkins MJ, Sharp R, Macfarlane GT. Age and disease related changes in intestinal bacterial populations assessed by cell culture, 16S rRNA abundance, and community cellular fatty acid profiles. Gut. BMJ Group; 2001 Feb;48(2):198–205.

515. Biagi E, Candela M, Fairweather-Tait S, Franceschi C, Brigidi P. Aging of the human metaorganism: the microbial counterpart. Age (Dordr). 2012 Feb;34(1):247–67.

516. Vinolo MAR, Rodrigues HG, Nachbar RT, Curi R. Regulation of Inflammation by Short Chain Fatty Acids. Nutrients. Molecular Diversity Preservation International; 2011 Dec;3(12):858–76.

517. Maslowski KM, Vieira AT, Ng A, Kranich J, Sierro F, Yu D, et al. Regulation of inflammatory responses by gut microbiota and chemoattractant receptor GPR43. Nature. 2009 Oct 29;461(7268):1282–6.

518. Blais M, Seidman EG, Asselin C. Dual effect of butyrate on IL-1beta--mediated intestinal epithelial cell inflammatory response. DNA Cell Biol. 2007 Mar;26(3):133–47.

519. Fukae J, Amasaki Y, Yamashita Y, Bohgaki T, Yasuda S, Jodo S, et al. Butyrate suppresses tumor necrosis factor alpha production by regulating specific messenger RNA degradation mediated through a cis-acting AU-rich element. Arthritis & Rheumatism. 2005 Sep;52(9):2697–707.

520. Waldecker M, Kautenburger T, Daumann H, Busch C, Schrenk D. Inhibition of histone-deacetylase activity by short-chain fatty acids and some polyphenol metabolites formed in the colon. J Nutr Biochem. 2008 Sep;19(9):587–93.

521. Bruewer M, Luegering A, Kucharzik T, Parkos CA, Madara JL, Hopkins AM, et al. Proinflammatory cytokines disrupt epithelial barrier function by apoptosis-independent mechanisms. The Journal of Immunology. 2003;171(11):6164–72.

522. Turgeon N, Gagne JM, Blais M, Gendron FP, Boudreau F, Asselin C. The acetylome regulators Hdac1 and Hdac2 differently modulate intestinal epithelial cell dependent homeostatic responses in experimental colitis. AJP: Gastrointestinal and Liver Physiology. 2014 Apr 1;306(7):G594–G605.

523. Marjoram L, Alvers A, Deerhake ME, Bagwell J, Mankiewicz J, Cocchiaro JL, et al. Epigenetic control of intestinal barrier function and inflammation in zebrafish. PNAS. 2015 Mar 3;112(9):2770–5.

524. Ware LB, Matthay MA. The acute respiratory distress syndrome. N Engl J Med. 2000 May 4;342(18):1334–49.

525. Saiki T, Mitsuyama K, Toyonaga A, Ishida H, Tanikawa K. Detection of pro- and anti-inflammatory cytokines in stools of patients with inflammatory bowel disease. Scand J Gastroenterol. 1998 Jun;33(6):616–22.